



Zuway, Khaled Yousff (2018) Development of new methods of detection and quantification of controlled and new psychoactive substances (NPS) using liquid chromatography-amperometric detection (LC-AD). Doctoral thesis (PhD), Manchester Metropolitan University.

Downloaded from: <https://e-space.mmu.ac.uk/622108/>

Usage rights: Creative Commons: Attribution-Noncommercial-No Derivative Works 4.0

Please cite the published version

<https://e-space.mmu.ac.uk>

**Development of New Methods of Detection and
Quantification of Controlled and New Psychoactive
Substances (NPS) using Liquid Chromatography-
Amperometric Detection (LC-AD)**

**A thesis submitted in partial fulfilment of the requirements of the
Manchester Metropolitan University for the degree of Doctor of
Philosophy.**

**By
Khaled Youssff Zuway**

School of Science and the Environment
Faculty of Science and Engineering
Manchester Metropolitan University

May 2018

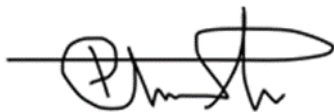
Author's declaration

"I declare that none of the work detailed herein has been submitted for any other award at Manchester Metropolitan University or any other Institution."

"I declare that, except where specifically indicated, all the work presented in this report is my own, and I am the sole author of all parts. I understand that any evidence of plagiarism and/or the use of unacknowledged third part data will be dealt with as a very seriousmatter."

Signature

Date: 04-February-2018

A handwritten signature in black ink, consisting of a stylized 'P' followed by a series of loops and a long horizontal stroke.

“Read! In the name of your Allah, who has created (all that exists).”

Al Qur'an Surah Al Alaq ayah 1

“And mankind has not been given of knowledge except a little.”

Al Qur'an Surah Al Isra ayah 85

Abstract

The global increase in the prevalence and abuse of new psychoactive substances (NPS) has required the development of new analytical methods for rapid, selective and inexpensive protocols for both their separation and detection. Electrochemical sensing of these compounds has been demonstrated to be an effective method for their in-field detection, either in their pure form or the presence of common adulterants. The electrochemical technique can differentiate between structurally-related phenethylamines (for example (±)-paramethoxyamphetamine and (±)-3,4-methylene dioxymethamphetamine, however it is limited in its ability to distinguish between structurally-related cathinone-derivatives, for example (±)-4-mephedrone and (±)-4-methyl-N-ethycathinone.

The HPLC-AD protocol obtained a cost-effective, reproducible, and reliable sensor platform for detection of the target analytes by simultaneous HPLC-UV and amperometric detection protocol. Additionally, the simultaneous HPLC-UV and amperometric detection protocol detailed herein shows a marked improvement in selectively discriminating between structurally related compounds.

This thesis demonstrates, for the first time, the combination of HPLC-UV with amperometric detection (HPLC-AD) for the detection and quantitative analysis of new psychoactive substances using a commercially available impinging jet (LC-FC-A system) or using a custom-made iCell channel flow-cell system (LC-FC-B), both incorporating embedded graphite screen-printed macroelectrodes. The method demonstrates the application of a cost-effective, reproducible, and reliable sensor platform for the simultaneous HPLC-UV and amperometric detection of target analytes.

Although the amperometric detection (HPLC-AD) system that has been developed is not as sensitive as standard HPLC-UV detection, both LC-FC-A and LC-FC-B show a good agreement between the quantitative electroanalytical data. Therefore, they are suitable for the detection and quantification of new psychoactive substances, either in their pure form or within complex mixtures.

Additionally, the simultaneous HPLC-AD protocol shows a marked improvement and advantage over previously reported electroanalytical methods. The electroanalytical methods were either unable to selectively differentiate between structurally related synthetic cathinones (e.g. (±)-mephedrone and (±)-4-MEC (Smith et al., 2014a), or utilised harmful and restrictive materials in their design by adding the illegal compounds in combination with the legal compounds.

Table of contents

Author's declaration	I
Abstract	III
Table of contents	V
List of tables	XII
List of figures	XXIV
List of equations	XXVIII
Published work (from this thesis)	XXIX
Abbreviation and Acronyms	XXX
Acknowledgments	XXXIV
1 Chapter 1: Introduction and literature review	1
1.1 New psychoactive substances.	1
1.2 Emergence/prevalence of NPS	3
1.3 Prevalence of NPSs	4
1.4 Misuse of Drugs Act (1971)	6
1.5 Classification of controlled and new/novel psychoactive substances	11
1.5.1 Phenethylamine (amphetamine, methamphetamine and MDMA)	12
1.5.2 Synthetic cathinones	16
1.5.3 Dissociative anaesthetics (regioisomers of methoxyphenidine and fluoroephendine)	23
1.6 Analytical techniques for the detection of NPS	26
1.6.1 The principle of chromatography	29
1.6.2 Electrochemistry	32
1.6.3 Application of high performance liquid chromatography-electrochemical detection (HPLC-D)	36
1.7 Study aims and objectives	39
2 Chapter 2: Materials and methods	41
2.1 Chemicals	41
2.1.1 Synthesis of (\pm)-methoxyphenidine regioisomers	42

2.1.2	Synthesis of (±)-fluoroephedrine regioisomers	43
2.2	Instrumental details	43
2.2.1	High performance liquid chromatography (HPLC)	43
2.2.2	Electrochemistry flow cells used in liquid chromatography-amperometric detection (HPLC-AD)	44
2.2.3	Screen-printing electrodes	45
2.2.4	HPLC-AD protocol	45
2.3	Preparation of buffer solutions:	46
2.3.1	Preparation of aqueous-50 mM potassium dihydrogen phosphate ($K_2H_2PO_4$)-100 mM potassium chloride buffer (pH 3.2).	46
2.3.2	Preparation of aqueous 10 mM ammonium acetate-100 mM potassium chloride buffer (pH 4.3)	47
2.3.3	Preparation of aqueous 10 mM ammonium formate-100 mM potassium chloride buffer (pH 3.5)	47
2.3.4	Preparation of aqueous 20 mM ammonium acetate-100 mM potassium chloride buffer (pH 7)	47
2.4	Preparation of mobile phases	48
2.5	Determination the void time (t_0) of HPLC	48
2.6	Detection and quantification of (±)-MDMA in the presence of (±)-MA and (±)-PMA by using high performance liquid chromatography-amperometric detection	49
2.6.1	Preparation of standard solutions for determination of λ_{max} of the UV detector	49
2.6.2	Sample preparation for HPLC method development	49
2.6.3	Optimisation of potential for amperometric detection (AD)	49
2.6.4	Optimisation of linear velocity for amperometric detection (AD)	50
2.6.5	Optimisation of HPLC-AD amperometric response under varying pH	50
2.6.6	Calibration standards (pure substances):	51
2.6.7	Specificity standards	51
2.6.8	Accuracy of the study	51
2.6.9	Street samples	52
2.7	Detection and quantification of (±)-mephedrone; (±)-4-MEC and caffeine using high performance liquid chromatography-amperometric detection	52
2.7.1	Preparation of solutions to determination λ_{max} of the UV detector:	52
2.7.2	Sample preparation for HPLC method development	52

2.7.3	Optimisation of potential for amperometric detection (AD)	53
2.7.4	Optimisation of linear velocity for amperometric detection (AD)	53
2.7.5	Optimisation of HPLC-AD amperometric response under varying pH	53
2.7.6	Calibration standards (pure substances):	54
2.7.7	Specificity standards	55
2.7.8	Accuracy of the study	55
2.7.9	Street samples	55
2.8	Detection and quantification of (±)-mexedrone and (±)-mephedrone	56
2.8.1	Characterisation	56
2.8.2	Preparation of solution to determine λ_{\max} :	57
2.8.3	Sample preparation for HPLC method development:	57
2.8.4	Optimisation of potential for amperometric detection (AD)	57
2.8.5	Optimisation of linear velocity for amperometric detection (AD)	58
2.8.6	Optimisation of HPLC-AD amperometric response under varying pH	58
2.8.7	Calibration standards (pure substances):	59
2.8.8	Specificity standards of HPLC-UV	59
2.8.9	Selectivity study of HPLC-UV	59
2.8.10	Accuracy study	60
2.8.11	Street samples	60
2.9	Detection and quantification of (±)-2-MEP, (±)-3-MEP and (±)-4-MEP.	60
2.9.1	Preparation of solutions to determine λ_{\max}	60
2.9.2	Sample preparation for HPLC method development	61
2.9.3	Optimisation of potential for amperometric detection (AD)	61
2.9.4	Optimisation of linear velocity for amperometric detection (AD)	61
2.9.5	Optimisation of HPLC-AD amperometric response under varying pH	61
2.9.6	Calibration standards (pure substances):	62
2.9.7	Specificity standards	63
2.9.8	Accuracy of the study	63
2.9.9	Street samples:	63

2.10	Detection and quantification of (±)-2-FEP, (±)-3-FEP and (±)-4-FEP.	64
2.10.1	Preparation of solutions to determine λ_{\max}	64
2.10.2	Sample preparation for HPLC method development:	64
2.10.3	Optimisation of potential for amperometric detection (AD)	64
2.10.4	Optimisation of linear velocity for amperometric detection (AD)	65
2.10.5	Optimisation of HPLC-AD amperometric response under varying pH	65
2.10.6	Calibration standards (pure substances):	66
2.10.7	Specificity standards	66
2.10.8	Accuracy of the study	66
2.10.9	Street samples	67
2.11	HPLC-UV validation	67
2.12	Amperometric detection validation:	67
3	Chapter 3: Detection and quantification of (±)-MDMA in the presence of (±)-MA and (±)-PMA by using high-performance liquid chromatography-amperometric detection (HPLC-AD)	68
3.1	Introduction	68
3.2	Ultraviolet-visible spectroscopy (UV) Determination of λ_{\max}	72
3.3	HPLC Method Development	72
3.4	Amperometric detection method development	74
3.4.1	Optimisation of the potential of amperometric detection:	74
3.4.2	Optimisation of the linear velocity of amperometric detection	77
3.4.3	Optimisation of pH of HPLC-UV and amperometric detection:	78
3.5	HPLC-AD method validation	79
3.5.1	System suitability test	82
3.5.2	Resolution (R_s)	84
3.5.3	Selectivity (separation) factor (α) and specificity:	84
3.5.4	Linearity	85
3.5.5	Limit of detection (LOD)	89
3.5.6	Limit of quantification	90
3.5.7	Robustness	91
3.5.8	Inter-and intra-day precision	93
3.5.9	Accuracy	94

3.6	Application of methodology in a forensic drug analysis context	97
3.7	Conclusions	99
4	Chapter 4: Detection and quantification of (±)-mephedrone (±)-4-MEC and common adulterants by using High Performance Liquid Chromatography-Amperometric Detection	100
4.1	Introduction:	100
4.2	Ultraviolet-visible spectroscopy (UV) determination of λ_{\max}	103
4.3	HPLC Method Development:	103
4.4	Amperometric detection method development:	105
4.4.1	Optimisation of potential of amperometric detection:	105
4.4.2	Optimisation of linear velocity of amperometric detection:	106
4.4.3	Optimisation of pH for HPLC-UV and amperometric detection	107
4.5	HPLC-AD method validation:	107
4.5.1	System suitability test	109
4.5.2	Resolution (R_s)	112
4.5.3	Selectivity factor (α)	112
4.5.4	Linearity	113
4.5.5	Limits of detection (LOD)	116
4.5.6	Limits of quantification (LOQ)	117
4.5.7	Robustness	118
4.5.8	Inter-and intra-day precision	120
4.5.9	Accuracy test	122
4.6	Application of the technique to forensic drug analysis	124
4.7	Conclusions	128
5	Chapter 5: Detection and quantification of (±)-mephedrone and (±)-mexedrone as new Psychoactive substances using the HPLC-AD protocol	130
5.1	Introduction	130
5.2	Characterisation	132
5.3	Nuclear magnetic resonance spectroscopy (NMR)	133
5.3.1	(±)-Mephedrone:	133
5.3.2	(±)-Mexedrone	136
5.4	Gas chromatography-mass spectrometry (GC-MS) analysis	139
5.5	Ultraviolet-visible spectroscopy (UV-vis) (determination of λ_{\max})	143

5.6	HPLC method development	143
5.7	Amperometric detection method development	145
5.7.1	Optimisation of anodic potential by amperometric detection (AD)	145
5.7.2	Optimisation of the linear velocity of amperometric detection	146
5.7.3	Optimisation of pH of HPLC-UV and amperometric detection	146
5.8	HPLC-AD method validation	147
5.8.1	System suitability test	148
5.8.2	Resolution (Rs)	150
5.8.3	Linearity	150
5.8.4	Limit of detection (LOD)	152
5.8.5	Limit of quantification (LOQ)	153
5.8.6	Robustness	153
5.8.7	Inter- and intra-day precision	155
5.8.8	Accuracy	156
5.9	Application of the methodology to forensic analysis	156
5.10	Conclusion	157
6	Chapter 6: Detection and quantification of regioisomers of new psychoactive substances (NPS) using high performance liquid chromatography-amperometric detection (HPLC-AD)	159
6.1	Introduction	159
6.2	Detection and quantification of regioisomers of methoxyphenidine using HPLC-AD	162
6.2.1	Ultraviolet-visible spectroscopy (UV) determination of λ_{\max}	162
6.2.2	HPLC method development	162
6.2.3	Amperometric detection method development	163
6.2.4	HPLC-AD method validation	166
6.2.5	Forensic Application	176
6.3	Detection and quantification of regioisomer of fluoroephenidine by using HPLC-AD protocol:	178
6.3.1	Ultraviolet-Visible Spectroscopy (UV) (Determination of λ_{\max})	178
6.3.2	HPLC Method Development:	178
6.3.3	Amperometric detection method development:	179
6.3.4	Method Validation	182
6.3.5	Forensic Application	192

6.4	Conclusions	193
7	Chapter 7: Conclusions & Future Perspectives	195
8	References	198
9	Appendix	219

List of tables

Table 1.1 Drug Class specifications within the Misuse of Drugs Act (1971) (HomeOffice, 2009)	7
Table 1.2 Penalties under the legalisation.gov.uk 2016 (Reuter and Pardo, 2017; UK-Government, 2016)	10
Table 1.3 Chemical structure of ephenidine, lefetamine, 2-MEP, 3-MEP and 4-MEP, 2-FEP, 3-FEP and 4-FEP.	25
Table 1.4 Analytical methods currently reported in the literature for the detection of New Psychoactive Substances and recreational drugs.	28
Table 1.5 Comparisons between LC-ED, LC-MS, and LC-UV for analysis of abused drugs.	35
Table 1.6 Analytical methods in the literature using high performance liquid chromatography-electrochemical detection	38
Table 2.1. The sources of the street samples utilised in this study.	42
Table 2.2 HPLC columns utilised in this project	43
Table 2.3. Mobile phases used in this study.	48
Table 2.4 Different pH of Mobile Phase 1	50
Table 2.5 Different pH of mobile phase 2	54
Table 2.6 Different pH of Mobile Phase 3	58
Table 2.7 Different pH of mobile phase 4	62
Table 2.8 Different pH of mobile phase 5	65
Table 3.1 Chemical structures of methamphetamine, PMA, and MDMA	68
Table 3.2 Analytical methods in the literature used to detect (±)-Paramethoxyamphetamine hydrochloride ((±)-PMA),(±)-3,4-methylenedioxymethamphetamine hydrochloride ((±)-MDMA).	71
Table 3.3. The anodic potential (80 µg mL ⁻¹) of (±)-MA, (±)-PMA and (±)-MDMA over the range + 1.1 to + 1.6 V ⁻¹ using mobile phase 1, column: an ACE 3 C ₁₈ column (150 mm × 4.6 mm i.d., particle size: 3 µm); at temperature = 22 °C, flow rate = 1.2 mL	

min ⁻¹ and pH = 3.2 using HPLC-AD detection in LC-FC-A and LC-FC-B systems.	75
Table 3.4 The linear velocity for (100 µg mL ⁻¹) of (±)-MA, (±)-PMA and (±)-MDMA over the range 0.9 to 1.2 mL min ⁻¹ using mobile phase 1, column: an ACE 3 C ₁₈ column (150 mm × 4.6 mm i.d., particle size: 3 µm); at temperature = 22 °C and pH = 3.2 by using HPLC-AD detection in LC-FC-A and LC-FC-B systems.	78
Table 3.5 Summary of the optimal conditions utilised for method validation in the analysis (±)-MA, (±)-PMA and (±)-MDMA by using LC-FC-A and LC-FC-B systems.	80
Table 3.6 Summary of HPLC-UV validation data for the quantification of (±)-MA, (±)-PMA and (±)-MDMA obtained on HPLC-UV with the LC-FC-A (impinging jet flow cell) or LC-FC-B (iCell flow cell) systems, using column (A) (Table 2.2); mobile phase 1(Section2.4); UV wavelength: 210 nm.	81
Table 3.7 Summary of HPLC-AD) validation data for quantification of (±)-MA, (±)-PMA and (±)-MDMA obtained on either the LC-FC-A (impinging jet flow cell) or LC-FC-B (iCell flow cell) systems using column (A) Table 2.2; mobile phase 2.	82
Table 3.8 Relative retention time (RRT) data of (±)-MA, (±)-PMA and (±)-MDMA using HPLC-UV detection in LC-FC-A and LC-FC-B systems with different temperatures used in the analysis.	93
Table 3.9 Relative retention time (RRT) of (±)-MA, (±)-PMA and (±)-MDMA using HPLC-UV detection in LC-FC-A and LC-FC-B systems with minor changes in the composition ratio of the mobile phase.	93
Table 3.10 The relative standard deviation (RSD %) of inter- and intra-day peak current values for (±)-MA, (±)-PMA and (±)-MDMA using HPLC-UV and HPLC-AD detection in both systems (LC-FC-A and LC-FC-B).	94
Table 3.11 Accuracy data expressed as the percentage recovery of a mixture of (±)-MA, (±)-PMA and (±)-MDMA by using HPLC-UV and HPLC-AD in both systems (LC-FC-A and LC-FC-B).	96

Table 3.12 Direct comparison between quantitative data obtained by HPLC-UV and amperometric detection (AD), using the LC-FC-A (impinging jet flow cell), or LC-FC-B (iCell channel flow cell) systems, for the analysis of the street samples.	98
Table 4.1 The chemical structures of (±)-mephedrone and (±)-4-MEC	101
Table 4.2 Analytical methods in the literature that have been used to detect (±)-mephedrone and (±)-4-MEC	102
Table 4.3 Representation of the anodic potential ($100\ \mu\text{g mL}^{-1}$) of (±)-caffeine, (±)-mephedrone and (±)-4-MEC over the range + 1 to + $1.5\ \text{V}$ using mobile phase 2, column : an ACE 3 C ₁₈ column (150 mm × 4.6 mm i.d., particle size: 3 μm); at temperature = 22 °C, flow rate = 0.8 mL min ⁻¹ and pH = 4.3 using HPLC-AD detection in LC-FC-A and LC-FC-B systems.	106
Table 4.4 Summary of the optimal conditions utilised for method validation of the analysis of (±)-caffeine, (±)-mephedrone and (±)-4-MEC using LC-FC-A and LC-FC-B systems.	108
Table 4.5 Summary of HPLC-UV (UV detection) validation data for the quantification of caffeine, (±)-mephedrone and (±)-4-MEC obtained on either the LC-FC-A (impinging jet flow cell) or LC-FC-B (iCell flow cell) systems, using column (A) (Table 2.2), mobile phase 2A (Section 2.4); UV wavelength: 264 nm.	110
Table 4.6 Summary of HPLC-AD (amperometric detection) validation data for quantification of caffeine, (±)-mephedrone and (±)-4-MEC obtained on either the LC-FC-A (impinging jet flow cell) or LC-FC-B (iCell flow cell) systems. Using column A (Table 2).2; mobile phase 2.	111
Table 4.7 The effect of minor changes of temperature on relative retention time (RRT) of (±)-caffeine, (±)-mephedrone and (±)-4-MEC using HPLC-UV detection in LC-FC-A systems (highlighted area is the standardised condition of this method).	119
Table 4.8 The effect of minor changes of organic composition of mobile phase 3 on Relative Retention Time (RRT) of (±)-caffeine, (±)-mephedrone and (±)-4-MEC using HPLC-UV	

detection in LC-FC-A systems (highlighted area is standardised condition of this method).	119
Table 4.9 The effect of minor changes of temperature on relative retention time (RRT) of (±)-caffeine, (±)-mephedrone and (±)-4-MEC using HPLC-UV detection in LC-FC-B systems (highlighted area is standardised condition of this method).	120
Table 4.10 The effect of minor changes in organic composition of mobile phase 3 on Relative Retention Time (RRT) of (±)-caffeine, (±)-mephedrone and (±)-4-MEC using HPLC-UV detection in LC-FC-B systems (highlighted area is standardised condition of this method).	120
Table 4.11 Relative standard deviations (RSD %) of inter- and intra-day precision for 400 µg mL ⁻¹ (±)-Caffeine, (±)-4-mephedrone and (±)-4-MEC using HPLC-UV and HPLC-AD in the LC-FC-A system.	121
Table 4.12 Accuracy data expressed as the percentage recovery of the mixture of (±)-caffeine, (±)-4-mephedrone and (±)-4-MEC using HPLC-UV and HPLC-AD detection in LC-FC-A and LC-FC-B systems.	123
Table 4.13 Direct comparison of LC-MS ^a and HPLC-UV data (obtained using either LC-FC-A (impinging jet flow cell) or LC-FC-B (iCell channel flow cell) systems) of purchased NRG-2 samples	124
Table 4.14 Direct comparison between quantitative data obtained by the HPLC-UV and HPLC-AD protocols for the analysis of the synthetic cathinones in a selection of purchased NRG-2 samples	127
Table 5.1 ¹ H, ¹³ C NMR spectral data and ¹ H- ¹³ C long-range correlations of (±)-mephedrone in d ₆ -DMSO. Chemical shifts (δ) in ppm; coupling constants (J) in Hz.	135
Table 5.2 ¹ H, ¹³ C NMR spectral data and ¹ H- ¹³ C long-range correlations of (±)-Mexedrone in d ₆ -DMSO. Chemical shifts (δ) in ppm; coupling constants (J) in Hz.	138
Table 5.3 The anodic potential of 300 µg mL ⁻¹ of (±)-mephedrone and (±)-Mexedrone over the range + 1.1 to + 1.5 v ⁻¹ using mobile phase 3, ACE 3 C ₁₈ column (150 mm x 4.6 mm i.d., particle	

size: 3 μm); temperature = 22 $^{\circ}\text{C}$, flow rate = 0.8 mL min^{-1} and pH = 3.5 using HPLC-AD in the LC-FC-A system.	145
Table 5.4 The linear velocity of 300 $\mu\text{g mL}^{-1}$ (\pm)-mephedrone and (\pm)-Mexedrone over the range 0.8 to + 1.2 mL min^{-1} using mobile phase 3, ACE 3 C_{18} column (150 mm x 4.6 mm i.d., particle size: 3 μm); at temperature = 22 $^{\circ}\text{C}$ and pH = 3.5 using HPLC-AD in the LC-FC-A system.	146
Table 5.5 The effect of pH of the mobile phase on the analysis of (\pm)-mephedrone and (\pm)-Mexedrone over the range 3.5 to 7 using mobile phase 3, ACE 3 C_{18} column (150 mm x 4.6 mm i.d., particle size: 3 μm); at temperature = 22 $^{\circ}\text{C}$ and flow rate = 0.8 mL min^{-1} using HPLC-AD in the LC-FC-A system.	147
Table 5.6 Summary of the optimal conditions used for method validation of (\pm)-mephedrone and (\pm)-mexedrone using the LC-FC-A system.	148
Table 5.7 Summary of HPLC-UV (UV detection) validation data for the quantification of (\pm)-mephedrone and (\pm)-Mexedrone using HPLC-UV in the LC-FC-A system, column A (Table 2.3 mobile phase 3; wavelength = 263 nm.	149
Table 5.8 Summary of HPLC-AD (amperometric detection) validation data for the quantification of (\pm)-mephedrone and (\pm)-mexedrone using HPLC-AD in the LC-FC-A system, column A, (Table 2.2), mobile phase 3; detector wavelength = 263 nm.	150
Table 5.9 The effect of minor changes of temperature on relative retention time (RRT) of analysis of 300 $\mu\text{g mL}^{-1}$ of (\pm)-mephedrone and (\pm)-mexedrone using HPLC-UV in the LC-FC-A system. (The highlighted area is a standardised condition for this study).	154
Table 5.10 The effect of a minor change in organic composition of mobile phase 3 on the relative retention time (RRT) of 300 $\mu\text{g mL}^{-1}$ of (\pm)-mephedrone and (\pm)-mexedrone using HPLC-UV in the LC-FC-A system. (The highlighted area is a standardised condition for this study).	155

Table 5.11 The relative standard deviation (RSD %) of inter- and intra-day precision for (±)-mephedrone and (±)-mexedrone by using HPLC-UV and HPLC-AD in the LC-FC-A system.	156
Table 5.12 Accuracy data expressed as the percentage recovery of a mixture of (±)-mephedrone and (±)-Mexedrone by using both HPLC-UV and HPLC-AD in the LC-FC-A system.	156
Table 5.13 Summary of the quantification analysis of street samples by using HPLC-UV and LC-FC-A systems.	157
Table 6.1 The anodic potentials for 100 µg mL ⁻¹ of (±)-2-MEP, (±)-3-MEP and (±)-4-MEP over the range 1.0 to + 1.5 V ⁻¹ using mobile phase 4, column: ACE 5 C ₁₈ AR column (150 mm × 4.6 mm i.d., particle size: 5 µm). Temperature = 50 °C, flow rate = 2 mL min ⁻¹ and pH = 7 using HPLC-AD detection in the LC-FC-A system.	164
Table 6.2 The linear velocity for 100 µg mL ⁻¹ of (±)-2-MEP, (±)-3-MEP and (±)-4-MEP over the range 0.9 to 1.2 ml min ⁻¹ using mobile phase 4, column: ACE 5 C ₁₈ AR column (150 mm × 4.6 mm i.d. particle size: 5 µm); at temperature = 50 °C, and pH = 7 using HPLC-AD detection in the LC-FC-A system.	164
Table 6.3 The effect of the pH of mobile phase on the analysis of 100 µg mL ⁻¹ of (±)-2-MEP, (±)-3-MEP and (±)-4-MEP over the range 3 to 7 ml min ⁻¹ using mobile phase 4, column: ACE 5 C ₁₈ AR column (150 mm × 4.6 mm i.d. particle size: 5 µm); temperature = 50 °C, potential = 1.2 EV ⁻¹ and flow rate 2 mL min ⁻¹ using HPLC-AD detection in the LC-FC-A system.	165
Table 6.4 Summary of the optimal conditions utilised in the analysis of (±)-4-FEP, (±)-2-FEP and (±)-3-FEP.	167
Table 6.5 Summary of HPLC-UV (UV detection) validation data for the quantification of (±)-4-MEP, (±)-2-MEP and (±)-3-MEP obtained in the LC-FC-A systems using column B, (Table 2.2); mobile phase: 4C (Section 2.4); UV wavelength: 279 nm.	168
Table 6.6 Summary of HPLC-AD (amperometric detection) validation data for the quantification of (±)-4-MEP, (±)-2-MEP and (±)-3-MEP obtained in the LC-FC-A (impinging jet flow cell) system	

using column B, (Table 2.2). Mobile phase: 4C (Section 2.4);
UV wavelength: 279 nm.

168

Table 6.7 The effect of minor changes of temperature on relative retention time (RRT) of the analysis of 300 $\mu\text{g mL}^{-1}$ of (\pm)-4-MEP, (\pm)-2-MEP and (\pm)-3-MEP using HPLC-UV in the LC-FC-A system, (the highlighted area is a standardised condition for this study).

174

Table 6.8 The effect of a minor change inorganic composition of the mobile phase 4 on the relative retention time (RRT) of 300 $\mu\text{g mL}^{-1}$ of (\pm)-4-MEP, (\pm)-2-MEP and (\pm)-3-MEP using HPLC-UV in the LC-FC-A system. The highlighted area is a standardised condition for this study.

174

Table 6.9 The relative standard deviation (RSD %) of inter- and intra-day measurements for (300 $\mu\text{g mL}^{-1}$) (\pm)-4-MEP, (\pm)-2-MEP and (\pm)-3-MEP using HPLC-UV detection and amperometric detection in the LC-FC-A system.

175

Table 6.10 Percentage recovery of (\pm)-4-MEP, (\pm)-2-MEP and (\pm)-3-MEP using both system HPLC-UV and LC-FC-A

176

Table 6.11 Direct comparison between quantitative data obtained by HPLC-UV and HPLC-AD (impinging jet flow cell) system, for the analysis 300 $\mu\text{g mL}^{-1}$ of the regioisomer of methoxyphenidine in a selection of purchased street samples

177

Table 6.12 The anodic potential of 300 $\mu\text{g mL}^{-1}$ (\pm)-4-FEP, (\pm)-2-FEP and (\pm)-3-FEP over the range + 0.0 to + 1.5 V at temperature = 50 $^{\circ}\text{C}$, flow rate = 1.5 mL min^{-1} and pH = 7 by using LC-FC-A

180

Table 6.13 the linear velocity of 300 $\mu\text{g mL}^{-1}$ of (\pm)-4-FEP, (\pm)-2-FEP and (\pm)-3-FEP over the range 0.5 to 1.5 mL min^{-1} at temperature = 50 $^{\circ}\text{C}$, potential = 1.2 V and pH = 7) by using LC-FC-A system.

180

Table 6.14 The effect of pH of mobile phase on analysis 100 $\mu\text{g mL}^{-1}$ of (\pm)-4-FEP, (\pm)-2-FEP and (\pm)-3-FEP over the range 3 to 7 at temperature = 50 $^{\circ}\text{C}$, potential = 1.2 V by using LC-FC-A system.

181

Table 6.15 Summary of the optimal conditions utilised in the analysis (±)-4-FEP, (±)-2-FEP and (±)-3-FEP	182
Table 6.16 Summary of HPLC-UV validation data for the quantification of regioisomers of fluoroephenidine obtained on the LC-FC-A (impinging jet flow cell) system, using column B, (Table 2.2) mobile phase 5; detector wavelength (UV): 270 nm.	183
Table 6.17 Summary of validation data for regioisomers of fluoroephenidine obtained on the LC-FC-A (impinging jet flow cell) system using column B, (Table 2.2) mobile phase 5, detector wavelength (UV): 270 nm.	184
Table 6.18 The effect of minor changes of temperature on relative retention time (RRT) of analysis of 300 µg mL ⁻¹ of (±)-4-FEP, (±)-2-FEP and (±)-3-FEP using HPLC-UV in the LC-FC-A system, (the highlighted area is a standardised condition for this study).	189
Table 6.19 The effect of a minor changes in organic composition of mobile phase 4 on the relative retention time (RRT) of 300 µg mL ⁻¹ of (±)-4-FEP, (±)-2-FEP and (±)-3-FEP using HPLC-UV in the LC-FC-A system, (the highlighted area is a standardised condition for this study).	190
Table 6.20 Relative standard deviation (RSD %) of inter- and intra-day peak values for (±)-4-FEP, (±)-2-FEP and (±)-3-FEP.	191
Table 6.21 Percentage recovery of (±)-4-FEP, (±)-2-FEP and (±)-3- FEP using both HPLC-UV and HPLC-AD in the LC-FC-A system.	192
Table 6.22 Direct comparison between quantitative data obtained by HPLC-UV and HPLC-AD (impinging jet flow cell) in LC-FC-A system, for the analysis of the regioisomers of fluoroephenidine in a selection of purchased street samples	193
Table 9.1 Results of linearity measurements for (±)-MA using HPLC-UV detection in the LC-FC-A system, column A (Table 2.2), Mobile phase 1, detector wavelength (UV): 210 nm.	219
Table 9.2 Results of linearity measurements for (±)-PMA using HPLC- UV detection in the LC-FC-A system, column A (Table 2.2), Mobile phase 1, detector wavelength (UV): 210 nm.	219

Table 9.3 Results of linearity measurements for (±)-MDMA using HPLC-UV detection in the LC-FC-A system, column A (Table 2.2), mobile phase 1, detector wavelength (UV): 210 nm.	219
Table 9.4 Results of linearity measurements for (±)-PMA by using HPLC-AD detection in the LC-FC-A system, column A (Table 2.2), mobile phase 1.	220
Table 9.5 Results of linearity measurements for (±)-MDMA using HPLC-AD detection in the LC-FC-A system, column A (Table 2.2), mobile phase 1.	220
Table 9.6 Results of linearity measurements for (±)-PMA using HPLC-AD detection in the LC-FC-B system, column (A) Table 2.2, mobile phase 1.	220
Table 9.7 Raw data of the inter- and intra-day peak values and relative standard deviations (RSD %) for (±)-MA, (±)-PMA and (±)-MDMA using HPLC-UV detection and amperometric detection in the LC-FC-A and LC-FC-B systems.	221
Table 9.8 Results of linearity measurements for (±)-caffeine using HPLC-UV in the LC-FC-A system, column A (Table 2.2), mobile phase 2, detector wavelength (UV): 264 nm.	222
Table 9.9 Results of linearity measurements for (±)-mephedrone using HPLC-UV in the LC-FC-A system, column A (Table 2.2), mobile phase 2, detector wavelength (UV): 264 nm.	222
Table 9.10 Results of linearity measurements for (±)-4-MEC using HPLC-UV in the LC-FC-A system, column A (Table 2.2), mobile phase 2 C, detector wavelengths (UV): 264 nm.	222
Table 9.11 Results of linearity measurements for (±)-caffeine using HPLC-AD in the LC-FC-A system, column A (Table 2.2), mobile phase 2, detector wavelength (UV): 264 nm.	223
Table 9.12 Results of linearity measurements for (±)-mephedrone using HPLC-AD in the LC-FC-A system, column A (Table 2.2), mobile phase 2, detector wavelength (UV): 264 nm.	223
Table 9.13 Results of linearity measurements for (±)-4-MEC using HPLC-AD in the LC-FC-A system, column A (Table 2.2), mobile phase 2, detector wavelength (UV): 264 nm.	223

Table 9.14 Results of linearity measurements for (±)-caffeine using HPLC-UV in the LC-FC-B system, column A (Table 2.2), mobile phase 2, detector wavelength (UV): 264 nm.	224
Table 9.15 Results of linearity measurements for (±)-mephedrone using HPLC-UV in the LC-FC-B system, column A (Table 2.2), mobile phase 2, detector wavelength (UV): 264 nm.	224
Table 9.16 Results of linearity measurements for (±)-4-MEC by using HPLC-UV in the LC-FC-B system, column A (Table 2.2), mobile phase 2, detector wavelength (UV): 264 nm.	224
Table 9.17 Results of linearity measurements for (±)-mephedrone using HPLC-AD in the LC-FC-B system, column A (Table 2.2), mobile phase 2, detector wavelength (UV): 264 nm.	225
Table 9.18 Results of linearity measurements for caffeine using HPLC-AD in the LC-FC-B system, column A (Table 2.2), mobile phase 2, detector wavelength (UV): 264 nm.	225
Table 9.19 Results of linearity measurements for (±)-4-MEC using HPLC-AD in the LC-FC-B system, column A (Table 2.2), mobile phase 2, detector wavelength (UV): 264 nm.	225
Table 9.20 Raw data of inter- and intra-day peak area values and relative standard deviations (RSD %) for (±)-caffeine, (±)-mephedrone and (±)-4-MEC using HPLC-UV detection and amperometric detection in the LC-FC-A system.	226
Table 9.21 Raw data of the inter- and intra-day peak area values and relative standard deviations (RSD %) of for (±)-caffeine, (±)-mephedrone and (±)-4-MEC using HPLC-UV detection and amperometric detection in the LC-FC-B system.	227
Table 9.22 Results of linearity measurements for (±)-mephedrone using HPLC-UV in the LC-FC-A system, column A (Table 2.2), mobile phase 3, detector wavelength (UV): 263 nm.	228
Table 9.23 Results of linearity measurements for (±)-mexedrone using HPLC-UV in the LC-FC-A system, column A (Table 2.2), mobile phase 3, detector wavelength (UV): 263 nm.	228
Table 9.24 Results of linearity measurements for (±)-mephedrone using HPLC-AD in the LC-FC-A system, column A (Table 2.2), mobile phase 3, detector wavelength (UV): 263 nm.	228

Table 9.25 Results of linearity measurements for (±)-mexedrone using HPLC-AD in the LC-FC-A system, column A (Table 2.2), mobile phase 3, detector wavelength (UV): 263 nm.	229
Table 9.26 Raw data of the inter- and intra-day peak values and relative standard deviations (RSD %) of for (±)-mephedrone, and (±)-mexedrone using HPLC-UV detection and amperometric detection in the LC-FC-A system.	230
Table 9.27 Results of linearity measurements for (±)-4-MEP using HPLC-UV in the LC-FC-A system, column B (Table 2.2), mobile phase 4, detector wavelength (UV): 279 nm.	231
Table 9.28 Results of linearity measurements for (±)-2-MEP using HPLC-UV in the LC-FC-A system, column B (Table 2.2), mobile phase 4, detector wavelength (UV): 279 nm.	231
Table 9.29 Results of linearity measurements for (±)-3-MEP using HPLC-UV in the LC-FC-A system, column B (Table 2.2), mobile phase 4, detector wavelength (UV): 279 nm.	231
Table 9.30 Results of linearity measurements for (±)-4-MEP using HPLC-UV in the LC-FC-A system, column B (Table 2.2), mobile phase 4, detector wavelength (UV): 279 nm.	232
Table 9.31 Results of linearity measurements for (±)-2-MEP using HPLC-AD in the LC-FC-A system, column B (Table 2.2), mobile phase 4, amperometric detector	232
Table 9.32 Results of linearity measurements for (±)-3-MEP using HPLC-AD in the LC-FC-A system, column B (Table 2.2), mobile phase 4, amperometric detector	232
Table 9.33 Results of linearity measurements for (±)-4-FEP using HPLC-UV in the LC-FC-A system, column B (Table 2.2), mobile phase 5; detector wavelength (UV): 270 nm.	233
Table 9.34 Results of linearity measurements for (±)-2-FEP using HPLC-UV in the LC-FC-A system, column B (Table 2.2), mobile phase 5, detector wavelength (UV): 270 nm.	233
Table 9.35 Results of linearity measurements for (±)-3-FEP using HPLC-UV in the LC-FC-A system, column B, (Table 2.2), mobile phase 5, detector wavelength (UV): 270 nm.	233

Table 9.36 Results of linearity measurements for (±)-4-FEP using HPLC-AD in LC-FC-A system, column B (Table 2.2), mobile phase 5, amperometric detector	234
Table 9.37 Results of linearity measurements for (±)-2-FEP using HPLC-AD in the LC-FC-A system, column B (Table 2.2), mobile phase 5, amperometric detector	234
Table 9.38 Results of linearity measurements for (±)-3-FEP using HPLC-AD in the LC-FC-A system, column B (Table 2.2), mobile phase 5, amperometric detector	234
Table 9.39 Raw data of inter- and intra-day peak area values and relative standard deviations (RSD %) for (±)-4-MEP, (±)-2-MEP and (±)-3-MEP by using HPLC-UV detection and amperometric detection in the LC-FC-A system.	235
Table 9.40 Raw data of the inter and intra-day peak values and relative standard deviations (RSD %) for (±)-4-FEP, (±)-2-FEP and (±)-3-FEP using HPLC-UV detection and amperometric detection in the LC-FC-A system.	236

List of figures

- Figure 1.1** Number of new psychoactive substances formally notified for the first time in Europe (dots) and the total number of new psychoactive substances monitored by the EMCDDA, 2005–16 (bars) (reproduced with permission from reference (EMCDDA, 2016). 4
- Figure 1.2** Number and categories of new psychoactive substances formally notified for the first time in Europe, 2005–16 (reproduced with permission from reference (EMCDDA, 2016)). 5
- Figure 1.3** Structures of representative new/novel psychoactive Substances (stimulants and empathogens). Chemically, the substances shown include phenethylamine: (a), amphetamine (b), (±)-methamphetamine, (c), (±)-MDMA (d), and (±)-PMA (e). 12
- Figure 1.4** The relationship between the cathinone (a) and amphetamine (b). 17
- Figure 1.5** The chemical structure of cathinone (a), (±)-mephedrone (b), (±)-4-MEC (c), and mexedrone (d). 18
- Figure 1.6** High Performance Liquid Chromatography diagram 30
- Figure 1.7** The cyclic voltammetry for cathinone derivatives (A) (Smith et al., 2014a) and cyclic voltammetry to differentiate between MDMA and PMA (B) (Cumba et al., 2016). 33
- Figure 2.1** (a) Impinging jet flow cell (LC-FC-A; closed). (b) The impinging jet flow cell (LC-FC-A; open). (c) iCell channel flow cell (LC-FC-B; closed). (d) iCell channel flow cell (LC-FC-B; open). 44
- Figure 2.2** Flow diagram of the High performance liquid chromatography-UV-amperometric detection (HPLC-AD) systems (LC-FC-A and LC-FC-B). 46
- Figure 3.1** Chromatogram of a solution containing (±)-MA, (±)-PMA and (±)-MDMA obtained on a HPLC-UV system (UV detection) using an ACE 3 C₁₈ column (150 mm × 4.6 mm i.d. particle

size: 3 μm); flow-rate: 1.2 mL min^{-1} ; mobile phase 1; detector wavelength (UV): 210 nm.	73
Figure 3.2 Mechanism for the electrochemical oxidation of (\pm)-MDMA (Garrido et al., 2010)	76
Figure 3.3 Electrochemical oxidation of aliphatic amines, E is the electrode surface (Adenier et al., 2004).	77
Figure 3.4 Amperogram of a solution containing (\pm)-MA, (\pm)-PMA (a) and (\pm)-MDMA (b) obtained on the LC-FC-A system (amperometric detection) using an ACE 3 C ₁₈ column (150 mm \times 4.6 mm i.d., particle size: 3 μm); flow-rate: 1.2 mL min^{-1} ; mobile phase 1.	79
Figure 3.5 Amperogram of a solution containing (\pm)-MA, (\pm)-PMA (a) and (\pm)-MDMA (b) obtained on the LC-FC-B system (amperometric detection) using an ACE 3 C ₁₈ column (150 mm \times 4.6 mm i.d., particle size: 3 μm); flow-rate: 1.2 mL min^{-1} ; mobile phase 1.	79
Figure 3.6 The linearity of (\pm)-MA (circles), (\pm)-PMA (squares) and (\pm)-MDMA (triangles) by using a) HPLC-UV of LC-FC-A and LC-FC-B systems. b) HPLC-AD detection of LC-FC-A system. c) HPLC-AD detection of LC-FC-B system.	88
Figure 4.1 Representative chromatogram and amperogram of a solution containing (\pm)-caffeine, (\pm)-4-mephedrone and (\pm)-4-MEC with mobile phase 2 obtained using: (a) HPLC-UV (UV detection) in LC-FC-A system with flow rate: 0.8 mL min^{-1} . (b) HPLC-AD (amperometric detection) in the LC-FC-A system (c) HPLC-UV (UV detection) in the LC-FC-B system with flow rate: 1 mL min^{-1} . (d) HPLC-AD (amperometric detection) in the LC-FC-B system. The t_0 (for both systems) was determined from the retention time of a solution of uracil (10 $\mu\text{g mL}^{-1}$). The peak (S) is a system peak associated with the sample injection.	105
Figure 4.2 The linearity of (\pm)-caffeine (triangles), (\pm)-mephedrone (squares) and (\pm)-4-MEC (circles) by using a) HPLC-UV in the LC-FC-A system. b) HPLC-UV detection in the LC-FC-B	

system. c) HPLC-AD detection in the LC-FC-A system. d) HPLC-AD detection in the LC-FC-B system.	115
Figure 5.1 Chemical structures of a- (±)-mephedrone.HCl and b- (±)- mexedrone.HCl.	131
Figure 5.2 ^1H NMR spectrum ($\text{d}_6\text{-DMSO}$, $60\text{ }^\circ\text{C}$) of (±)-mephedrone.	134
Figure 5.3 Chemical structure of (±)-mephedrone.HCl	135
Figure 5.4 ^{13}C NMR spectrum ($\text{d}_6\text{-DMSO}$, $60\text{ }^\circ\text{C}$) of (±)-mephedrone.	135
Figure 5.5 Determination of ^1H NMR spectrum ($\text{d}_6\text{-DMSO}$, $60\text{ }^\circ\text{C}$) of (±)-mexedrone.	137
Figure 5.6 Chemical structure of (±)-mexedrone.HCl	138
Figure 5.7 ^{13}C NMR spectrum ($\text{d}_6\text{-DMSO}$, $60\text{ }^\circ\text{C}$) of (±)-mexedrone.	138
Figure 5.8 Gas chromatograms of a mixture containing $100\text{ }\mu\text{g mL}^{-1}$ of (a) (±)-mephedrone (b) (±)-Mexedrone and (c) eicosane (internal standard).	140
Figure 5.9 The proposed fragmentation of (±)-mephedrone and (±)- mexedrone, under EI-MS conditions.	141
Figure 5.10 Mass spectra of $100\text{ }\mu\text{g mL}^{-1}$ of (±)-mephedrone.	142
Figure 5.11 Mass spectra of $100\text{ }\mu\text{g mL}^{-1}$ of (±)-mexedrone.	142
Figure 5.12 The chromatogram of a solution containing uracil (a) $200\text{ }\mu\text{g mL}^{-1}$, (±)-mephedrone (b), -and (±)-Mexedrone (c) obtained on a HPLC-UV system (UV detection) using an ACE 3 C_{18} column ($150\text{ mm} \times 4.6\text{ mm i.d.}$, particle size: $3\text{ }\mu\text{m}$); flow-rate: 0.8 mL min^{-1} ; mobile phase 3; detector wavelength (UV): 264 nm .	144
Figure 5.13 Amperogram of a solution containing $200\text{ }\mu\text{g mL}^{-1}$ (±)- mephedrone (a), and (±)-Mexedrone (b) obtained on the LC- FC-A system (amperometric detection) using an ACE 3 C_{18} column ($150\text{ mm} \times 4.6\text{ mm i.d.}$, particle size: $3\text{ }\mu\text{m}$); flow-rate: 0.8 mL min^{-1} ; mobile phase 3.	147
Figure 5.14 The linearity of (±)-mephedrone (squares) and (±)- mexedrone (triangles) by using a) HPLC-UV in the LC-FC-A system b) HPLC-AD in the LC-FC-A system.	152
Figure 6.1 The chromatogram of a solution containing $300\text{ }\mu\text{g mL}^{-1}$ of (±)-4-MEP (a), (±)-2-MEP (b) and (±)-3-MEP (c) obtained using HPLC-UV in the LC-FC-A system using an ACE 5 C_{18}AR	

column (150 mm × 4.6 mm i.d., particle size: 5 µm); mobile phase 4 detector wavelength (UV): 279 nm. 163

Figure 6.2 Amperogram of a solution containing 300 µg mL⁻¹ of (±)-4-MEP (a), (±)-2-MEP (b) and (±)-3-MEP (c) obtained on the LC-FC-A system (amperometric detection) using an ACE 5 C₁₈AR column (150 mm × 4.6 mm i.d., particle size: 5 µm); flow-rate: 2 mL min⁻¹; mobile phase 4. 166

Figure 6.3 The linearity of (±)-4-MEP (triangles), (±)-2-MEP (squares) and (±)-3-MEP (circles) using the LC-FC-A system a) HPLC-UV (UV detection), b) HPLC-AD (amperometric detection). 171

Figure 6.4 The chromatogram for 200 µg mL⁻¹ of (±)-4-FEP (a), (±)-2-FEP (b) and (±)-3-FEP (c) obtained by using HPLC-UV detection in LC-FC-A system using an ACE 5 C₁₈AR column (150 mm × 4.6 mm i.d., particle size: 5 µm); Mobile phase: mobile phase 4; UV wavelengths 279 nm, the peak (S) is a system peaks associated with the sample. 179

Figure 6.5 Amperogram of 200 µg mL⁻¹ (±)-4-FEP (a), (±)-2-FEP (b) and (±)-3-FEP (c) obtained on the HPLC-AD system using an ACE 5 C₁₈AR column (150 mm × 4.6 mm i.d., particle size: 5 µm); mobile phase 5; detector wavelengths (UV): 279 nm. 181

Figure 6.6 The linearity of (±)-4-FEP (circles), (±)-2-FEP (squares) and (±)-3-FEP (triangles) by using a) HPLC-UV and b) HPLC-AD in LC-FC-A system. 187

List of equations

Equation 3.1 Number of Plates	83
Equation 3.2 Capacity factor (K)	83
Equation 3.3 Resolution (R_s)	84
Equation 3.4 Selectivity (separation) factor (α)	85
Equation 3.5 Limit of detection	89
Equation 3.6 Limit of quantification	90

Published work (from this thesis)

- 1- Zuway, K. Y., Smith, J. P., Foster, C. W., Kapur, N., Banks, C. E. and Sutcliffe, O. B. (2015) 'Detection and quantification of new psychoactive substances (NPSs) within the evolved "legal high" product, NRG-2, using high performance liquid chromatography-amperometric detection (HPLC-AD).' *Analyst*, 140(18), Sep 21, pp. 6283-6294.
- 2- Cumba, L. R., Smith, J. P., Zuway, K. Y., Sutcliffe, O. B., do Carmo, D. R. and Banks, C. E. (2016) 'Forensic electrochemistry: simultaneous voltammetric detection of MDMA and its fatal counterpart "Dr Death" (PMA).' *Analytical Methods*, 8(1) pp. 142-152.

Reprints of these two articles are provided (for reference) in the appendix.

Abbreviation and Acronyms

ACMD	Advisory Council on the Misuse of Drugs
AD	Amperometric Detection
Ag/AgCl	Silver/Silver Chloride
As	Asymmetric
BBB	Blood-Brain Barrier
BRC	Buy Research Chemical- Fine Chemicals
CAHID	Centre for Anatomy and Human Identification
Cm	Centimetre
CNS	Central Nervous System
CV	Cyclic Voltammetry
d6-DMSO	Dimethyl sulfoxide-d6
DA	Dopamine
DAD	Diode-Array Detector
DAT	Dopamine transporter
DEPT	Distortion less Enhancement by Polarisation Transfer
DME	Dropping Mercury Electrode
E	Potential
E V	Electron Volt
EI	Electron Ionisation
EL-MS	Electron Ionisation- Mass Spectroscopy
EMCDDA	European Monitoring Centre for Drugs and Drug Addiction
EPE	Ephedrine
EU	Europe
EWS	Early Warning System
FTIR	Fourier-Transform Infrared Spectroscopy
GC	Gas Chromatography
GC-MS	Gas Chromatography-Mass Spectrometry
GHB	Gamma HydroxyButyrate
GMP	Great Manchester Police
gov.	Government
GSPE	Graphite Screen Printed Electrode
H	High
HCl	Hydrochloride

HMBC	Heteronuclear Multiple Bond Correlation
HMQC	Heteronuclear Multiple-Quantum Correlation
HPLC	High Performance Liquid Chromatography
HPLC-AD	High Performance Liquid Chromatography- Amperometric Detection
HPLC-DAD	High Performance Liquid Chromatography- Diode-Array Detector
HPLC-ED	High Performance Liquid Chromatography- Electrochemical Detector
HPLC-FL	High Performance Liquid Chromatography-Fluorescence Detection
HPLC-MS	High Performance Liquid Chromatography- Mass Spectroscopy
HPLC-UV	High Performance Liquid Chromatography-Ultraviolet Spectroscopy
HX	HCl/ HBr
ICH	International Council for Harmonisation
IR	Infrared Spectroscopy
k'	Capacity Factor
KCl	Potassium Chloride
LC-FC-A	Liquid Chromatography-Flow Cell-A
LC-FC-B	Liquid Chromatography-Flow Cell-B
LC-MS	Liquid Chromatography-Mass Spectroscopy
LC-MS/MS	Liquid Chromatography-Mass Spectroscopy/ Mass Spectroscopy
LC-UV	Liquid Chromatography-Ultraviolet
LOD	Limit of Detection
LOQ	Limit of Quantification
LSD	Lysergide
λ_{max}	Maximum Wavelength
m	Metre
M	Molar
mM	Millimolar
m/z	Mass (m) to Charge (z) Ratio
MA	Methamphetamine
MAO	Monoamine Oxidase
mAU	Milliabsorption Units

MDA	3,4-Methylenedioxyamphetamine
MDEA	3,4-Methylenedioxyethamphetamine
MDMA	3,4-Methylenedioxymethamphetamine
MDPBP	3,4-Methylenedioxy- α -pyrrolidinobutyrophenone
MDPV	3,4-Methylenedioxypropylone
MEC.HBr	(\pm)-4-Methyl-N-ethylcathinone hydrobromide
MECD	Multichannel electrochemical detection
MEX	Mexedrone
mg mL ⁻¹	Milligram per Millilitre
min ⁻¹	Per Minute
mM	Millimolar
MPPP	4-Methyl- α -pyrrolidinopropiophenone
MSD	Mass Selective Detector
μ mol L ⁻¹	Micromoles per Litre
μ A	Microampere
μ g mL ⁻¹	Microgram per Millilitre
μ L	Microlitre
μ L	Microlitre
μ M	Micro molar
N	Number of plates
n.d.	Not Detected
NE	Norepinephrine
NEDPA	N-Ethyl-1, 2-Diphenyl Ethylamine
NET	Norepinephrine Transporter
ng	Nanogram
ng mL ⁻¹	Nanogram per Millilitre
nm	Nanometre
NMDA	N-methyl-D-aspartate receptor Antagonist
NMR	Nuclear Magnetic Resonance Spectroscopy
NPSs	New Psychoactive Substances
NRG	Suspected Second-generation Cathinone Product
PCP	Phencyclidine
pH	Potential of Hydrogen
PMA	Paramethoxyamphetamine
ppm	Parts per million

PS Act	Psychoactive Substances Act
PSTrace	Palmsens (Palm Instruments BV, The Netherlands)
PTFE	Polytetrafluoroethylene
R ²	Coefficient of determination
RRT	Relative Retention Time
R _s	Resolution
RSD	Relative Standard Deviation
SD	Standard Deviation
SERT	Serotonin Transporter
SPEs	Screen Printed Electrodes
t ₀	Dead Volume or Time
THC	Thin Layer Chromatography
THC-COOH	11-Nor-9-carboxy-Δ ⁹ -tetrahydrocannabinol
t _R	Retention Time
UK	United Kingdom
UNODC	United Nations Office on Drugs and Crime
UV	Ultraviolet
V	Volt
v/v	Volume for Volume
Ver	Version
w/w	Weight for Weight
WHO	World Health Organization
Δ	Delta
(±)-4MMC	(±)-Mephedrone
¹³ C NMR	Carbon 13 Nuclear Magnetic Resonance Spectroscopy
¹ H NMR	Proton Nuclear Magnetic Resonance Spectroscopy
2-FEP	2-Fluoroephedrine
2-MEP	2-Methoxyephedrine
3-FEP	3-Fluoroephedrine
3-MEP	3-Methoxyephedrine
4-FEP	4-Fluoroephedrine
4-MBC	4'-methyl-N-benzylcathinone
4-MEP	4-Methoxyephedrine
5-HT	Serotonin

Acknowledgments

First and foremost, I would like to thank Almighty God for help in blessing me and supporting me to complete this work. I would like to express my sincere gratitude to my supervisors, Dr Oliver Sutcliffe and Professor Craig Banks, for their continuous support in my PhD study and related research, for their patience, motivation, and immense knowledge. Their guidance helped me in all the time of study. Special thanks to Dr Sutcliffe who looked after me through the writing of this thesis. I could not have imagined how I could have completed my PhD study without his encouragement and advice. My sincere thanks also go to Dr Saeed Gulzar, Mr Bill Ellison, Mr Lee Harman and Dr Chris Foster who provided me with an opportunity to learn something new, and who gave access to the laboratory and research facilities.

Last, but not the least; I would like to thank my family: my father for encouraging and supporting me. My heartfelt regard goes to my mother who prayed for me every time; I would not have been able to complete much of what I have done, and become who I am, without my mother. My most profound gratitude towards my wife for her eternal support and understanding of my goals and aspirations. Her infallible love and support has always been my strength. I am thankful to my son Abdelmalike and my daughter Malak for giving me happiness during my studies. Their patience and sacrifice will remain my inspiration throughout my life. I feel a deep sense of gratitude to my brothers for supporting my life and me spiritually throughout the PhD in general. Special thanks to my friends who supported me.

1 Chapter 1: Introduction and literature review

1.1 New psychoactive substances.

New psychoactive substances (NPS) are defined by the Advisory Council on the Misuse of Drugs (ACMD) as: *“Psychoactive drugs which are not prohibited by the United Nations Single Convention on Narcotic Drugs or by the Misuse of Drugs Act (1971), and which people in the UK are seeking for intoxicant use”* (ACMD, 2011).

The designer drugs, legal highs, herbal highs and bath salts in the market have been termed ‘new psychoactive substances’ (NPS) (Addiction, 2012; Wilkins, 2014), and this preferred term was adopted by the European Community in 2005 (King and Kicman, 2011; Council Decision, 2005; EMCDDA, 2007) (King and Kicman, 2011). The new psychoactive substances (designer or synthetic drugs) include legal highs and club drugs (Dunne et al., 2015); the term ‘designer drugs’ was created in 1984 and in recent times these have been described informally as ‘legal highs’ (King and Kicman, 2011). Designer drugs are defined as ‘analogues, or chemical cousins, of controlled substances that are designed to produce effects similar to the controlled substances they mimic’ (King and Kicman, 2011). These substances have the pharmacological effect to cause euphoria, central nervous system stimulation, and/or hallucination (Dunne et al., 2015). These effects are based on the chemical formula of opioids, mescaline, and cannabis, and they are synthesised in the laboratory under lax conditions for no defined medical purposes.

NPSs are potentially dangerous for the user due to the variation in the composition from batch to batch. Furthermore, laboratories are continually changing the chemical structure of the substances to avoid legislative control; therefore, the

user often does not know exactly what they are taking. These substances are produced by altering the molecular structure of controlled psychoactive drugs. The term 'designer drugs' includes all substances which are used recreationally and not controlled by the Misuse of Drugs Act (1971) (UK-Government, 1971) , and not licensed for legal use and not regulated under the Medicines Act (1986) (Dunne et al., 2015).

NPS fall outside legislative controls and include a diverse range of chemical classes including (but not limited to): synthetic cathinones, phenethylamines, piperazines, aminoindanes and synthetic cannabinoids, their chemistry or process of synthesis have been slightly modified to produce effects similar to known illicit substances (UNODC, 2013). These substances are not entirely new phenomena and many were synthesized and patented in the early 1970s or even earlier, but only recently they have been controlled under the Psychoactive Substances Act (PSA) 2016 (UK-Government, 2016). The descriptor 'legal high' is a media-coined term which is considered by many professionals to be misleading as it can lead to the misconception that these substances which, though legal to possess prior to the PSA 2016, were indeed safe to use – which has been shown in some cases not to be true (UK-Government, 1971).

Some NPSs have been identified as having some negative side effects on health, but, because they are relatively new materials, there is very little research undertaken on the short and long-term health risks of prolonged use (Addiction, 2012). Many of these substances are created by subtly changing the chemical structure of the parent psychotropic substance (for example a cathinone or amphetamine) that is already controlled, to produce a similar pharmacological response (i.e. CNS stimulatory effect) but which fall outside the definitions of the

controlling legislation. The most well-known example of a synthetic cathinone is (±)-mephedrone hydrochloride (±)-mephedrone (Zuba, 2012) (Section 1.5.2). Herbal dietary supplements, herbal highs, and party pills, which contain products from natural sources, are also considered NPSs in many regions. Pre 2016 these products could be legally possessed and purchased online or through high street retail stores known as 'head shops'. According to a UK-based internet market survey at the time, their low cost, ease of supply and the relatively high quality of the active ingredients made these products extremely attractive to recreational drug users (Arunotayanun and Gibbons, 2012; Gibbons and Zloh, 2010).

1.2 Emergence/prevalence of NPS

In recent years, the world has seen the emergence of new drugs (NPS) that have similar effects to drugs that are internationally controlled. These drugs are represented worldwide as an underestimated health risk (Zanda and Fattore, 2017; Dargan and Wood, 2013). NPS are a global issue and the widespread trade of such substances is drawing international concern.

The brand names of NPSs are used to describe them such as Benzo Fury, NRG-1 and NRG-2. These names do not always pertain to what is the actual psychoactive substance present, for example, (±)-mephedrone was sold as naphyrone (or NRG-1) in the UK after it was banned (Brandt et al., 2010). In addition, another study reported 70 % of NRG-1 and NRG-2 analysed were found to be a mixture of substituted cathinones (Smith et al., 2015). The typical marketing for NPSs is as 'not for human consumption' or labelled as plant food or bath salts in order to bypass legislative controls pre-PSA 2016 (Johnson et al., 2013; Smith et al., 2015). The identification of NPSs are a novel investigation field (Smith et al., 2015). The customers purchasing such products have

no assurance that these products contain what they are advertised as containing (Smith et al., 2015).

1.3 Prevalence of NPSs

In 2009, the abuse of NPSs had been reported to have increased and has continued to be an ever-growing market (EMCDDA, 2013), emerging at an extraordinary rate of online vendors in the UK reflected in the online marketplace increasing by more than 300% between 2010 and 2011 (EMCDDA, 2011; Smith et al., 2015). NPSs notification increased between 2012-2015 as shown in figure 1.1. and were reported for the first time to the EU early warning system (EWS) run by the European Monitoring Center for Drugs and Drug Addiction EMCDDA (EMCDDA, 2015).

In addition, sixty-six NPSs were notified during for the first time in 2016 in Europe. Recently, the total number of NPSs monitored by the EMCDDA increased to more than 620, more than twice the total number of substances currently controlled under the United Nations drug conventions (Figure 1.1) (EMCDDA, 2016).

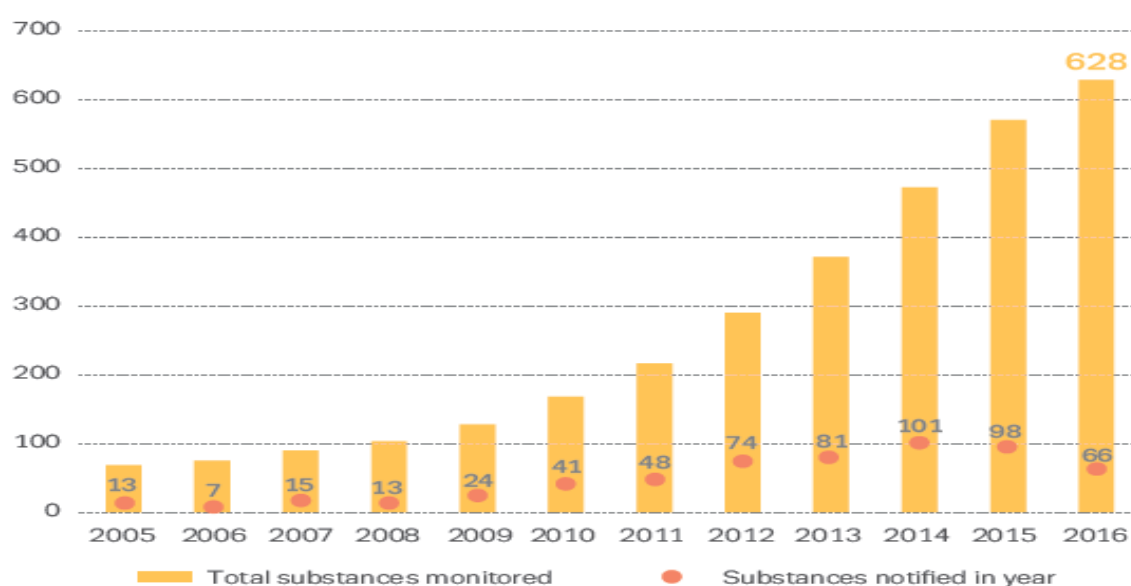


Figure 1.1 Number of new psychoactive substances formally notified for the first time in Europe (dots) and the total number of new psychoactive substances monitored by the EMCDDA, 2005–16 (bars) (reproduced with permission from reference (EMCDDA, 2016).

The two most significant categories of new psychoactive substances identified by the EMCDDA through the EU Early Warning System in 2016 were the synthetic cathinones (14) and synthetic cannabinoids (11). Moreover, nine opioids, six phenethylamines, six arylcyclohexylamines, six benzodiazepines, three arylalkylamines, one piperidine/pyrrolidine and ten other substances that do not conform to any of the previous groups were identified for the first time (Figure 1.2) (EMCDDA, 2016).

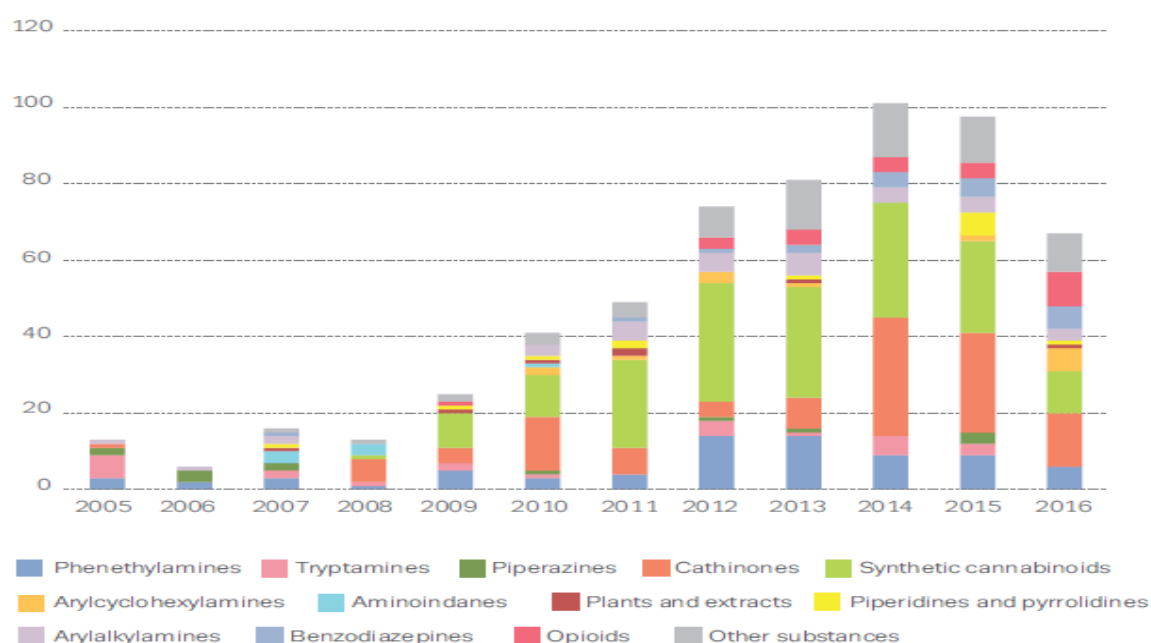


Figure 1.2 Number and categories of new psychoactive substances formally notified for the first time in Europe, 2005–16 (reproduced with permission from reference (EMCDDA, 2016)).

The internet is the main method of supply of such drugs in the UK. Synthetic cathinones, piperazines and synthetic cannabinoids are being used as substances of abuse. The most popular abused recreational drugs such as ‘ecstasy’, amphetamine, cocaine, and LSD are taken to make the user awake, energetic, feel euphoric and feel intoxicated. Some of these substances can cause relaxation and create a sense of wellbeing (empathogens), and some stimulants lead to euphoria.

However, these compounds were banned in the UK under the revision of Misuse of Drugs Act (1971) (UK-Government, 1971).

1.4 Misuse of Drugs Act (1971)

The United Kingdom has legalisation to control the drugs of abuse and this was called the Misuse of Drugs Act (1971) (UK-Government, 1971). (UK-Government, 2016; Reuter and Pardo, 2017). In 1971, the United Kingdom government established the Misuse of Drugs Act for the control of substances, which were believed to pose a significant risk to society and the individual. This legislation was in alignment with the United Kingdom's obligations under the United Nation's Conventions on Narcotic Drugs (1961) (UNODC, 1961; UNODC, 2013) and Psychotropic Substances (1971) (UK-Government, 1971; UNODC, 2013) and supported the development of the 1988 international agreement to limit the illicit traffic in narcotic drugs and psychotropic substances (Neue, 1997).

The Misuse of Drugs Act (1971) refers to what cannot be done with a controlled substance and the level of control relates to a drugs potential for harm. Drug addiction is a state of physical or psychological dependence on a drug (Dragan, 2003). All substances, which are capable of producing a psychoactive effect in a person who consumes it, and which are not controlled under the Misuse of Drugs Act (1971)(UK-Government, 1971), are controlled under the Psychoactive Substances Act 2016

The UK Government has had to evolve drug control legislation to allow the regulation of NPS. In 2014, the UK government convened an NPS expert panel looking for a range of approaches and as a result, on the 26th May 2016, the

Psychoactive Substances Act (2016) came into force in the UK (UK-Government, 2016).

Under the Misuse of Drugs Act (1971), it is an offence to produce, possess or possess with intent to supply a controlled drug (Phillips et al., 1997). The Misuse of Drugs Act (1971) divided drugs into three different classes: Class A, B, and C. Class A, considered most dangerous substances, while class C substances are considered the least dangerous (Table 1.1) (Gibbons and Zloh, 2010; Brandt et al., 2010; UK-Government, 1971).

Table 1.1 Drug Class specifications within the Misuse of Drugs Act (1971) (HomeOffice, 2009)

Class	Class A	Class B	Class C
Example of drugs	<ul style="list-style-type: none"> - 'ecstasy' - LSD - heroin - cocaine - crack - magic mushrooms - amphetamines (if prepared for injection) 	<ul style="list-style-type: none"> - amphetamines - cannabis - methylphenidate (Ritalin) - Pholcodine. - synthetic cathinones - synthetic cannabinoids 	<ul style="list-style-type: none"> - tranquilisers - some painkillers - gamma hydroxybutyrate (GHB) - ketamine
Possession	Up to seven years in prison or an unlimited fine or both.	Up to five years in prison or an unlimited fine or both	Up to two years in prison or an unlimited fine or both.
Supplying	Up to life in prison or an unlimited fine or both.	Up to 14 years in prison or an unlimited fine or both	Up to 14 years in prison or an unlimited fine or both.

Additionally, there are regulations (Misuse of Drugs Regulations (2001)) (UK-Government, 2001) which are concerned with the supply, import, and export of the controlled drugs. Misuse of Drugs Regulations (2001) essentially states what can be done with a controlled substance and has five schedules for controlled drugs, which are based on their medical use. Substances in the first schedule, such as (±)-mephedrone, are considered to have no medical use, with the following schedules

relating to materials which have a therapeutic use but remain controlled due to their risk of abuse (Neue, 2010). The schedules, as specified by the Misuse of Drugs Regulations (2001)(UK-Government, 2001), are as follows:

Schedule 1 Controlled Drugs: It includes the most stringently controlled drugs. These drugs are not permitted for medical use and can be supplied, possessed or administered only by a person authorised by a licence issued by the Home Office. The licences are approved for research or particular purposes. Schedule 1 Controlled Drugs are subject to the Misuse of Drugs (Safe Custody) Regulations (1973) to safe custody requirements. Drugs in Schedule 1 must be stored in a locked cabinet or approved safe, which can be opened only by the person in lawful possession of the controlled drugs, or a person authorised by him/her. These drugs are not allowed to be prescribed by doctors or dispensed by pharmacists; this is the closest that British law comes to total prohibition. Examples of drugs listed in Schedule 1 include cannabis and cannabis resin, ecstasy (MDMA) and lysergide (LSD).

Schedule 2 Controlled Drugs: Schedule 2 controlled drugs include heroin, cocaine, morphine, pethidine, quinalbarbitone, and amphetamine. It is illegal to possess drugs in Schedule 2 without a prescription or other authority. For production, import, export or supply substances in this Schedule require a Home Office licence.

Schedule 3 Controlled Drugs: Schedule 3 drugs include the majority of barbiturates (excluding quinalbarbitone), temazepam and buprenorphine. It is not legal to possess drugs in Schedule 3 without a prescription or other authority. A Home Office licence is required to export, or import and authority is needed for production, possession, and supply. Certain Schedule 3 controlled

drugs, e.g. temazepam are also subject under the Misuse of Drugs (Safe Custody) Regulations (1973) (UK-Government, 1973).

Schedule 4 Controlled Drugs: This Schedule is currently split into two parts, Part 1 and Part 2. Part 1 contains mainly the benzodiazepines, e.g. diazepam, lorazepam, nitrazepam, and oxazepam. Schedule 4 controlled drugs are subject to minimal control, but they need a prescription or other authority to legally possess them, so long as it is in the form of a medicinal product. The licences are not needed to import or export Schedule 4 controlled drugs.

Part 2 contains mainly drugs such as anabolic steroids, e.g. nandrolone, stanozolol and testosterone, but also contains specific growth hormones and clenbuterol. All the substances listed in Part 2 are substances, which may be (mis)used by athletes and/or bodybuilders.

Schedule 5 Controlled Drugs: The drugs in Schedule 5 are considered to pose minimal risk of abuse. These non-injectable, low-dose preparations are not necessary to have a prescription for because they can be purchased over the counter at a pharmacy but, once obtained, it is illegal to supply them to another person. Many of these preparations include well-known cough mixtures and painkillers. However, some Schedule 5 controlled drugs are prepared from drugs that appear in Schedule 2 and therefore make misuse a risk. The safe custody and register requirements do not apply to these types of drugs (UK-Government, 2001).

In 2001, the UK parliament passed an amendment to the Misuse of Drugs Act (1971). The amendments were slight changes to the wording within the original legislation (for example: removal of the definition “medicinal product”). The most significant amendment was to allow a nurse independent prescriber and/or a

pharmacist independent prescriber to prescribe, possess, supply, offer to supply, administer and give directions for the administration of any controlled drug specified in Schedules 2 to 5 of the 2001 Regulations. The amendments also allow a nurse independent prescriber and a pharmacist independent prescriber to supply certain articles for administering or preparing controlled drugs.

The Psychoactive Substances Act (2016) (UK-Government, 2016) became law on 26th of May 2016. The Act made it an offence to produce, supply or offer psychoactive substances with the exception of caffeine, nicotine, alcohol and medicinal products as defined by the Human Medicines Regulations (2012) (UK-Government, 2012). It is important to note that the PSA 2016 does not replace the Misuse of Drug Act (1971) and substances controlled under the early legislation remain unchanged (Reuter and Pardo, 2017; UK-Government, 2016).

In general, the Psychoactive Substances Act (2016) defines many offences such as possession, importation, supply, production, penalties (Table 1.2), powers to stop and search; whereas the police will have powers for that and also for premises and prohibition notices (UK-Government, 2016; Reuter and Pardo, 2017).

Table 1.2 Penalties under the legalisation.gov.uk 2016 (Reuter and Pardo, 2017; UK-Government, 2016)

Offence	Summary (Magistrates Court)	Indictment (Crown Court)
Possession	Not an offence	Not an Offence
Possession in a custodial institution	Up to 12 months and/or a fine	Up to 2 years and/or a fine
Possession with intent to supply	Up to 12 months and/or a fine	Up to 7 years and/or a fine
Supply/offer to supply etc.	Up to 12 months and/or a fine	Up to 7 years and/or a fine
Production	Up to 12 months and/or a fine	Up to 7 years and/or a fine
Importation/exportation	Up to 12 months and/or a fine	Up to 7 years and/or a fine
Failure to comply with a Prohibition or Premises notice	Up to 12 months and/or a fine	Up to 2 years and/or a fine

1.5 Classification of controlled and new/novel psychoactive substances

Controlled substances are classified based on their psychotropic effects as stimulants, empathogens/entactogens (such as (±)-MDMA, 'ecstasy'), hallucinogens or classified depending on their chemical family as phenethylamines, amphetamines, cathinones, piperazines, pipradrol/piperidines, aminoindanes, benzofurans, and tryptamines (Hill and Thomas, 2011; Liechti, 2015). In addition, controlled substances are also classified by the United Nations Office on Drugs and Crime (UNODC) and the EMCDDA to the following sub-categories: phenethylamines (Hanson et al., 2015), synthetic cathinones (Valente et al., 2014), ketamine (Wolff and Winstock, 2006), synthetic cannabinoids (Shevyrin et al., 2016), piperazines (Castaneto et al., 2015), plant-based substances (Kalix, 1996): Khat, Kratom, *Salvia divinorum* and miscellaneous examples (which fall outside the classes listed above): aminoindanes, phencyclidine, tryptamines (Smith et al., 2015).

This section provides an overview of the most common/prevalent substances of abuse, relevant to this study. The group of substances collectively referred to as NPSs include a wide range of primarily synthetic compounds that fit into pre-existing categories of existing drugs. They include phenethylamines: ((±)-methamphetamine, (±)-Paramethoxyamphetamine ((±)-PMA), and (±)-3,4-Methylenedioxymethamphetamine ((±)-MDMA), synthetic cathinone, and its derivatives ((±)-mephedrone, (±)-4-Methyl-N-ethylcathinone (±)-4-MEC, and (±)-mexedrone) and dissociative anaesthetic substances (methoxyphenidine regioisomers and fluoroephedrine regioisomers).

1.5.1 Phenethylamine (amphetamine, methamphetamine and MDMA)

Phenethylamine molecules (Figure 1.3a) are the backbone of many stimulant NPS (Whelpton, 2007; Liechti, 2015; Dargan and Wood, 2013; Freeman and Alder, 2002). The amphetamines (Figure 1.3b) are formed by inserting an alpha methyl group into phenethylamine that protects against metabolism by monoamine oxidase (MAO). The higher CNS activity of methamphetamine (Figure 1.3c) is produced from the methylation of the terminal amine of amphetamine, which increases the duration of sympathomimetic activity and protects against metabolism by MAO(Whelpton, 2007; Liechti, 2015; Dargan and Wood, 2013; Freeman and Alder, 2002; Shulgin, 1978).

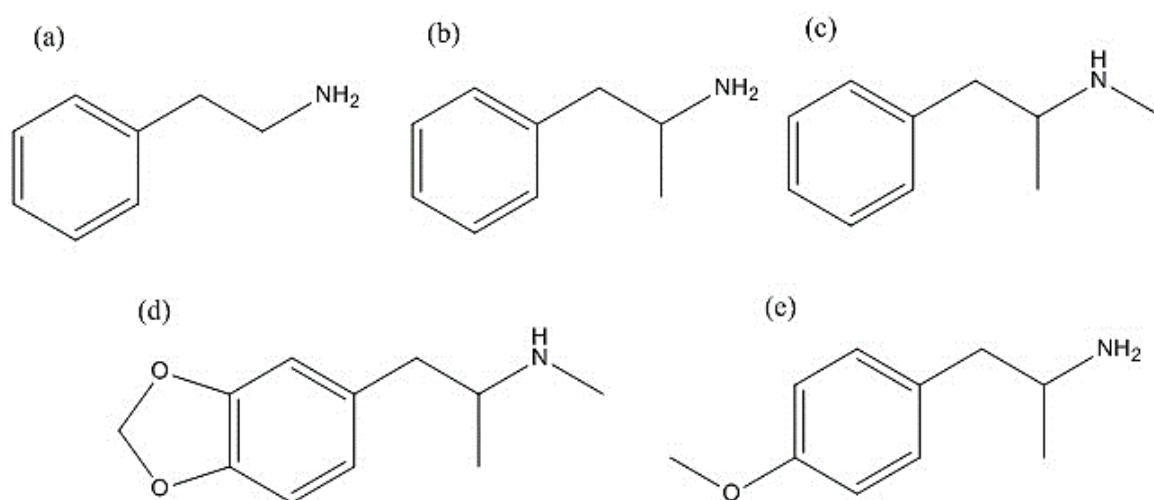


Figure 1.3 Structures of representative new/novel psychoactive Substances (stimulants and empathogens). Chemically, the substances shown include phenethylamine: (a), amphetamine (b), (\pm)-methamphetamine, (c), (\pm)-MDMA (d), and (\pm)-PMA (e).

Amphetamine and methamphetamine have been used clinically as classic psychostimulants recreationally and by the military services since the 1930s (Whelpton, 2007; Liechti, 2015). The term 'designer amphetamine' is used to describe the synthetic chemical substances that are derived from amphetamine or methamphetamine such as (\pm)-MDMA (Figure 1.3d) and (\pm)-PMA (Figure 1.3e)).

1.5.1.1 (±)-3,4-Methylenedioxymethylamphetamine ((±)-MDMA)

One of the most important of the amphetamine-derivatives is (±)-MDMA; Figure 1.3d), which is not a novel psychoactive substance as it has been used for decades. (±)-MDMA, commonly known as 'ecstasy', is one of the most popular addictive synthetic drugs (synthetic amphetamine). (±)-MDMA was first synthesised by the German pharmaceutical company Merck in 1912 as part of a new pathway for a potential appetite suppressants, and over the next seventy years, a number of researchers explored its psychedelic properties of (±)-MDMA with little success (Isabel Colado et al., 2007).

During the 1970s, (±)-MDMA surfaced on the recreational drugs market. Its widespread abuse and potential long-term health effects led many countries to prohibit its possession, supply and manufacture. In the 1980s, (±)-MDMA entered the lists of internationally controlled substances (Muller and Windberg, 2005). Currently, in the UK, (±)-MDMA (or 'ecstasy') is controlled as a Class A, Schedule 1 substance due to its illicit use as a recreational drug and its implication in some highly publicised fatalities (Soar et al., 2001; Liechti and Vollenweider, 2001; Verschraagen et al., 2007; White et al., 2014; Cumba et al., 2016).

(±)-MDMA is usually found in tablet form (containing 60–70 mg (±)-MDMA) with each batch being stamped with a particular motif, e.g. a Mitsubishi™ logo, smiley faces, or letters. However, it has also been seized as a high purity (circa. 95 – 98%) crystalline powder sold in wraps. Since the global prohibition of (±)-MDMA and its precursors (e.g. 3,4-methylenedioxyphenyl-2-propanone, piperonal, safrole and isosafrole), a wide range of structurally-related phenethylamines have

appeared on the recreational drugs market, including the designer drug, (±)-PMA (Cumba et al., 2016).

Currently, (±)-MDMA is predominantly a 'club drug' and is commonly used recreationally within many "night time economies". In addition, (±)-MDMA is one of the recreational drugs widely used, and many of new psychoactive substances were synthesised and designed to mimic effects of (±)-MDMA and added in 'ecstasy' pills instead of the (±)-MDMA. (±)-MDMA used to enhance sociability and produces feelings of empathy or 'being touched' because it has the prototypical empathogen or entactogen activity (Morgan et al., 2013). In some studies, (±)-MDMA is used to increase emotional empathy, extroversion, trust, and sociality relatively (Hysek et al., 2014).

The term 'ecstasy' is commonly used to refer to (±)-MDMA, but a number of different amphetamine derivatives, and other drugs may be present in 'ecstasy tablets'. The majority of 'ecstasy' product contains another related chemical such as 3,4-methylenedioxyamphetamine (MDA), 3,4-methylenedioxyethamphetamine (MDEA), (±)-PMA and methamphetamine, amphetamine, or sometimes another type of drug like ketamine, ephedrine and over-the-counter painkiller (Cole et al., 2002; Soares et al., 2004).

1.5.1.2 (±)-Paramethoxyamphetamine [(±)-PMA]

(±)-PMA is one of the monomethoxy derivatives of amphetamine [para-(4)-phenyl-substituted (serotonergic) amphetamines] (Figure 1.3e) (Dargan and Wood, 2013). (±)-PMA is typically sold as 'ecstasy' although; its substitution for (±)-MDMA is unwanted because (±)-PMA is associated with higher morbidity and mortality particularly attributable to hyperthermia (Paton et al., 1975; Martin, 2001; Lurie et

al., 2012). In addition, this para-substituted amphetamine had hyperthermic properties which are stronger than those of (±)-MDMA (Daws et al., 2000) and associated with serotonergic and adrenergic receptor activation (Carmo et al., 2003). Therefore, hyperthermic complications are of particular concern when the amphetamines or new psychoactive substances with a comparable pharmacological profile are used (Simmler et al., 2014).

In addition, (±)-PMA is structurally related to phenethylamine and acts on the CNS producing mood enhancement, heightened sexual arousal and energy by increasing the release of intra-synaptic serotonin and inhibiting its reuptake resulting in hyperthermia (i.e. serotonin syndrome). Animal models suggest that (±)-PMA is more toxic than (±)-MDMA (Paton et al., 1975; Martin, 2001; Caldicott et al., 2003).

1.5.1.3 Pharmacological activity of synthetic amphetamine and its derivatives

All of the novel psychoactive drugs have the same psychostimulants of cocaine, amphetamine and (±)-MDMA, although with differences in their psychological effects. The prototypical psychostimulant of amphetamine produces agitation, insomnia, and loss of appetite, and produces amphetamine psychosis that is characterised by paranoia, hallucinations and delusions at high doses. (±)-MDMA and 'ecstasy' have both properties of a psychostimulant effect leading to euphoria and an intense love of self and others. It is described as an 'empathogen' (Iversen, 2008; Iversen et al., 2014). There is the difficulty of a clear distinction between 'empathogen' and 'psychostimulants'. The amphetamines, (±)-MDMA and (±)-PMA designer drugs' act by increasing extracellular levels of the monoamines dopamine (DA), serotonin (5-HT) and noradrenaline (norepinephrine) (NE) (Iversen et al., 2014). Many new/novel psychoactive substances have interacted with neurotransmitter transporters.

Amphetamine and its derivatives including methamphetamine and (±)-MDMA decrease the dopamine (DAT), serotonin (SERT) and noradrenaline (norepinephrine; NET) transporters and release these monoamines through their respective transporter. Methamphetamine predominantly increases dopamine and noradrenaline, but (±)-MDMA mostly increases serotonin, noradrenaline, and oxytocin (Hysek et al., 2014; Hysek et al., 2012; Liechti, 2015). (±)-MDMA has the entactogenic effects dependent on its serotonergic effects (Liechti, 2015).

Consequently, all substances releasing serotonin, similar to (±)-MDMA, can be expected to produce (±)-MDMA -like entactogenic effects. (±)-MDMA and these substances are also associated with serotonergic toxicity including serotonin syndrome, hyponatremia, hyperthermia, and seizures (Liechti et al., 2005; Simmler et al., 2011; Liechti, 2015). In contrast, methamphetamine, is a psychostimulants and mostly enhances dopaminergic neurotransmission (Simmler et al., 2013a; Simmler et al., 2013b).

1.5.2 Synthetic cathinones

Synthetic cathinone's are a subgroup of NPS structurally derived from cathinone (Figure 4.1 a). Cathinone is the principal active ingredient in the Khat plant (*Catha Edulis*) (Kalix and Braenden, 1985). In addition, cathinone and its derivatives are structurally related to the phenethylamine family such as amphetamine (Figure 4.1b). Most people who use Khat mainly within the East African and Arabic peninsula, chew the fresh leaves to ingest the principal natural ingredient, cathinone, to produce a psychostimulatory effect. The natural monoamine alkaloids, cathinone, and norephedrine are present within the fresh leaves (Kalix, 1981; Litman et al., 1986; Al-Motarreb et al., 2002).

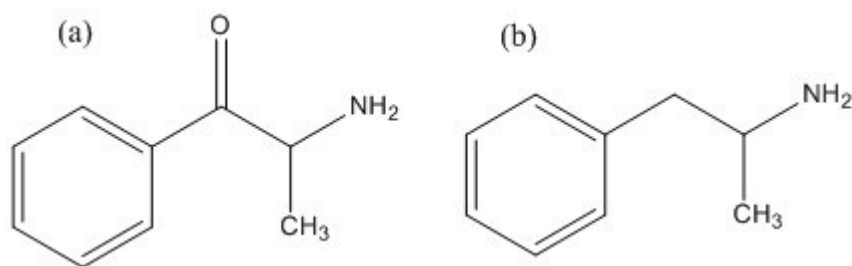


Figure 1.4 The relationship between the cathinone (a) and amphetamine (b).

In the early 1980s, Khat use was prominent in some countries and can be considered the forerunner of the 'designer drugs' phenomenon, which developed in the 1990s. The seriousness of the use of this plant recreationally led the World Health Organization (WHO) to classify Khat as a drug of abuse with the ability to produce mild-to-moderate psychological dependence (Neville, 1995). Since the late 1990s, with the increase in restrictions on the supply and production of recreational amphetamines and designer drugs, such as (±)-MDMA, clandestine drug manufacturers began seeking 'legal alternatives to fill the void on the club market. Although the initial motivation was probably to drive the development of novel psychoactive agents and sidestep drug laws, it did not take long for a broad range of products enter the recreational drug market (Neville, 1995).

The popularity of these drugs has grown. One of the most prominent classes are the synthetic cathinone's, leading to sensationalised media attention. In addition to the wide availability of these products through the internet, synthetic cathinone's have been marketed under some different guises including legal highs, bath salts or plant food and are usually labelled as 'not for human consumption' to circumvent drug legislation. Since the early 2000s, these recreational drugs have appeared on the European market with unregulated ring-substituted cathinone derivatives, such as (±)-mephedrone (Figure 1.5a) (Santali et al., 2011), (±)-4-MEC; Figure 1.5b) (Gil

et al., 2013; Santali et al., 2011), (\pm)-flephedrone ((\pm)-4-FMC; Figure 1.5c) (Prosser and Nelson, 2012) and (\pm)-mexedrone (Figure 1.5d) (Gillman, 2005). International legislation regarding synthetic cathinone derivatives are now in place, for example, cathinone's are illegal in the UK, Germany, and many others countries (Fass et al., 2012; Morris, 2010).

The EMCDDA) Early Warning System (EWS) has reported the seventy-four new synthetic cathinones between 2005 and 2014, with 30 synthetic cathinones detected in 2014 alone. The development of methods for their detection and quantification is timely and urgently required.

This project focuses on three synthetic cathinones, which are (\pm)-mephedron, (\pm)-4-MEC, and (\pm)-mexedrone and the application of new analytical methods for their detection and quantification.

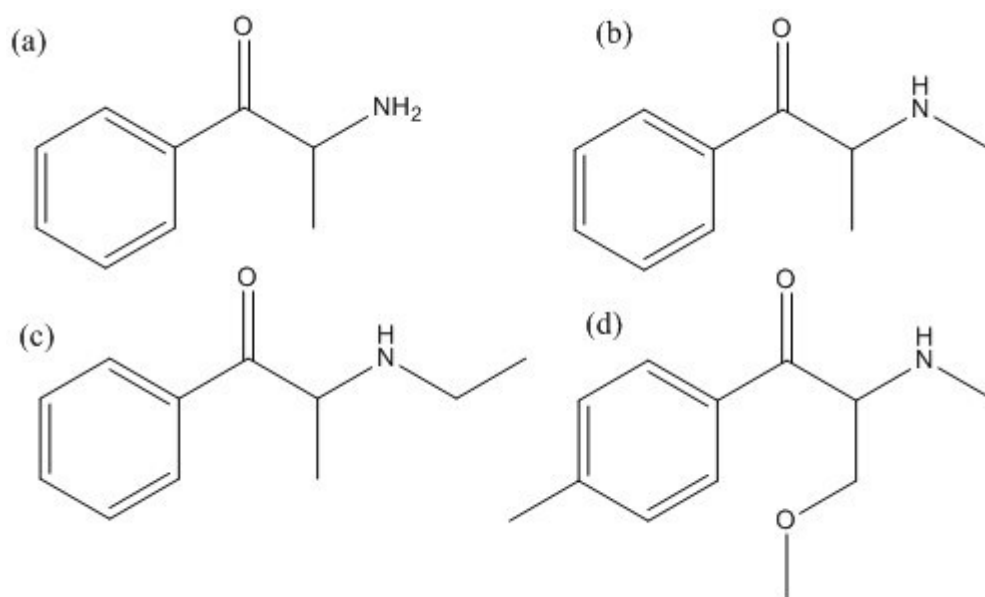


Figure 1.5 The chemical structure of cathinone (a), (\pm)-mephedrone (b), (\pm)-4-MEC (c), and mexedrone (d).

1.5.2.1 (±)-Mephedrone [(±)-4-MMC]

The most infamous synthetic cathinone, which has appeared since 2000, is (±)-mephedrone which was first reported in 1929 and was little more than a chemical footnote before its rediscovery, by recreational users, in the mid-2000s. (±)-mephedrone is a substituted methcathinone, with a degree of divergence from the parent molecule that has been found in NPS products such as Benzo Fury, Afghan incense, NRG-1 and NRG-2 (Smith et al., 2015).

Subsequent media reports about incidents of fatalities through the alleged use of this material across many countries led to the UK, Germany, Sweden, Ireland, Denmark and Norway, Israel and United States to legislate and control this substance (McElrath and O'Neill, 2011; Kelly, 2011). In the UK, an online survey of 1006 secondary school, college, and university students in February 2010, indicated that 20.3% had tried (±)-mephedrone at least once (Dargan et al., 2010). In the US, it has enjoyed similar growth in popularity. In 2009, no calls reporting bath salt overdoses were received by the poison control centres, but about 303 calls were fielded in 2010, and in 2011 there were about 5625 calls received (Winstock et al., 2010).

1.5.2.2 (±)-4-Methylethcathinone [(±)-4-MEC]

(±)-4-MEC [(±)-4-methyl-*N*-ethylcathinone] is derived from cathinone. Its effects are very similar to (±)-mephedrone, but it is apparently not as euphoric, has a shorter duration and is less potent than (±)-mephedrone (Brandt et al., 2010). In 2010, (±)-4-MEC was available for sale over the internet as 'NRG-2' (Brandt et al., 2010; Gil et al., 2013), but now all cathinone derivatives are banned.

(±)-4-MEC appeared as an alternative product following the ban on (±)-mephedrone in June 2010 (Gil et al., 2013). It was detected in powder form in both Hungary and the United Kingdom (Jankovics et al., 2011; Gil et al., 2013). In 2011, the Institute of Forensic Research (IFR, Poland) reported that (±)-4-MEC was the most prevalent substitute of (±)-mephedrone in Poland (Gil et al., 2013). (±)-4-MEC has often been described as a 'legal replacement for (±)-mephedrone', 'mephedrone – new formula' or 'modified mephedrone' – suggesting similar psychoactive action. The UK introduced a broad ban through an amendment of the MDA 1971 on all substituted cathinones, including (±)-4-MEC in April 2010 (Ayres and Bond, 2012).

People are aware that these substances labelled with 'not for human use', are 'legal highs' and sold not only as a sole compound but also as mixtures with other psychoactive substances, especially substituted cathinones such as 3',4'-methylenedioxy- α -pyrrolidinobutyrophenone (MDPBP) and 3,4-methylenedioxy-pyrovalerone (MDPV), and rarely with 4'-methyl- α -pyrrolidinopropiophenone (MPPP), pentylone, benzedrone, and other substances. There is little available information on the effects of (±)-4-MEC, but it appears to be less potent than most other cathinones. The effects of (±)-4-MEC include excitation, gentle euphoria, mood elevation, relaxation, feeling of bliss, empathy, increased tactile and musical appreciation (Gil et al., 2013).

1.5.2.3 (±)-Mexedrone

(±)-Mexedrone [3-methoxy-2-(methylamino)-1-(4-methylphenyl) propane-1-one.hydrochloride], is a (±)-mephedrone derivative created by adding an alpha-methoxy to the (±)-mephedrone structure. The effect of (±)-mexedrone is to inhibit the re-uptake of serotonin and dopamine, depending on the dose, and it has an

affinity for serotonin and dopamine membrane transporters and receptors (5-HT₂ and DA₂ receptors), producing similar sympathomimetic effects to amphetamines (Gillman, 2005). To date, mephedrone use has rarely been analytically confirmed (Gillman, 2005). However, mephedrone has a weak releasing activity at the serotonin transporter (SERT) and is a weak non-selective uptake blocker at the dopamine transporter (DAT) and norepinephrine transporter (NET).

1.5.2.4 Pharmacological activity of synthetic cathinone derivatives

Pharmacologically, cathinone is classed as stimulant. However, it is significantly less potent than amphetamine, despite having structural similarities to the phenethylamine family i.e. cathinone (Figure 1.4a) contains a β -keto group adjacent to the aromatic ring of amphetamine (Figure 1.4b) (Al-Motarreb et al., 2002; Kalix, 1996). The presence of the β -keto group in the cathinone derivatives increases the polarity of the synthetic cathinones and results in a decrease in their ability to cross the blood-brain barrier (BBB). Therefore, their psychostimulatory (CNS stimulant and sympathomimetic) effects have been shown to be markedly lower than their closest relatives, the amphetamines (Schifano et al., 2011; Valente et al., 2014; Kalix, 1992; Kalix, 1983; Kalix and Braenden, 1985).

The presence of the α -methyl group in the phenylethylamine side chain prevents the metabolism and inactivation of cathinones through monoamine oxidase (MAO), and they have been shown to inhibit this enzyme (Siegel and Agranoff, 1999). Furthermore, cathinones strongly inhibit MAO to a greater extent than amphetamine (Nencini et al., 1984) and have been shown to be more selective toward the isoenzyme MAO-B (Osorio-Olivares et al., 2004; Simmler, 2018). Cathinones are more lipophilic than their corresponding metabolites and are believed to be able to penetrate the CNS more effectively (Kalix, 1991). However,

with the lack of *in vivo* studies, many of the conclusions drawn are anecdotal and resort to comparisons with illicit drugs with similar subjective effects and chemical structures (i.e. cocaine, amphetamines, and (±)-MDMA) (Carvalho et al., 2012). In the central nervous system, it is believed that the main effects of cathinone are to increase the release of the dopamine, noradrenaline, and serotonin (Kalix and Braenden, 1985; Gibbons and Zloh, 2010) in a similar way that amphetamine, methamphetamine and (±)-MDMA exert their CNS activities (McElrath and O'Neill, 2011; Carhart-Harris et al., 2011; Hadlock et al., 2011).

If a synthetic cathinone is taken orally, for example (±)-mephedrone, the effects will appear within 15–45 minutes; but if administered intranasal, the effects start within a few minutes, producing a maximum effect within half an hour and will last between two and three hours. Other reported effects include euphoria, increased sexual stimulation, sociability and re-dosing (Brunt et al., 2011). In same survey (February 2010), 947 of (±)-mephedrone users who reported that they had previously used cocaine; 20.4% said the effects of (±)-mephedrone, were as rewarding as cocaine with 54.6% reporting that (±)-mephedrone effects were significantly better (Winstock et al., 2011).

In 2011, the US National Poison Information Service summarised this evidence and concluded that, (±)-mephedrone and its derivatives may have significant effects on:

- (i) The cardiovascular system (e.g. palpitations, tachycardia, arrhythmias, hypertension, and hot flushes).
- (ii) The central nervous system (e.g. headaches, light-headedness, dizziness, tremors, convulsions, loss of concentration, and memory loss).
- (iii) The gastrointestinal system (e.g. abdominal pain, nausea and vomiting).

(iv) The respiratory system (e.g. chest pain and respiratory difficulties).

Nasal insufflation of (±)-mephedrone has been reported to be associated with significant nasal irritation and pain, which has led to some users switching to the oral use of (±)-mephedrone. The long-term effects of (±)-mephedrone are currently unknown (EMCDDA, 2010).

1.5.3 Dissociative anaesthetics (regioisomers of methoxyephedrine and fluoroephedrine)

In 2008, ephedrine appeared on the NPS scene together with isopropylphenidine (NPDPA) (another leftamine derivative) as reported by the German police (Beharry and Gibbons, 2016). In some countries, ephedrine is illegal as a structural isomer of the banned opioid drug lefetamine (Wink et al., 2014; Wink et al., 2015).

Phencyclidine (PCP) and ketamine were developed as potential general anaesthetics (Greifenstein et al., 1958; Kang et al., 2017). Both were globally abused for their dissociative effects (Kang et al., 2017). The misuse of PCP has reduced in Europe because of severe and long lasting psychotomimetic effects, including lethality (Moeller et al., 2008). Interestingly, 1,2-diarylethylamines, e.g. ephedrine (Kang et al., 2017), diphenidine and 2-methoxydiphenidine are the most common structures, like phencyclidine (Morris and Wallach, 2014).

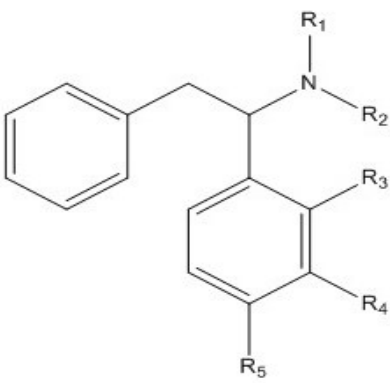
In 2013, the UK controlled all arylcyclohexylamines under the MDA (1971) in an attempt to decrease the spread of novel PCP and ketamine derivatives (NPS class). The dissociative diarylethylamines (Table 1.3a) are not new compounds, being originally synthesised as far back as 1924. They have appeared on the NPS market as crystal or powder ephedrine (Beharry and Gibbons, 2016).

In addition, ephenidine (Table 1.3b) is a diarylethylamine and synthesised recently to become popular with recreational users for its dissociative hallucinogenic effect (Kang et al., 2017). Recent studies show that the new psychoactive substance, ephenidine, is a selective NMDA receptor antagonist with a voltage-dependent profile similar to phencyclidine (PCP) and ketamine. Such properties help explain the dissociative, cognitive and hallucinogenic effects in man (Kang et al., 2017). Ephenidine [N-ethyl-1, 2-diphenyl ethylamine; NEDPA; EPE] is dissociative anaesthetic which elicits activity by antagonizing (inhibiting) N-methyl-D-aspartate (NMDA) receptors. It has been used as an anaesthetic drug for animals and humans, therefore, ephenidine's action is referred to as 'dissociative anaesthesia' and used as a recreational drug (Morris and Wallach, 2014).

Table 1.3 shows the chemical structure of the ephenidine derivatives methoxyephenidine and fluoroephenidine and their regioisomers, (2-methoxyephenidine (Table 1.3c), 3-methoxyephenidine (Table 1.3d), 4-methoxyephenidine (Table 1.3e), 2-fluoroephenidine (Table 1.3f), 3-fluoroephenidine (Table 1.3g), and 4-fluoroephenidine (Table 1.3h).

There is little information reported in the literature about the derivatives of ephenidine and their regioisomers, however, the pharmacological effect of ephenidine and ephenidine derivatives and its regioisomers are likely to be similar as they have the same backbone of chemical structure (Table 1.3).

Table 1.3 Chemical structure of ephenidine, lefetamine, 2-MEP, 3-MEP and 4-MEP, 2-FEP, 3-FEP and 4-FEP.

					
Compound	R ₁	R ₂	R ₃	R ₄	R ₅
Lefetamine	CH ₃	CH ₃	H	H	H
Ephenidine	H	CH ₂ CH ₃	H	H	H
2-MEP	H	CH ₂ CH ₃	O-CH ₃	H	H
3-MEP	H	CH ₂ CH ₃	H	O-CH ₃	H
4-MEP	H	CH ₂ CH ₃	H	H	O-CH ₃
2-FEP	H	CH ₂ CH ₃	F	H	H
3-FEP	H	CH ₂ CH ₃	H	F	H
4-FEP	H	CH ₂ CH ₃	H	H	F

1.5.3.1 Pharmacological effect of ephenidine (synthetic diarylethylamine) and its derivatives

Dissociative anaesthetic substances including ketamine, PCP, and dextromethorphan produce feelings of detachment and induce a state of anaesthesia by antagonising ionotropic N-methyl-D-aspartate receptors (NMDAR) in the central nervous system (Morris and Wallach, 2014). One of the most recent classes of NMDAR antagonists to emerge on the NPS market are the diarylethylamines, e.g. diphenidine (Wallach et al., 2015), and 2-methoxyphenidine (McLaughlin et al., 2016).

The pharmacological effect of ephenidine (and its derivatives) and its neural actions were investigated by assessing its effect on central nervous system receptor in targeted electrophysiological studies (Kang et al., 2017). The ephenidines also

showed modest activity at dopamine and noradrenaline transporters and at sigma 1 and sigma two binding sites (Kang et al., 2017).

Ephenidine has mild psychedelic effects, inducing fear (Beharry and Gibbons, 2016). Recently, ephenidine became available and anecdotally appears popular with dissociative users (e.g. an alternative to ketamine). In the previous study comparison of ephenidine and ketamine showed that ephenidine is a relatively selective, voltage-dependent NMDA antagonist, explaining the psychotomimetic effects of ephenidine and predicts the side-effects including memory impairment (Kang et al., 2017).

1.6 Analytical techniques for the detection of NPS

There is an increasing interest in the study and development of rapid, selective, and sensitive methods for the identification and quantification of phenethylamines, synthetic cathinones, dissociative anaesthetic substances and their derivatives in seized samples and biological fluids. Numerous studies have demonstrated the analysis of NPS drugs and described the significant improvements in analytical methods for analysis of the drugs in biological specimens (Table 1.4).

In the literature, there are currently no validated methods reported for each of the (±)-Mexedrone or for the regioisomers of methoxyephenidine or fluoroephenidine. McLaughlin et al. reported the GC-MS and HPLC-MS separation for (±)-Mexedrone but without validation information. The regioisomers of methoxyephenidine and fluoroephenidine have not been reported in the literature because they are new substances (McLaughlin et al., 2017).

The separation, identification and quantification of NPSs in biological samples have been described using, for example, high performance liquid chromatography (HPLC) (Butler and Guilbault, 2004; Kumihashi et al., 2007) or gas chromatography (GC) (Dams et al., 2003), capillary electrophoresis (Nieddu et al., 2007) and electrochemistry techniques (Smith et al., 2014b; Cumba et al., 2016; Michel et al., 1993) and other analytical techniques. The chromatography technique is the most commonly used methodology for the separation of NPS and the recreational drug (\pm)-MDMA (Butler and Guilbault, 2004; Kumihashi et al., 2007; Garrido et al., 2010). Liquid chromatography with UV spectrometry (Soares et al., 2004; Khreit et al., 2012), diode array detector (DAD) (de Figueiredo et al., 2010), mass spectrometry (Lee, 2013; Saito et al., 2011; Arora et al., 2016; Xiang et al., 2015; Brandt et al., 2010; Jankovics et al., 2011) and gas chromatography (Saito et al., 2011; Arora et al., 2016) with mass spectrometry have been widely used.

Table 1.4 Analytical methods currently reported in the literature for the detection of New Psychoactive Substances and recreational drugs.

Analyte	Analytical method	Matrix	Analytical, linear range	Limit of detection	References
MDMA	HPLC-UV	urine	4.2-150.0 $\mu\text{g mL}^{-1}$	84.0 $\mu\text{g mL}^{-1}$	(Soares et al., 2004)
MDMA	HPLC-DAD	Potassium phosphate buffer: acetonitrile (90:10 v/v) pH = 3.2 \pm 0.02	1.4-111.0 $\mu\text{g mL}^{-1}$	1.0 $\mu\text{g mL}^{-1}$	(Muller and Windberg, 2005)
PMA	HPLC-DAD	Potassium phosphate buffer: acetonitrile (90:10 v/v) pH = 3.2 \pm 0.02	N/A	N/A	(Muller and Windberg, 2005)
PMA	Capillary electrophoresis with diode array	Plasma Urine	50.0-5000.0 ng mL ⁻¹	20.92 ng mL ⁻¹ 24.26 ng mL ⁻¹	(Nieddu et al., 2007)
MDMA	HPLC-DAD	Methanol: water (90:10 v/v)	5.0-100.0 ppm	2.94 ppm	(de Figueiredo et al., 2010)
MDMA	fluorescence HPLC-chemiluminescence	Plasma Hair root Hair shaft	0.01-1.0 ng mL ⁻¹ 0.10-10.0 ng mL ⁻¹ 0.10-10.0 ng mL ⁻¹	3.0 ng mL ⁻¹ 17.0 ng mL ⁻¹ 14.0 ng mL ⁻¹	(Wada et al., 2012)
MDMA	Square wave voltammetry	Supporting electrolytes Human serum	8.0-45.0 μM 12.0-45.0 μM	1.2 μM 2.4 μM	(Garrido et al., 2010)
MDMA	Cyclic voltammetry – dip coating/ spin coating	KCl (0.1 mol L ⁻¹)	4.2-48.0 $\mu\text{mol L}^{-1}$	3.5/2.7 $\mu\text{mol L}^{-1}$	(Tadini et al., 2014)
MDMA PMA MDMA/PMA	Electrochemical analysis (cyclic voltammetry-dip coating/spin coating)	Potassium phosphate buffer and KCl (0.1 mol L ⁻¹): acetonitrile) (90:10 v/v) pH = 3.2 \pm 0.02	0.50-4.98 $\mu\text{g mL}^{-1}$ 0.50-4.98 $\mu\text{g mL}^{-1}$ 2.0-19.60 $\mu\text{g mL}^{-1}$	0.04 $\mu\text{g mL}^{-1}$ 0.03 $\mu\text{g mL}^{-1}$ 0.25 $\mu\text{g mL}^{-1}$ / 0.14 $\mu\text{g mL}^{-1}$	(Cumba et al., 2016)
MDMA PMA MDMA/PMA	HPLC-UV	Potassium phosphate buffer acetonitrile (90:10 v/v) pH = 3.2 \pm 0.02	0.50-4.98 $\mu\text{g mL}^{-1}$ 0.50-4.98 $\mu\text{g mL}^{-1}$	0.04 $\mu\text{g mL}^{-1}$ 0.08 $\mu\text{g mL}^{-1}$	(Cumba et al., 2016)
MA	HPLC-FL	Plasma Hair	1.49-746 ng mL ⁻¹ 0.149-149.2 ng mL ⁻¹	0.87 ng mL ⁻¹ 0.12 ng mL ⁻¹	(Nakashima et al., 2003)
4-MEC	LC-MS/MS	Acetonitrile: Water: formic acid (50:50:1%)		2.0 ng mL ⁻¹	(Jankovics et al., 2011)
4-MMC	HPLC-UV	Methanol:10 mM ammonium formate (40:60 v/v) pH = 3.5 \pm 0.02	0.5-10.0 $\mu\text{g mL}^{-1}$	0.09 $\mu\text{g mL}^{-1}$	(Santali et al., 2011)
4-MMC 4-MEC	HPLC-UV	Methanol:10 mM ammonium formate (46:54 v/v) pH = 3.5	0.5-10.0 $\mu\text{g mL}^{-1}$	0.03 $\mu\text{g mL}^{-1}$ 0.03 $\mu\text{g mL}^{-1}$	(Khreit et al., 2012)
4-MMC 4-MEC	Electrochemistry (electrochemical oxidation)	Phosphate buffer solution (pH = 2)	16–350 mg mL ⁻¹	39.8 $\mu\text{g mL}^{-1}$ 84.2 mg mL ⁻¹	(Smith et al., 2014a)
4-MEC	HPLC-DAD	Acetonitrile: water (containing 100 mL 85% orthophosphoric acid per 1 L)	200-400 ng mL ⁻¹	0.5 %	(Gil et al., 2013)
4-MEC	LC-MS/MS	Blood Urine	10-1000 ng mL ⁻¹	0.96 ng mL ⁻¹ 0.68 ng mL ⁻¹	(Gil et al., 2013)
4-MEC	LC-MS/MS	Hair	1-1000 pg mg ⁻¹	0.5 pg mg ⁻¹	(Alvarez et al., 2017)

1.6.1 The principle of chromatography

In pharmaceutical analysis, chromatography is the most frequently analytical technique. For example, liquid chromatography with UV spectroscopy (LC-UV) has gained more and more popularity for drug analysis because it is generally faster, easy to use and has good sensitivity and specificity (Soares et al., 2004; Khreit et al., 2012) compared to other analytical techniques.

The fundamental purpose of chromatography is to separate compounds in complex mixtures of individual components using a variety of interactions on the surface of an adsorbent. The process of separation depends on the mobile phase, which can be a liquid, or a gas phase and a stationary phase which can be solid or liquid. Furthermore, affinity is a measure of the strength of the interaction between the stationary phase and the components in the dissolved mobile phase. The stronger the interaction, the higher the affinity of the analyte to the stationary phase and the longer the retention time (Kazakevich and Lobrutto, 2007) .

1.6.1.1 High performance liquid chromatography

High performance liquid chromatography is the most valuable tool used for quality control in the pharmaceutical industry. HPLC-UV is a technique to separate mixtures of substances into their components based on their molecular structure and molecular composition (Kazakevich and Lobrutto, 2007). This involves a stationary phase (a solid) and a mobile phase (a liquid). The mobile phase flows through the stationary phase and carries the components of the mixture with it. Sample components that display stronger interactions with the stationary phase will move more slowly through the column than components with weaker interactions. This difference in rates causes the separation of the various components. The sample is introduced into the mobile phase flow through an injector. HPLC columns

contain the stationary phase. The different types of stationary phase include C₁₈ (octadecylsilyl) which is the most widely used (c. 90% of chromatographic applications) (Figure 1.6). In this study, reverse phase HPLC was used, in which the stationary phase is nonpolar (hydrophobic) in nature, while the mobile phase is a polar liquid, such as mixtures of water and methanol or acetonitrile. It works on the principle of hydrophobic interactions, hence the more nonpolar the analyte is, the longer it will be retained on the column and the longer it will take to elute.

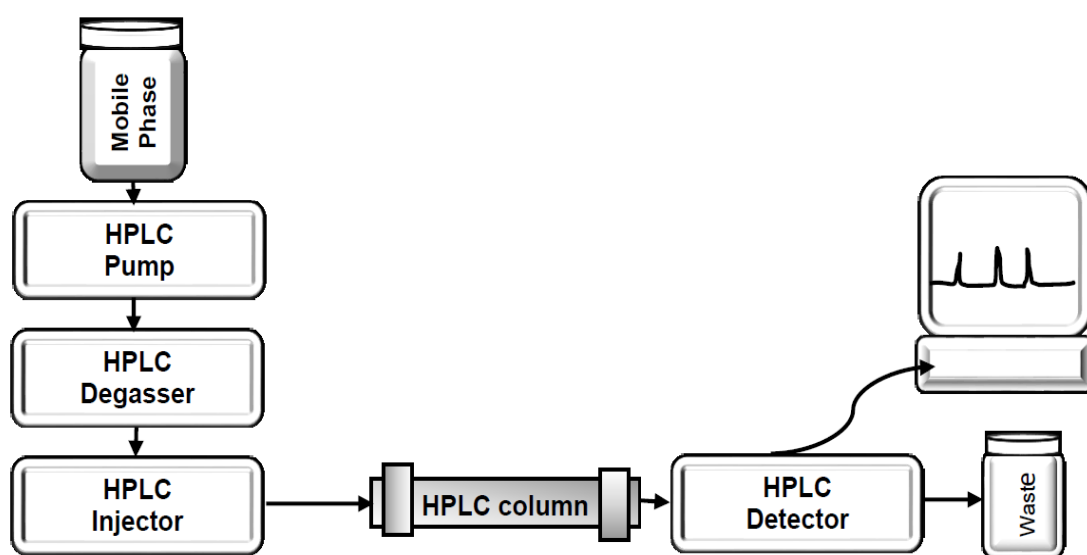


Figure 1.6 High Performance Liquid Chromatography diagram

Muller and Windberg described the HPLC method for the quantitation of the (±)-MDMA in the presence other (±)-MDMA derivatives and adulterants (amphetamine, ephedrine, metamphetamine, phentermine, MDE, PMA, paramethoxymetamphetamine (PMMA) and caffeine). In most cases the MDMA derivatives (or caffeine) were fully resolved from (±)-MDMA, however, samples containing PMMA were unable to be discriminated using the method and required secondary confirmation using GC-MS. (±)-MDMA linearity and accuracy were confirmed, and the precision was acceptable for routine testing of bulk samples

(Muller and Windberg, 2005). Cumba et al. used HPLC-UV for the detection and quantification of (±)-MDMA in the presence of (±)-PMA and reported the development and validation of the analytical method (Cumba et al., 2016).

In addition, Santali et al. reported for the first time the fully validated chromatographic methods for the detection and quantitative analysis of (±)-mephedrone in its pure form, and the presence of a number of common adulterants used in illicit drug manufacture (Santali et al., 2011). In 2012, Khreit et al. presented full synthetic and chemical characterisation data for the two (±)-mephedrone derivatives (±)-4-MEC and 4'-methyl-N-benzylcathinone (4-MBC) which have been identified in purchased NRG-2 samples. Khreit et al. described for the first time the fully validated chromatographic methods for the detection and quantitative analysis of (±)-mephedrone derivatives in their pure form, and the presence of adulterants used in illicit drug manufacture (Khreit et al., 2012). McLaughlin et al. reported the analysis of (±)-Mexedrone using HPLC-MS but did not present the limit of detection and limit of quantification (McLaughlin et al., 2017). However, in the literature there are no reported analytical methods for analysis of the regioisomers of methoxyphenidine and regioisomers of fluoroephenidine.

Principally, the detection by UV-visible and fluorescence spectroscopy and mass spectrometry have been utilised with liquid chromatography (Honeychurch, 2016). The UV-visible and fluorescence spectrometry methods are based on the absorbance of light. Liquid chromatography combined with mass spectrometry is widely used in industry and forensic analysis. LC-MS is extremely selective and sensitive and can be successfully used for a wide range of analytes (Honeychurch, 2016). However, it is relatively expensive and suffers from issues with selectivity resulting from 'isobaric' interferences and unpredictable ion yield attenuations from

'ion suppression effects' (Seger, 2012). Nevertheless, these issues can be overcome by using deuterated internal standards, however, these can be expensive.

1.6.2 Electrochemistry

Electrochemical techniques are powerful analytical techniques that have high sensitivity, accuracy, precision and relatively inexpensive instrumentation. These techniques are more regularly used in the pharmaceutical industry for drug analysis in their dosage forms and forensic science for the analysis of biological samples (Farghaly et al., 2014). The concept of most electroanalytical techniques is based on continuously changing the applied potentials on the electrode-solution interface and the resulting measured current (Uslu and Ozkan, 2011; Farghaly et al., 2014). Most of the chemical compounds have electrochemical activity (Farghaly et al., 2014). Voltammetry is based on the relation between the potential, current and time. This relationship could be explained when the applied potential (E) serves as a driving force for the reaction (reduction or oxidation reactions) on the working electrode and records the resulting current (i) flowing through the electrochemical cell over a period (t) (Farghaly et al., 2014). Cyclic voltammetry and amperometry are electroanalytical techniques that are widely used for the analysis of NPSs and other pharmaceutical compounds (Smith et al., 2014b; Zuway et al., 2015; Waddell et al., 2017).

Cyclic voltammetry (CV) is widely used for the study of reduction-oxidation reactions, and a rapid voltage scan technique with reversed direction of voltage scan. While the potential is applied to the working electrode in both forward and reversed directions, the resulting current is recorded (Farghaly et al., 2014). Cyclic voltammetry has previously been used for the analysis of NPSs. Smith et al. used

CV for the analysis of the cathinone derivatives such as (±)-mephedrone and (±)-4-MEC) but could not discriminate between them (Figure 1.7A) (Smith et al., 2014a). Also, Cumba et al. used CV for the differentiation of MDMA and PMA in mixtures (Figure 1.7B) (Cumba et al., 2016).

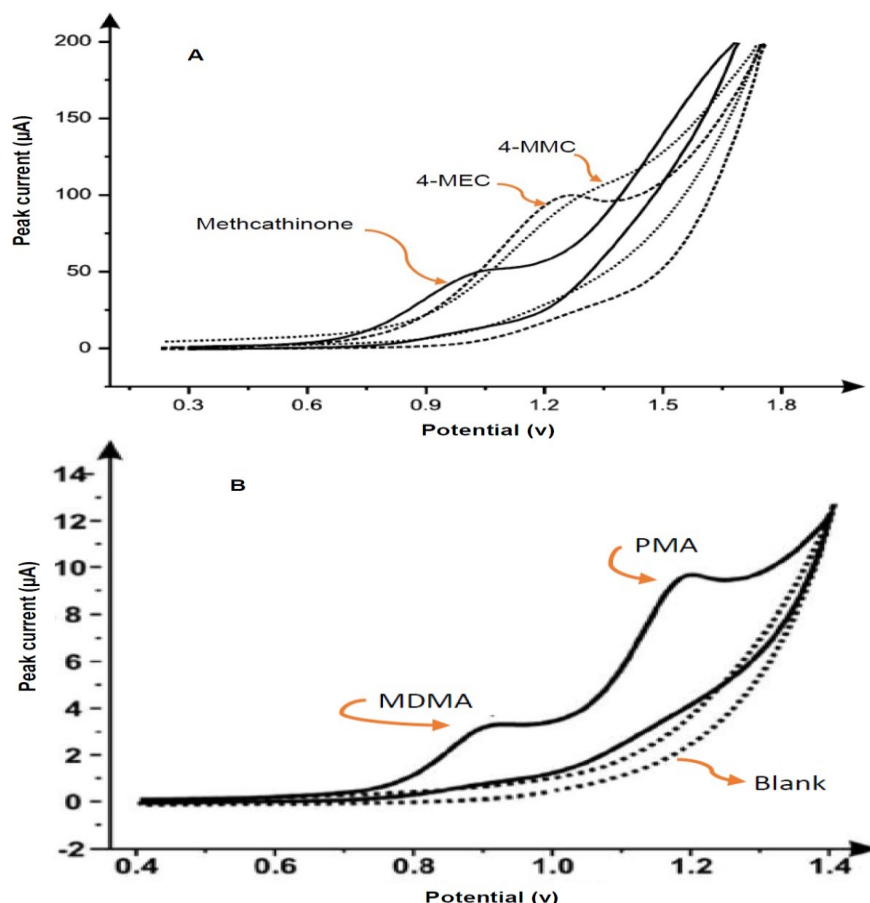


Figure 1.7 The cyclic voltammetry for cathinone derivatives (A) (Smith et al., 2014a) and cyclic voltammetry to differentiate between MDMA and PMA (B) (Cumba et al., 2016).

Amperometry is used by applying a constant potential to the working electrode and measuring the current as a function of time. In addition, the amperometric measurement depends on recording the current flow in the flow cell at a single applied potential (Stradiotto et al., 2003). Recently, several types of disposable electrochemical sensors have been developed. Screen-printed electrodes (SPEs) have offered high-volume production of extremely inexpensive, and yet highly reproducible and reliable single-use sensors (Ochiai et al., 2017).

Graphite screen-printed electrodes have received significant consideration in recent years due to their simplicity, efficiency, speed, cost-effectiveness and disposability (Cumba et al., 2015). They offer a reproducible and reliable sensor platform for amperometric detection for target analytes (Zuway et al., 2015).

The detection of illegal drugs at low concentrations can be carried out using voltammetry techniques. These techniques can be quite selective, quantitative and low-cost and have been used in the determination of cocaine (Ribeiro et al., 2016; de Oliveira et al., 2013), as well as (±)-MDMA; 'ecstasy' (Balbino et al., 2016; Tadini et al., 2014; Cumba et al., 2016; Garrido et al., 2010).

A comparison between the detection limits reported for HPLC-MS, HPLC-ED, and HPLC-UV for several drugs of abuse are shown in **Error! Reference source not found.** For a number of compounds, detection limits of the HPLC-ED technique are better; however, as a general approach LC-MS is a better technique across the range of analytes investigated. Liquid chromatography combined with UV detection (LC-UV) is simple, reliable and can be gained using various wavelength by using diode array detection (DAD) where spectra can be obtained for each eluting peak. LC-ED offers, in some cases, better detection limits and is considerably less expensive than LC-MS (Honeychurch, 2016). However, the limitation of HPLC-ED is its being affected by fouling of the electrodes leading to loss of sensitivity. In addition, the presence of oxygen in the mobile phase can be an issue, but this can be overcome by degassing.

Table 1.5 Comparisons between LC-ED, LC-MS, and LC-UV for analysis of abused drugs.

Analyte	LC-ED $\mu\text{g mL}^{-1}$	Ref.	LC-MS $\mu\text{g mL}^{-1}$	Ref.	LC-UV $\mu\text{g mL}^{-1}$	Ref.
THC	0.5	(Nakahara et al., 1989)	1.0	(Hudson et al., 2013)	0.746	(de MenezesA et al., 2012)
Methadone	9×10^{-4}	(Somaini et al., 2011)	1×10^{-4}	(Liu et al., 2015)	/	/
Morphine	5×10^{-4}	(Masui et al., 1968)	5×10^{-4}	(Liu et al., 2015)	0.01	(Masui et al., 1968)
Codeine	0.024	(Huettl et al., 1999)	1×10^{-3}	(Liu et al., 2015)	6×10^{-3}	(He et al., 1998)
Amphetamine	<0.05	(Santagati et al., 2002)	25×10^{-5}	(Liu et al., 2015)	0.1	(Moeller et al., 1998)
Rohypnol	0.02	(Honeychurch and Hart, 2008)	2×10^{-4}	(Bogusz, 2000)	0.03	(Borges et al., 2009)
Nitrozepam	0.1	(Honeychurch et al., 2006)	125×10^{-5}	(Glover and Allen, 2010)	/	/

This technique has been used for analysis a wide range of abused substances, including cannabinoids, ethanol, opiates, morphine, and benzodiazepines. The target analytes are separated chromatographically depending on their interactions with the stationary phase (column) and mobile phase. Different electrochemical detector systems have been utilised; including conductivity, potentiometric, amperometry and coulometry (Honeychurch, 2016). One of the most common electrochemical detection modes employed is amperometry which is based on the analyte being oxidised or reduced at the electrode interface (Honeychurch, 2016). The current formed from the redox reaction is linearly related to the concentration of the analytes and can therefore be used for the quantification of the analytes. In amperometric detection, the analytes flow over the surface of the working electrode (Honeychurch, 2016).

1.6.3 Application of high performance liquid chromatography-electrochemical detection (HPLC-D)

Table 1.6 details published studies where the use of HPLC-AD was reported. Nakahara et al. used HPLC-ED for the highly sensitive and simultaneous determination of free cannabinoids and cannabinoid acids without derivatisation in marijuana cigarettes and in tar and ash obtained by using an automatic smoking machine (Nakahara and Sekine, 1985). The linear range was 5 to 500 ng/injection for all cannabinoids and the LOD of this method was 0.5-0.9 ng/injection for free cannabinoids and 1.2-2.5 ng/injection for cannabinoid acids (Nakahara and Sekine, 1985).

Nyoni et al. described a method for determining small quantities of Δ^9 -THC in rat brain tissue using a high performance liquid chromatography-electrochemical detector (HPLC-ED) (Nyoni et al., 1996). The solvent employed was methanol-hexane-ethyl acetate, followed by HPLC-ED using a linear range up to $10 \mu\text{g mL}^{-1}$ and the LOD was 1.5 ng mL^{-1} (Nyoni et al., 1996).

In addition, Bourquin and Brenneisen utilised the reverse phase in HPLC-ED for analysis of urine to determine the metabolite of THC, 11-nor- Δ^9 -tetrahydrocannabinol-9-carboxylic acid (II) (THC-COOH) (Bourquin and Brenneisen, 1987; ElSohly et al., 1983). Further investigations using HPLC-ED for the simultaneous determination of the pure synthetic form of THC which has been developed as the drug dronabinol by Kokubun et al. (Kokubun et al., 2014). Kokubun et al. developed a HPLC-amperometric method to investigate the

pharmacokinetics of dronabinol in cancer patients and its quantitation in blood (Kokubun et al., 2014). The calibration curve was linear in the range of $10\text{--}00\text{ ng mL}^{-1}$ and the lower limit of quantification was 0.5 ng mL^{-1} (Kokubun et al., 2014).

Sawyer et al. developed an HPLC-ED method for the analysis of morphine, heroin, and hydromorphone in post-mortem tissues. Whole blood, urine, or vitreous humours were assayed without pre-treatment. The LODs for extracted samples were reported to be 0.5 ng mL^{-1} , 3.1 ng mL^{-1} and 12.5 ng mL^{-1} for morphine, hydromorphone and heroin respectively (Sawyer et al., 1988).

The use of HPLC-ED was recommended for the determination of morphine in biological fluids for its high sensitivity (Tagliaro et al., 1989). Xu et al. developed HPLC and amperometric determination of morphine in rat brain microdialysates. The amperometric detection of morphine was performed by using potential of $+0.60\text{ V}$ (vs Ag/AgCl), and a linear response for morphine was reported over the range $1.0 \times 10^{-6} - 5.0 \times 10^{-4}\text{ M}$ with a detection limit of $5.0 \times 10^{-7}\text{ M}$ (Xu et al., 2002). Moreover, the determination of morphine using liquid chromatography with amperometric determination at a glassy carbon electrode was investigated by Jordan and Hart (Jordan and Hart, 1991). They reported that the LOD for the morphine was $1.24 \times 10^{-13}\text{ M}$ over the linear range $1.2 \times 10^{-12} - 4.0 \times 10^{-10}\text{ M}$ of morphine injected (Jordan and Hart, 1991). The high-performance liquid chromatography with dual-electrode electrochemical detection has been successfully used in the redox mode to determine the benzodiazepine tranquilizer, Nitrazepam, in serum (Honeychurch et al., 2006). A large number of psychoactive compounds required a technique that was capable of separating, identifying and quantifying such compounds in complex samples. Min et al. reported a liquid chromatographic multichannel electrochemical detection (MECD) method for the

determination of 31 different tryptamines, phenethylamines and piperazines. These compounds were separated by using reverse phase HPLC (Min et al., 2010).

Table 1.6 Analytical methods in the literature using high performance liquid chromatography-electrochemical detection

Analytes	Technique HPLC-AD	Reference Electrode	Matrix	Linear range	Limit of detection	Ref.
THC-COOH	Amperometric mode; +1.2 V	Ag/AgCl	Urine	25-300 ng mL ⁻¹	5 ng mL ⁻¹	(ElSohly et al., 1983)
Δ ⁹ -Tetrahydrocannabinol levels	Amperometric mode; +1.2 V	Ag/AgCl	Brain tissue	Up to 10 µg/mL	1.5 ng on column	(Nyoni et al., 1996)
Cannabinoid contents	Amperometric mode; +1.2 V	Ag/AgCl	In marijuana cigarettes and tar and ash	5-500 ng/injection	0.5 to 0.9 ng/injection for free cannabinoids and 1.2 to 2.5 ng/injection for cannabinoid acids	(Nakahara and Sekine, 1985)
THC levels in patients given the drug dronabinol	Amperometric mode; +0.40 V	Ag/AgCl	Blood	10–100 ng/mL	0.5 ng/mL	(Kokubun et al., 2014)
Morphine	Amperometric mode; +0.60 V.	Ag/AgCl	Rat brain dialysates	1.0×10^{-6} – 5.0×10^{-4} M	5.0×10^{-7} M	(Xu et al., 2002)
Morphine	Amperometric mode; +0.45 V	Ag/AgCl	Serum	1.2×10^{-12} – 4×10^{-10} M	1.24×10^{-13} M	(Jordan and Hart, 1991)
Heroin, morphine and hydromorphone	Amperometric mode; +0.5 V	Ag/AgCl	Post-mortem sample of whole blood, urine, or vitreous humour	10 to 500 ng/mL (morphine), 62 to 1000 ng/mL (hydromorphone), and 250 to 2000 ng/mL (heroin)	0.5 ng/mL (morphine), 3.1 ng/mL (hydromorphone), and 12.5 ng/mL (heroin)	(Sawyer et al., 1988)
Rohypnol (flunitrazepam)	Dual amperometric reductive-reductive mode; electrode 1; –2.4 V and electrode 2; –0.2 V	Stainless steel (generator cell); Ag/AgCl (detector cell)	Bovine and human serum	0.5–100 mg/mL	20 ng/mL	(Honeychurch et al., 2006)

1.7 Study aims and objectives

The principle of basic analytical testing in a forensic science laboratory begins with receiving the drug sample(s) and then recording the physical description, evidential information (e.g. evidence bag number). This allows the forensic scientist to fully document the sample and ensure tracability through the analytical processes. The bulk sample may be qualitatively tested to ascertain the type of substance present (i.e. presumptive tests and/or instrumental analysis). In some cases the substance may require quantitative analysis to determine the amount of the principle component (or adulterants) which are present or trace analysis which may determine impurities and provide information on routes of manufacture (Cole, 2003). In the case of bulk samples, where potentially the ability to discriminate between either new substances or potentially regioisomers of a substance of concern, the need for robust and novel methods (though these may be extensions or new applications of existing technologies) are of interest to refine the capabilities within laboratory environments. The overall aim of this study is to develop novel applications of high performance liquid chromatography with amperometric detection (HPLC-AD) to the detection, analysis and quantification of controlled materials (for example: MDMA and mephedrone) and NPS (for example, regioisomeric methoxephedrinines and fluoroephedrinines) both in their pure form and in the presence of their derivatives or the common adulterants. The specific objectives are as follows:

1. To design, develop and validate (using ICH guidelines) a HPLC-AD protocol for detection and quantification of the controlled substance (±)-MDMA in the presence of two other illicit amphetamines: MA and (±)-PMA. The technique/protocol will be tested on seized samples (e.g. MDMA tablets) to

demonstrate its potential for forensic application towards rapid separation and detection of the principle components.

2. To develop, optimise and validate (using ICH guidelines) a suitable method to discriminate between controlled N-alkylcathinones such as (±)-mephedrone and (±)-4-MEC, which cannot be discriminated using other electrochemical analytical techniques (Smith et al., 2014a). The technique/protocol will be tested on seized bulk forensic samples of NRG-2, for the detection and quantification of the active components and levels of adulterants, and to demonstrate its potential application to the rapid forensic detection of these materials.
3. Carry out full physical and chemical characterisation, using NMR, IR, UV and GC-MS analysis, of the synthetic cathinone-derivative, mexedrone. Develop, optimise and validate (using ICH guidelines) an HPLC-AD protocol for the analysis of mexedrone (both in its pure form and in bulk forensic samples).
4. Extend this HPLC-AD methodology to study the separation, detection and quantification of regioisomeric new psychoactive substances – namely methoxyphenidines and fluoroephenidines, which have recently emerged on the recreational market. The optimised method will be ICH validated and then tested against seized samples, obtained from law enforcement agencies, to determine its forensic application to the discrimination of regioisomeric substances.

2 Chapter 2: Materials and methods

2.1 Chemicals

All chemicals used in this project were of analytical grade, obtained from commercial sources (Sigma-Aldrich, Gillingham, UK and Alfa-Aesar Limited, Heysham, UK) and used without any further purification. Acetonitrile, methanol (HPLC grade) supplied by Fisher Scientific International Company (Loughborough, UK). All solutions were prepared with deionised water with resistivity not less than 18.2 Ω cm, and vigorously degassed with nitrogen gas to remove all oxygen before the analysis. (±)-MDMA.HCl and (±)-MA.HCl were obtained, under Home Office licence, from Sigma-Aldrich (Gillingham, UK) and used without further purification. (±)-PMA.HCl was prepared in-house as described by Cumba et al. in previous work (Cumba et al., 2016). (±)-mexedrone.HCl was obtained from BRC Fine Chemicals (London UK), recrystallised from acetone and structurally characterised by NMR, IR, UV and GC-MS before use. (±)-mephedrone.HCl and (±)-4-MEC.HCl were synthesised, from the prerequisite α -bromopropiophenones, in-house under Home Office licence, using adaptations of the published methods (Santali et al., 2011; Khreit et al., 2012). Table 2.1 shows the street samples utilised in this study were obtained in accordance with Home Office licence requirements.

All samples were provided by authorised/licenced personnel in accordance with the legislation and under the approved Memorandum of Understanding operating between MANchester DRug Analysis & Knowledge Exchange (MANDRAKE) and Greater Manchester Police. All materials were stored, transferred, used and destroyed in compliance with the UK Misuse of Drugs Act (1971) and the UK Misuse of Drugs Regulations (2001).

Table 2.1. The sources of the street samples utilised in this study.

Street sample	Purported contents	Source
MDMA-1	MDMA	CAHID, University of Dundee
MDMA-2	MDMA	CAHID, University of Dundee
MDMA-3	MDMA.	CAHID, University of Dundee
MDMA-4	MDMA	CAHID, University of Dundee
MDMA-5	MDMA	CAHID, University of Dundee
NRG-2-A	4-MEC	EuChemicals (www.euchemicals.com)
NRG-2-B	4-MMC	EuChemicals (www.euchemicals.com)
NRG-2-C	4-MEC	EuChemicals (www.euchemicals.com)
NRG-2-D	4-MMC	EuChemicals (www.euchemicals.com)
NRG-2-E	4-MEC	EuChemicals (www.euchemicals.com)
MEX-1	Mexedrone	Research Chemicals (www.rcnetchemicals.com)
MEX-2	Mexedrone	Research Chemicals UK (www.rcuk.co.uk)
MEX-3	Mexedrone	Research Chemicals (www.rcnetchemicals.com)
MEX-4	Mexedrone	Buckled.eu (www.buckled.eu)
MEP-1	2-MEP	Greater Manchester Police (GMP)
MEP-2	2-MEP	Greater Manchester Police (GMP)
FEP-1	2-FEP	Greater Manchester Police (GMP)
FEP-2	2-FEP	Greater Manchester Police (GMP)
FEP-3	2-FEP	Greater Manchester Police (GMP)

2.1.1 Synthesis of (±)-methoxyphenidine regioisomers

Synthesis of (±)-2-methoxyphenidine.HCl [(±)-2-MEP], (±)-3-methoxyphenidine.HCl [(±)-3-MEP] and (±)-4-methoxyphenidine.HCl [(±)-4-MEP] was performed by Mr Matthew Hulme (unpublished work) using an adaptation of the published method for substituted diphenidine derivatives (Le Gall et al., 2009). The target compounds were fully characterised using NMR, IR, GC-MS and elemental analysis and confirmed to have a >99.5% purity. The analytes were used without further purification.

2.1.2 Synthesis of (±)-fluoroephenidine regioisomers

Synthesis of the (±)-2-fluoroephenidine.HCl [(±)-2-FEP], (±)-3-fluoroephenidine.HCl [(±)-3-FEP] and (±)-4-fluoroephenidine.HCl [(±)-4-FEP] was performed by Mr Matthew Hulme (unpublished work) using an adaptation of the published method for substituted diphenidine derivatives (Le Gall et al., 2009). The target compounds were fully characterised using NMR, IR, GC-MS and elemental analysis and confirmed to be of >99.5% purity. The analytes were used without further purification.

2.2 Instrumental details

2.2.1 High performance liquid chromatography (HPLC)

High performance liquid chromatography (HPLC) was performed with an integrated Agilent HP Series 1100 Liquid Chromatograph (Agilent Technologies, Wokingham, UK) fitted with an in-line degasser (G1322A, Serial # JP73017007), pump (G1310A, Serial # DE80301064), 100-place autosampler (G1313A, Serial # DE54901543), column compartment (G1318A, Serial # DE91610205), and UV absorbance detector (G1314A, Serial # JP73705698). Data collection and analysis were carried out using ChemStation for LC (Ver. 10.02) software (Agilent Technologies, Wokingham, UK). Columns were used with different stationary phases provided by HiChrom Limited (Reading, UK) as shown in Table 2.2.

Table 2.2 HPLC columns utilised in this project

Column	Stationary Phase	Length [cm]	Internal diameter [mm]	Particle size [µm]	Pore size [Å]	HPLC mode
A	ACE-3-C ₁₈	15	4.6	3	150	Reverse Phase
B	ACE-5-C ₁₈ AR	15	4.6	5	150	Reverse Phase

2.2.2 Electrochemistry flow cells used in liquid chromatography-amperometric detection (HPLC-AD)

One of the flow cells used in this study were obtained from Metrohm UK, Runcorn, UK (impinging jet flow cell; product code: DRP-FLWCL-TEF-71306; $3.3 \times 6.0 \times 3.3$ cm, flow chamber volume = $8 \mu\text{L}$; denoted as LC-FC-A, Figure 2.1a and Figure 2.1b). The second flow cell was obtained from the University of Leeds, UK (iCell channel flow cell; $4.5 \times 4.5 \times 4.0$ cm, flow-chamber volume = $120 \mu\text{L}$; denoted as LC-FC-B, Figure 2.1c and 2.1d). The iCell (LC-FC-B) was fabricated as previously reported (Pike et al., 2012).

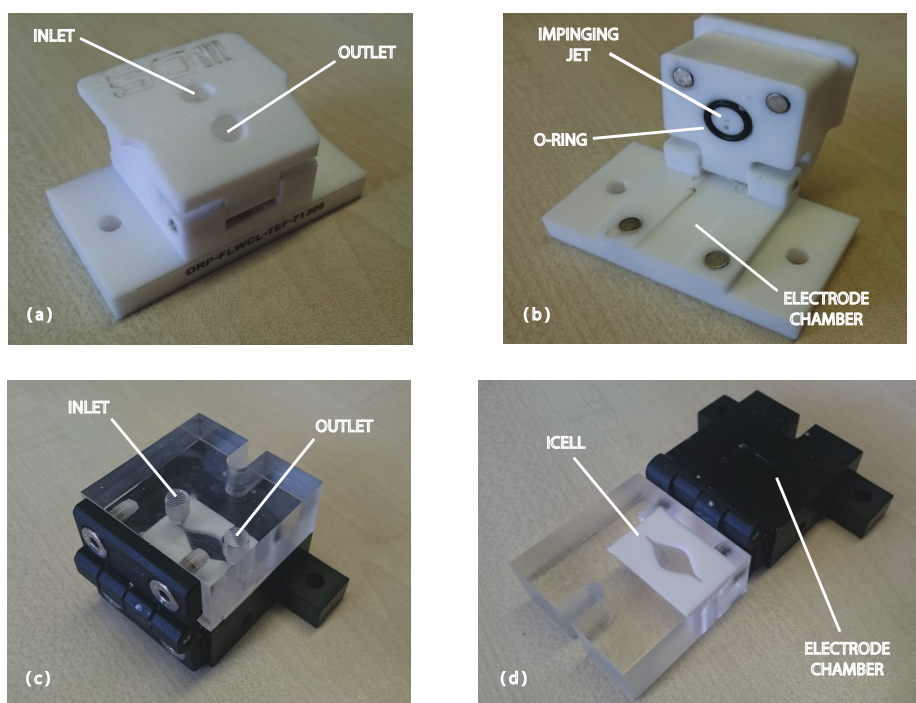


Figure 2.1(a) Impinging jet flow cell (LC-FC-A; closed). (b) The impinging jet flow cell (LC-FC-A; open). (c) iCell channel flow cell (LC-FC-B; closed).(d) iCell channel flow cell (LC-FC-B; open).

The HPLC-UV was connected, in series with the flow-cell (LC-FC-A or LC-FC-B). The flow cells housed the Graphite Screen-printed electrode (GSPE) **Error! Reference source not found.**) to give the HPLC-AD protocol. To distinguish the HPLC-AD system employing either of the flow-cells, the two systems were denoted LC-FC-A and LC-FC-B respectively. Data analysis (HPLC-UV) was carried out using Chemstation for LC (Ver. 10.02) software (Agilent Technologies, Wokingham, UK)

and amperometric measurements were performed using a Palmsens (Palm Instruments BV, The Netherlands) potentiostat/galvanostat and controlled by PSTrace (Ver. 4.4-4.8) (Zuway et al., 2015).

2.2.3 Screen-printing electrodes

GSPEs with a working electrode (3 mm diameter) were fabricated in-house with appropriate stencil designs using a DEK 248 screen-printing machine (DEK, Weymouth, UK) (Smith et al., 2014b). To produce the screen-printed sensors, a carbon-graphite ink formulation (Gwent Electronic Materials Ltd, UK; Product Code: C2000802P2) was screen-printed onto a polyester (Autostat, 250 µm thickness) flexible film (denoted throughout as standard screen-printed electrodes). This layer was cured in a fan oven (60 °C/30 min) and an Ag/AgCl reference electrode incorporated by screen-printing Ag/AgCl paste (Gwent Electronic Materials Ltd, UK; Product Code: C2040308D2) onto the polyester substrate. Finally, a dielectric paste (Gwent Electronic Materials Ltd, UK; Product Code: D2070423D5) was then printed onto the polyester substrate to cover the connections. After curing (60 °C/30 min) the screen-printed electrodes were ready to be used. Note that Dr Christopher W. Foster performed the GSPEs fabrication (Zuway et al., 2015; Blanco et al., 2016), and a new GSPE utilised for each experiment performed, including during the 'street sample' analysis study.

2.2.4 HPLC-AD protocol

There is a demand for analytical techniques capable of determining the drugs and their metabolites in different sample mixtures (Honeychurch, 2016).

HPLC combined with electrochemical detection has been shown to be highly sensitive and specific as well as it's a more economical option than the HPLC-UV technique (Honeychurch, 2016). This technique has been used for the analysis of a

wide range of abused substances, The target analytes are separated chromatographically depending then the separated compounds pass with the mobile phase into the UV detector, then the electrochemical detector (Figure 2.2). Different electrochemical detector systems have been utilised, including amperometry (Honeychurch, 2016). One of the most common electrochemical detection modes employed is amperometry which is based on the analyte being oxidised or reduced at the electrode interface (Honeychurch, 2016). The current formed from the redox reaction is linearly related to the concentration of the analyte and can therefore be used for the quantification of the analytes. In amperometric detection, the analytes flow over the surface of the working electrode (Honeychurch, 2016).

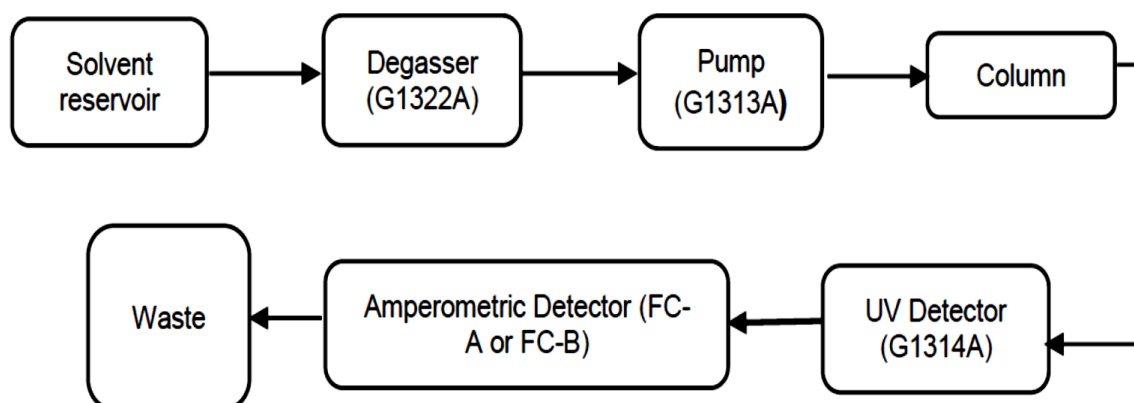


Figure 2.2 Flow diagram of the High performance liquid chromatography-UV-amperometric detection (HPLC-AD) systems (LC-FC-A and LC-FC-B).

2.3 Preparation of buffer solutions:

2.3.1 Preparation of aqueous-50 mM potassium dihydrogen phosphate ($\text{K}_2\text{H}_2\text{PO}_4$)-100 mM potassium chloride buffer (pH 3.2).

Potassium dihydrogen phosphate (6.8 g) and potassium chloride (7.46 g; supporting electrolyte) were weighed accurately, transferred into a 1 L clear glass volumetric flask, and dissolved in deionised water (800 mL). The pH of the solution

was adjusted by dropwise phosphoric acid to pH 3.2, then the solution was made up to volume (1L) using ultra-pure deionised water.

2.3.2 Preparation of aqueous 10 mM ammonium acetate-100 mM potassium chloride buffer (pH 4.3)

Ammonium acetate (0.77 g), and potassium chloride (7.46 g; supporting electrolyte) were weighed accurately, transferred into a 1 L clear glass volumetric flask and dissolved in deionised water (800 mL). The pH of the solution was adjusted by dropwise addition of glacial acetic acid to pH 4.3. The solution was made up to volume (1L) using ultra-pure deionised water.

2.3.3 Preparation of aqueous 10 mM ammonium formate-100 mM potassium chloride buffer (pH 3.5)

Ammonium formate (0.63 g) and potassium chloride (7.46 g; supporting electrolyte) were weighed accurately, transferred into a 1 L clear glass volumetric flask, and dissolved in deionised water (800 mL). The pH of the solution was adjusted by dropwise addition of formic acid (98–100%) to pH 3.5. The solution was made up to volume (1L) using ultra-pure deionised water.

2.3.4 Preparation of aqueous 20 mM ammonium acetate-100 mM potassium chloride buffer (pH 7)

Ammonium acetate (1.54 g) and potassium chloride (7.46 g; supporting electrolyte) were weighed accurately, transferred into a 1 L clear glass volumetric flask and dissolved in deionised water (800 mL). The pH of the solution was adjusted by dropwise addition of glacial acetic acid to pH 7. The solution was made up to volume (1L) using ultra-pure deionised water.

2.4 Preparation of mobile phases

The mobile phases were prepared by mixing amounts of the buffer solution with an organic solution in the appropriate proportions as mentioned in Table 2.3. The mobile phase was vacuum-filtered by using a 0.45 mm pore filter paper and degassed by ultrasonication for 10 mins and the residue of oxygen removed by flashing nitrogen gas through the mobile phase.

Table 2.3. Mobile phases used in this study.

Mobile phase	Composition
1	10:90 % v/v acetonitrile: buffer solution pH = 3.2, Section 2.3.1
2	30:70 % v/v methanol: buffer solution pH = 4.3, Section 2.3.2
3	38:62 % v/v methanol: buffer solution pH = 3.5, Section 2.3.3
4	18:82 % v/v acetonitrile: buffer solution pH = 7, Section 2.3.4
5	25:75 % v/v acetonitrile: buffer solution pH = 7, Section 2.3.5

2.5 Determination the void time (t_0) of HPLC

Uracil (10 mg) was weighed accurately and transferred into a 100 mL clear glass volumetric flask, dissolved in the mobile phase (50 mL). The solution was made up to 100 mL with mobile phase to give a solution containing uracil at 100 $\mu\text{g mL}^{-1}$ then the resultant solution was diluted to obtain 10 $\mu\text{g mL}^{-1}$. The void time was determined from duplicate injections of this solution and the retention time of uracil (un-retained component) eluting from the column.

2.6 Detection and quantification of (±)-MDMA in the presence of (±)-MA and (±)-PMA by using high performance liquid chromatography-amperometric detection

2.6.1 Preparation of standard solutions for determination of λ_{max} of the UV detector

(±)-MDMA (1 mg) was weighed accurately and transferred into a 10 mL clear glass volumetric flask, dissolved and made up to the mark with mobile phase: Mobile Phase 1 (Table 2.3). The resultant solution ($100 \mu\text{g mL}^{-1}$) was used in the determination of the wavelength of maximum absorbance. Solutions of (±)-PMA ($100 \mu\text{g mL}^{-1}$) and (±)-MA ($100 \mu\text{g mL}^{-1}$) were prepared in an analogous manner.

2.6.2 Sample preparation for HPLC method development

(±)-MDMA (1.0 mg) was weighed accurately and transferred into a 10.0 mL clear volumetric glass flask, dissolved in mobile phase 1 (Table 2.3) (5.0 mL). The resultant solution was made up to the mark with mobile phase 1 to give a solution of (±)-MDMA ($100.0 \mu\text{g mL}^{-1}$). This solution was further diluted with mobile phase 1 to a standard solution containing (±)-MDMA ($10.0 \mu\text{g mL}^{-1}$). In addition, (±)-MA (1.0 mg), (±)-PMA (1.0 mg) and a solution containing [(±)-MDMA (1.0 mg), (±)-MA (1.0 mg) and (±)-PMA (1.0 mg)] were prepared in the same manner. Three replicate injections were performed for each of the individual analytes using LC-FC-A and LC-FC-B systems.

2.6.3 Optimisation of potential for amperometric detection (AD)

The resultant mixture solution of (±)-MDMA, (±)-MA and (±)-PMA ($100.0 \mu\text{g mL}^{-1}$ for each component) was prepared as in Section 2.6.1. The solution was injected, in triplicate, into both LC-FC-A and LC-FC-B systems and the amperometric response (peak current, μA) was measured for each analyte, as a

function of anodic potential ($E \text{ V}^{-1}$) between the range +1.1 to +1.8 $E \text{ V}^{-1}$. The data was analysed by using PSTrace version 4.6.

2.6.4 Optimisation of linear velocity for amperometric detection (AD)

A solution of (\pm)-MDMA, (\pm)-MA and (\pm)-PMA ($100.0 \mu\text{g mL}^{-1}$ for each component) was prepared as in Section 2.6.1. The solution was injected ten times in both LC-FC-A and LC-FC-B systems and the amperometric response (peak current, μA) was measured for each analyte, as a function of flow rate between the range 0.9 to 1.2 mL min^{-1} . The data was analysed under the same conditions using PSTrace version 4.6.

2.6.5 Optimisation of HPLC-AD amperometric response under varying pH

Different pH mobile phases were prepared by adjusting Mobile Phase 1 (Table 2.3) by dropwise addition of phosphoric acid to obtain the desired pH in the modified mobile phases (Table 2.4).

Table 2.4 Different pH of Mobile Phase 1

Mobile phase 1	pH
Mobile phase 1A	7.2
Mobile phase 1B	5.2
Mobile phase 1	3.2

(\pm)-MDMA (1.0 mg), (\pm)-MA (1.0 mg) and (\pm)-PMA (1.0 mg) were weighed accurately and transferred into a 10.0 mL clear glass volumetric flask, and dissolved in the appropriate mobile phase (Table 2.4) (5 mL). The resultant solution was made up to 10.0 mL to give a solution containing $100.0 \mu\text{g mL}^{-1}$ of each analyte. The resultant solution of (\pm)-MDMA, (\pm)-MA and (\pm)-PMA ($100.0 \mu\text{g mL}^{-1}$) was injected (ten replicates) using both LC-FC-A and LC-FC-B systems. The amperometric response (peak current, μA), was measured by using a different range of pH (3.2-

7.2), and the data analysed under the same conditions by using PSTrace version 4.6. In addition, the HPLC-UV data was analysed by using Chem-Station for LC (Ver. 10.02) software.

2.6.6 Calibration standards (pure substances):

A solution of (±)-MDMA, (±)-MA and (±)-PMA ($100.0 \mu\text{g mL}^{-1}$) was prepared in Section 2.6.1, and diluted with mobile phase 1 (Table 2.3) to give calibration standards containing $100.0 \mu\text{g mL}^{-1}$, $80.0 \mu\text{g mL}^{-1}$, $60.0 \mu\text{g mL}^{-1}$, $40.0 \mu\text{g mL}^{-1}$, $20.0 \mu\text{g mL}^{-1}$ and $10.0 \mu\text{g mL}^{-1}$ of (±)-MDMA, (±)-MA and (±)-PMA (containing $5.0 \mu\text{g mL}^{-1}$ of uracil). Six replicate injections of each calibration standard were performed by using both systems LC-FC-A and LC-FC-B. The column A (Table 2.2) was used as stationary phase. The column was fitted with C_{18} and maintained at an isothermal temperature of 22°C with an Agilent HP series 1100 column oven with a programmable controller. The detection wavelength was 210 nm; flow rate was 1.2 mL min^{-1} and the injection volume $10.0 \mu\text{L}$.

2.6.7 Specificity standards

Sucrose (5.0 mg), mannitol (5.0 mg) and lactose (5.0 mg) were weighed accurately into separate 10.0 mL clear glass volumetric flasks, then dissolved with mobile phase 1 (Table 2.3) (5.0 mL). The resultant solution was made up to volume with mobile phase 1 to give solutions containing the components at $500.0 \mu\text{g mL}^{-1}$ of each analyte.

2.6.8 Accuracy of the study

5.0 mg (±)-MA, (±)-PMA and (±)-MDMA were weighed accurately into a 10 mL clear volumetric glass flask and diluted to volume with mobile phase 1 (Table 2.3) to give a solution containing $500.0 \mu\text{g mL}^{-1}$ (±)-MA, (±)-PMA and (±)-MDMA. This solution was then further diluted with mobile phase 1 to give solutions containing

60.0 $\mu\text{g mL}^{-1}$, 80.0 $\mu\text{g mL}^{-1}$ and 100.0 $\mu\text{g mL}^{-1}$ of (\pm)-MA, (\pm)-PMA and (\pm)-MDMA.

Three replicate injections of each solution were performed.

2.6.9 Street samples

Five samples of (\pm)-MDMA were obtained from CAHID (University of Dundee, Dundee, UK) and were arbitrarily labelled as MDMA-1, MDMA-2, MDMA-3, MDMA-4 and MDMA-5 (Table 2.1). Each sample (8.0 mg) was weighed in duplicate and transferred into a 100 mL clear glass volumetric flask, then dissolved with mobile phase 1 (Table 2.3) (5 mL). The resultant solution was made up to volume to give a solution of 80.0 $\mu\text{g mL}^{-1}$ which was then injected in triplicate.

2.7 Detection and quantification of (\pm)-mephedrone; (\pm)-4-MEC and caffeine using high performance liquid chromatography-amperometric detection

2.7.1 Preparation of solutions to determination λ_{max} of the UV detector:

(\pm)-mephedrone (1 mg) was weighed accurately and transferred into a 10 mL clear glass volumetric flask, dissolved and made up to the mark with mobile phase 2 (Table 2.3). The resultant solution of (\pm)-mephedrone (100 $\mu\text{g mL}^{-1}$) was used to determine the wavelength of maximum absorbance. The solutions of (\pm)-4-MEC (100 $\mu\text{g mL}^{-1}$) and caffeine (100 $\mu\text{g mL}^{-1}$) were prepared in an analogous manner.

2.7.2 Sample preparation for HPLC method development

(\pm)-mephedrone (5.0 mg) was weighed accurately and transferred into a 10.0 mL clear glass volumetric flask, then dissolved with mobile phase 2 (Table 2.3) (5 mL). The resultant solution was made up to the mark with the mobile phase 2 to give a solution containing 500.0 $\mu\text{g mL}^{-1}$ of (\pm)-mephedrone. This solution was further diluted with mobile phase 2 to a standard solution containing 50.0 $\mu\text{g mL}^{-1}$ (\pm)-mephedrone. In addition, (\pm)-4-MEC (5.0 mg), caffeine (5.0 mg) and a solution

containing [(±)-mephedrone (5.0 mg), (±)-4-MEC (5.0 mg) and caffeine (5.0 mg)] were prepared by using the same above procedure. Three replicate injections were performed for all analytes by using LC-FC-A and LC-FC-B.

2.7.3 Optimisation of potential for amperometric detection (AD)

A mixture of (±)-4-MMC, (±)-4-MEC and caffeine ($500.0 \mu\text{g mL}^{-1}$), as prepared in Section 2.7.2, was diluted with mobile phase 2 to give a standard solution containing $100 \mu\text{g mL}^{-1}$. Three replicate injections of $100 \mu\text{g mL}^{-1}$ of the resultant mixture solution [(±)-mephedrone, (±)-4-MEC and caffeine] were injected using both LC-FC-A and LC-FC-B systems, and the amperometric responses (peak current, μA) were measured for each analyte as a function of anodic potential ($E \text{ V}^{-1}$) over the range +1.1 to +1.4 $E \text{ V}^{-1}$. The data was analysed by using PSTrace version 4.4.

2.7.4 Optimisation of linear velocity for amperometric detection (AD)

A solution of (±)-mephedrone, (±)-4-MEC and caffeine ($500.0 \mu\text{g mL}^{-1}$) was prepared in Section 2.7.2. This solution was then further diluted with mobile phase 2 (Table 2.3) to a standard solution containing $150 \mu\text{g mL}^{-1}$ of mixture solution [(±)-mephedrone, (±)-4-MEC and caffeine]. Ten replicate injections were performed (using both LC-FC-A and LC-FC-B systems) and the amperometric responses (peak current, μA) were measured for each analyte as a function of flow rate between the range 0.8 to 1.0 mL min^{-1} . The data was analysed under the same conditions using PSTrace version 4.4. The optimisation of linear velocity for amperometric detection, for LC-FC-B, was carried out in an analogous manner.

2.7.5 Optimisation of HPLC-AD amperometric response under varying pH

Mobile phase 2 at three different pH was prepared by dropwise addition of glacial acetic acid to obtained three mobile phases.

Table 2.5 Different pH of mobile phase 2

Mobile phase 2	pH
Mobile phase 2A	7.3
Mobile phase 2B	5.3
Mobile phase 2	4.3

(±)-mephedrone (1.0 mg), (±)-4-MEC (1.0 mg) and caffeine (1.0 mg) were weighed accurately and transferred into a 10.0 mL clear glass volumetric flask, then dissolved with different pHs of mobile phase 2 (Table 2.5). The resultant solution was made up to 10.0 mL to give a solution containing 100.0 $\mu\text{g mL}^{-1}$ of each analyte. The resultant mixture solution was injected as ten replicates using the LC-FC-A. The amperometric response (peak current, μA), was measured as a function of pH over the different range of pH (4.3-7.3), and the data analysed under the same conditions by using PSTrace version 4.4. In addition, the HPLC-UV data was analysed by using ChemStation for LC (Ver. 10.02) software. The optimisation of pH for amperometric detection for LC-FC-B, was carried out in an analogous manner.

2.7.6 Calibration standards (pure substances):

The resultant mixture solution (500.0 $\mu\text{g mL}^{-1}$) of (±)-mephedrone, (±)-4-MEC and caffeine was prepared as in Section 2.7.2. The resultant solutions were further diluted with mobile phase 2 (Table 2.3) to give calibration standards containing 500.0 $\mu\text{g mL}^{-1}$, 400.0 $\mu\text{g mL}^{-1}$, 300.0 $\mu\text{g mL}^{-1}$, 200.0 $\mu\text{g mL}^{-1}$, 100.0 $\mu\text{g mL}^{-1}$ and 50.0 $\mu\text{g mL}^{-1}$ of (±)-mephedrone, (±)-4-MEC and caffeine (containing 5.0 $\mu\text{g mL}^{-1}$ of uracil). Six replicate injections of each calibration standard were performed. Column A (Table 2.2) was used as the stationary phase. The column was fitted with a guard cartridge and maintained at an isothermal temperature of 22°C with an Agilent HP series 1100 column oven with a programmable controller. The detection wavelength was 264 nm; flow rate was either 0.8 mL min^{-1} (using LC-FC-A) or 1.0 mL min^{-1} (using LC-FC-B) with an injection volume of 10.0 μL .

2.7.7 Specificity standards

Sucrose (5.0 mg), mannitol (5.0 mg) and lactose (5.0 mg) were weighed accurately into separate 10.0 mL clear glass volumetric flasks, dissolved with mobile phase 2 (Table 2.3) (5 mL) and sonicated using an ultrasonic bath to completely dissolve them. The resultant solution was made up to volume with mobile phase 2 to give solutions containing 500.0 $\mu\text{g mL}^{-1}$ of each analyte.

2.7.8 Accuracy of the study

5.0 mg (\pm)-mephedrone and (\pm)-4-MEC were weighed accurately into a 10 mL clear glass volumetric flask and diluted to volume with mobile phase 2 (Table 2.3) to give a solution containing 500.0 $\mu\text{g mL}^{-1}$ (\pm)-mephedrone and (\pm)-4-MEC. This solution was then further diluted with mobile phase 2 to give solutions containing 240.0 $\mu\text{g mL}^{-1}$, 300.0 $\mu\text{g mL}^{-1}$ and 360.0 $\mu\text{g mL}^{-1}$ of (\pm)-mephedrone and (\pm)-4-MEC. Three replicate injections of each solution were performed.

2.7.9 Street samples

Five street samples of NRG-2 were obtained from web vendors in January 2013 as off-white crystalline powders in sealable bags. These samples were arbitrarily labelled NRG-2-A, NRG-2-B, NRG-2-C, NRG-2-D and NRG-2-E (Table 2.1). 5.0 mg of each substance was weighed (in triplicate) accurately into a 10.0 mL clear glass volumetric flask, dissolved with mobile phase 2 (Table 2.3) (5.0 mL) and the solution sonicated using an ultrasonic bath for 10 mins to completely dissolve them. The resultant solution was made up to volume with mobile phase 2 to give a 500.0 $\mu\text{g mL}^{-1}$ solution. Each sample was injected in duplicate.

2.8 Detection and quantification of (±)-mexedrone and (±)-mephedrone

2.8.1 Characterisation

Melting points were determined using a Stuart melting point apparatus SMP10 (Stuart, Bibby Sterlin Ltd, UK). Thin-Layer Chromatography (TLC) was carried out on aluminium-backed SiO₂ plates (Merck, Darmstadt, Germany) and spots visualised using ultra-violet light (254 nm). Infrared spectra were obtained in the range of 4000–400 cm⁻¹ using a ThermoScientific Nicolet FTIR Smart ITR instrument (ThermoScientific, Rochester, USA). ¹H and ¹³C NMR spectra were recorded on a JEOL ECS-400 (400 MHz) instrument (JEOL, Tokyo, Japan). Ultraviolet spectra were obtained using a Cary 100 Bio UV-visible spectrophotometer (Agilent Technologies, Wokingham, UK).

2.8.1.1 Gas chromatography–mass spectrometry (GC–MS)

Santali et al. reported a gas chromatography-mass spectrometry method for the analysis of mephedrone (Santali et al., 2011). GC–MS analysis was performed using an Agilent HP 5890 Series II GC and a HP 5972 mass selective detector (MSD) (Agilent Technologies, Wokingham, UK). The mass spectrometer was operated in the electron ionisation mode at 70 eV. Using a capillary column (HP5 MS, 30 m × 0.25 mm i.d., 0.25 µm) with helium as the carrier gas at a constant flow rate of 1.2 mL min⁻¹, separation was achieved. The temperature programme of the oven started at 50 °C for 1 minute. It was increased to 220 °C at a rate of 30 °C min⁻¹ and held for 7 minutes then increased by 30 °C min⁻¹ to 320 °C and held for 2 mins. Solutions of 1 mg mL⁻¹ (±)-mexedrone and (±)-mephedrone were prepared in methanol (including 1 mg mL⁻¹ of eicosane as internal standard). A 1 µL aliquot of each solution was injected in the split (100:1) mode with a purge time of 1 minute. The injector and the GC interface temperatures were kept constant at 280 °C. The MS source and quadrupole temperature were set at 230 °C and 150 °C,

respectively. The full scan mode (40-550 amu) was utilised for the mass spectra and the chromatographic separation was monitored in SIM mode. Overall, run time was 16 minutes and mass detected temperature at 300 °C.

2.8.2 Preparation of solution to determine λ_{max} :

(±)-Mexedrone (1.0 mg) was weighed accurately and transferred into a 10 mL clean glass volumetric flask, dissolved and made up to the mark with mobile phase 3 (Table 2.3). The solution of (±)-Mexedrone ($100.0 \mu\text{g mL}^{-1}$) was diluted to obtain a solution containing $9.1 \mu\text{g mL}^{-1}$. This solution was used to determine the wavelength of maximum absorbance. The same procedure was used to prepare a solution of (±)-mephedrone with a concentration of $9.1 \mu\text{g mL}^{-1}$.

2.8.3 Sample preparation for HPLC method development:

(±)-Mexedrone (1.0 mg) was weighed accurately and transferred into a 10.0 mL clean glass volumetric flask, and dissolved with mobile phase 3 (Table 2.3) (5 mL). The resultant solution was made up to the mark with the mobile phase 3 to give a solution containing $100.0 \mu\text{g mL}^{-1}$ of (±)-mexedrone. This solution was further diluted with mobile phase 3 to make a standard solution containing $10.0 \mu\text{g mL}^{-1}$. In addition, (±)-mephedrone (1.0 mg) and a solution containing [(±)-Mexedrone (1.0 mg) and (±)-mephedrone (1.0 mg)] were prepared by the same procedure. Three replicate injections were performed by using LC-FC-A.

2.8.4 Optimisation of potential for amperometric detection (AD)

A solution ($100.0 \mu\text{g mL}^{-1}$) of (±)-Mexedrone and (±)-mephedrone mixture was prepared as described in Section 2.8.3. This solution was injected three times using LC-FC-A. The amperometric response (peak current, μA), for the analyte, was measured as a function of anodic potential (E V^{-1}) over the range +1.1 to +1.4 E V^{-1} . The data were analysed under the same conditions using PSTrace version 4.4.

2.8.5 Optimisation of linear velocity for amperometric detection (AD)

A solution ($100.0 \mu\text{g mL}^{-1}$) of (\pm)-Mexedrone and (\pm)-mephedrone mixture was prepared as described in Section 2.8.3 and injected ten times using LC-FC-A. The amperometric response (peak current, μA), for each analyte, was measured as a function of flow rate over the range 0.8 to 1.2 mL min^{-1} . The data were analysed under the same conditions using PSTRace version 4.4.

2.8.6 Optimisation of HPLC-AD amperometric response under varying pH

Different pH mobile phases 3 were prepared by adjusting mobile phase 3 (Table 2.3) by dropwise addition of formic acid to obtain the desired pH in the modified mobile phases 3 – 3B (Table 2.6).

Table 2.6 Different pH of Mobile Phase 3

Mobile phase 3	pH
Mobile phase 3A	7.5
Mobile phase 3B	5.5
Mobile phase 3	3.5

(\pm)-Mexedrone (1.0 mg) and (\pm)-mephedrone (1.0 mg) were weighed accurately and transferred into 10.0 mL clear glass volumetric flask, dissolved with different pHs of mobile phase 3 (Table 2.3) (5.0 mL). The resultant solutions were made up to 10.0 mL to give a solution containing $100.0 \mu\text{g mL}^{-1}$ of each analyte. The resultant mixture solution ($100.0 \mu\text{g mL}^{-1}$) of (\pm)-Mexedrone and (\pm)-mephedrone mixture was injected ten times by using LC-FC-A. The amperometric response (peak current, μA), was measured as a function of pH over the range of pH 3.5 - 7.5 , and the data analysed under the same conditions by using PSTRace version 4.4. In addition, the HPLC-UV data were analysed by using ChemStation for LC (Ver. 10.02) software.

2.8.7 Calibration standards (pure substances):

A solution ($100.0 \mu\text{g mL}^{-1}$) of (\pm)-Mexedrone and (\pm)-mephedrone mixture was prepared as described in Section 2.8.3. This solution was further diluted with mobile phase 3 (Table 2.3) to give calibration standards containing $500.0 \mu\text{g mL}^{-1}$, $400.0 \mu\text{g mL}^{-1}$, $300.0 \mu\text{g mL}^{-1}$, $200.0 \mu\text{g mL}^{-1}$ and $100.0 \mu\text{g mL}^{-1}$ (\pm)-Mexedrone and (\pm)-mephedrone (containing $5.0 \mu\text{g mL}^{-1}$ of uracil). Six replicate injections of each calibration standard were performed by using LC-FC-A. Column A (Table 2.2) was used as the stationary phase. The column was maintained at an isothermal temperature of 22°C with an Agilent HP series 1100 column oven with a programmable controller. The detection wavelength was 264 nm ; flow rate was 0.8 mL min^{-1} with an injection volume of $10 \mu\text{L}$.

2.8.8 Specificity standards of HPLC-UV

Sucrose (5.0 mg), mannitol (5.0 mg) and lactose (5.0 mg) were weighed accurately into separate 10.0 mL clear glass volumetric flasks, and dissolved with mobile phase 3 (Table 2.3) (5 mL). The resultant solutions were made up to volume with mobile phase 3 to give solutions containing the components at $500.0 \mu\text{g mL}^{-1}$ of each analyte.

2.8.9 Selectivity study of HPLC-UV

10.0 mg of each component (paracetamol, caffeine, (\pm)-mexedrone and (\pm)-mephedrone) was weighed accurately into a 100 mL clear glass volumetric flask and diluted to volume with mobile phase 3 to give a solution containing each component at $10.0 \mu\text{g mL}^{-1}$ (containing $5 \mu\text{g mL}^{-1}$ of uracil as internal standard). Three replicate injections of the solution were performed.

2.8.10 Accuracy study

5.0 mg (\pm)-Mexedrone and (\pm)-mephedrone were weighed accurately into a 10 mL clear glass volumetric flask and diluted to volume with mobile phase 3 (Table 2.3) to give a solution containing $500.0 \mu\text{g mL}^{-1}$ (\pm)-Mexedrone and (\pm)-mephedrone. This solution was then further diluted with mobile phase 3 to give solutions containing $240.0 \mu\text{g mL}^{-1}$, $300.0 \mu\text{g mL}^{-1}$ and $360.0 \mu\text{g mL}^{-1}$ (\pm)-Mexedrone and (\pm)-mephedrone. Three replicate injections of each solution were performed.

2.8.11 Street samples

Four street samples of (\pm)-Mexedrone were obtained from internet vendors (MEX-1, MEX-2 and MEX-3 obtained from Research Chemicals, and MEX-4 obtained from Buckled.eu as explained in table 1 Section 2.1). 3.0 mg of each (\pm)-Mexedrone street sample was weighed (in duplicate) accurately into a 10.0 mL clear glass volumetric flask and diluted to volume with mobile phase 3 (Table 2.3) to give solutions containing the samples at $300 \mu\text{g mL}^{-1}$. The solutions were injected in triplicate for each sample.

2.9 Detection and quantification of (\pm)-2-MEP, (\pm)-3-MEP and (\pm)-4-MEP.

2.9.1 Preparation of solutions to determine λ_{max}

(\pm)-2-MEP (1 mg) was weighed accurately and transferred into a 10 mL clear glass volumetric flask, dissolved and made up to the mark with mobile phase 4 (Table 2.3). The resultant solution of (\pm)-2-MEP ($100 \mu\text{g mL}^{-1}$) was used in determination of the wavelength of maximum absorbance. The solutions of (\pm)-3-MEP ($100 \mu\text{g mL}^{-1}$) and (\pm)-4-MEP ($100 \mu\text{g mL}^{-1}$) were prepared in an analogous manner.

2.9.2 Sample preparation for HPLC method development

(±)-2-MEP (3.0 mg) was weighed accurately and transferred into a 10.0 mL clear glass volumetric flask, dissolved with mobile phase 4 (Table 2.3) (5 mL). The resultant solution made up to the volume with the mobile phase 4 (Table 2.3) to give a solution containing $300.0 \mu\text{g mL}^{-1}$ of (±)-2-MEP. This solution was further diluted with mobile phase 4 (Table 2.3) to a standard solution containing at $20 \mu\text{g mL}^{-1}$. In addition, (±)-3-MEP (3.0 mg), (±)-4-MEP (3.0 mg) and a solution containing [(±)-2-MEP (3.0 mg), (±)-3-MEP (3.0 mg) and (±)-4-MEP (3.0 mg)] were prepared using the same procedure. Three replicate injections were performed by using LC-FC-A.

2.9.3 Optimisation of potential for amperometric detection (AD)

A solution ($100.0 \mu\text{g mL}^{-1}$) of (±)-2-MEP, (±)-3-MEP and (±)-4-MEP mixture was prepared as described in Section 2.9.1 and injected three times by using LC-FC-A and the amperometric response (peak current, μA), for each analyte, was measured as a function of anodic potential (E V^{-1}) over the range +1.0 to +1.4 E V^{-1} . The data were analysed under the same conditions using PSTRace version 4.6.

2.9.4 Optimisation of linear velocity for amperometric detection (AD)

A solution ($300.0 \mu\text{g mL}^{-1}$) of (±)-2-MEP, (±)-3-MEP and (±)-4-MEP mixture was prepared as described in Section 2.9.2 and injected ten times by using LC-FC-A and the amperometric response (peak current, μA), for all analytes, was measured as a function of flow rate over the range 1, 1.5 and 2 mL min^{-1} . The data were analysed under the same conditions using PSTRace version 4.6.

2.9.5 Optimisation of HPLC-AD amperometric response under varying pH

Three mobile phases with different pH were prepared by dropwise glacial acetic acid to produced mobile phases 4 -4B (Table 2.7).

Table 2.7 Different pH of mobile phase 4

Mobile phase 4	pH
Mobile phase 4	7
Mobile phase 4A	5
Mobile phase 4B	3

(\pm)-2-MEP (3.0 mg), (\pm)-3-MEP (3.0 mg) and (\pm)-4-MEP (3.0 mg) were weighed accurately and transferred into 10.0 mL clear glass volumetric flasks, then dissolved in mobile phase 4 of different pHs (Table 8) (5 mL). The resultant solutions were made up to 10.0 mL to give a solution containing 300.0 $\mu\text{g mL}^{-1}$ of each analyte. The resultant mixture solution was injected three times by using LC-FC-A and the amperometric response (peak current, μA), was measured as a function of pH over the range of pH (3-7). The data were analysed under the same conditions by using PSTRace version 4.6. In addition, the HPLC-UV data was analysed by using Chem-Station for LC (Ver. 10.02) software.

2.9.6 Calibration standards (pure substances):

(\pm)-2-MEP (50.0 mg), (\pm)-3-MEP (50.0 mg) and (\pm)-4-MEP (50.0 mg) were weighed accurately and transferred into a 100.0 mL clear glass volumetric flask, and dissolved with mobile phase 4 (Table 2.3) (5 mL). The resultant solution was made up to the volume with mobile phase 4 to give a solution containing the components at 500 $\mu\text{g mL}^{-1}$. This solution was further diluted with mobile phase 4 to give calibration standards containing 500 $\mu\text{g mL}^{-1}$, 400 $\mu\text{g mL}^{-1}$, 300 $\mu\text{g mL}^{-1}$, 200 $\mu\text{g mL}^{-1}$ and 100 $\mu\text{g mL}^{-1}$ of each analyte. Six replicate injections of each calibration standard were performed by using LC-FC-A. Column B (Table 2.2) was maintained at an isothermal temperature of 50°C with an Agilent HP series 1100 column oven with a programmable controller. The detection wavelength was 279 nm; flow rate was 2 mL min^{-1} with an injection volume of 10 μL .

2.9.7 Specificity standards

Sucrose (5.0 mg), mannitol (5.0 mg) and lactose (5.0 mg) were weighed accurately into separate 10.0 mL clear glass volumetric flasks, and dissolved with mobile phase 4 (Table 2.3) (5 mL). The resultant solutions were made up to volume with mobile phase 4 to give solutions containing the components at $500.0 \mu\text{g mL}^{-1}$ for each analyte.

2.9.8 Accuracy of the study

5.0 mg (\pm)-4-MEP, (\pm)-2-MEP and (\pm)-3-MEP were weighed accurately into a 10 mL clear glass volumetric flask and diluted to volume with mobile phase 4 (Table 2.3) to give a solution containing $500.0 \mu\text{g mL}^{-1}$ of (\pm)-4-MEP, (\pm)-2-MEP and (\pm)-3-MEP. This solution was then further diluted with mobile phase 4 to give solutions containing $240.0 \mu\text{g mL}^{-1}$, $300.0 \mu\text{g mL}^{-1}$ and $360.0 \mu\text{g mL}^{-1}$ (\pm)-4-MEP, (\pm)-2-MEP and (\pm)-3-MEP. Three replicate injections of each solution were performed.

2.9.9 Street samples:

Two street samples of (\pm)-MEP were obtained from Greater Manchester Police (GMP) and arbitrarily labelled as MEP-1 and MEP-2 (Table 2.1). 5.0 mg of each street sample of (\pm)-MEP were twice weighed accurately and labelled as (MEP-1-A, MEP-1-B, MEP-2-A and MEP-2-B) into a 100.0 mL clear glass volumetric flask, and dissolved with mobile phase 4 (Table 2.3) (50 mL). The resultant solution made up to volume with Mobile Phase 4 (Table 2.3) to obtain a solution with $50 \mu\text{g mL}^{-1}$ and each sample was injected in triplicate.

2.10 Detection and quantification of (±)-2-FEP, (±)-3-FEP and (±)-4-FEP.

2.10.1 Preparation of solutions to determine λ_{max}

(±)-2-FEP (1 mg) was weighed accurately and transferred into a 10 ml clear glass volumetric flask, dissolved and made up to the mark with mobile phase 5 (Table 2.3). The resultant solution (±)-2-FEP ($100 \mu\text{g mL}^{-1}$) was used in determination of the wavelength of maximum absorbance. The solutions of (±)-3-FEP ($100 \mu\text{g mL}^{-1}$) and (±)-4-FEP ($100 \mu\text{g mL}^{-1}$) were prepared in an analogous manner.

2.10.2 Sample preparation for HPLC method development:

(±)-FEP (5.0 mg) was weighed accurately and transferred into a 10.0 mL clear glass volumetric flask, and dissolved with mobile phase 5 (Table 2.3) (5 mL). The resultant solution made up to the mark with the mobile phase 5 to give a solution containing $500.0 \mu\text{g mL}^{-1}$. This solution was further diluted with mobile phase 5 to a standard solution containing $50.0 \mu\text{g mL}^{-1}$ of (±)-2-FEP. In addition, (±)-3-FEP (5.0 mg), (±)-4-FEP (5.0 mg) and a solution containing [(±)-2-FEP (5.0 mg), (±)-3-FEP (5.0 mg) and (±)-4-FEP (5.0 mg)] were prepared by using the same procedure. Three replicate injections were performed by using LC-FC-A.

2.10.3 Optimisation of potential for amperometric detection (AD)

The resultant solution mixture ($500.0 \mu\text{g mL}^{-1}$) of (±)-2-FEP, (±)-3-FEP and (±)-4-FEP was prepared as in Section 2.10.1. This solution was further diluted to obtain a solution mixture of ($300.0 \mu\text{g mL}^{-1}$) of each analyte. By using LC-FC-A, three replicate injections were performed and the response (peak current, μA), for each analyte, was measured as a function of anodic potential (E V^{-1}) over the range +1.0 to +1.4 E V^{-1} . The data were analysed under the same conditions using PSTrace version 4.8.

2.10.4 Optimisation of linear velocity for amperometric detection (AD)

The resultant solution mixture ($500.0 \mu\text{g mL}^{-1}$) of (\pm)-2-FEP, (\pm)-3-FEP and (\pm)-4-FEP was prepared as in Section 2.10.1. This solution was further diluted to obtain a solution mixture ($300.0 \mu\text{g mL}^{-1}$) of each analyte. Ten replicate injections were made by using LC-FC-A. The amperometric response (peak current, μA), for all analytes, was measured as a function of flow rate over the range 1, 1.5 and 2 mL min^{-1} . The data were analysed under the same conditions using PSTRace version 4.8.

2.10.5 Optimisation of HPLC-AD amperometric response under varying pH

Mobile phase 5 at different pH was prepared by dropwise addition of glacial acetic acid to obtain three mobile phases with different pH (mobile phase 5-5B; table 9).

Table 2.8 Different pH of mobile phase 5

Mobile phase 5	pH
Mobile phase 5	7
Mobile phase 5A	5
Mobile phase 5B	3

(\pm)-2-FEP (1.0 mg), (\pm)-3-FEP (1.0 mg) and (\pm)-4-FEP (1.0 mg) were weighed accurately and transferred into a 10.0 mL clear glass volumetric flask, then dissolved with different pHs of mobile phase 5 (Table 2.3) (5 mL). The resultant solutions were made up to 10.0 mL to give a solution containing $100.0 \mu\text{g mL}^{-1}$ of each analyte. Ten replicate injections were performed by using the LC-FC-A. The amperometric response (peak current, μA), was measured as a function of pH over the range of pH 3-7, and the data analysed under the same conditions by using PSTRace version 4.8. In addition, the HPLC-UV data were analysed by using Chem-Station for LC (Ver. 10.02) software.

2.10.6 Calibration standards (pure substances):

The resultant solution mixture ($500.0 \mu\text{g mL}^{-1}$), of (\pm)-2-FEP, (\pm)-3-FEP and (\pm)-4-FEP was prepared as in Section 2.10.1. This solution was then further diluted with mobile phase 5 (Table 2.3) to give calibration standards containing $500 \mu\text{g mL}^{-1}$, $400 \mu\text{g mL}^{-1}$, $300 \mu\text{g mL}^{-1}$, $200 \mu\text{g mL}^{-1}$ and $100 \mu\text{g mL}^{-1}$ of each analyte. Six replicate injections of each calibration standard were performed by using LC-FC-A. Column B (Table 2.2) was fitted with a guard cartridge and maintained at an isothermal temperature of 50°C with an Agilent HP series 1100 column oven with a programmable controller. The detection wavelength was 270 nm ; flow rate was 1.5 mL min^{-1} with an injection volume of $10.0 \mu\text{L}$.

2.10.7 Specificity standards

Sucrose (5.0 mg), mannitol (5.0 mg) and lactose (5.0 mg) were weighed accurately into separate 10.0 mL clear glass volumetric flasks, then dissolved with mobile phase 5 (Table 2.3) (5 mL) and sonicated using an ultrasonic bath to completely dissolve them. The resultant solutions were made up to volume with mobile phase 5 to give solutions containing the components at $500.0 \mu\text{g mL}^{-1}$ for each analyte.

2.10.8 Accuracy of the study

5.0 mg (\pm)-4-FEP, (\pm)-2-FEP and (\pm)-3-FEP were weighed accurately into a 10 mL clear glass volumetric flask and diluted to volume with mobile phase 5 (Table 2.3) to give a solution containing $500.0 \mu\text{g mL}^{-1}$ (\pm)-4-FEP, (\pm)-2-FEP and (\pm)-3-FEP. This solution was then further diluted with mobile phase 5 to give solutions containing $240.0 \mu\text{g mL}^{-1}$, $300.0 \mu\text{g mL}^{-1}$ and $360.0 \mu\text{g mL}^{-1}$ of (\pm)-4-MEP, (\pm)-2-MEP and (\pm)-3-MEP. Three replicate injections of each solution were performed.

2.10.9 Street samples

Two samples of fluoroephedrine obtained from Greater Manchester Police were arbitrarily labelled as FEP-1 and FEP-2. 5.0 mg of each street sample were weighed (in duplicate) into 100.0 mL clear glass volumetric flasks then diluted to volume with mobile phase 5 to obtain a solution of 50.0 $\mu\text{g mL}^{-1}$. Each sample was injected in triplicate.

2.11 HPLC-UV validation

HPLC-UV method was validated in accordance with the ICH guidelines(ICH, 1996; Marchand et al., 2005)(by using the following parameters: linearity, precision, specificity, limit of detection (LOD), limit of quantification (LOQ) and system suitability [resolution (R_s), column efficiency (N), peak asymmetry (A_s)]. Six replicate injections of the calibration standard solutions were performed to obtain the data of the system suitability, linearity, precision, specificity, %RSD, LOD and LOQ for the HPLC-UV method validation. The LOD and LOQ were calculated based on the standard deviation of the response and the slope.

2.12 Amperometric detection validation:

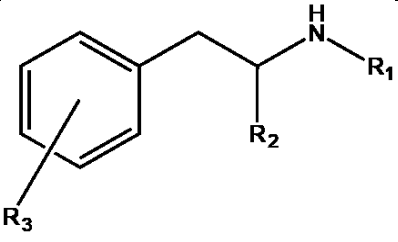
The validation of Amperometric detection (AD) method was performed according to the ICH guidelines(ICH, 1996; Marchand et al., 2005)by using the following parameters: linearity, precision, limit of detection (LOD) and limit of quantification (LOQ). Six replicate injections of the calibration standard solutions were performed to obtain the linearity, precision, LOD and LOQ and the data were analysed. The LOD and LOQ were calculated based on the standard deviation of the response and the slope. The RSD% was calculated for each 6 replicate injections of the samples.

3 Chapter 3: Detection and quantification of (±)-MDMA in the presence of (±)-MA and (±)-PMA by using high-performance liquid chromatography-amperometric detection (HPLC-AD)

3.1 Introduction

The detection of controlled drugs and substances of concern that may be present in the recreationally (ab)used drugs is becoming increasingly essential. (±)-PMA; (Table 3.1a) has attracted considerable media and scientific attention due to its being linked to fatalities internationally, and is often found either in isolation or in combination with (±)-MDMA (Table 3.1b) in recreational drug products sold under the alias 'ecstasy'. Both (±)-MDMA and (±)-MA (Table 3.1c)] are increasingly popular drugs amongst recreational users (Clemens et al., 2007). The (±)-MA has a similar structure to (±)-MDMA and sometimes (±)-MA is sold as, or with, (±)-MDMA in combination. (±)-MDMA and (±)-MA in combination are potentially more dangerous than using each drug in isolation, as suggested by recent research, because they may produce greater adverse neurochemical and behavioural effects (Clemens et al., 2007). This is of some concern given recent evidence that party drug users may frequently be exposed to this combination of drugs (Clemens et al., 2007).

Table 3.1 Chemical structures of methamphetamine, PMA, and MDMA

					
	Name	Acronym	R ₁	R ₂	R ₃
a)	Para-methoxyamphetamine	(±)-PMA	H	CH ₃	4-methoxy
b)	3,4-Methylenedioxymethamphetamine	(±)-MDMA	CH ₃	CH ₃	3,4-methylenedioxy
c)	Methamphetamine	MA	CH ₃	CH ₃	H

The chromatographic analysis of (±)-MDMA is routinely performed in forensic laboratories around the world but not fully validated (Natalia Biziak de Figueiredo¹ and Oliveira^{1*}, 2010; Cumba et al., 2016). The detection of MDMA in biological specimens has been obtained using high performance liquid chromatography (HPLC) with electrochemical (Michel et al., 1993; Zhao et al., 2001), UV (Soares et al., 2004), or diode array detection (DAD) (Helmlin et al., 1996; de Figueiredo et al., 2010), or with fluorescence detection (da Costa and Chasin, 2004).

In previous work, Cumba et al. reported a HPLC separation methodology for (±)-MDMA and (±)-PMA. The limit of detection and quantification for (±)-MDMA were 0.04 µg mL⁻¹ and 0.12 µg mL⁻¹ respectively and for (±)-PMA were 0.08 and 0.26 µg mL⁻¹ (Cumba et al., 2016). In the literature, various analytical methods have been used in the detection of (±)-MA (±)-PMA and (±)-MDMA (Gura et al., 2009; Pichini et al., 2003; Riezzo et al., 2010; Chèze et al.; Martin, 2001; Garrido et al., 2010; Moreno et al., 2012; Nieddu et al., 2007; Tadini et al., 2014; Kato et al., 2008; Wada et al., 2012; Clemens et al., 2007). Table 3.2 summarises the different protocols. The utilisation of electrochemical detection (ED) alongside HPLC has been used for a range of applications such as toxicology, therapeutic drug monitoring, drug metabolism, and pharmacokinetics (Zuway et al., 2015; Kusu, 2015; R. J. Flanagan).

Electrochemical detection using screen-printed graphite electrodes (SPEs) has been studied as a potential analytical technique for simultaneous quantification of (±)-MDMA and (±)-PMA. These SPEs allow for disposable electrochemical devices, potentially providing a simple, cost-effective point-of-care analytical screening tool (Zuway et al., 2015; Kusu, 2015; R. J. Flanagan).

The electroanalytical technique was used in the previous study by Cumba et al. for the detection of (±)-MDMA and (±)-PMA (in their pure form), and gave a detection limit of 0.04 mL and 0.08 $\mu\text{g mL}^{-1}$ respectively. In addition, the differentiation between (±)-MDMA and (±)-PMA utilising cyclic voltammetry has also been reported, where two oxidation peaks were observed at +0.92 V (vs Ag/AgCl) and +1.20 V (vs Ag/AgCl) with limits of detection determined to be 0.25 $\mu\text{g mL}^{-1}$ and 0.14 $\mu\text{g mL}^{-1}$ (Cumba et al., 2016).

This chapter investigates a new methodological approach for the qualitative and quantitative analysis of the psychoactive substances (±)-MDMA, and (±)-MA present in NPSs such as (±)-PMA, using a combination of high performance liquid chromatography with amperometric detection (HPLC-AD). In addition, the difference between commercially available flow cells with an impinging jet flow cell (LC-FC-A) and an iCell channel flow-cell (LC-FC-B) (D. J. Pike) with both incorporating embedded graphitic screen-printed macroelectrodes (GSPE), is presented. GSPEs offer a cost-effective, reproducible and reliable sensor platform for the amperometric detection (AD) of the target analytes and the validation of the technique. Validation has been carried out using the recommended ICH guidelines for analytical confirmation and the most characteristic analytical performances were used ; such as the stability of the solution, and the selectivity, recovery, accuracy, precision, linearity, limits of detection, and limits of quantification were investigated (ICH, 1996; ICH, 2017).

Table 3.2 Analytical methods in the literature used to detect (±)-Paramethoxyamphetamine hydrochloride ((±)-PMA),(±)-3,4-methylenedioxymethamphetamine hydrochloride ((±)-MDMA).

Analyte	Analytical method	Matrix	Analytical linear range	Limit of detection	References
PMA	GC equipped with a nitrogen phosphorus	Peripheral and heart blood	0.125 mg L ⁻¹ to 1.0 mg L ⁻¹	N/A	(Martin, 2001)
MDMA	Square wave voltammetry	Supporting electrolytes, human serum	8 - 45 µM 12 - 45 µM	1.2 µmol L ⁻¹ - 2.4 µmol L ⁻¹	(Garrido et al., 2010)
PMA	Capillary electrophoresis with diode array	Plasma Urine	50 - 5000 ng mL ⁻¹	20.92 ng mL ⁻¹ 24.26 ng mL ⁻¹	(Nieddu et al., 2007)
MDMA	Turn-on fluorogenic probe	Water	N/A - not disclosed	0.13 µM	(Moreno et al., 2012)
MDMA	Thin layer chromatography/ fluorescence	Urine	N/A - not disclosed	50 ng mL ⁻¹	(Kato et al., 2008)
MDMA	HPLC-chemiluminescence	Plasma Hair root Hair shaft	0.01 - 1.0 ng mL ⁻¹ 0.10 - 10 ng mL ⁻¹ 0.10 - 10 ng mL ⁻¹	3 ng mL ⁻¹ 17 ng mL ⁻¹ 14 ng mL ⁻¹	(Wada et al., 2012)
MDMA	Cyclic voltammetry – dip coating/ spin coating	KCl (0.1 mol L ⁻¹)	4.2 - 48 µmol L ⁻¹	3.5/2.7 µmol L ⁻¹	(Tadini et al., 2014)
MDMA PMA MDMA/PMA	Differential plus voltammetry	Mobile phase	0.50 - 4.98 µg mL ⁻¹ 0.50 - 4.98 µg mL ⁻¹ 2.00 – 19.6 µg mL ⁻¹ (for both)	0.04 µg mL ⁻¹ 0.03 µg mL ⁻¹ 0.25 µg mL ⁻¹ / 0.14 µg mL ⁻¹	(Cumba et al., 2016)
MDMA PMA	HPLC-UV	Mobile phase	1.25-40 µg mL ⁻¹	0.08 µg mL ⁻¹ 0.04 µg mL ⁻¹	(Cumba et al., 2016)

3.2 Ultraviolet-visible spectroscopy (UV) Determination of λ_{\max}

The UV/vis spectrophotometer was used to determine the wavelength of maximum absorbance for (±)-MA, (±)-MDMA and (±)-PMA. The strongest absorption for all was obtained at $\lambda_{\max} = 210 \text{ nm}$, and provided the highest absorbance reading for (±)-MA ($A = 0.4794, 1.0 \times 10^{-3} \text{ g } 100\text{mL}^{-1}$), (±)-MDMA ($A = 0.671, 1.0 \times 10^{-3} \text{ g } 100\text{mL}^{-1}$) and (±)-PMA ($A = 0.4661, 1.0 \times 10^{-3} \text{ g } 100\text{mL}^{-1}$), in agreement with the results of (Muller and Windberg, 2005).

3.3 HPLC Method Development

Other researchers have reported utilising HPLC and LC-MS techniques to determine (±)-MDMA and (±)-PMA separately in the toxicological screening of the target analytes (Muller and Windberg, 2005; Stoll et al., 2006). The HPLC method was developed by employing a modified isocratic elution protocol (Section 2.6), to ensure both optimal detection of the analytes and a rapid analysis time. The aim was to develop a HPLC-UV method which could resolve and detect (±)-MDMA, (±)-PMA and (±)-MA with good resolution and a short overall run time. The method was adapted from the HPLC-UV method of Cumba et al. (Cumba et al., 2016), which was itself adapted from the method reported by (Muller and Windberg, 2005). They used a Chromspher B column as the stationary phase (C_{18} , 100 x 3 mm; particle size: 5 μm) with a mobile phase consisting of 0.05M phosphate buffer (pH 3.2): acetonitrile (90:10, % v/v).

In the current study, column A (Table 2.2) was used, with a 3 μm particle size to decrease the eddy diffusion and mass transfer effects, and to improve both the efficiency of the column and the resolution of (±)-MDMA, (±)-PMA and (±)-MA. Decreasing the particle size from 5 μm to 3 μm is known to limit the effect of flow rate on peak efficiency. In this case, reducing the particle size increased the surface

area of the column and improved mass transfer, thereby reducing the effect of band-broadening. Moreover, the smaller particle sizes yielded better overall efficiencies, or less peak dispersion, across a much wider range of proper flow rates. The mobile phase of Muller's et al. method was modified by adding KCl as electrolyte support to improve the electrochemical conductivity of the mobile phase. In addition, the flow rate of the mobile phase in this study was increased to 1.2 mL min⁻¹ to decrease longitudinal diffusion according to the Van Deemter equation and to improve the resolution between the peaks of analytes. The final modification was a decrease in the injection volume to 10 µL from 20 µL to decrease peak width and improve the resolution between peaks (Ren et al., 2013). The temperature was decreased from 30°C to the ambient temperature (22°C).

Using this new method, (±)-MA, (±)-PMA and (±)-MDMA were eluted at 10.56 (10.84), 11.36 (11.68) and 12.09 (12.40) mins respectively by using HPLC-UV detection in LC-FC-A (or LC-FC-B) systems. The resolution for all analytes in both systems was in the range 2.13-2.36 (Figure 3.1).

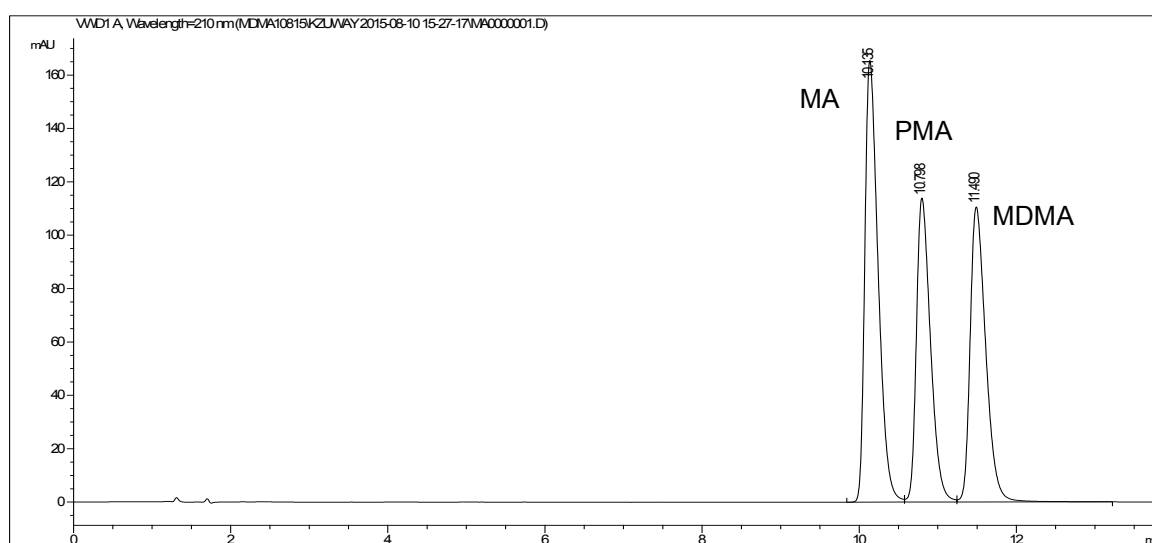


Figure 3.1 Chromatogram of a solution containing (±)-MA, (±)-PMA and (±)-MDMA obtained on a HPLC-UV system (UV detection) using an ACE 3 C₁₈ column (150 mm × 4.6 mm i.d. particle size: 3 µm); flow-rate: 1.2 mL min⁻¹; mobile phase 1; detector wavelength (UV): 210 nm.

Both amperometric detectors used in this study were either of impinging jet flow cell (LC-FC-A) (Gunasingham et al., 1984; Gunasingham, 1984) or iCell channel flow cell (LC-FC-B) design (Pike et al., 2012). These flow cells accommodated graphite screen-printed electrodes without any further modification. The HPLC-AD system required the amperometric detector to be connected behind the UV detector, via PTFE tubing (230 × 1.6 mm, i.d. 0.3 mm, internal volume: 16.25 µL). This configuration reduced the system back pressure and thereby prevented leakages from the flow-cells. To distinguish the HPLC-AD system employing the impinging jet (LC-FC-A) from the iCell channel (LC-FC-B) flow-cells, the two systems were denoted LC-FC-A and LC-FC-B respectively.

3.4 Amperometric detection method development

Optimisation of the anodic potential, linear velocity and pH were performed to achieve the optimal current response and determine the optimal conditions for the maximum electrochemical response before applying this method to the purchased street samples.

3.4.1 Optimisation of the potential of amperometric detection:

The anodic potential was determined using the peak maxima for a solution of (±)-MA, (±)-PMA and (±)-MDMA (all 80 µg mL⁻¹) in mobile phase 1 (Table 2.3), in using optimised instrumental configuration. The optimal instrumental conditions were used for optimisation of the potential according to the best conditions obtained in the method development in Section 3.3 (temperature = 22 °C, flow rate = 1.2 mL min⁻¹ and pH = 3.2). The potential required to obtain the optimal response for the mixture was determined for both LC-FC-A and LC-FC-B systems, by measuring the amperometric response (peak current, µA) as a function of the anodic potential (E V⁻¹), using the range +1.1 to +1.6 E V⁻¹.

Table 3.3. The anodic potential (80 $\mu\text{g mL}^{-1}$) of (\pm)-MA, (\pm)-PMA and (\pm)-MDMA over the range + 1.1 to + 1.6 V^{-1} using mobile phase 1, column: an ACE 3 C_{18} column (150 mm \times 4.6 mm i.d., particle size: 3 μm); at temperature = 22 $^{\circ}\text{C}$, flow rate = 1.2 mL min^{-1} and pH = 3.2 using HPLC-AD detection in LC-FC-A and LC-FC-B systems.

Flow rate	Linear velocity = 1.2 mL min^{-1}					
System	LC-FC-A			LC-FC-B		
Detection	Peak Current (μA)			Peak Current (μA)		
Potential (V)	MA	PMA	MDMA	MA	PMA	MDMA
1.1	n.d.	n.d.	0.755	n.d.	n.d.	0.286
1.2	n.d.	0.299	1.874	n.d.	0.103	0.338
1.3	n.d.	0.310	1.252	n.d.	0.113	0.369
1.4	n.d.	0.800	1.037	n.d.	0.299	0.367
1.5	n.d.	0.887	0.954	n.d.	0.197	0.218
1.6	n.d.	0.677	0.807	n.d.	0.189	0.163
Key: n.d. = not detected						

Table 3.3 shows no response for (\pm)-MA, however, there was a high response for both (\pm)-PMA and (\pm)-MDMA (0.800 μA and 1.037 μA respectively) at 1.4 E V^{-1} and pH = 3.2 using LC-FC-A system. In addition, using the LC-FC-B system also gave no response for (\pm)-MA, but (\pm)-PMA and (\pm)-MDMA produced a good response (0.299 μA and 0.367 μA respectively) at 1.4 E V^{-1} and pH = 3.2. The anodic peaks observed for (\pm)-PMA and (\pm)-MDMA were produced due to the oxidation of the aromatic nucleus of the molecules leading to the formation of a radical cation at low pH (pH = 3.2), but the anodic peak of (\pm)-MA cannot be observed at pH < 9 (Garrido et al., 2010; Masui et al., 1968; Adenier et al., 2004; Gulaboski et al., 2007; Švorc et al., 2014).

Garrido et al. described the electrochemical oxidation mechanism of amphetamine-like drugs and this mechanism matched and explained the reasons why (\pm)-MDMA and (\pm)-PMA oxidised and produced an anodic peak at pH = 3.2 but no response was observed for (\pm)-MA at the same pH (Garrido et al., 2010). Methamphetamine has just one functional group (a secondary amine group) and the anodic peak was not observed because the secondary amine is present only in the

aliphatic part of (±)-MA. This is the most likely electro-oxidisable group (Garrido et al., 2010). The oxidation of the secondary amine group of (±)-MA occurs more readily in alkaline solution, and that was in agreement with the pKa = 9.5 of the amino group in (±)-MA (Logan, 2002; Švorc et al., 2014). Garrido et al. reported that at pH 2, (±)-MDMA produced an anodic peak corresponding to an oxidation on the aromatic nucleus of the (±)-MDMA molecules leading to the formation of a radical cation (Figure 3.2a). At pH 4, another anodic peak corresponding to the oxidation of a species formed by dimerisation of the initial radical cation was observed (Figure 3.2b). Above pH 9, there is another anodic peak due to the oxidation of the secondary amine (Figure 3.2c) and this behaviour has been previously observed within the voltametric profile of (±)-MA (Garrido et al., 2010).

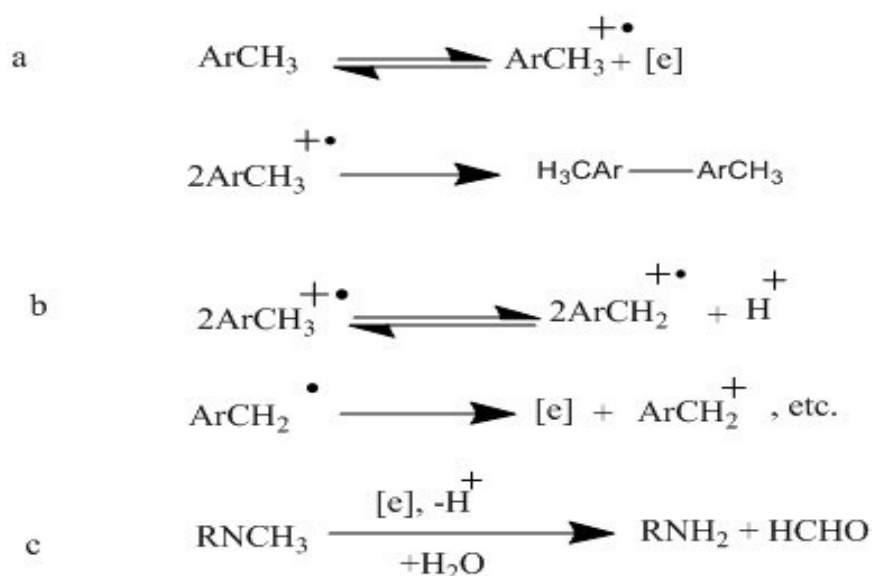


Figure 3.2 Mechanism for the electrochemical oxidation of (±)-MDMA (Garrido et al., 2010)

(±)-MDMA and (±)-PMA are electroactive drugs due to the oxidation of the primary and secondary amino groups and oxidation of the aromatic nucleus (Garrido et al., 2010; Milhazes et al., 2007; Adenier et al., 2004; Švorc et al., 2014). The oxidation of aliphatic amines in aqueous solution is believed to follow the mechanism shown in Figure 3.3 through the abstraction of an electron from the lone-

pair of electrons on the nitrogen atom. In the case of (±)-PMA and (±)-MDMA, the oxidative process occurs more readily under acidic conditions (pH <5) (Garrido et al., 2010; Masui et al., 1968) (Figure 3.3).

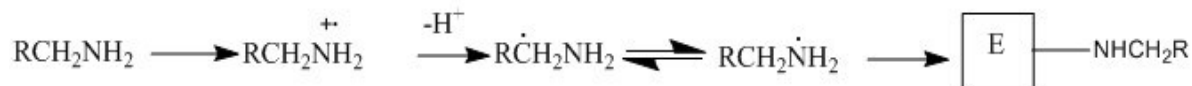


Figure 3.3 Electrochemical oxidation of aliphatic amines, E is the electrode surface (Adenier et al., 2004).

3.4.2 Optimisation of the linear velocity of amperometric detection

The flow rate used in Section 3.3 and Section 3.4.1 was 1.2 mL min⁻¹ because this flow rate produced the optimal response in both sections. However, in this part, due to the variation of the internal chamber volumes of the flow cells (LC-FC-A = 8 µL vs LC-FC-B = 120 µL), the solution of the mixture (100 µg mL⁻¹; prepared in section 2.6.2) was injected (n = 10) over the range of flow rates 0.9-1.2 mL min⁻¹. The amperometric response was measured to determine the optimal linear velocity required for each system. Table 3.4 shows no response for (±)-MA (the reason is as explained in Section 3.3), but a good response for both (±)-PMA and (±)-MDMA (0.800 µA and 1.037 µA respectively) at a flow rate of 1.2 mL min⁻¹, 1.4 E V⁻¹ and pH = 3.2 using the LC-FC-A system. In addition, using the LC-FC-B system gave no response for (±)-MA, but with both (±)-PMA and (±)-MDMA, produced a good response (0.299 V and 0.367 V respectively) at a flow rate of 1.2 mL min⁻¹, 1.4 E V⁻¹. In fact, no response was observed at a flow rate less than 1 mL min⁻¹ or more than 1.2 mL min⁻¹.

Table 3.4 The linear velocity for (100 $\mu\text{g mL}^{-1}$) of (\pm)-MA, (\pm)-PMA and (\pm)-MDMA over the range 0.9 to 1.2 mL min^{-1} using mobile phase 1, column: an ACE 3 C_{18} column (150 mm \times 4.6 mm i.d., particle size: 3 μm); at temperature = 22 $^{\circ}\text{C}$ and pH = 3.2 by using HPLC-AD detection in LC-FC-A and LC-FC-B systems.

Potential	1.4 V^{-1}					
System	LC-FC-A			LC-FC-B		
Detection	Peak Current (μA)			Peak Current (μA)		
Linear Velocity (mL min^{-1})	MA	PMA	MDMA	MA	PMA	MDMA
1.0	n.d.	0.555	0.786	n.d.	0.223	0.257
1.2	n.d.	0.800	1.037	n.d.	0.299	0.367
Key: n.d. = not detected						

3.4.3 Optimisation of pH of HPLC-UV and amperometric detection:

Different pH (3.2– 7.2) were used to find the best pH to obtain the highest response for the analytes. However, the best response for HPLC-UV and HPLC-AD systems were at pH = 3.2. When the pH was increased, the detection response decreased. At pH 9, the drugs are in their free-base form with the ionisation in basic solution, , and will be precipitated from the solution.

At pH extremes (2 or 8), the silica support of the HPLC columns begins to degrade via dissolution, reducing the performance of the column. The maximum amperometric response using the LC-FC-A system was 0.80 μA for (\pm)-PMA and 1.03 μA for (\pm)-MDMA) observed at +1.4 E V^{-1} and a flow rate of 1.2 mL min^{-1} pH = 3.2. As before, there was no response with (\pm)-MA. For the LC-FC-B system, the best amperometric responses were 0.30 μA for (\pm)-PMA and 0.37 μA for (\pm)-MDMA) observed at +1.4 E V^{-1} , flow rate of 1.2 mL min^{-1} and pH = 3.2. Also, there was no response with the (\pm)-MA. In addition, the HPLC-UV detection in both systems was affected when the pH changed from 3.2 with a loss of resolution.

Following the optimisation of amperometric detection (Sections 3.4.1, 3.4.2, and 3.4.3) in LC-FC-A and LC-FC-B systems, the analytes were eluted at 11.38 and

12.11 minutes for (±)-PMA and (±)-MDMA respectively in LC-FC-A system. In LC-FC-B system, the elution was at 11.70 for (±)-PMA and 11.42 for (±)-MDMA. In addition, there was no peak current observed for (±)-MA in both systems (Figure 3.4 and Figure 3.5).

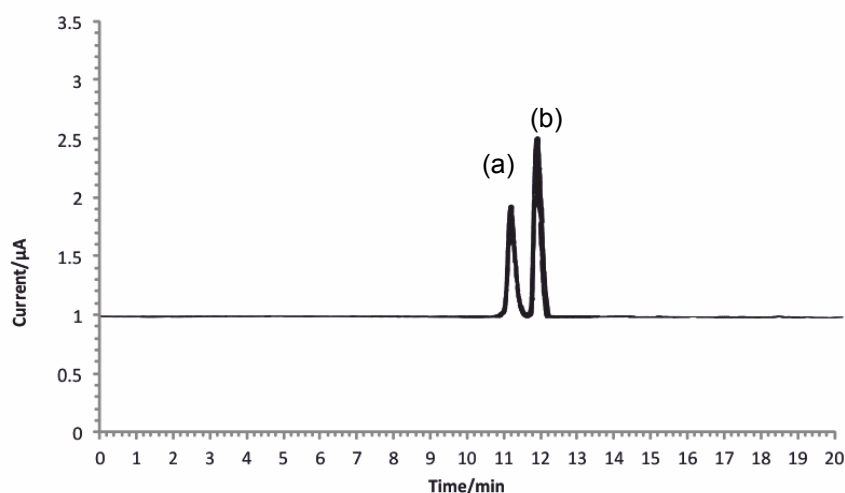


Figure 3.4 Amperogram of a solution containing (±)-MA, (±)-PMA (a) and (±)-MDMA (b) obtained on the LC-FC-A system (amperometric detection) using an ACE 3 C₁₈ column (150 mm × 4.6 mm i.d., particle size: 3 μm); flow-rate: 1.2 mL min⁻¹; mobile phase 1.

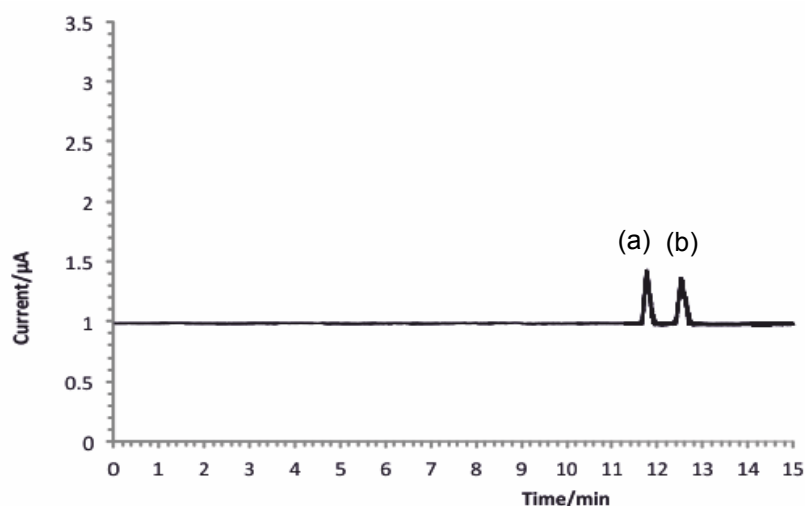


Figure 3.5 Amperogram of a solution containing (±)-MA, (±)-PMA (a) and (±)-MDMA (b) obtained on the LC-FC-B system (amperometric detection) using an ACE 3 C₁₈ column (150 mm × 4.6 mm i.d., particle size: 3 μm); flow-rate: 1.2 mL min⁻¹; mobile phase 1.

3.5 HPLC-AD method validation

Method validation was performed by evaluating system suitability, selectivity and specificity, resolution, linearity, LOD, LOQ, robustness, inter- and intra-day

precision, and accuracy parameters in accordance with the ICH guideline (ICH, 1996). Using simultaneous UV and amperometric detection to separate and detect a standard mixture of (±)-MA, (±)-PMA and (±)-MDMA, the HPLC-UV (UV detection) system and the two HPLC-AD systems (amperometric detection) (LC-FC-A and LC-FC-B), required validation prior to deploying them in the analysis of the purchased street samples. The optimal conditions were used in this study are shown in Table 3.5. The HPLC-UV and HPLC-AD systems used in this study were validated using standard mixtures containing (±)-MA, (±)-PMA and (±)-MDMA over a 10–100.0 $\mu\text{g mL}^{-1}$ range.

Table 3.5 Summary of the optimal conditions utilised for method validation in the analysis (±)-MA, (±)-PMA and (±)-MDMA by using LC-FC-A and LC-FC-B systems.

Optimised chromatographic conditions	
Column	Column A (Section 2.2.1; ACE 3 C18 column (150 mm × 4.6 mm i.d. particle size: 3 μm))
Flow rate	1.2 mL min^{-1}
Solvent	Mobile phase 1 (Table 2.3)
Column temperature ($^{\circ}\text{C}$)	22
Wavelength (nm)	210
Injection volume (μL)	10
Run time (mins)	15
Optimised amperometric detection parameters	
Potential (V)	+1.4
Equilibration time (s)	10
Data interval (s)	0.05
Current range (mA)	$1 \times 10^{-6} - 1$
Total run time (s)	5000

Table 3.6 summarises the validation data for the quantification of (±)-MA, (±)-PMA and (±)-MDMA obtained by HPLC-UV (UV detection) in both LC-FC-A and LC-FC-B systems and using a column A (Section 2.2.1), mobile phase 2 (Table 2.3) and detector wavelength (UV): 210 nm.

Table 3.6 Summary of HPLC-UV validation data for the quantification of (±)-MA, (±)-PMA and (±)-MDMA obtained on HPLC-UV with the LC-FC-A (impinging jet flow cell) or LC-FC-B (iCell flow cell) systems, using column (A) (Table 2.2); mobile phase 1(Section2.4); UV wavelength: 210 nm.

System (Detection)	LC-FC-A (HPLC-UV)		
Analyte	MA	PMA	MDMA
$t_R(\text{min})$	10.56 ^a	11.36 ^a	12.09 ^a
RRT ^c	1.14	1.06	1
Capacity factor (k')	9.56	10.36	11.09
N (plates) ^d	20860.5 (139070)	21077 (140513)	20780 (138533)
H (m)	7.19×10^{-06}	7.12×10^{-06}	7.22×10^{-06}
Resolution (R_s)	-	2.36	2.13
Asymmetry factors	0.81	0.83	0.83
LOD ^c ($\mu\text{g mL}^{-1}$) ^e	0.35	0.33	0.54
LOQ ^d ($\mu\text{g mL}^{-1}$) ^f	1.05	0.99	1.62
Co-efficient of regression (r^2)	0.999 ^g	0.999 ^h	0.999 ⁱ
10 $\mu\text{g mL}^{-1}$	0.71	0.95	0.44
20 $\mu\text{g mL}^{-1}$	0.17	0.38	0.31
40 $\mu\text{g mL}^{-1}$	0.26	0.42	0.16
60 $\mu\text{g mL}^{-1}$	0.10	0.27	0.10
80 $\mu\text{g mL}^{-1}$	0.06	0.13	0.05
100 $\mu\text{g mL}^{-1}$	0.16	0.20	0.08
^a Measured from the retention time of uracil (10 $\mu\text{g mL}^{-1}$) eluting from the column ($t_0 = 1.3$). ^b Measured from the retention time of uracil (10 $\mu\text{g mL}^{-1}$) eluting from the column ($t_0 = 1.45$) ^c Relative retention time (concerning MDMA). ^d N is plates per m. ^e Limit of Detection. ^f Limit of Quantification. ^g $y = 18.436x - 1.782$. ^h $y = 14.133x - 1.7333$. ⁱ $y = 14.233x - 1.6383$.			

Table 3.7 shows a summary of the validation data for the quantification of (±)-MA, (±)-PMA and (±)-MDMA obtained on either flow cell LC-FC-A (impinging jet flow cell; amperometric detection) or LC-FC-B (iCell channel flow cell; amperometric detection) systems using a column A (Section 2.2.1), mobile phase 2 (Table 2.3).

Table 3.7 Summary of HPLC-AD) validation data for quantification of (±)-MA, (±)-PMA and (±)-MDMA obtained on either the LC-FC-A (impinging jet flow cell) or LC-FC-B (iCell flow cell) systems using column (A) Table 2.2; mobile phase 2.

System (Detection)	LC-FC-A (AD)			LC-FC-B (AD)		
Analyte	MA	PMA	MDMA	MA	PMA	MDMA
t_R (min)	n.d.	11.37 ^b	12.10 ^b	n.d.	11.69 ^a	12.41 ^a
RRT ^c	n.d.	1.06	1.00	n.d.	1.06	1.00
LOD ^d (µg mL ⁻¹)	n.d.	5.86	4.68	n.d.	6.12	4.64
LOQ ^e (µg mL ⁻¹)	n.d.	17.60	14.19	n.d.	18.56	14.07
Co-efficient of regression (r^2)	n.d.	0.975 ^h	0.984 ⁱ	n.d.	0.969 ^f	0.982 ^g
Precision (%RSD) (n=6)						
10 µg /mL	n.d.	0.99	0.51	n.d.	0.88	0.81
20µg /mL	n.d.	0.62	0.25	n.d.	0.50	0.81
40µg mL ⁻¹	n.d.	0.70	0.11	n.d.	0.65	0.47
60µg mL ⁻¹	n.d.	0.58	0.12	n.d.	0.73	0.43
80µg mL ⁻¹	n.d.	0.60	0.11	n.d.	0.94	0.54
100 µg mL ⁻¹	n.d.	0.39	0.08	n.d.	0.45	0.41
^a Measured from the retention time of uracil (10 µg mL ⁻¹) eluting from the column (t_0 = 1.3). ^b Measured from the retention time of uracil (10 µg mL ⁻¹) eluting from the column (t_0 = 1.45). ^c Relative retention time (with respect to MDMA). ^d Limit of Detection Limit of Quantification, ^f y = 0.0022x + 0.0814. ^g y = 0.0029x + 0.0733. ^h y = 0.0104x - 0.0699. ⁱ y = 0.0154x - 0.0991. Note: n.d. = not detected.						

3.5.1 System suitability test

These tests were used for both systems (LC-FC-A and LC-FC-B) to confirm that the resolution and reproducibility of the chromatographic system were suitable and that the entire chromatographic system was effective, not only before use, but also during the time of analysis. System suitability was established by using UV detection data (resolution, number of plates and peak asymmetry factor obtained from HPLC-UV software) (ICH, 1996).

The number of theoretical plates (N) explained the sharpness of the peaks and efficiency of the column. The number of theoretical plates of all analytes in HPLC-UV for both LC-FC-A and LC-FC-B systems were >20,000). The greater the number

of theoretical plates, the greater the efficiency of the column. For (±)-MA, the number of theoretical plates was determined (Equation 3.1) to be about 20860.5 and, in addition, the parameter was calculated for the other two analytes: $N = 21077$ for (±)-PMA and $N = 20780$ for (±)-MDMA respectively using both the LC-FC-A and LC-FC-B systems (Table 3.6). Moreover, the similarity in the number of theoretical plates in both systems (LC-FC-A and LC-FC-B) confirmed that both systems were stable and had the same performance and effectiveness of the columns.

$$N = 5.54 \left(\frac{t_R}{W_{0.5}} \right)^2$$

Equation 3.1 Number of Plates

Where: N = number of theoretical plates
 t_R = retention time of peak of interest
 $W_{0.5}$ = width at half the peak height

Capacity factor (K) indicated how long each compound was retained by stationary phase in the column and was calculated as follows:

$$K = t_R - t_0 / t_0$$

Equation 3.2 Capacity factor (K)

Where: t_0 = unrestrained peak retention time
 t_R = retention time of peak of interest

The capacity factor(s) were calculated to be found in both LC-FC-A and LC-FC-B systems as 9.56 for (±)-MA, 10.36 for (±)-PMA and 11.09 (±)-for MDMA (Table 3.6).

Asymmetry factor (A_s)

It's characterised the peak shape of the chromatogram and any deviation of the peak shape makes difficulty to acquisition of information from the chromatographic signal, such as the retention time, the peak area, the peak overlapping, etc. (Pápai and Pap, 2002).

If asymmetric factor > 1, there is peak tailing. In this study, the asymmetric factor for all analytes using both LC-FC-A and LC-FC-B (UV detection data) systems were found within the limit < 1 (Table 3.6).

3.5.2 Resolution (R_s)

The resolution is defined in a chromatographic separation as a quantitative measure of how well two elution peaks are differentiated from each other (Equation 3.3). It is expressed as the difference of the distance between the two peak in retention times ($t_{R2} - t_{R1}$), divided by the combined widths (w_1 and w_2) of the two closely eluting peaks (ICH, 1996).

$$R_s = (t_{R2} - t_{R1}) / 2(W_1 + W_2)$$

Equation 3.3 Resolution (R_s)

Where: t_{R2} = retention time of second peak

t_{R1} = retention time of first peak

W_1 = width of first peak

W_2 = width of second peak

Table 3.6 shows (±)-MA was eluted in both LC-FC-A and LC-FC-B systems at 10.56 min, (±)-PMA eluted at 11.36 min with a high resolution of 2.36 and (±)-MDMA eluted at 12.09 min with a high resolution of 2.13. Therefore, the values of 2.36 and 2.13 obtained in this present study suggest that the HPLC-UV system was able to sufficiently separate target compounds during the analysis.

3.5.3 Selectivity (separation) factor (α) and specificity:

Selectivity is the most important parameter used in analytical method validation. It is the ability to separate the target analyte from interference present in the sample to provide accurate analyte measurements. Commonly, the term 'selectivity' refers to the ability of the method to produce responses for a number of analytes in a complex matrix and its ability to discriminate between them (Vessman, 1996). The selectivity factor is usually measured as a ratio of the retention factors

(capacity factor, k) of the two peaks in Equation 3.4 and can be visualised as the distances between the two peaks.

$$\alpha = K_2/K_1 = (t_2 - t_0)/(t_1 - t_0)$$

Equation 3.4 Selectivity (separation) factor (α)

Where: K_2 = capacity factor of second peak
 K_1 = capacity factor of first peak
 t_2 = retention time of first peak
 t_1 = retention time of second peak
 t_0 = unrestrained peak retention time

Selectivity, therefore, is greatest priority in analytical method developments (Aboul-Enein, 2000). By using UV detection in HPLC analysis, the term of selectivity is very common since it can detect many components present in a sample. The selectivity should be tested against all components present in the sample matrix and these components or interferences have to be separated with acceptable resolution ($R_s > 1.5$) (Maldener, 1989).

The selectivity, tested by using both LC-FC-A and LC-FC-B systems, showed that (\pm)-MA eluted at 10.56 mins and (\pm)-PMA at 11.36 mins with a resolution (R_s) of 2.36 and (\pm)-MDMA eluted at 12.09 mins, $R_s = 2.13$. That means this method has good selectivity to separate (\pm)-MDMA from the other analytes (Figure 3.1). In addition, the specificity of this method was expressed by using the solutions of the UV-inactive analytes sucrose, mannitol, and lactose (which are commonly used as diluents, prepared in Section 2.6.7). These were shown not to interfere with the three target analytes – thereby confirming the specificity of the proposed method.

3.5.4 Linearity

Linearity is used to assess the ability (within a given range) of obtaining a directly proportional relationship between an analyte response and its concentration. Linearity was evaluated across a range of concentrations by visual

inspection of the plot of signals as a function of analyte concentration or using the correlation coefficient, r (usually represented as R^2). Moreover, the statistical calculation was performed to provide the degree of linearity (ICH, 1996). The standards used were 10-100 $\mu\text{g mL}^{-1}$ injected as six replicates using the optimised chromatographic condition at 210 nm using an ACE 3 C₁₈ column (150 mm \times 4.6 mm i.d., particle size: 3 μm). The calibration was constructed (Figure 3.6a) and a good linear response was obtained for HPLC-UV detection in LC-FC-A and LC-FC-B systems. For (\pm)-MA, $R^2 = 0.999$ with precision (%RSD = 0.06–0.71%; $n = 6$); for (\pm)-PMA, $R^2 = 0.999$ with precision (%RSD = 0.13–0.95%; $n = 6$) and for (\pm)-MDMA, $R^2 = 0.999$ with precision (%RSD = 0.05–0.44%; $n = 6$). That explained the excellent linearity for the HPLC-UV system (Appendix Table 9.1, Table 9.2, and Table 9.3).

The corresponding liquid chromatography-amperometric detection system, [LC-FC-A], employing the commercially available, impinging jet, flow cell (LC-FC-A), was validated using standard mixtures containing 10-100 $\mu\text{g mL}^{-1}$ of (\pm)-MA, (\pm)-PMA and (\pm)-MDMA. However, there was not an electrochemical response to (\pm)-MA Figure 3.6c. The good linear response of HPLC-AD (amperometric detection) in LC-FC-A system for (\pm)-PMA, $R^2 = 0.975$ with precision (%RSD = 0.39–0.99%; $n = 6$), and for (\pm)-MDMA, $R^2 = 0.984$ with precision (%RSD = 0.08–0.51%; $n = 6$) (Appendix Table 9.4 and Table 9.5).

The liquid chromatography-amperometric detection system [LC-FC-B], employing the iCell channel flow cell (LC-FC-B), was validated (in terms of UV-detection) using standard mixtures containing the strongly UV-absorbing components (\pm)-MA, (\pm)-PMA and (\pm)-MDMA over a 10–100 $\mu\text{g mL}^{-1}$ range. There was no electrochemical response observed for (\pm)-MA (Figure 3.6d) as explained in Section 3.4.1. The good linear response of amperometric detection in the LC-FC-B

system for (±)-PMA, $R^2 = 0.969$ with precision (%RSD = 0.50 – 0.94%; n = 6) and for (±)-MDMA, $R^2 = 0.982$ with precision (%RSD = 0.41 – 0.81%; n = 6) (Appendix: Table 9.6). In comparing the linearity of three systems (HPLC-UV, LC-FC-A and LC-FC-B), it was observed that the linearity of HPLC-UV is the best, and then the linearity of LC-FC-A and the last one is the linearity of LC-FC-B. Therefore, the HPLC-UV system still the best analytical technique with high sensitivity for the analysis of (±)-MA, (±)-PMA and (±)-MDMA.

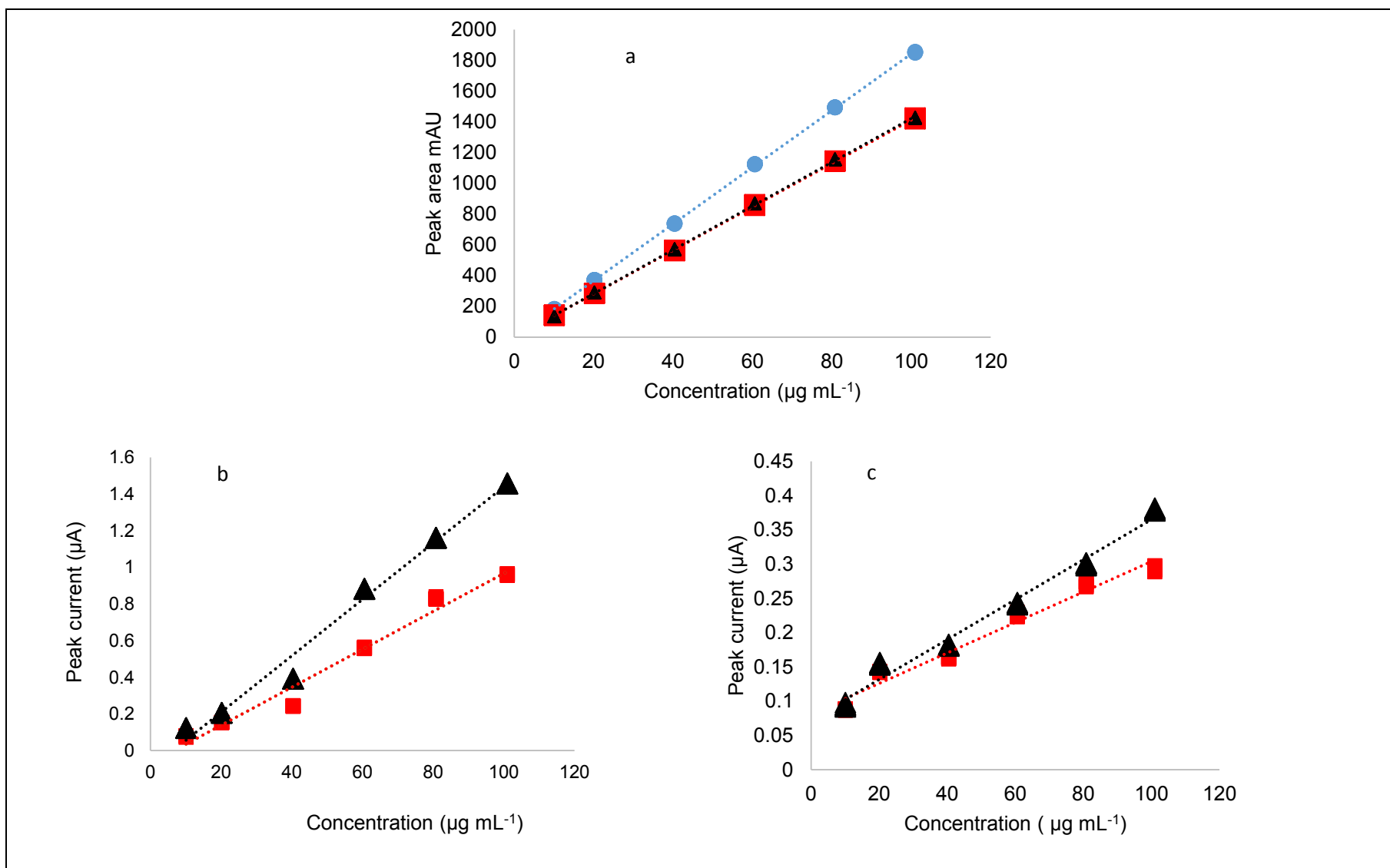


Figure 3.6 The linearity of (±)-MA (circles), (±)-PMA (squares) and (±)-MDMA (triangles) by using a) HPLC-UV of LC-FC-A and LC-FC-B systems. b) HPLC-AD detection of LC-FC-A system. c) HPLC-AD detection of LC-FC-B system.

3.5.5 Limit of detection (LOD)

The detection limit was calculated to determine the lowest analyte concentration which can be detected, and not necessarily to quantitate it. There are several methods to determine the LOD (ICH, 1996), and in this study, the LOD was determined based on the standard deviation of the response and the slope of the calibration curve expressed as:

$$LOD = 3.3(SD)/S$$

Equation 3.5 Limit of detection

Where: S = the slope of the calibration curve (estimated from the calibration curve of the analyte)
SD = the standard deviation of the response (determined based on calibration curve, the standard deviation of y-intercepts of regression lines used as the standard deviation (Shabir, 2003).

The limits of detection of (±)-MA, (±)-PMA and (±)-MDMA obtained using HPLC-UV detection of LC-FC-A and LC-FC-B systems (using the standard deviation of the response and the slope of the calibration graph) were found to be 0.35, 0.33 and 0.54 µg mL⁻¹ respectively (the validation parameters, for the HPLC-UV system, are summarised in Table 3.6). In a previous study, the LOD reported by Cumba et al. (Cumba et al., 2016) for (±)-MDMA and (±)-PMA was lower than the LOD reported in this study, 0.04 µg mL⁻¹ and 0.08 µg mL⁻¹ respectively. This variation is because in this study the linear range used was 10-100 µg mL⁻¹, which is higher than the linear range of by Cumba et al. (1.25-40 µg mL⁻¹) in their previous study.

In the corresponding amperometric detection; the limits of detection using HPLC-AD detection of LC-FC-A system for (±)-PMA and (±)-MDMA were determined (using the standard deviation of the response and the slope of the calibration graph) as being 5.86 µg mL⁻¹ and 4.45 µg mL⁻¹ respectively. The LODs using HPLC-AD in LC-FC-B system for (±)-PMA and (±)-MDMA were 6.12 µg mL⁻¹ and 4.64 µg mL⁻¹ respectively. In addition, the LODs using HPLC-AD detection of

LC-FC-B system for PMA and (±)-MDMA were 6.12 µg mL⁻¹ and 4.64 µg mL⁻¹ respectively. The validation parameters, for the LC-FC-A system, are summarised in Table 3.7.

The LODs for amperometric detection in both LC-FC-A and LC-FC-B systems were higher than the limit of detection of HPLC-UV detection techniques due to used high analytical linear range (high concentration). The LODs in this study by using amperometric detection are higher than the LODs were described by Cumba et al. using cyclic volumetric detection (0.04 µg mL⁻¹ of (±)-MDMA and 0.03 µg mL⁻¹ of (±)-PMA). This variation is because in this study a dynamic system through the flow cell was used instead of the static system used by Cumba et al. Therefore, the time of the analytes on the surface of the electrode was not long for oxidation.

3.5.6 Limit of quantification

The limit of quantification was performed to determine the lowest concentration of the analytes in the sample with acceptable precision and accuracy under the stated operating conditions of the method. The LOQ was determined based on the standard deviation of the response and the slope expressed as:

$$LOQ = 10(SD/S)$$

Equation 3.6 Limit of quantification

Where S = the slope of the calibration curve (estimated from the calibration curve of the analyte)

SD = the standard deviation of the response (estimated based on calibration curve, the standard deviation of y-intercepts of regression lines used as the standard deviation (Shabir, 2003).

The calculation of LOQs for (±)-MA, (±)-PMA and (±)-MDMA using HPLC-UV detection (LC-FC-A and LC-FC-B systems) was determined by the standard deviation of the response and the slope to be 1.05, 0.99 and 1.62 µg mL⁻¹ respectively as summarised in Table 3.6. The LOQs of Cumba's et al. study were

0.26 and 0.12 $\mu\text{g mL}^{-1}$ for (\pm)-PMA and (\pm)-MDMA respectively. These LOQs were lower than the LOQs in this study because Cumba et al. used a lower linear range concentration (1.25-40 $\mu\text{g mL}^{-1}$).

The limit of quantification using HPLC-AD detection of LC-FC-A system was calculated to be 17.60 $\mu\text{g mL}^{-1}$ for (\pm)-PMA and 14.19 $\mu\text{g mL}^{-1}$ for (\pm)-MDMA (Table 3.7). The limits of quantification by using HPLC-AD detection of LC-FC-B for (\pm)-PMA and (\pm)-MDMA were 18.56 $\mu\text{g mL}^{-1}$ and 14.07 $\mu\text{g mL}^{-1}$ respectively (Table 3.7). In comparing the LOQs of this study with that obtained by Cumba et al. (0.04 $\mu\text{g mL}^{-1}$ and 0.03 $\mu\text{g mL}^{-1}$ of (\pm)-PMA and (\pm)-MDMA respectively (pure sample), or 0.25 $\mu\text{g mL}^{-1}$ and 0.14 $\mu\text{g mL}^{-1}$ of (\pm)-PMA and (\pm)-MDMA as mixture), in this study, the LOQs were higher due to this study using a linear range concentration of 10-100 $\mu\text{g mL}^{-1}$ in the LOD, (Section 3.7.6).

3.5.7 Robustness

ICH defined the robustness as a measure of the capacity of the analytical procedure to remain unaffected by small variations in method parameters, and it indicates the reliability during normal usage. One of the robustness evaluations is the system suitability test (resolution test etc.) to ensure the validity of the HPLC method. The HPLC experimental variations include: 1) the effect of a minor change in temperature; 2) the effect of minor variations in the composition of the mobile phase; 3) chromatographic column variation; 4) the effect of minor changes in flow rate; 5) the effect of minor changes in pH of the mobile phase (USE, 2005; Kumar et al., 2010; Bhoomaiah, 2012; Kumar et al., 2012; Baldania et al., 2008; Kaur et al., 2010; Sreedevi et al., 2013; Dhakane and Ubale, 2012; PYLA et al.; Sandhya et al., 2013).

In this study, the effect of temperature variation and change of composition ratio of the mobile phase were analysed to ensure that the HPLC-UV method was

unaffected by these changes. Solutions of (±)-MA, (±)-PMA and (±)-MDMA (all at 60 $\mu\text{g mL}^{-1}$) using six injections at different temperatures (20°C, 22°C, and 24°C) were tested on the HPLC-UV equipment for both LC-FC-A and LC-FC-B systems (the optimal conditions are highlighted and represented for comparison in Tables 3.8 and 3.9). The tables present the effect of small changes of temperature by measuring the relative retention time (RRT) of (±)-MA, (±)-PMA and (±)-MDMA. There was no change with the different temperatures that were used. That means this method has good robustness. At the same time, in comparing the relative retention time data in Table 3.8 (the optimal conditions are highlighted and presented for comparison for both systems LC-FC-A and LC-FC-B), no change was found in the RRT with minor modifications of temperature although both systems had the same method conditions. These results produced confirmation that this method has excellent robustness.

Mixture solutions of (±)-MA, (±)-PMA and (±)-MDMA (all at 60 $\mu\text{g mL}^{-1}$) were prepared with different proportions of acetonitrile: 10mM phosphate buffer – 100mM potassium chloride (pH 3.2) in mobile phase 1. The proportions were 11: 89 v/v, 10:90 v/v and 9:91v/v and six injections were made for each mixture solution. Table 3.9 shows the effect of a minor change in the composition ratio of mobile phase on the HPLC-UV analysis method by measuring relative retention time of (±)-MA, (±)-PMA and (±)-MDMA. The data in Table 3.9 (the optimal conditions are highlighted and represented for comparison) confirm the method was unaffected by changing the composition ratio of the mobile phase. Moreover, in comparing the results of systems LC-FC-A and LC-FC-B, there were similar RRTs, confirming that this method has good robustness.

Table 3.8 Relative retention time (RRT) data of (±)-MA, (±)-PMA and (±)-MDMA using HPLC-UV detection in LC-FC-A and LC-FC-B systems with different temperatures used in the analysis.

Concentration ($\mu\text{g mL}^{-1}$)	RRT (20 °C)			RRT (22 °C)			RRT (24 °C)		
	MA	PMA	MDMA	MA	PMA	MDMA	MA	PMA	MDMA
60	1.141	1.062	1.000	1.146	1.063	1.000	1.148	1.063	1.000
60	1.141	1.062	1.000	1.146	1.063	1.000	1.148	1.063	1.000
60	1.149	1.062	1.000	1.148	1.063	1.000	1.151	1.063	1.000
60	1.150	1.062	1.000	1.142	1.062	1.000	1.143	1.063	1.000
60	1.148	1.063	1.000	1.145	1.062	1.000	1.147	1.063	1.000
60	1.147	1.063	1.000	1.141	1.062	1.000	1.149	1.063	1.000
Average	1.146	1.062	1.000	1.145	1.062	1.000	1.148	1.063	1.000
RSD%	0.330	0.044	0.000	0.220	0.040	0.000	0.229	0.021	0.000

Table 3.9 Relative retention time (RRT) of (±)-MA, (±)-PMA and (±)-MDMA using HPLC-UV detection in LC-FC-A and LC-FC-B systems with minor changes in the composition ratio of the mobile phase.

Concentration $\mu\text{g mL}^{-1}$	RRT								
	(12: 88% v/v) acetonitrile: buffer solution pH = 3.2, Section 2.4			(10:90% v/v) acetonitrile: buffer solution pH = 3.2, Section 2.4			(8:92% v/v) acetonitrile: buffer solution pH = 3.2, Section 2.4		
	MA	PMA	MDMA	MA	PMA	MDMA	MA	PMA	MDMA
60	1.132	1.064	1.000	1.139	1.065	1.000	1.132	1.061	1.000
60	1.133	1.065	1.000	1.139	1.065	1.000	1.134	1.065	1.000
60	1.132	1.064	1.000	1.138	1.065	1.000	1.134	1.065	1.000
60	1.132	1.064	1.000	1.138	1.065	1.000	1.133	1.065	1.000
60	1.132	1.064	1.000	1.138	1.065	1.000	1.133	1.065	1.000
60	1.131	1.064	1.000	1.137	1.065	1.000	1.133	1.065	1.000
Average	1.132	1.064	1.000	1.138	1.065	1.000	1.133	1.064	1.000
RSD%	0.039	0.023	0.000	0.047	0.024	0.000	0.073	0.172	0.000

3.5.8 Inter-and intra-day precision

The precision of the analytical procedure was measured over a short interval of time (repeatability) (ICH, 1996; Kumar et al., 2010; Bhoomaiah, 2012; Kumar et al., 2012; Baldania et al., 2008; Kaur et al., 2010). Twelve replicate injections of a mixed solution of (±)-MA, (±)-PMA and (±)-MDMA (all at $60 \mu\text{g mL}^{-1}$; section 2.6.2) were made on the same day (6 in the morning and 6 in the afternoon). The same procedure was repeated with six injections on the following day. However, the results' precision showed little change between the HPLC-UV detection and amperometric detection in both systems LC-FC-A and LC-FC-B, and the HPLC-

UV detection in both systems had an excellent precision for the three compounds as shown by the RSD% of less than 1% (Table 3.10). In terms of amperometric detection, both systems (LC-FC-A and LC-FC-B) did not detect (±)-MA, as explained in Section 3.4.1, but achieved good precision for both (±)-PMA and (±)-MDMA.

Table 3.10 The relative standard deviation (RSD %) of inter- and intra-day peak current values for (±)-MA, (±)-PMA and (±)-MDMA using HPLC-UV and HPLC-AD detection in both systems (LC-FC-A and LC-FC-B).

RSD %				
n =12	detection	HPLC-UV peak area (mAU)	HPLC-AD (LC-FC-A) peak current (µA)	HPLC-AD (LC-FC-B) peak current (µA)
Inter-day precision	MA	0.099	n.d.	n.d.
	PMA	0.199	0.933	0.943
	MDMA	0.115	0.128	0.412
intra-day precision	MA	0.069	n.d.	n.d.
	PMA	0.223	0.740	0.943
	MDMA	0.161	0.664	0.412
Key: (n.d.) = not detected.				

Table 3.10 shows the RSD% values were calculated from raw data (Appendix: Table 9.7) of the peak area of HPLC-UV detection (RSD% = 0.069 – 0.223 for LC-FC-A and LC-FC-B) or peak current of amperometric detection (RSD% = 0.128 – 0.933 for LC-FC-A and 0.412 - 0.943 for LC-FC-B) were less than 1%. The value of the RSD% is suggested to be $\leq 1\%$ as an appropriate precision criterion for repetitive injections to assess the precision of the instrument in analytical method validation (Green, 1996). These results illustrate the ability of this method and the efficiency of these systems to be applied to routine analysis.

3.5.9 Accuracy

The accuracy test was performed to determine the closeness of agreement between the experimental values to an actual value, which is acceptable, either as a true conventional value or an accepted reference value (ICH, 1996; Kumar et al.,

2010; Bhoomaiah, 2012; Kumar et al., 2012; Baldania et al., 2008; Kaur et al., 2010). Accuracy studies were performed at the 75, 100 and 125 % level of target concentration. Recovery data were obtained from triplicate samples at each level of label claim. Percentage recovery for (±)-MDMA and (±)-PMA were calculated for each sample and demonstrated an excellent accuracy range of 98.2% - 101.9% by using HPLC-UV and HPLC-AD in both system LC-FC-A and LC-FC-B. However, the percentage recovery for (±)-MA was between 99.5% - 101.1% using HPLC-UV but no peak was observed using HPLC-AD in either flow cells LC-FC-A or LC-FC-B (Table 3.11).

Table 3.11 Accuracy data expressed as the percentage recovery of a mixture of (±)-MA, (±)-PMA and (±)-MDMA by using HPLC-UV and HPLC-AD in both systems (LC-FC-A and LC-FC-B).

Detection			HPLC-UV		HPLC-AD (LC-FC-A)		HPLC-AD (LC-FC-B)	
Compound	Concentration (µg mL ⁻¹)	Theoretical recovery (µg mL ⁻¹)	Actual recovery (µg mL ⁻¹)	%Recovery (n=3)	Actual recovery (µg mL ⁻¹)	%Recovery (n=3)	Actual recovery (µg mL ⁻¹)	%Recovery (n=3)
MA	60 (75%)	60.6	61.29	101.1 (±0.22)	n.d.	n.d.	n.d.	n.d.
PMA		60.6	61.21	101.0 (±0.35)	60.5	99.8 (±0.52)	61.36	101.2 (±0.90)
MDMA		60.6	61.43	101.3 (±0.03)	63.76	105.2 (±0.11)	61.62	101.6 (±0.56)
MA	80 (100%)	80.8	81.39	100.7 (±0.06)	n.d.	n.d.	n.d.	n.d.
PMA		80.8	81.35	100.6 (±0.10)	81.04	100.2 (±1.94)	82.39	101.9 (±0.32)
MDMA		80.8	81.65	101.1 (±0.03)	81.87	101.3 (±0.11)	82.3	101.8 (±0.40)
MA	100 (125%)	101.0	100.75	99.7 (±0.14)	n.d.	n.d.	n.d.	n.d.
PMA		101.0	101.04	100.0 (±0.20)	99.24	98.2 (±0.44)	101.08	100.0 (±0.88)
MDMA		101.0	100.58	99.5 (±0.02)	101.1	100.0 (±0.08)	101.97	100.9 (±0.59)

3.6 Application of methodology in a forensic drug analysis context

The viability of the proposed electroanalytical oxidation approach for detecting MA, PMA and MDMA in street samples was tested on five MDMA street samples that were obtained from the University of Dundee and who had previously analysed these samples and determined that these samples contained MDMA. These samples were arbitrarily labelled as MDMA-1, MDMA-2, MDMA-3, MDMA-4, and MDMA-5.

The street samples were analysed (in triplicate) using the validated HPLC-AD protocol, using both flow cells (LC-FC-A and LC-FC-B), at a concentration of $80\text{ }\mu\text{g mL}^{-1}$ [section 2.6.9]. The results of HPLC-UV in both systems, were similar and the five street samples contained MDMA (Table 3.12) the qualitative and quantitative results, obtained from the amperometric detector (HPLC-AD) in both systems also confirmed the constitution of the five street samples a containing MDMA (Table 3.12). The variation in the results was due to the adsorption of the analytes onto the electrode surface of the GSPE. However, as the iCell channel flow cell (LC-FC-B) had a larger chamber volume that had an effect on reducing mass transfer/ diffusion to the electrode surface, due to sample dispersion which may also have been a factor in reducing the sensitivity of the GSPE sensor platform (Zuway et al., 2015). The above results indicate that the HPLC-AD (amperometric detection) system has lower sensitivity than simple HPLC-UV (UV detection). In this work, the proposed HPLC-AD protocol can be considered suitable for the detection and quantification of the MDMA either in its pure form or as a mixed product. In addition, MA and PMA were studied with MDMA in this chapter but not detected in all street samples. That means all the street samples of MDMA were pure.

Table 3.12 Direct comparison between quantitative data obtained by HPLC-UV and amperometric detection (AD), using the LC-FC-A (impinging jet flow cell), or LC-FC-B (iCell channel flow cell) systems, for the analysis of the street samples.

Detection	HPLC-UV (%w/w) (n=3)			HPLC-AD (LC-FC-A) (%w/w) (n=3)			HPLC-AD (LC-FC-B) (%w/w) (n=3)		
Sample	MA	PMA	MDMA	MA	PMA	MDMA	MA	PMA	MDMA
MDMA-1	n.d.	n.d.	35.89 (± 0.27)	n.d.	n.d.	32.29 (± 2.70)	n.d.	n.d.	36.2 (± 2.66)
MDMA-2	n.d.	n.d.	14.94 (± 2.89)	n.d.	n.d.	16.71 (± 2.95)	n.d.	n.d.	16.62 (± 1.78)
MDMA-3	n.d.	n.d.	15.69 (± 0.49)	n.d.	n.d.	16.51 (± 1.64)	n.d.	n.d.	16.40 (± 1.76)
MDMA-4	n.d.	n.d.	28.49 (± 1.31)	n.d.	n.d.	24.77 (± 2.34)	n.d.	n.d.	25.84 (± 1.59)
MDMA-5	n.d.	n.d.	22.14 (± 0.66)	n.d.	n.d.	19.64 (± 2.20)	n.d.	n.d.	21.62 (± 2.54)

3.7 Conclusions

For the first time, the qualitative and quantitative analysis of (\pm)-MDMA using a combination of HPLC with amperometric detection has been reported using two types of flow cell, either an impinging jet flow cell (LC-FC-A) or iCell channel flow (LC-FC-B) cell, incorporating disposable, embedded graphite, screen-printed macroelectrodes (GSPE).

The limit of detection and limit of quantification for both flow cell were similar. Both flow cells have higher detection limits than standard HPLC-UV detection, nevertheless, both flow cells showed good agreement between the quantitative electroanalytical data, thereby making them suitable for the detection and quantification of MDMA, either in its pure form or within a mixed product. However, this protocol can be used to detect and quantify MDMA and PMA using both UV-detection and amperometric detection in LC-FC-A and LC-FC-B systems, but still has some limitations. The limitations of this protocol are such that it can be used just for electroactive analytes and analytes that can become oxidised over the pH range 2-8 to be suitable with the HPLC system (column).

In addition, HPLC-AD cannot be used for oxidizing the analytes at potentials higher than those allowed by the potential window of electrodes (e.g. compounds containing primary amines such as amphetamine and methamphetamine (Pecková, 2011)). The composition of the mobile phase must be compatible with the material of the detection cells housing GSPEs (Pecková, 2011). Despite these limitations to using the high performance liquid chromatography–amperometric detection protocol, it was used in chapter 4 for the detection and quantification of NSPs which are the synthetic cathinones, (\pm)-mephedrone and (\pm)-4-MEC, in presence the common adulterant, caffeine.

4 Chapter 4: Detection and quantification of (±)-mephedrone (±)-4-MEC and common adulterants by using High Performance Liquid Chromatography-Amperometric Detection

4.1 Introduction:

The increase in the abuse and production of cathinone-derived of NPS led to the requirement for rapid, selective and sensitive methods for their qualitative and quantitative analysis. The electrochemical detection for cathinone derivatives has been demonstrated to be an effective method either in their pure form or in mixtures with adulterants (Smith et al., 2014a; Smith et al., 2014b). However, the reported electrochemical techniques are limited in their ability to distinguish between structurally similar cathinone derivatives (for example: (±)-mephedrone and (±)-4-MEC (Table 4.1) when they are both present in a mixture.

The analytical method developed in chapter 3 was successful in detecting and quantifying (±)-MDMA in its pure form or in the presence (±)-PMA. The aim of this chapter was to demonstrate the combination of high performance liquid chromatography HPLC and amperometric detection (AD) for the qualitative and quantitative analysis of (±)-4-mephedrone and (±)-4-MEC using either a commercially available impinging jet (LC-FC-A) or custom-made iCell channel (LC-FC-B) flow-cell system incorporating embedded graphite screen-printed macroelectrodes (GSPEs).

Table 4.1 The chemical structures of (±)-mephedrone and (±)-4-MEC

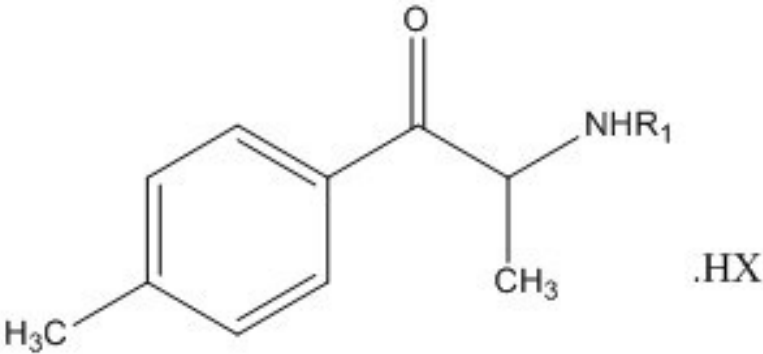
	
Compound	R ₁
(±)-Mephedrone	CH ₃
(±)-4-MEC	CH ₂ CH ₃

Table 4.2 summarises various analytical methods reported in the literature that have been used for the detection of (±)-mephedrone and (±)-4-MEC. The results of different protocols that have been used include the results of this study for comparison.

Table 4.2 Analytical methods in the literature that have been used to detect (±)-mephedrone and (±)-4-MEC

Analyte	Analytical method	Matrix	Analytical linear range	Limit of detection	References
(±)-Mephedrone.HCl	LC-MS/MS	Plasma	78–10,000 ng mL ⁻¹	39 ng mL ⁻¹	(Maskell et al., 2011)
(±)-4-MEC.HBr	LC-MS/MS	Blood, urine	10–1,000 ng mL ⁻¹	0.96 ng mL ⁻¹ (blood), 0.68 ng mL ⁻¹ (urine)	(Gil et al., 2013)
(±)-Mephedrone.HCl	LC-MS/MS	Blood	1–100 ng mL ⁻¹	0.08 ng mL ⁻¹	(Adamowicz et al., 2013)
(±)-Mephedrone.HCl	LC-MS/MS	Blood, urine	20–2,000 ng mL ⁻¹	1 ng mL ⁻¹ (blood), 2 ng mL ⁻¹ (urine)	(Cosbey et al., 2013)
(±)-Mephedrone.HCl	HPLC-UV	Mobile phase	0.5 -25 µg mL ⁻¹	0.1 µg mL ⁻¹	(Santali et al., 2011)
(±)-Mephedrone.HCl	HPLC-UV	Mobile phase	0.5-10 µg mL ⁻¹	0.03 µg mL ⁻¹	(Khreit et al., 2012)
(±)-4-MEC.HBr				0.03 µg mL ⁻¹	
(±)-Mephedrone.HCl	Electrochemistry (electrochemical reduction)	Mobile phase	2.7×10 ⁻⁴ – 1.8 µg mL ⁻¹	2.2 × 10 ⁻⁴ µg mL ⁻¹	(V. Krishnaiah)
(±)-Mephedrone.HCl	Electrochemistry (electrochemical reduction)	Mobile phase	0.00–200.00 µg mL ⁻¹	11.80 µg mL ⁻¹	(Smith et al., 2014b)
(±)-4-MEC.HBr				11.60 µg mL ⁻¹	
(±)-Mephedrone.HCl	Electrochemistry (electrochemical oxidation)	Mobile phase	16–350 µg mL ⁻¹	39.8 µg mL ⁻¹	(Smith et al., 2014a)
(±)-4-MEC.HBr				84.2 µg mL ⁻¹	

4.2 Ultraviolet-visible spectroscopy (UV) determination of λ_{max}

The UV/vis spectrophotometer was used to determine the wavelength producing the highest absorption for (±)-mephedrone and (±)-4-MEC. The wavelength (λ_{max} = 264 nm) showing the most intense absorption was recorded and provided the highest absorbance reading for (±)-mephedrone (A = 0.895, c = 9.1×10^{-4} g/100 mL) and (±)-4-MEC (A = 0.382, c = 9.1×10^{-4} g/100 mL). This wavelength matched data reported by Santali et al. for (±)-mephedrone obtained in deionised water (λ_{max} = 263.5 nm, A = 0.651, c = 9.1×10^{-4} g/100 mL) or 0.1 M aqueous hydrochloric acid (λ_{max} = 263.5 nm, A = 0.662, c = 9.1×10^{-4} g/100 mL) (Santali et al., 2011).

4.3 HPLC Method Development:

The application of HPLC-UV and LC-MS techniques for the analysis of NRG-2 products has been reported by Khreit et al. using an ACE 3 C₁₈ column (150 mm x 4.6 mm i.d., particle size: 3 μm) and a mobile phase consisting of methanol: 10 mM ammonium formate (46:54 % v/v) (Khreit et al., 2012). The validated HPLC-UV method (which can detect (±)-mephedrone hydrochloride, (±)-4-MEC and (±)-caffeine at levels of $0.02 \mu\text{g mL}^{-1}$), was further developed and reported by Smith et al. to analysis the analytes in the presence of other synthetic cathinones and benzocaine based on new intelligence received from law enforcement agencies (Smith et al., 2014a).

A gradient elution program was employed to ensure a rapid analysis time with the optimal detection of the analytes. Gradient elution can change the performance of electrochemical detectors, due to changes in the composition of the electrolyte/eluent employed (Gunasingham et al., 1984).

The original isocratic method was reported by Khreit et al. and adapted to screen the mixture of (±)-caffeine, (±)-mephedrone and (±)-4-MEC in this study, by using HPLC-UV and amperometric detection simultaneously and employing mobile phase 2 (Table 2.3). The percentage of organic modifier in mobile phase 2 was a reduced (30% v/v methanol) and mixed with 10 mM ammonium acetate buffer containing a suitable electrolyte (100 mM KCl, as electrolyte support). The pH of the eluent was adjusted to (4.3) both to ensure the cathinones ((±)-mephedrone: $pK_a = 8.69$ (Santali et al., 2011); (±)-4-MEC: $pK_a = 8.88$ (Khreit et al., 2012)) were fully ionised and, as the electrochemical responses of (±)-mephedrone and (±)-4-MEC have been shown to be sensitive to pH, to optimise their detection amperometrically (Smith et al., 2013; Smith et al., 2014a).

The same amperometric detectors used in the previous study (chapter 3 section 3.3) were used in this study. Based on the previous reported and validated HPLC-UV methods, (Santali et al., 2011; Smith et al., 2014b; Khreit et al., 2012) employed in the separation of (±)-caffeine, (±)-mephedrone and (±)-4-MEC (Santali et al., 2011; Khreit et al., 2012; Smith et al., 2014), an ACE 3 C₁₈ column (150 mm x 4.6 mm i.d. particle size: 3 µm) was selected. The extra-column volumes associated with the system (e.g. connective tubing and /or flow cell internal

volumes) were reduced to minimise the contribution from the LC-FC-A and LC-FC-B parameters respectively - thereby optimising the efficiency of a chromatographic resolution between components within a mixture and ensuring the accuracy of their quantification.

Following the incorporation of the above modifications, (±)-caffeine, (±)-mephedrone and (±)-4-MEC were eluted at 5.5, 9.4 and 11.7 mins respectively as detected using HPLC-UV detection with the LC-FC-A, and eluted at 4.3, 7.5 and 9.3 mins respectively by using HPLC-UV detection in the LC-FC-B system. The resolutions for all analytes in both system was > 2 (Figure 4.1 a & c).

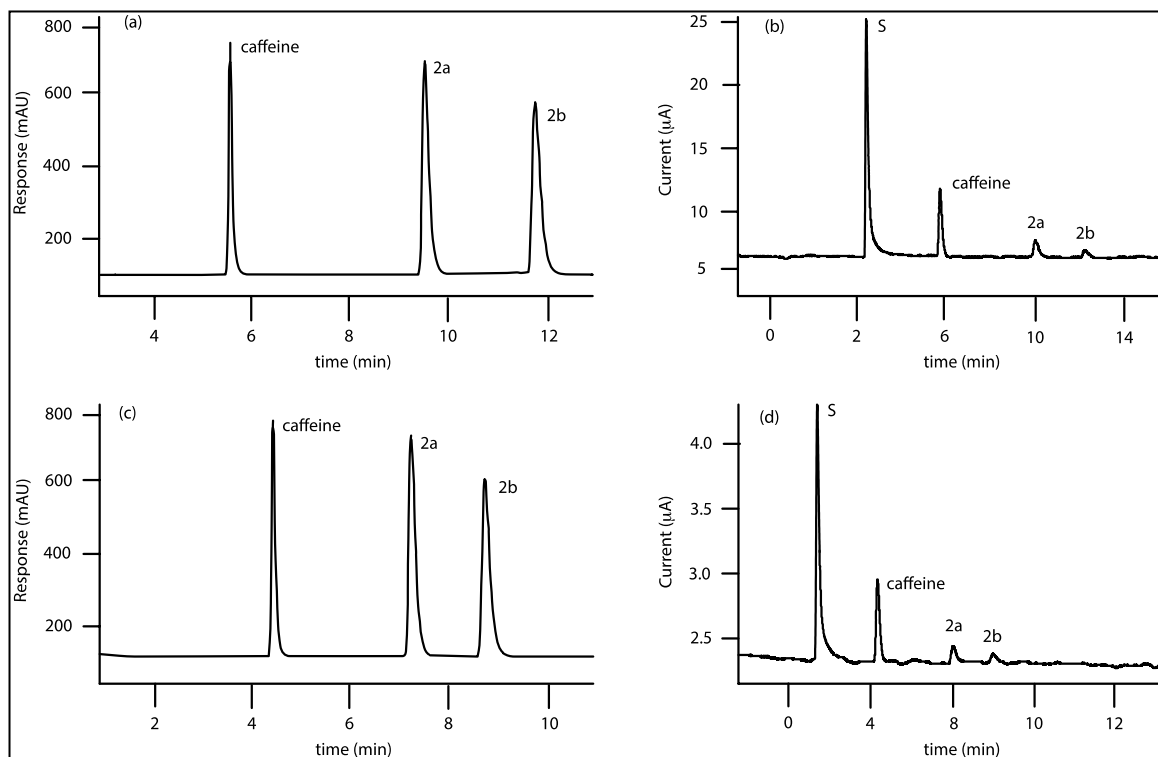


Figure 4.1 Representative chromatogram and amperogram of a solution containing (±)-caffeine, (±)-4-mephedrone and (±)-4-MEC with mobile phase 2 obtained using: (a) HPLC-UV (UV detection) in LC-FC-A system with flow rate: 0.8 mL min^{-1} . (b) HPLC-AD (amperometric detection) in the LC-FC-A system (c) HPLC-UV (UV detection) in the LC-FC-B system with flow rate: 1 mL min^{-1} . (d) HPLC-AD (amperometric detection) in the LC-FC-B system. The t_0 (for both systems) was determined from the retention time of a solution of uracil ($10 \text{ } \mu\text{g mL}^{-1}$). The peak (S) is a system peak associated with the sample injection.

4.4 Amperometric detection method development:

4.4.1 Optimisation of potential of amperometric detection:

The anodic over-potential for (±)-caffeine, (±)-mephedrone and (±)-4-MEC ($100 \mu\text{g mL}^{-1}$, Section 2.7.3) in the mobile phase 2 (Table 2.3) was determined using the peak maxima. In conjunction with the optimised instrumental configuration, the potentials required to achieve the optimal detector response for (±)-caffeine, (±)-mephedrone and (±)-4-MEC, were determined for both LC-FC-A and LC-FC-B, by measuring the amperometric response (peak current, μA) as a function of the anodic potential (E V^{-1}), over the range +1.1 to +1.5 E V^{-1} . The maximum responses were observed by using HPLC-AD in the LC-FC-A system, for caffeine ($1.36 \mu\text{A}$, $n = 3$), (±)-mephedrone ($0.25 \mu\text{A}$, $n = 3$) and (±)-4-MEC ($0.17 \mu\text{A}$, $n = 3$) at +1.4 E V^{-1} and this potential, which was also shown to be optimal, was used herein for the detection of the target analytes.

In terms of the LC-FC-B system, Table 4.3 shows the anodic potential (E V^{-1}) by using HPLC-AD. The maximum peak response was observed for (±)-caffeine ($0.596 \mu\text{A}$, $n = 3$), (±)-mephedrone ($0.124 \mu\text{A}$, $n = 3$) and (±)-4-MEC ($0.07 \mu\text{A}$, $n = 3$) at +1.4 E V^{-1} and this potential was used as the best potential for the detection of the target analytes.

Table 4.3 Representation of the anodic potential (100 $\mu\text{g mL}^{-1}$) of (\pm)-caffeine, (\pm)-mephedrone and (\pm)-4-MEC over the range + 1 to + 1.5 V using mobile phase 2, column : an ACE 3 C_{18} column (150 mm \times 4.6 mm i.d., particle size: 3 μm); at temperature = 22 $^{\circ}\text{C}$, flow rate = 0.8 mL min^{-1} and pH = 4.3 using HPLC-AD detection in LC-FC-A and LC-FC-B systems.

System	LC-FC-A			LC-FC-B		
Flow rate	0.8 mL min^{-1}			1 mL min^{-1}		
Detection	Peak Current (μA)			Peak Current (μA)		
Potential (V)	Caffeine	mephedrone	4-MEC	Caffeine	mephedrone	4-MEC
1.2	0.041	0.059	0.038	0.38	0.041	0.039
1.3	0.259	0.167	0.110	0.4	0.059	0.047
1.4	1.36	0.25	0.17	0.596	0.124	0.07

4.4.2 Optimisation of linear velocity of amperometric detection:

The variation in the volume of the internal chamber of both flow cells (LC-FC-A = 8 μL vs. LC-FC-B = 120 μL) a solution of (\pm)-mephedrone (150 $\mu\text{g mL}^{-1}$, Section 2.7.4) was injected ten times at different flow rates (over the range 0.8 – 1 mL min^{-1}) and the amperometric response measured to determine the optimal linear velocity required for a maximum amperometric response. The system employing the impinging jet flow cell (LC-FC-A, internal chamber volume = 8 μL) gave the highest response, 1.58, 0.47 and 0.39 μA for caffeine, (\pm)-mephedrone and (\pm)-4-MEC, respectively, at a flow rate of 0.8 mL min^{-1} . Increasing the flow rate gave a decreased response with an increase in backpressure, due to the nature of the impinging jet design. The corresponding system employing the iCell channel flow cell (LC-FC-B, internal chamber volume = 120 μL) gave, under similar conditions, the highest response, 0.596, 0.124 and 0.07 μA for caffeine, (\pm)-mephedrone and (\pm)-4-MEC, respectively at flow rate of 1.0 mL min^{-1} .

4.4.3 Optimisation of pH for HPLC-UV and amperometric detection

The pH of the eluent was adjusted to 4.3 to ensure that the analytes were fully ionised. The electrochemical responses of (±)-mephedrone and (±)-4-MEC have been previously been shown to be sensitive to pH, to optimise their detection amperometrically (Smith et al., 2013; Smith et al., 2014a).

By the optimisation of the amperometric detection (section 4.4.1, 4.4.2, and 4.4.3) in LC-FC-A and LC-FC-B systems, the analytes were eluted at 5.52, 9.42 and 11.72 minutes for caffeine, (±)-mephedrone and (±)-4-MEC respectively in LC-FC-A system. In HPLC-FC-B system, the elution was at 4.32 for caffeine, 7.52 for (±)-mephedrone and 9.32 for (±)-4-MEC. (Table 4.1b & d).

4.5 HPLC-AD method validation:

The separation and detection of a standard mixture (500 µg mL⁻¹) of (±)-caffeine, (±)-mephedrone and (±)-4-MEC had been demonstrated using simultaneous UV and amperometric detection. Both HPLC-AD systems (LC-FC-A and LC-FC-B) required validation before deploying them in the analysis of the purchased NRG-2 (street sample) products. The liquid chromatography-amperometric detection system (LC-FC-A), employing the commercially available, impinging jet flow cell (LC-FC-A), was validated (in terms of UV-detection) using standard mixtures

containing strongly UV-absorbing components, (±)-caffeine, (±)-mephedrone and (±)-4-MEC, over a 50 – 500.0 µg mL⁻¹ range. Table 4.4 summarises the optimal conditions used in this study.

Table 4.4 Summary of the optimal conditions utilised for method validation of the analysis of (±)-caffeine, (±)-mephedrone and (±)-4-MEC using LC-FC-A and LC-FC-B systems.

Optimised chromatographic conditions	
Column	Column A (Section 2.2.1; ACE 3 C18 column (150 mm × 4.6 mm i.d., particle size: 3 µm))
Flow rate	0.8 mL min ⁻¹ for LC-FC-A system 1 mL min ⁻¹ for LC-FC-B system
Solvent	Mobile phase: mobile phase 2 C (Table 2.3)
Column temperature (°C)	22
Wavelength (nm)	264
Injection volume (µL)	10
Run time (mins)	15
pH	4.3
Optimised amperometric detection parameters	
Potential (V)	+1.4
Equilibration time (s)	10
Data interval (s)	0.05
Current range (mA)	1 × 10 ⁻⁶ – 1
Total run time (s)	5000

The validation data for the quantification of (±)-caffeine, (±)-mephedrone and (±)-4-MEC are summarised in Table 4.5. These data were obtained by HPLC-UV (UV detection) in both LC-FC-A and LC-FC-B systems and using a column A (Section 2.2.1), mobile phase 2 C, (Table 2.3); detector wavelength (UV): 264 nm.

Table 4.6 Table 4.6 summarises the data of amperometric detection for (±)-caffeine, (±)-mephedrone and (±)-4-MEC by using either the LC-FC-A (impinging jet flow cell) or LC-FC-B (iCell flow cell) systems using column A (Section 2.2.1); mobile phase 2.

4.5.1 System suitability test

System performance was verified to ensure confidence in the analytical method and the results obtained. Table 4.5 shows the retention time, capacity factor, theoretical plates, resolution and asymmetric factor. These parameters are very important to confirm that the analytical equipment and method are suitable for their intended use. The high resolution >2 in both systems. In addition, the theoretical plates were >2000 and the asymmetric factor <1 for all analytes in both systems, which explained that both systems were stable, and they had similar efficiencies with good separation. The developed method, for both systems LC-FC-A or LC-FC-B, showed that all of the standard system suitability parameters were within acceptable limits according to ICH guidelines (ICH, 1996). The HPLC validation parameters, for both systems in Table 4.5 and Table

Table 4.6 were obtained from the calibration standard analysis with their respective correlation coefficients, slopes, and intercepts resulting from linear regression analysis.

Table 4.5 Summary of HPLC-UV (UV detection) validation data for the quantification of caffeine, (±)-mephedrone and (±)-4-MEC obtained on either the LC-FC-A (impinging jet flow cell) or LC-FC-B (iCell flow cell) systems, using column (A) (Table 2.2 mobile phase 2A (Section 2.4); UV wavelength: 264 nm.

System	HPLC-UV with LC-FC-A			HPLC-UV with LC-FC-B		
Flow rate (mL min ⁻¹)	0.8 mL min ⁻¹ (t ₀ = 2.01 min)			1 mL min ⁻¹ (t ₀ = 1.57 min)		
Analyte	Caffeine	mephedrone	4-MEC	Caffeine	mephedrone	4-MEC
Rt ^a (min)	5.5	9.4	11.7	4.3	7.5	9.3
RRt ^b	0.56	1	1.24	0.57	1	1.24
RRF ^c	0.8	1	1.1	0.8	1	1.1
Capacity Factor (k')	1.7	3.7	4.8	1.7	3.7	4.9
N (plates)	10,700 (71,300) ^d	13,000 (86,700) ^d	13,500 (90,000) ^d	10,200 (68,000) ^d	12,800 (85,300) ^d	13,000 (86,700) ^d
H (m)	1.40 x 10 ⁻⁵	1.15 x 10 ⁻⁵	1.11 x 10 ⁻⁵	1.47 x 10 ⁻⁵	1.17 x 10 ⁻⁵	1.15 x 10 ⁻⁵
Resolution (R _s)	-	14.3	5.9	-	14.2	5.98
Asymmetry Factor(A _s)	0.59	0.54	0.53	0.64	0.58	0.56
LOD ^e (µg mL ⁻¹)	2.03	2.50	2.99	1.79	1.95	2.41
LOQ ^f (µg mL ⁻¹)	6.14	7.58	9.05	5.43	5.90	7.29
Co-efficient of Regression	0.999 ^g	0.999 ^h	0.999 ⁱ	0.999 ^j	0.999 ^k	0.999 ^l
Precision (%RSD, n = 6)						
50 µg mL ⁻¹	0.06	0.06	0.05	0.03	0.06	0.03
100 µg mL ⁻¹	0.02	0.01	0.03	0.02	0.01	0.04
200 µg mL ⁻¹	0.04	0.02	0.03	0.03	0.03	0.03
300 µg mL ⁻¹	0.03	0.01	0.03	0.02	0.01	0.01
400 µg mL ⁻¹	0.06	0.05	0.05	0.01	0.02	0.06
500 µg mL ⁻¹	0.02	0.04	0.04	0.02	0.16	0.16
Key: (a) Measured from the retention time of uracil (10 µg mL ⁻¹) eluting from the column. (b) Relative retention time (with respect to (±)-mephedrone). (c) Relative response factor (with respect to (±)-mephedrone). (d) N expressed in plates per m. (e) Limit of Detection. (f) Limit of Quantification. (g) y = 28.005x + 17.842. (h) y = 42.457x – 59.662. (i) y = 40.176x – 72.103. (j) y = 22.325x + 31.399. (k); y = 33.8x – 16.925. (l) y = 32.083x – 34.811.						

Table 4.6 Summary of HPLC-AD (amperometric detection) validation data for quantification of caffeine, (±)-mephedrone and (±)-4-MEC obtained on either the LC-FC-A (impinging jet flow cell) or LC-FC-B (iCell flow cell) systems. Using column A (Table 2.2; mobile phase 2).

System	HPLC-FC-A			HPLC-FC-B		
Analyte	Caffeine	mephedrone	4-MEC	Caffeine	mephedrone	4-MEC
Rt ^a (min)	5.52	9.42	11.72	4.32	7.52	9.32
RRT ^b (min)	0.59	1	1.24	0.57	1	1.24
LOD ^c (µg mL ⁻¹)	12.23	14.66	9.35	23.38	57.92	26.91
LOQ ^d (µg mL ⁻¹)	37.06	44.42	28.33	70.86	175.51	81.54
Co-efficient of regression	0.995 ^d	0.993 ^e	0.997 ^f	0.992 ^g	0.953 ^h	0.990 ⁱ
Precision (%RSD, n = 6)						
50 µg mL ⁻¹	0.58	0.55	0.74	n.d.	n.d.	n.d.
100 µg mL ⁻¹	0.32	0.87	0.81	n.d.	n.d.	n.d.
200 µg mL ⁻¹	0.53	0.91	1.00	0.07	0.19	0.74
300 µg mL ⁻¹	0.53	0.81	0.80	0.32	0.45	0.68
400 µg mL ⁻¹	0.71	0.91	1.00	0.15	0.55	0.45
500 µg mL ⁻¹	0.57	0.87	0.48	0.10	0.87	0.38
<p>Key: n.d. = not determined. (a) Measured from the retention time of uracil (10 µg mL⁻¹) eluting from the column. (b) Relative retention time (with respect to 4-mephedrone). (c) Limit of Detection. (d) Limit of Quantification. (e) $y = 0.0105x + 0.2039$. (f) $y = 0.0025x - 0.0211$. (g) $y = 0.0011x + 0.0082$. (h) $y = 0.0013x + 0.0563$. (i) $y = 0.0003x + 0.0053$. (j) $y = 0.00009x + 0.026$.</p>						

4.5.2 Resolution (R_s)

Both systems (LC-FC-A and LC-FC-B) provided excellent analyte peak resolution ($R_s = >2$) for the UV detection data. The resolution for all analytes was obtained by injecting $500 \mu\text{g mL}^{-1}$ (prepared in Section 2.7.6; $n = 6$) and found the resolution of (\pm)-mephedrone was 14.3 and (\pm)-4-MEC was 5.9 by using the LC-FC-A system. In terms of LC-FC-B system, the resolution of (\pm)-mephedrone was 14.2 and (\pm)-4-MEC was 5.98.

4.5.3 Selectivity factor (α)

Using the optimised parameters (Table 4.4) a mixture of $500 \mu\text{g mL}^{-1}$ of (\pm)-caffeine, (\pm)-mephedrone and (\pm)-4-MEC (prepared in Section 2.7.6) was rapidly separated on both systems. The three analytes eluted at different retention times using LC-FC-A system (Table 4.5), and LC-FC-B system (Table 4.5), exhibiting a baseline resolution $R_s > 2$ and a slight peak fronting (asymmetry factor, $A_s \sim 0.53 - 0.64$) in each case.

The amperometric response corresponding to these solutions showed a slight delay of 1.22 (LC-FC-A, flow-rate = 0.8 mL min^{-1}) and 0.98 sec (LC-FC-B, flow-rate = 1 mL min^{-1}) respectively, due to variation in flow rates and connecting PTFE tubing ($230 \times 1.6 \text{ mm}$, i.d. 0.3 mm , internal volume: $16.25 \mu\text{L}$) between the HPLC-UV and amperometric detectors.

There was no interference of the three target analytes with solution of the UV-inactive analytes sucrose, mannitol and lactose (which are commonly used as diluents) - thereby confirming the specificity of the proposed method.

4.5.4 Linearity

The liquid chromatography-amperometric detection system employing the commercially available, impinging jet, flow cell (LC-FC-A), was validated (in terms of UV-detection) using standard mixtures containing strongly UV-absorbing components (\pm)-caffeine, (\pm)-mephedrone and (\pm)-4-MEC over a 50 – 500.0 $\mu\text{g mL}^{-1}$ range (prepared in Section 2.7.6). All three analytes demonstrated a linear response ($R^2 = 0.999$) (Figure 4.2a) with excellent repeatability ($\text{RSD} = 0.01 - 0.06\%$; $n = 6$) for (\pm)-caffeine, (\pm)-mephedrone and (\pm)-4-MEC (Appendix:

Table 9.8, Table 9.9 and Table 9.10).

In terms of amperometric detection (LC-FC-A), this was carried out using calibration standards 50.0 – 500.0 $\mu\text{g mL}^{-1}$ (prepared in Section 2.7.6) employed in the UV-detection validation study. The data show that the three analytes (\pm)-caffeine, (\pm)-mephedrone and (\pm)-4-MEC gave a linear response ($R^2 = 0.99$) (Figure 4.2b), with good repeatability ($\text{RSD} = 0.32 - 1.00\%$; $n = 6$) (Appendix: Table 9.11, Table 9.12 and Table 9.13).

The corresponding liquid chromatography-amperometric detection system employing the iCell channel flow cell (LC-FC-B) was also validated in terms of UV-detection, after increasing the flow rate to 1 mL min^{-1} to ensure a satisfactory elution time of the three target analytes. As the HPLC-UV detection system was identical to that employed with the impinging jet flow cell (LC-FC-A), the repeatability, specificity and linear response showed no significant differences over the 50.0–500.0 $\mu\text{g mL}^{-1}$ range (prepared in Section 2.7.6) to the system employing the impinging jet flow cell (LC-FC-A). The UV detection in the LC-FC-B system obtained

excellent linearity for all analytes, in which $R^2 = 0.999$ (Figure 4.2c), with good repeatability (RSD = 0.01 – 0.16%; $n = 6$) for (±)-caffeine, (±)-mephedrone and (±)-4-MEC (Appendix: Table 9.14, Table 9.15 and Table 9.16).

Interestingly, in terms of the amperometric detection, the modified system incorporating the iCell channel flow cell (LC-FC-B) demonstrated linearity 0.95-0.99 with good repeatability (RSD = 0.07 – 0.87%; $n = 6$) for the three analytes (Appendix: Table 9.17, Table 9.18 and Table 9.19), However, the linear response was significantly reduced ($R^2 = 0.95 – 0.99$) (Figure 4.2d) over the 200.0 – 500.0 $\mu\text{g mL}^{-1}$ range (Section 2.7.6).

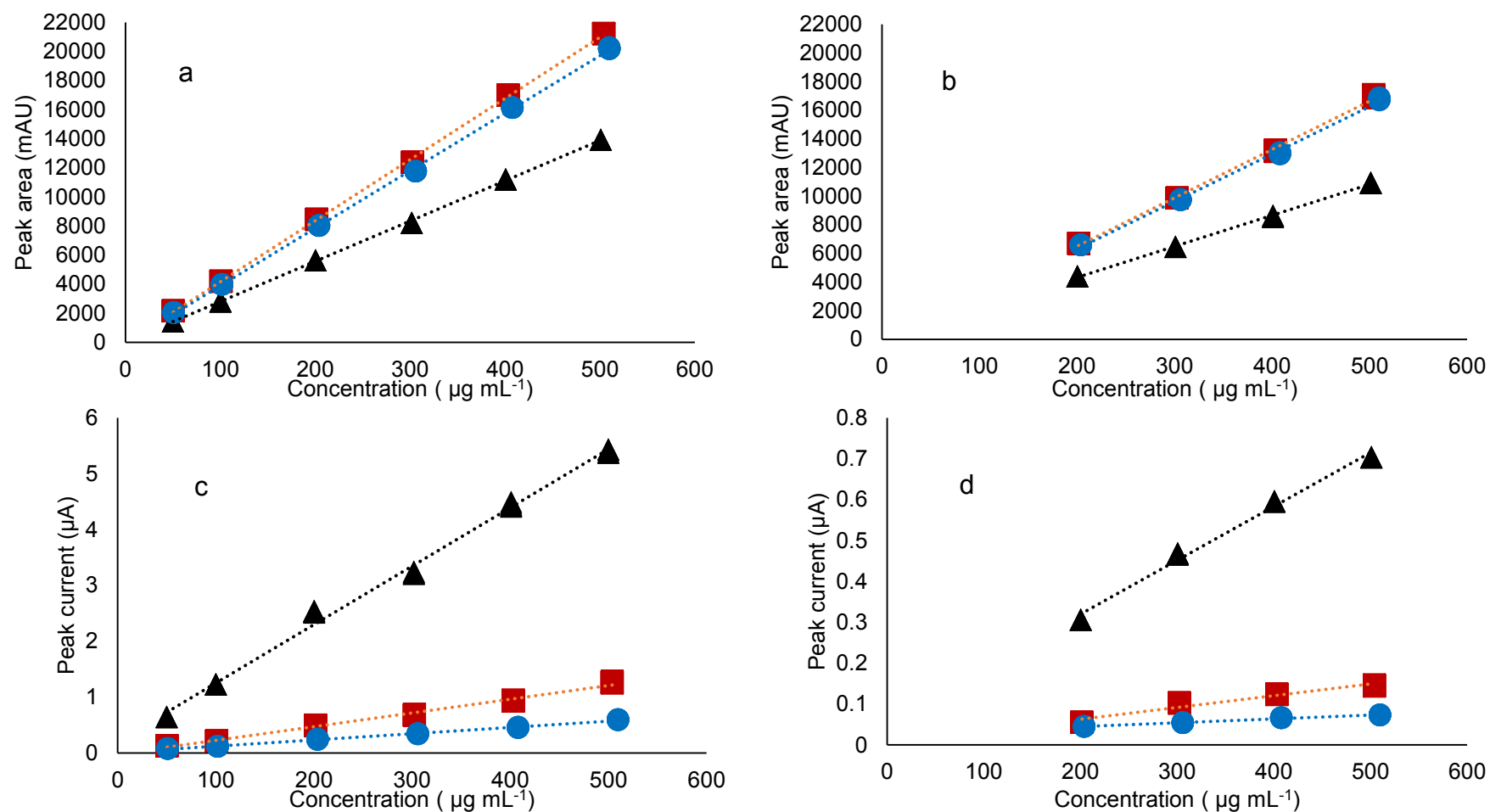


Figure 4.2 The linearity of (±)-caffeine (triangles), (±)-mephedrone (squares) and (±)-4-MEC (circles) by using a) HPLC-UV in the LC-FC-A system. b) HPLC-UV detection in the LC-FC-B system. c) HPLC-AD detection in the LC-FC-A system. d) HPLC-AD detection in the LC-FC-B system.

4.5.5 Limits of detection (LOD)

The limits of detection for the LC-FC-A system for (±)-caffeine, (±)-mephedrone and (±)-4-MEC (using the standard deviation of the response and the slope of the calibration graph; (Section 2.7.6)) were determined to be 2.03, 2.5 and 2.99 $\mu\text{g mL}^{-1}$ respectively, by using HPLC-UV (UV detection)(Table 4.5). In amperometric detection by using impinging jet flow-cell [LC-FC-A], LODs of (±)-caffeine, (±)-mephedrone and (±)-4-MEC were 12.23, 14.66 and 9.35 $\mu\text{g mL}^{-1}$ respectively (Table 4.6), though these are approximately 5× higher than UV-detection, they agree with the previously reported levels of 11.6 $\mu\text{g mL}^{-1}$ for (±)-mephedrone, and 11.8 $\mu\text{g mL}^{-1}$ for (±)-4-MEC) reported by Smith et al. (Smith et al., 2014b).

In the LC-FC-B system using HPLC-UV (UV detection), the LODs were 1.79, 1.95 and 2.41 $\mu\text{g mL}^{-1}$ for (±)-caffeine, (±)-mephedrone and (±)-4-MEC respectively (Table 4.5). The LODs for these components by amperometric detection using the iCell channel flow cell were confirmed as being 23.38, 57.92 and 26.91 $\mu\text{g mL}^{-1}$ for (±)-caffeine, (±)-mephedrone and (±)-4-MEC respectively (Table 4.6), These values are significantly higher than those obtained for the impinging jet flow-cell (LC-FC-A). It is suggested that in the case of the iCell channel flow cell, the larger chamber volume (120 μL), increased sample dispersion, diluting the analytes, and thereby reducing the sensitivity of the GSPE sensor platform via mass transfer/diffusion to the electrode surface (Guidelli, 1971b; Guidelli, 1971a; Oldham, 1973). Therefore, by using LC-FC-B the concentration range was 200-500 $\mu\text{g mL}^{-1}$ unlike the LC-FC-A range that was 50-500 $\mu\text{g mL}^{-1}$.

The LODs calculated using amperometric detection in both systems (LC-FC-A and LC-FC-B) were higher than the limits of detection for UV detection. In addition,

the LODs calculated using amperometric detection (HPLC-AD) were higher than the LODs obtained using UV detection (HPLC-UV) and HPLC-MS/MS. This was because in HPLC-AD, a high range of analyte concentrations were needed in this study.

4.5.6 Limits of quantification (LOQ)

The LOQs of (±)-caffeine, (±)-mephedrone and (±)-4-MEC by using UV detection of the LC-FC-A system were determined using the standard deviation of the response and the slope of the calibration graph (Section 2.7.6) to be 6.14 $\mu\text{g mL}^{-1}$ for (±)-caffeine, 7.58 $\mu\text{g mL}^{-1}$ for (±)-mephedrone and 9.05 $\mu\text{g mL}^{-1}$ for (±)-4-MEC. The LOQ was approximately 50× less sensitive in these terms than with the previously reported HPLC methods employing UV detection, (Santali et al., 2011; Khreit et al., 2012; Smith et al., 2014a; Smith et al., 2014b). At concentrations lower than 50 $\mu\text{g mL}^{-1}$, the ability to detect and accurately quantify the analytes using amperometry was shown not to be viable. In terms of amperometric detection by using LC-FC-A, the limits of quantification were determined from the standard deviation of the response and the slope of the calibration graph (Section 2.7.6), to be 37.06 for (±)-caffeine, 44.42 for (±)-mephedrone and 28.33 $\mu\text{g mL}^{-1}$ for (±)-4-MEC. The validation parameters for the LC-FC-A system are summarised in Table 4.5 and Table 4.6.

The LOQ of (±)-caffeine, (±)-mephedrone and (±)-4-MEC using UV detection of the LC-FC-B system were found to be 5.43 for (±)-caffeine, 5.90 for (±)-mephedrone and 7.29 $\mu\text{g mL}^{-1}$ for (±)-4-MEC. These results were lower than those obtained for UV detection using LC-FC-A. The LOQ of amperometric detection using the LC-FC-B system were found to be 70.86 for (±)-caffeine, 175.5 for (±)-mephedrone and 81.54 $\mu\text{g mL}^{-1}$ for (±)-4-MEC. In comparing, the LOQ of both

systems LC-FC-A and LC-FC-B, the LC-FC-A had a higher sensitivity than the LC-FC-B system (as explained in the LOD Section 4.5.5). The detection validation parameters, for the LC-FC-B system, are summarised in Table 4.5 and Table 4.6.

4.5.7 Robustness

This test described the ability to reproduce the HPLC-AD method under different circumstances and in different laboratories without the occurrence of unexpected differences in the obtained results. The assays for the robustness evaluation of the analytical method were carried out simultaneously in both systems.

Minor changes in temperature were used as one of the parameters to ensure the reliability of the robustness test using LC-FC-A and LC-FC-B systems for the analysis of (±)-caffeine, (±)-mephedrone and (±)-4-MEC. The robustness of this method was obtained by injecting $400\text{ }\mu\text{g mL}^{-1}$ of analytes ((±)-caffeine, (±)-mephedrone and (±)-4-MEC, Section 2.7.6). The relative standard deviation (RSD %) of the relative retention time for all runs at different temperatures ($20\text{ }^{\circ}\text{C}$, $22\text{ }^{\circ}\text{C}$ and $24\text{ }^{\circ}\text{C}$) was found to be less than 1 using LC-FC-A system (Table 4.7; the optimal conditions are highlighted for comparison). By using the LC-FC-B system, the RSD% were less than one (Table 4.9; the optimal conditions are highlighted for comparison). Therefore, this method is robust and indicated the methods' reliability during normal usage.

The second parameter of the robustness test was a change in the ratio of the organic composition of the mobile phase: mobile phase 2 (Table 2.3) by using different ratios (28:72, 30:70 and 32:68 % v/v of methanol: buffer solution A, Section

2.3.1). The RSDs% of relative retention time for all analytes were less than 1 as demonstrated in Table 4.8 and Table 4.10 (the optimal conditions are highlighted for comparison). This showed that this method is suitable to use in routine analysis under any minor change in ratio of mobile phase 2 composition.

Table 4.7 The effect of minor changes of temperature on relative retention time (RRT) of (±)-caffeine, (±)-mephedrone and (±)-4-MEC using HPLC-UV detection in LC-FC-A systems (highlighted area is the standardised condition of this method).

Concentration ($\mu\text{g mL}^{-1}$)	RRT								
	(20 °C)			(22 °C)			(24 °C)		
	Caffeine	4-MMC	4-MEC	Caffeine	4-MMC	4-MEC	Caffeine	4-MMC	4-MEC
400	0.589	1.000	1.216	0.571	1.000	1.226	0.569	1.000	1.227
400	0.590	1.000	1.217	0.571	1.000	1.227	0.570	1.000	1.228
400	0.590	1.000	1.216	0.571	1.000	1.226	0.570	1.000	1.227
400	0.590	1.000	1.216	0.571	1.000	1.226	0.570	1.000	1.227
400	0.590	1.000	1.217	0.571	1.000	1.227	0.570	1.000	1.227
400	0.591	1.000	1.216	0.572	1.000	1.226	0.570	1.000	1.227
Average	0.590	1.000	1.216	0.571	1.000	1.226	0.570	1.000	1.227
RSD%	0.591	0.692	0.746	0.611	0.692	0.740	0.612	0.692	0.739

Table 4.8 The effect of minor changes of organic composition of mobile phase 3 on Relative Retention Time (RRT) of (±)-caffeine, (±)-mephedrone and (±)-4-MEC using HPLC-UV detection in LC-FC-A systems (highlighted area is standardised condition of this method).

Concentration ($\mu\text{g mL}^{-1}$)	RRT								
	(28:72% v/v) methanol: buffer solution pH = 4.3 \pm , Section 2.4			(28:72% v/v) methanol: buffer solution pH = 4.3, Section 2.4			(28:72% v/v) methanol: buffer solution pH = 4.3, Section 2.4		
	Caffeine	4-MMC	4-MEC	Caffeine	4-MMC	4-MEC	Caffeine	4-MMC	4-MEC
400	0.577	1.000	1.252	0.571	1.000	1.226	0.569	1.000	1.227
400	0.577	1.000	1.253	0.571	1.000	1.227	0.570	1.000	1.228
400	0.578	1.000	1.253	0.571	1.000	1.226	0.570	1.000	1.227
400	0.578	1.000	1.253	0.571	1.000	1.226	0.570	1.000	1.227
400	0.578	1.000	1.253	0.571	1.000	1.227	0.570	1.000	1.227
400	0.578	1.000	1.253	0.572	1.000	1.226	0.570	1.000	1.227
Average	0.578	1.000	1.253	0.571	1.000	1.226	0.570	1.000	1.227
RSD%	0.604	0.692	0.724	0.611	0.692	0.740	0.612	0.692	0.739

Table 4.9 The effect of minor changes of temperature on relative retention time (RRT) of (±)-caffeine, (±)-mephedrone and (±)-4-MEC using HPLC-UV detection in LC-FC-B systems (highlighted area is standardised condition of this method).

Concentration ($\mu\text{g mL}^{-1}$)	RRT								
	(20 °C)			(22 °C)			(24 °C)		
	Caffeine	4-MMC	4-MEC	Caffeine	4-MMC	4-MEC	Caffeine	4-MMC	4-MEC
400	0.563	1.000	1.230	0.570	1.000	1.226	0.572	1.000	1.226
400	0.564	1.000	1.231	0.571	1.000	1.227	0.573	1.000	1.226
400	0.564	1.000	1.230	0.571	1.000	1.226	0.573	1.000	1.225
400	0.564	1.000	1.230	0.571	1.000	1.226	0.573	1.000	1.225
400	0.564	1.000	1.230	0.571	1.000	1.227	0.573	1.000	1.226
400	0.565	1.000	1.230	0.572	1.000	1.226	0.573	1.000	1.225
Average	0.564	1.000	1.230	0.571	1.000	1.226	0.573	1.000	1.226
RSD%	0.103	0.000	0.024	0.099	0.000	0.024	0.099	0.000	0.024

Table 4.10 The effect of minor changes in organic composition of mobile phase 3 on Relative Retention Time (RRT) of (±)-caffeine, (±)-mephedrone and (±)-4-MEC using HPLC-UV detection in LC-FC-B systems (highlighted area is standardised condition of this method).

Concentration ($\mu\text{g mL}^{-1}$)	RRT								
	(28:72% v/v) methanol: buffer solution pH = 4.3 , Section 2.4			(30:70% v/v) methanol: buffer solution pH = 4.3, Section 2.4			(32:68% v/v) methanol: buffer solution pH = 4.3, Section 2.4		
	Caffeine	4-MMC	4-MEC	Caffeine	4-MMC	4-MEC	Caffeine	4-MMC	4-MEC
400	0.567	1.000	1.228	0.570	1.000	1.226	0.574	1.000	1.224
400	0.568	1.000	1.228	0.571	1.000	1.227	0.575	1.000	1.225
400	0.569	1.000	1.228	0.571	1.000	1.226	0.576	1.000	1.224
400	0.569	1.000	1.228	0.571	1.000	1.226	0.575	1.000	1.224
400	0.569	1.000	1.228	0.571	1.000	1.227	0.576	1.000	1.224
400	0.569	1.000	1.227	0.572	1.000	1.226	0.576	1.000	1.224
Average	0.568	1.000	1.228	0.571	1.000	1.226	0.575	1.000	1.224
RSD%	0.101	0.000	0.024	0.099	0.000	0.024	0.097	0.000	0.024

4.5.8 Inter-and intra-day precision

Intra- and inter-day precision was determined by the evaluation of (±)-caffeine, (±)-mephedrone and (±)-4-MEC using UV and amperometric detection in LC-FC-A and LC-FC-B systems. This test was applied to ensure that this method could be used in routine analysis. Table 4.11 shows the relative standard deviation using the LC-FC-A system for three analytes that were obtained from 12 replicate injections of a mixture solution of 400 $\mu\text{g mL}^{-1}$ of (±)-caffeine, (±)-mephedrone and (±)-4-MEC (Section 2.7.6) in the same day (6 in the morning and 6 in the afternoon) or on different days. The RSD% of the three analytes of inter- and intra-day precision ranged from 0.012 to 0.0947% and precision ranged from 0.544 to 0.967 %. Both

RSD% were < 1, confirming that this method is precise. The value of RSD% was calculated by the supplementary data in Appendix Table 9.20 where the RSD% of all analytes were found to be < 1%. This is an appropriate precision criterion for repetitive injections to assess the precision of an instrument in analytical method validation (Green, 1996).

Table 4.11 Relative standard deviations (RSD %) of inter- and intra-day precision for 400 µg mL⁻¹ (±)-Caffeine, (±)-4-mephedrone and (±)-4-MEC using HPLC-UV and HPLC-AD in the LC-FC-A system.

Number of injections =12	System	RSD % of LC-FC-A		RSD % of LC-FC-B	
	Detection	HPLC-UV peak area, (mAU)	HPLC-AD peak current, (µA)	HPLC-UV peak area, (mAU)	HPLC-AD peak current, (µA)
Inter-day precision	Caffeine	0.249	0.656	0.55	0.95
	Mephedrone	0.047	0.860	0.35	0.72
	4-MEC	0.053	0.829	0.35	0.97
Intra-day precision	Caffeine	0.012	0.544	0.87	0.91
	Mephedrone	0.814	0.830	0.68	0.59
	4-MEC	0.947	0.967	0.67	0.86

In terms of the LC-FC-B system, the intra-day and inter-day tests were applied to confirm the suitability of this method to use in routine analysis. Inter- and intra-day test swere carried out using the same analytes that were used by the LC-FC-A system with the same procedure. In the inter- and intra-day variation studies, RSDs%, were calculated and ranged from 0.35 to 0.87% using HPLC-UV and ranged from 0.59 to 0.95% using HPLC-AD (Table 4.11). RSDs for both inter- and Intra-day studies of the LC-FC-B system were less than 1, therefore this method was found to be precise. These results illustrate the ability of this method and the efficiency of these systems to be applied to routine analysis. The values of RSDs% were calculated by the supplementary data in Appendix Table 9.21 and were found to be< 1% for all the analytes. This is an appropriate precision criterion for repetitive

injections to assess the precision of an instrument in analytical method validation (Green, 1996).

4.5.9 Accuracy test

This test was used to determine the closeness of agreement of experimental data to actual data. The accuracy studies were carried out at three levels of standard concentrations prepared as 80, 100, and 120% of (±)-caffeine, (±)-mephedrone and (±)-4-MEC (section 2.7.8). The prepared solutions were injected three times and detected using UV and amperometric detection in the LC-FC-A and LC-FC-B systems. The percentage recovery was calculated and presented in Table 4.12. This showed excellent recovery within the range of $100 \pm 2\%$, which in the LC-FC-A system were in the range 98.8 – 101% with RSD% $\pm 0.01 - 0.53$ by UV detection, and 99-100.6% with RSD% $\pm 0.45 - 0.14$ using amperometric detection. In terms of using the LC-FC-B system, the percentages of recovery were over the range 98.8 – 101% with RSDs% of $\pm 0.01 - 0.56$ by UV detection and 99.8 – 100.9% with RSDs% of $\pm 0.07 - 0.8$. In both systems, the percentage recovery indicated that both protocols were accurate and precise.

Table 4.12 Accuracy data expressed as the percentage recovery of the mixture of (±)-caffeine, (±)-4-mephedrone and (±)-4-MEC using HPLC-UV and HPLC-AD detection in LC-FC-A and LC-FC-B systems.

System			LC-FC-A				LC-FC-B			
Detection			HPLC-UV		HPLC-AD		HPLC-UV		HPLC-AD	
Analyte	Concentration ($\mu\text{g mL}^{-1}$)	Theoretical recovery ($\mu\text{g mL}^{-1}$)	Actual recovery ($\mu\text{g mL}^{-1}$)	%Recovery (n=3)	Actual recovery ($\mu\text{g mL}^{-1}$)	%Recovery (n=3)	Actual recovery ($\mu\text{g mL}^{-1}$)	%Recovery (n=3)	Actual recovery ($\mu\text{g mL}^{-1}$)	%Recovery (n=3)
Caffeine	240 (80%)	241.0	236.5	98.0 (± 0.015)	240.9	99.9 (± 0.54)	243.8	101 (± 0.01)	239.5	99.8 (± 0.07)
4-MMC		241.0	239.5	99.37 (± 0.04)	241.0	100.0 (± 0.89)	245.1	101 (± 0.04)	241.0	100.6 (± 0.14)
4-MEC		241.0	237.9	98.7 (± 0.037)	242.0	100.5 (± 0.98)	247.9	101 (± 0.02)	240.9	99.9 (± 0.45)
Caffeine	300 (100%)	301.0	297.0	98.6 (± 0.01)	302.0	100.4 (± 0.54)	298.4	99 (± 0.04)	298.3	99.5 (± 0.36)
4-MMC		301.0	293.3	97.7 (± 0.011)	299.7	99.5 (± 0.73)	299.6	99.5 (± 0.02)	301.0	100.9 (± 0.53)
4-MEC		301.0	293.4	100.0 (± 0.017)	301.5	100.1 (± 0.34)	303.0	100.7 (± 0.15)	301.5	99.9 (± 0.80)
Caffeine	360 (120%)	361.5	357.3	98.8 (± 0.22)	358.6	99.21 (± 0.73)	357.0	98.8 (± 0.56)	359.4	99.8 (± 0.16)
4-MMC		361.5	360.9	101 (± 0.33)	359.5	99.47 (± 0.92)	358.0	99 (± 0.34)	360.6	100.3 (± 0.32)
4-MEC		361.5	356.8	98.8 (± 0.53)	358.0	99.0 (± 0.39)	362.0	100 (± 0.34)	361.0	100.1 (± 0.73)

4.6 Application of the technique to forensic drug analysis

The five NRG-2 samples (Table 2.1) obtained from the internet vendors EuChemicals (www.euchemicals.com) (January 2013) were all purported to be > 99 % pure and to contain 1 g of NRG-2. The samples were homogenised and arbitrarily labelled NRG-2-A, NRG-2-B, NRG-2-C, NRG-2-D and NRG-2-E. Preliminary LC-MS analysis indicated that all five samples contained synthetic cathinones (Table 4.13).

Table 4.13 Direct comparison of LC-MS^a and HPLC-UV data (obtained using either LC-FC-A (impinging jet flow cell) or LC-FC-B (iCell channel flow cell) systems) of purchased NRG-2 samples

Street sample	LC-MS ^(a) (n = 3)	HPLC-UV in LC-FC-A (n = 3)	HPLC-UV in LC-FC-B (n = 3)
NRG-2-A	$t_R = 5.34$ min [$m/z = 192.2$ [M+H] ⁺ , 4-MEC]	$t_R = 11.7$ min [24.03% w/w ± 0.03 , 4-MEC.]	$t_R = 9.3$ min [24.01% w/w ± 0.05 , 4-MEC.]
NRG-2-B	$t_R = 4.48$ min $m/z = 178.1$ [M+H] ⁺ , 4-MMC]	$t_R = 9.4$ min [49.24% w/w ± 0.03 , 4-MMC]	$t_R = 7.5$ min [48.18% w/w ± 0.02 , 4-MMC]
NRG-2-C	$t_R = 2.57$ min [major, $m/z = 195.1$ [M+H] ⁺ , caffeine; 5.34 min [minor, $m/z = 192.2$ [M+H] ⁺ , 4-MEC]	$t_R = 5.5$ min [major, 76.19% w/w ± 0.22 , caffeine; 11.7 min [minor, 23.58% w/w ± 0.49 , 4-MEC]	$t_R = 4.3$ min [major, 74.83% w/w ± 0.16 , caffeine; 9.3 min [minor, 25.81% w/w ± 0.23 , 4-MEC]
NRG-2-D	$t_R = 2.57$ min [major, $m/z = 195.1$ [M+H] ⁺ , caffeine; 4.48 min [minor, $m/z = 178.1$ [M+H] ⁺ , 4-MMC]	$t_R = 5.5$ min [major, 83.04% w/w ± 0.03 , caffeine; 9.4 min [minor, 15.64% w/w ± 0.45 , 4-MMC]	$t_R = 4.3$ min [major, 82.93% w/w ± 0.35 , caffeine; 7.5 min [minor, 16.58% w/w ± 1.13 , 4-MMC]
NRG-2-E	$t_R = 2.57$ min [$m/z = 195.1$ [M+H] ⁺ , caffeine; 4.48 min [$m/z = 178.1$ [M+H] ⁺ , 4-MMC]; 5.34 min [$m/z = 192.2$ [M+H] ⁺ , 4-MEC]	$t_R = 5.5$ min [36.55% w/w ± 0.08 , caffeine; 9.4 min [15.64% w/w ± 0.46 , 4-MMC]; 11.7 min [24.03% w/w ± 0.03 , 4-MEC]	$t_R = 4.3$ min [34.09% w/w ± 0.77 , caffeine; 7.5 min [16.71% w/w ± 0.05 , 4-MMC]; 9.3 min [25.84% w/w ± 0.01 , 4-MEC]

Key: (a) results of sample analysed using the method reported by Khreit et al. (Khreit et al., 2012)

The synthetic cathinones [mephedrone or 4-MEC] were either pure (Khreit et al., 2012)[NRG-2-A contained 4-MEC and NRG-2-B contained mephedrone] or adulterated with significant quantities of caffeine (Smith et al., 2014b). [NRG-2-C contained caffeine and 4-MEC, and NRG-2-D caffeine and mephedrone] or combined together with caffeine (NRG-2-E caffeine, mephedrone and 4-MEC) (Table 2.1). With substantial evidence supporting an electroanalytical oxidation approach for detecting various substituted cathinones in street samples, the viability of the proposed protocol was tested. The NRG-2 samples were reanalysed (in triplicate) using the validated HPLC-AD method at a concentration of 500 $\mu\text{g mL}^{-1}$.

The HPLC-UV results (Table 4.14) were obtained using the commercial flow-cell (LC-FC-A). That confirmed two of the samples contained only synthetic cathinones [NRG-2-A: 24.03 \pm 0.03% w/w 4-MEC and NRG-2-B: 49.24 \pm 0.03% w/w mephedrone]. Two of the samples contained caffeine predominantly (80% w/w) in combination with mephedrone or 4-MEC [NRG-2-C: 76.19 \pm 0.22% w/w caffeine, 23.58 \pm 0.49% w/w 4-MEC and NRG-2-D: 83.04 \pm 0.03% w/w caffeine, 15.64 \pm 0.45% w/w mephedrone]. One sample contained a complex mixture of the three analytes [NRG-2-E: 36.55 \pm 0.08% w/w caffeine, 15.64 \pm 0.46% w/w mephedrone, 24.03 \pm 0.03% w/w 4-MEC].

These observations are in agreement with the information reported by Khreit et al., Brandt et al. and Smith et al., who noted that many second-generation “legal high” products contained increased levels of commonly used diluents and adulterants (Khreit et al., 2012; Brandt et al., 2010; Smith et al., 2014b). The qualitative results, obtained from the HPLC-AD (amperometric detector) in the LC-FC-A system, also confirmed the constitution of the five NRG-2 samples and comparison of two detection methods (UV detection vs. amperometric detection,

Table 4.14) indicated that in samples containing caffeine (NRG-2-C, NRG-2-D and NRG-2-E), the two methods were comparable in terms of their ability to quantify the components present (Table 4.13). The two samples containing only synthetic cathinones (NRG-2-A and NRG-2-B), however, show a significant increase in the estimation of the quantities of mephedrone and 4-MEC present (Table 4.13). However, a new GSPE was utilised during each sample analysis, the loss in analytical performance may be due to adsorption of the analytes onto the surface of the GSPE during the time scale of the analysis. Despite the loss in analytical performance, it is still adequate for quantifying the synthetic cathinones present within the samples. Similar results were observed with the iCell unit (LC-FC-B, Table 4.14).

The amperometric limits of detection (for the electrochemical oxidation of mephedrone and 4-MEC reported herein are similar to the values reported in our previous work (Smith et al., 2014a) (mephedrone: $39.8 \mu\text{g mL}^{-1}$ and 4-MEC: $84.2 \mu\text{g mL}^{-1}$). This is sufficient for use in the field as opposed to the values reported by Krishnaiah et al. (V. Krishnaiah) who utilised a dropping mercury electrode (DME) which is not suitable for use in the field and banned in many countries. This work also demonstrates an improvement over our previous work (Smith et al., 2014a), which indicated that there was no electrochemical selectivity for the electrochemical detection of mephedrone and 4-MEC. By coupling the amperometric detector to a high performance liquid chromatograph, one can now rapidly separate, discriminate between and quantify, two structurally related cathinones within a complex street sample mixture (NRG-2-E, Table 4.14) indicating that the proposed HPLC-AD protocol can be considered suitable for the detection and quantification of the two synthetic cathinones either in their pure form, in the presence of common adulterants e.g. caffeine or simultaneously within blended street samples of the evolved “legal high” product, NRG-2.

Table 4.14 Direct comparison between quantitative data obtained by the HPLC-UV and HPLC-AD protocols for the analysis of the synthetic cathinones in a selection of purchased NRG-2 samples

System	LC-FC-A						LC-FC-B					
Flow rate	0.8 mL min ⁻¹						1 mL min ⁻¹					
Detection	HPLC-UV (% w/w) (n =3)			HPLC-AD (% w/w) (n =3)			HPLC-UV (% w/w) (n =3)			HPLC-AD (% w/w) (n =3)		
Sample	Caffeine	4-MMC	4-MEC	Caffeine	4-MMC	4-MEC	Caffeine	4-MMC	4-MEC	Caffeine	4-MMC	4-MEC
tR	5.5	9.4	11.7	5.52	9.42	11.72	4.3	7.5	9.3	4.32	7.52	9.32
NRG-2-A	n.d.	n.d.	24.03 (±0.03)	n.d.	n.d.	54.39 (±1.24)	n.d.	n.d.	24.01 (±0.05)	n.d.	n.d.	65.07 (±1.21)
NRG-2-B	n.d.	49.24 (±0.03)	n.d.	n.d.	60.8 (±0.57)	n.d.	n.d.	48.18 (±0.02)	n.d.	n.d.	75.28 (±1.71)	n.d.
NRG-2-C	76.19 (±0.22)	n.d.	23.58 (±0.49)	78.26 (±0.68)	n.d.	20.69 (±1.72)	74.83 (±0.16)	n.d.	25.81 (±0.23)	80.35 (±0.99)	n.d.	18.77 (±2.45)
NRG-2-D	83.04 (±0.03)	15.64 (±0.45)	n.d.	80.54 (±2.06)	18.95 (±2.96)	n.d.	82.93 (±0.35)	16.58 (±1.13)	n.d.	85.38 (±0.48)	8.82 (±2.21)	n.d.
NRG-2-E	36.55 (±0.08)	15.64 (±0.46)	24.03 (±0.03)	42.22 (±1.43)	8.56 (±3.30)	54.39 (±1.24)	34.09 (±0.77)	16.71 (±0.05)	25.84 (±0.01)	36.42 (±1.14)	27.53 (±0.32)	44.01 (±1.59)
Key: n.d. = not detected.												

4.7 Conclusions

The combination of HPLC with electrochemical detection was used for the first time for the separation and detection of synthetic cathinones (±)-mephedrone and (±)-4-MEC using either an impinging jet (LC-FC-A) or iCell channel (LC-FC-B) flow cell incorporating disposable embedded graphite screen-printed macroelectrodes (GSPE). The validated HPLC-AD protocol was shown to have similar LODs [HPLC-AD in the LC-FC-A system: $14.66 \mu\text{g mL}^{-1}$ for (±)-mephedrone and $9.35 \mu\text{g mL}^{-1}$ for (±)-4-MEC; HPLC-AD in the LC-FC-B system: $57.92 \mu\text{g mL}^{-1}$ for (±)-mephedrone and $26.91 \mu\text{g mL}^{-1}$ for (±)-4-MEC] to the previously reported oxidative electrochemical protocol [$39.8 \mu\text{g mL}^{-1}$ for (±)-mephedrone and $84.2 \mu\text{g mL}^{-1}$ for (±)-4-MEC].

The impinging jet and iCell channel flow cells show an excellent agreement with respect to the quantitative electroanalytical and chromatographic data making them suitable for the detection and quantification of (±)-mephedrone and (±)-4-MEC, either in their pure form or in combination with adulterant. However, the commercial flow cell (LC-FC-A) appeared to be slightly more sensitive than the custom-made flow cell (LC-FC-B). This reduction in sensitivity is due to the larger internal volume of the LC-FC-B, which increases sample dispersion, thereby reducing the sensitivity of the GSPE sensor platform.

This work demonstrates the effect of the design of the flow-cell on the sensitivity of the detection system, with the commercial flow cell (LC-FC-A) giving a greater response because it has the smaller method volume. The designs of both flow cells are significantly different regarding the flow delivery to the electrode; however, the iCell having a volume 15 times that of the commercial cell gives detection results of a similar order. This suggests further optimisation of the shape

may yield greater sensitivity. The method detailed herein shows a significant improvement over previously reported electroanalytical methods (Smith et al., 2014a), which were either unable to selectively discriminate between structurally related synthetic cathinones, or utilised harmful and restrictive materials in their design. In addition, this chapter explained the suitability of this protocol for use in routine analysis for detection and quantification of (±)-mephedrone and its derivative in testing purchased samples. The next chapter presents the analysis of (±)-mephedrone with (±)-Mexedrone a new (±)-mephedrone derivative. It is envisaged that the data presented will be useful to law enforcement officials, for the development of robust, electroanalytical detection systems for new psychoactive substances and related compounds as they emerge on the recreational drugs market.

5 Chapter 5: Detection and quantification of (±)-mephedrone and (±)-mexedrone as new Psychoactive substances using the HPLC-AD protocol

5.1 Introduction

(±)-mephedrone (Figure 5.1a) is a synthetic cathinone derivative that entered the illicit drugs market about a decade ago and was placed under legislative control measures across Europe in 2010. Mephedrone was subjected to international control measures by its addition to Schedule 2 of the Convention on Psychotropic Substances (1971) in 2015 (McLaughlin et al., 2017; Council Decision, 2010). NPS manufacturers continue to design new compounds that (potentially) circumvent drugs legislation to exploit any gaps created in the market by prohibition/control of certain substances.

In August 2015 a “legal” replacement for (±)-mephedrone appeared on the NPS market in the UK and Ireland (McLaughlin et al., 2017). The substance was the alpha-methoxy-derivative of (±)-mephedrone to be called ‘(±)-mexedrone (Figure 5.1b) (McLaughlin et al., 2017; Roberts et al., 2017). (±)-Mexedrone was targeted at markets in countries where generic cathinone bans had been enforced (McLaughlin et al., 2017). Although (±)-Mexedrone has the generic cathinone backbone, it was uncontrolled in the UK due to the methoxy moiety at the terminal amine of the existing mephedrone molecular (methoxy group on the propane-1-one sidechain). The structure of the substance is similar to mephedrone Figure 5.1, however, it had been specifically designed to fall outside the generic cathinone ban in the UK (UK-Government, 2016).

Due to the rapid rise in the misuse, (±)-mephedrone and its related synthetic cathinone derivatives are controlled under the MDA (1979) as class B substances.

According to the Misuse of Drugs Act 1971, any stereoisomeric form and salt of a controlled substance, as well as any preparation or other product containing the substance is now controlled under Legalisation.gov.uk. 2016 (Morris and Wallach, 2014; UK-Government, 2016).

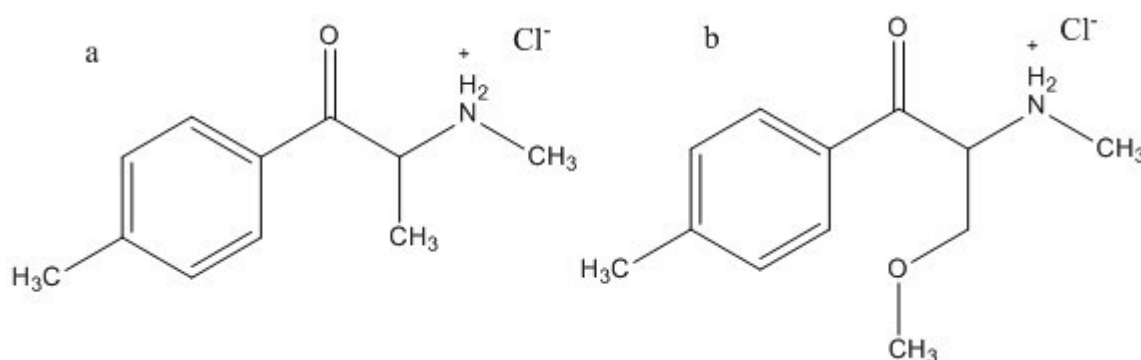


Figure 5.1 Chemical structures of a- (±)-mephedrone.HCl and b- (±)-mexedrone.HCl.

This chapter presents full characterisation data for mexedrone and compares the data with (±)-mephedrone using a range of instrumental techniques. The development for high performance liquid chromatography in combination with amperometric detection HPLC-AD in a LC-FC-A system has been successful in chapter 3 and chapter 4 for the analysis of MDMA, PMA, mephedrone and 4-MEC. This chapter represents the novel high-performance liquid chromatographic (HPLC-UV) method combined with amperometric detection (HPLC-AD) for the qualitative and quantitative analysis of (±)-Mexedrone and (±)-mephedrone using a commercially available impinging jet flow-cell system incorporating embedded graphite screen-printed macro-electrodes. In this study, just a commercially impinging jet flow-cell system was used because in chapter 3 it showed a higher sensitivity than the iCell channel flow cell due to the difference in chamber volumes of the two flow cells, as explained in chapter 4 (Zuway et al., 2015). Both detectors (UV and amperometric) allow discrimination between the two compounds, however, HPLC-UV was the more sensitive technique.

5.2 Characterisation

A reference standard of (±)-mephedrone was prepared in-house using the method reported by Santali et al. (Santali et al., 2011). The reference standard of (±)-Mexedrone was obtained from BRC Fine Chemicals (London, UK), and recrystallised from the minimum amount of acetone prior to use. (±)-mephedrone is an off-white powder (m.p. 249-251 °C) which is in agreement with the data published by Santali et al. (m.p. 251.18 °C) by differential scanning calorimetry (DSC) (Santali et al., 2011). In addition, (±)-Mexedrone was obtained as white-coloured crystals (m.p. 189-190 °C), in agreement with the melting point reported by McLaughlin et al. (m.p. 190-192 °C) (McLaughlin et al., 2017). TLC was performed using ethyl acetate and methanol as the solvent (1:3). Results showed that the two analytes were pure, as only one spot was observed per analyte. In addition, it was possible to distinguish between both analytes. The retention factor of each spot was measured, that for (±)-Mexedrone was 0.49 cm and for (±)-mephedrone was 0.32 cm.

The infrared spectra for (±)-mephedrone produced for C=C at 1606 cm⁻¹ is indicative of an aromatic nucleus. Also, the absorption of C=O was obtained at 1685 cm⁻¹, and at 2717.5 cm⁻¹ the absorption of the NH₂⁺ stretch, and that was similar to what was reported for (±)-mephedrone by Santali et al. (Santali et al., 2011), the infrared spectra for (±)-Mexedrone represent a strong C=O absorption band at 1690 cm⁻¹. It also displays C=C absorptions at 1605 cm⁻¹ indicating the presence of an aromatic nucleus. The absorption band observed at 2775 cm⁻¹ is indicative of the NH₂⁺. These results confirmed the similarity of (±)-mephedrone and (±)-mexedrone. However, there is a strong absorption at 1247 cm⁻¹ corresponding to the C-O in (±)-Mexedrone spectra and this absorption is not presented in (±)-mephedrone data,

therefore, this spectrum distinguishes between (±)-mephedrone and (±)-mexedrone.

5.3 Nuclear magnetic resonance spectroscopy (NMR)

NMR results obtained for (±)-mephedrone and (±)-Mexedrone were very similar, as expected.

5.3.1 (±)-Mephedrone:

A ^1H NMR spectrum of the (±)-mephedrone salt was obtained at 60 °C in d_6 -DMSO. Figure 5.2 shows that $\delta = 9.98$ ppm represents the ammonium salt protons (2H, br s, $\text{CH}(\text{NH}_2^+\text{CH}_3)\text{CH}_3$); and the characteristic AA'BB' aromatic system for an asymmetrically para-di-substituted aromatic system at 8.41 ppm (2H, d, $J = 8.0$ Hz, AA'BB', Ar-H), 7.88 ppm (2H, d, $J = 8.0$ Hz, AA'BB', Ar-H), a de-shielded one-hydrogen quartet at 5.62 ppm (1H, q, $J = 7.6$ Hz $\text{CH}(\text{NH}_2^+\text{CH}_3)\text{CH}_3$), a de-shielded three-hydrogen singlet at 3.04 ppm (3H, s, $\text{CH}(\text{NH}_2^+\text{CH}_3)\text{CH}_3$), a slightly de-shielded methyl singlet corresponding to the methyl attached to the aromatic ring at 2.88 ppm (3H, s, ArCH_3) and lastly a methyl doublet at 1.91 ppm (3H, d, $J = 7.6$ Hz, $\text{CH}(\text{NH}_2^+\text{CH}_3)\text{CH}_3$). The results obtained are similar to what was reported by Santali et al. (Santali et al., 2011).

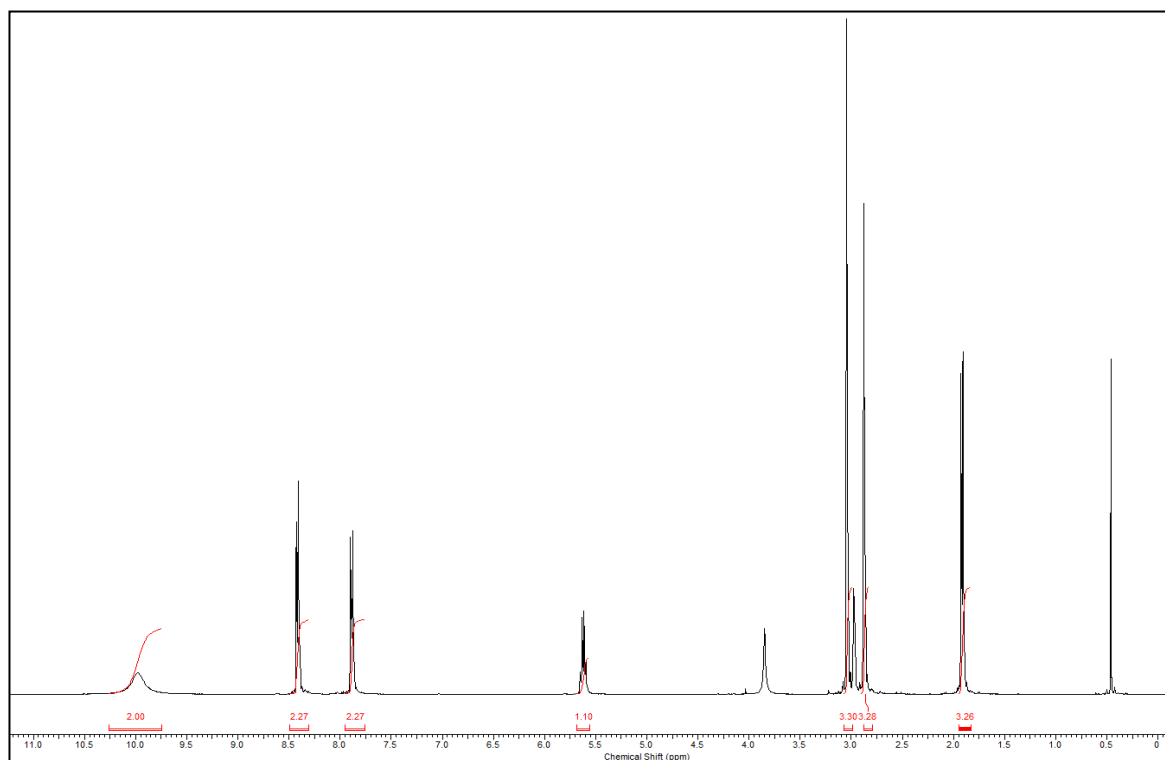


Figure 5.2 ¹H NMR spectrum (d₆-DMSO, 60 °C) of (±)-mephedrone.

¹³C NMR spectra (obtained at 60 °C in d₆-DMSO, Figure 5.3&Figure 5.4) support purity with nine distinct carbon signals. The δ = 196.86 (C=O, C1), 146.47 (ArC, C4*), 131.49 (ArC, C1*), 130.76 (2 x ArCH, C3*/C5*), 129.96 (2 x ArCH, C2*/C6*), 59.10 (CHCH₃, C2), 31.64 (NCH₃), 22.33 (ArCH₃, C7*) and 16.56 (CHCH₃, C3). The N-methyl resonance (δ = 3.04 ppm) gave a ³J correlation to C2 which is in turn coupled to the methyl doublet (C3). In the HMBC spectrum, the protons of the methyl resonance (δ = 1.91 ppm) are coupled to a de-shielded carbon (δ = 196.86 ppm, C1) completing the assignment of the 2-aminomethyl-propane-1-one side chain. Further couplings in the HMBC spectrum between H2*/H6* and C1 (³J) support the assignment of the propane-1-one side chain at C1* on the aromatic nucleus (between C6* and C2*) and the correlations between H2*/H6* and H3*/H5* confirmed the AA'BB' aromatic system. The methyl singlet at 2.88 ppm (C7') displays a ³J HMBC correlation to C3*/C5* and a ²J correlation to C4* finalising the assignment of all resonances (Table 5.1). The results obtained are similar to the current literature reported for (±)-mephedrone. (Santali et al., 2011).

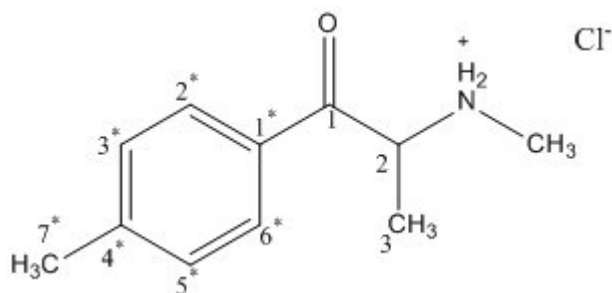


Figure 5.3 Chemical structure of (±)-mephedrone.HCl

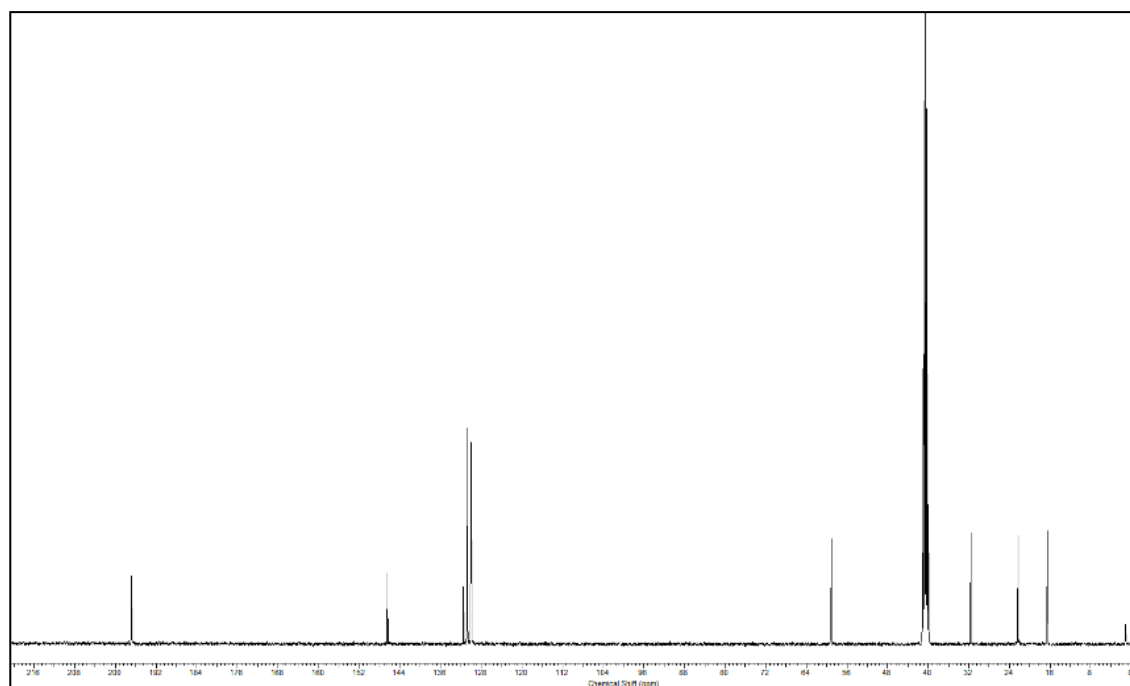


Figure 5.4 ^{13}C NMR spectrum ($\text{d}_6\text{-DMSO}$, $60\text{ }^\circ\text{C}$) of (±)-mephedrone.

Table 5.1 ^1H , ^{13}C NMR spectral data and ^1H - ^{13}C long-range correlations of (±)-mephedrone in $\text{d}_6\text{-DMSO}$. Chemical shifts (δ) in ppm; coupling constants (J) in Hz.

Position (±)-Mephedrone				
	^1H	^{13}C	2J	3J
1	-	196.86	-	-
2	5.62 q, $J = 7.6\text{ Hz}$	59.10	C1, C3	NCH_3
3	1.91 d, $J = 7.6\text{ Hz}$	16.56	C2	C1
1*	-	131.49	-	-
2*/6*	8.41 d, $J = 8.0\text{ Hz}$	130.76	$\text{C3}^*/\text{C5}^*$	$\text{C2}^*/\text{C6}^*$, C1
3*/5*	7.88 d, $J = 8.0\text{ Hz}$	129.96	$\text{C2}^*/\text{C6}^*$	$\text{C3}^*/\text{C5}^*$
4*	-	146.47	-	-
7*	2.88 s	22.33	-	$\text{C3}^*/\text{C5}^*$
NCH_3	3.04 s	31.64	-	C2
NH_2^+	9.98 br s	-	-	-

The DEPT profile (obtained at $60\text{ }^\circ\text{C}$ in $\text{d}_6\text{-DMSO}$) further supports the structure and shows six signals corresponding to the three CH and three CH_3 resonances. The two signals at $\delta = 129.96\text{ ppm}$ and 130.76 ppm correspond to the two different CH environments in the aromatic ring, and the aromatic methyl signal is observed at

δ = 22.33 ppm. The three signals signifying the resonances in the aliphatic 2-aminomethyl-propane-1-one chain are observed at δ = 59.10, 31.64, 16.56 ppm (the aliphatic CH, aminomethyl and methyl respectively).

5.3.2 (\pm)-Mexedrone

The ^1H NMR spectrum of (\pm)-Mexedrone salt was obtained at 60 $^\circ\text{C}$ in d_6 -DMSO. Figure 5.5 at δ = 9.98 ppm represents the ammonium salt protons (2H, br s, $\text{CH}(\text{NH}_2^+\text{CH}_3)\text{CH}_3$); and the characteristic AA'BB' aromatic system for an asymmetrically para-disubstituted aromatic system at 8.47 ppm (2H, d, J = 8.0 Hz, AA'BB'), 7.95 ppm (2H, d, J = 8.0 Hz, AA'BB'), a de-shielded one hydrogen singlet at 5.88 ppm (1H, m, $\text{C}(\text{O})\text{CHN}$), a de-shielded two-hydrogen doublet at 4.36 ppm (2H, dd, J = 7.79 Hz; CH_2OCH_3), a de-shielded three-hydrogen singlet at 3.73 ppm (3H, s, J = 7.79, OCH_3) a de-shielded three-hydrogen singlet at 3.17 ppm (3H, s, NHCH_3) and finally a slightly de-shielded methyl singlet corresponding to the methyl attached the aromatic ring at 2.96 ppm (3H, s, ArCH_3). The results obtained in this study are similar to what was reported by McLaughlin et al. (McLaughlin et al., 2017).

^{13}C NMR spectra (obtained at 60 $^\circ\text{C}$ in d_6 -DMSO, Figure 5.6 & Figure 5.7) support the idea that the substance is primarily pure, with ten distinct carbon signals. The δ = 194.06 ($\text{C}=\text{O}$, C1), 146.44 (ArC , C4*), 132.16 (ArC , C1*), 130.75 (2 x ArCH , C3*/C5*), 129.87 (2 x ArCH , C2*/C6*), 70.29 (CH_2 , C3), 64.10 (CH , C2), 59.87 (OCH_3), 32.67 (NCH_3) and 22.35 (ArCH_3 , C7*). These results are similar to what was reported by McLaughlin et al (McLaughlin et al., 2017).

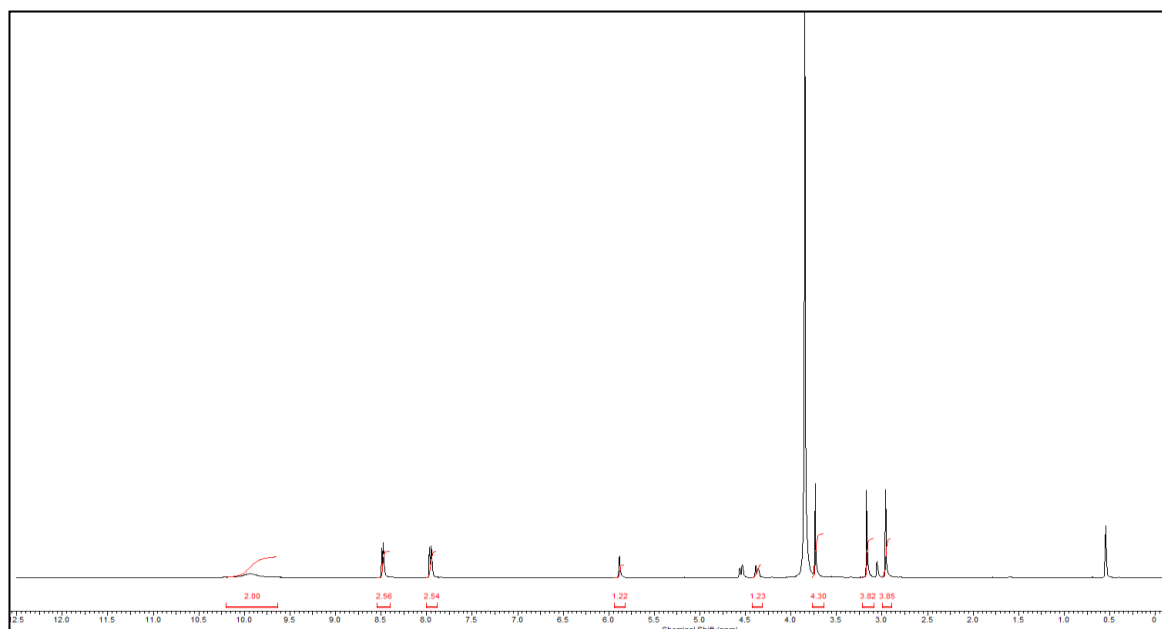


Figure 5.5 Determination of ^1H NMR spectrum ($\text{d}_6\text{-DMSO}$, $60\text{ }^\circ\text{C}$) of (\pm) -mexedrone.

Confident assignments of all carbon and hydrogen resonances were achieved using both HMQC and HMBC methods for a full spectral analysis, which signified that the sample was (\pm) -mexedrone. The N-methyl resonance ($\delta = 3.17\text{ ppm}$) gave a ^3J correlation to C2 which is in turn coupled to the methylene doublet (C3). The protons of the methylene resonance ($\delta = 3.73\text{ ppm}$) are coupled to a de-shielded carbon ($\delta = 194.06\text{ ppm}$, C1) and a de-shielded methoxy singlet ($\delta = 5.88\text{ ppm}$) completing the assignment of the 3-methoxy-2-aminomethyl-propane-1-one side chain. Further couplings in the HMBC spectrum between $\text{H}2^*/\text{H}6^*$ and C1 (^3J) supports the assignment of the propane-1-one side chain at C1* on the aromatic nucleus (between C6* and C2*) and correlations between $\text{H}2^*/\text{H}6^*$ and $\text{H}3^*/\text{H}5^*$ confirmed the AA'BB' aromatic system. The methyl singlet at 2.96 ppm (C7*) exhibits a ^3J HMBC correlation to C3*/C5* and a ^2J correlation to C4* concluding the assignment of all resonances (Table 5.2).

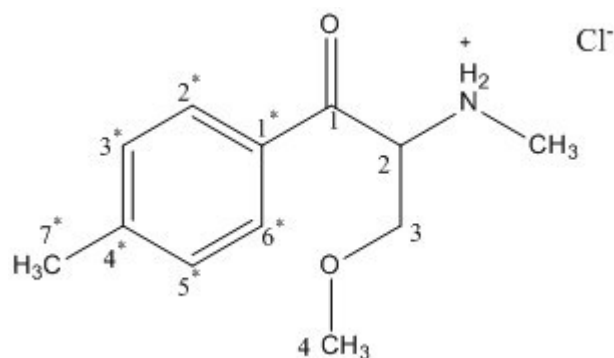


Figure5.6 Chemical structure of (±)-mexedrone.HCl

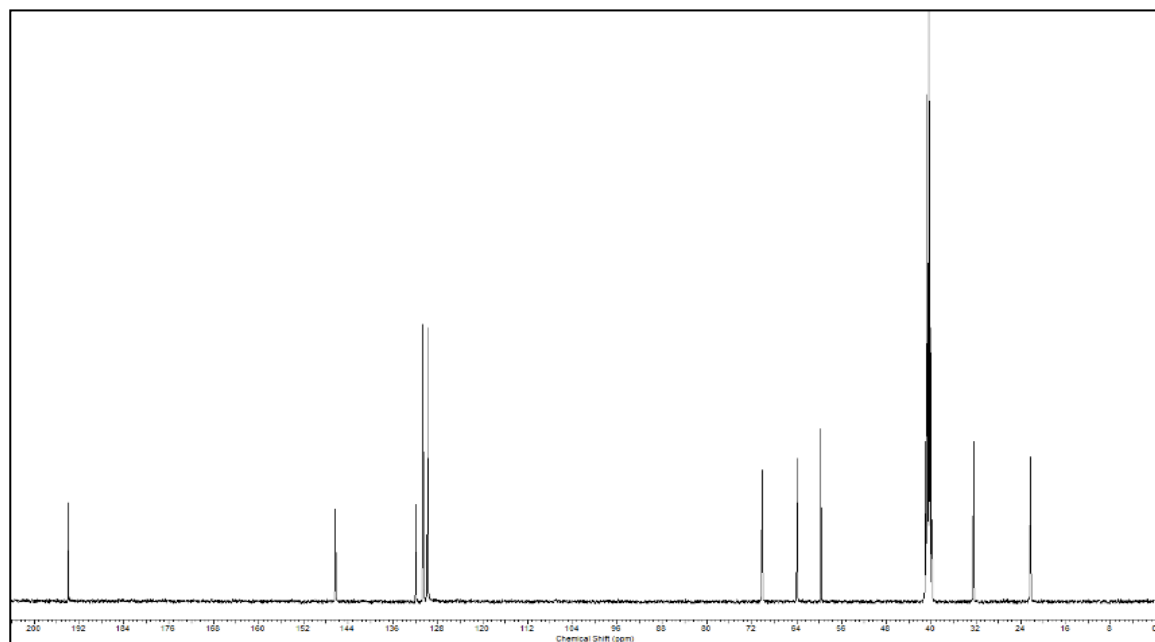


Figure 5.7 ^{13}C NMR spectrum ($\text{d}_6\text{-DMSO}$, $60\text{ }^\circ\text{C}$) of (±)-mexedrone.

Table 5.2 ^1H , ^{13}C NMR spectral data and ^1H - ^{13}C long-range correlations of (±)-Mexedrone in $\text{d}_6\text{-DMSO}$. Chemical shifts (δ) in ppm; coupling constants (J) in Hz.

Position (±)-Mexedrone				
	^1H	^{13}C	2J	3J
1	-	194.06	-	-
2	3.73 s	59.87	C1, C2, C3	NCH_3
3	4.36 d, $J = 7.79$	70.29	C2	C1
4	5.88 s	64.10	-	C2^*
1^*	-	132.16	-	-
$2^*/6^*$	8.47 d, $J = 8.0$	130.75	$\text{C3}^*/\text{C5}^*$	$\text{C2}^*/\text{C6}^*$, C4^* , C1
$3^*/5^*$	7.95 d, $J = 8.0$	129.87	$\text{C2}^*/\text{C6}^*$	$\text{C3}^*/\text{C5}^*$, C1^*
4^*	-	146.44	-	-
7^*	2.96 s	22.35	C4^*	$\text{C3}^*/\text{C5}^*$
NCH_3	3.17 s	32.67	-	C2
NH_2^+	9.94 br s	-	-	-

The DEPT profile (obtained at $60\text{ }^\circ\text{C}$ in $\text{d}_6\text{-DMSO}$) further supports the structure and shows seven signals corresponding to the single CH_2 , 3 CH and 3 CH_3

resonances. The two signals at $\delta = 130.75$ ppm and 129.87 ppm correspond to the two different CH environments in the aromatic ring, and the aromatic methyl signal is observed at $\delta = 22.35$ ppm. The four signals signifying the resonances in the aliphatic 3-methoxy-2-aminomethyl-propane-1-one chain are observed at $\delta = 70.29$, 64.10 , 59.87 , 32.67 ppm (the aliphatic CH₂, methoxy group, aliphatic CH, and aminomethyl group respectively).

5.4 Gas chromatography-mass spectrometry (GC-MS) analysis

GC-MS methods have been previously used for the analysis of (\pm)-mephedrone and (\pm)-Mexedrone in isolation (Santali et al., 2011; McLaughlin et al., 2017). The combined method for the analysis of these substances in combination has not previously been reported and the method was developed (see Section 2.8.1.1) which allowed rapid analysis within 8 minutes and high resolution of two target compounds (Figure 5.8). This method was used to quantitatively analyse the target substances and determine their electronic impact fragmentation pattern.

Mephedrone was eluted at 5.4 minutes and (\pm)-mexedrone was eluted at 6.1 minutes, so that means this method can be used to separate and differentiate between the two compounds (Figure 5.8).

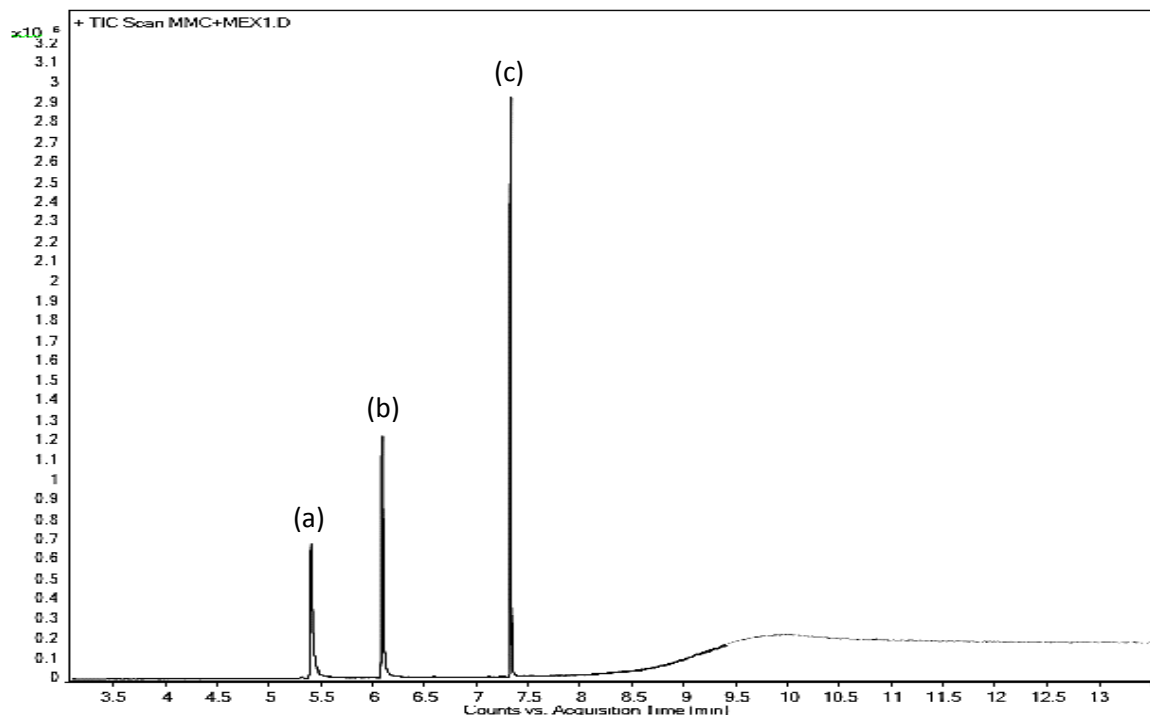
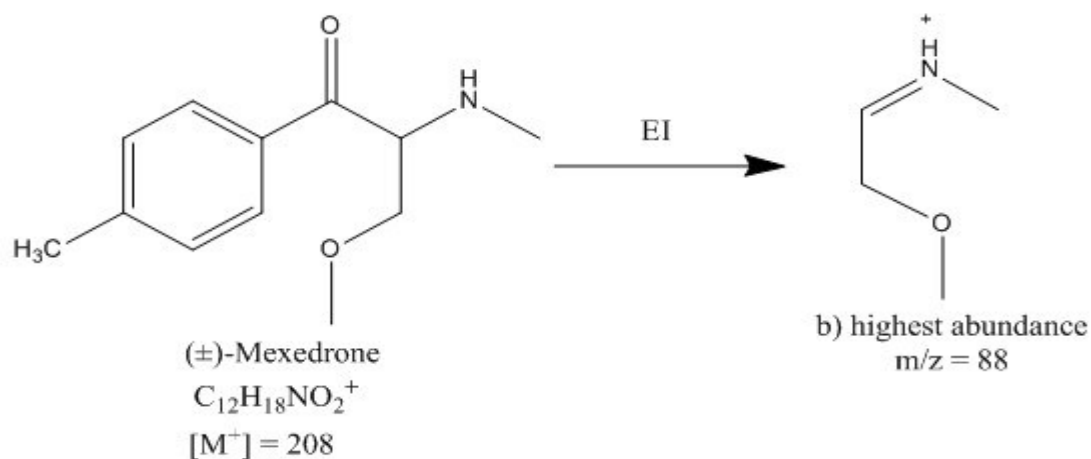
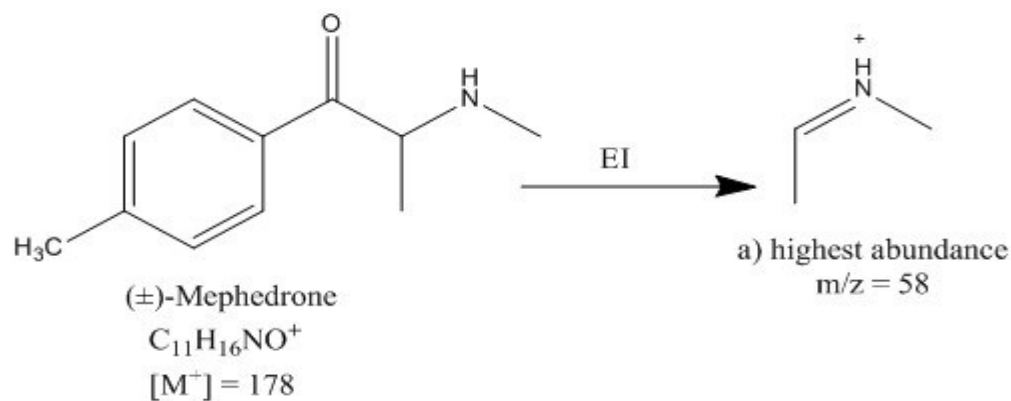


Figure 5.8 Gas chromatograms of a mixture containing $100 \mu\text{g mL}^{-1}$ of (a) (\pm)-mephedrone (b) (\pm)-Mexedrone and (c) eicosane (internal standard).

A comparison of both electron ionisation mass spectra shows that both compounds have similar fragmentation patterns. In the EI-MS of both compounds, some fragments were observed in their mass spectra (Figure 5.9). However, mass spectrometry allows unambiguous identification of the two molecules as no two molecules give the same mass spectrum. The peak with the highest abundance for (\pm)-mephedrone is observed at $m/z = 58$ (Figure 5.10), whereas, for (\pm)-Mexedrone it appears at $m/z = 88$ (Figure 5.11). The mass spectra also indicate the $[M^+]$ at $m/z = 178$ for (\pm)-mephedrone and $[M^+]$ at $m/z = 208$ for (\pm)-Mexedrone (Figure 5.9).



c) common fragments are observed in both compounds:

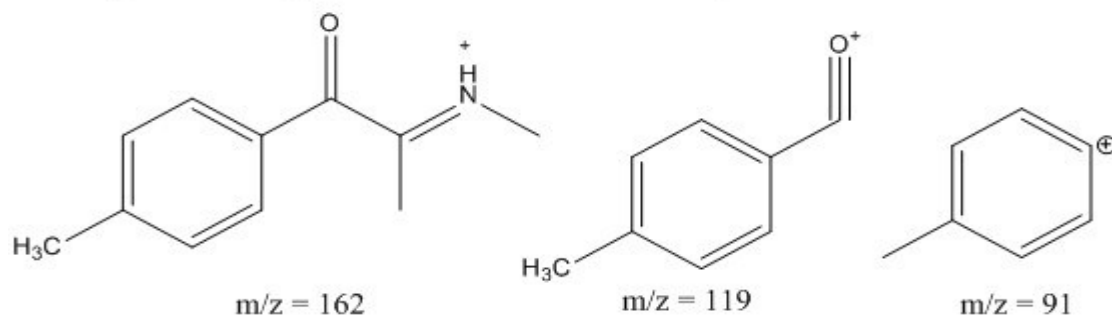


Figure 5.9 The proposed fragmentation of (±)-mephedrone and (±)-mexedrone, under EI-MS conditions.

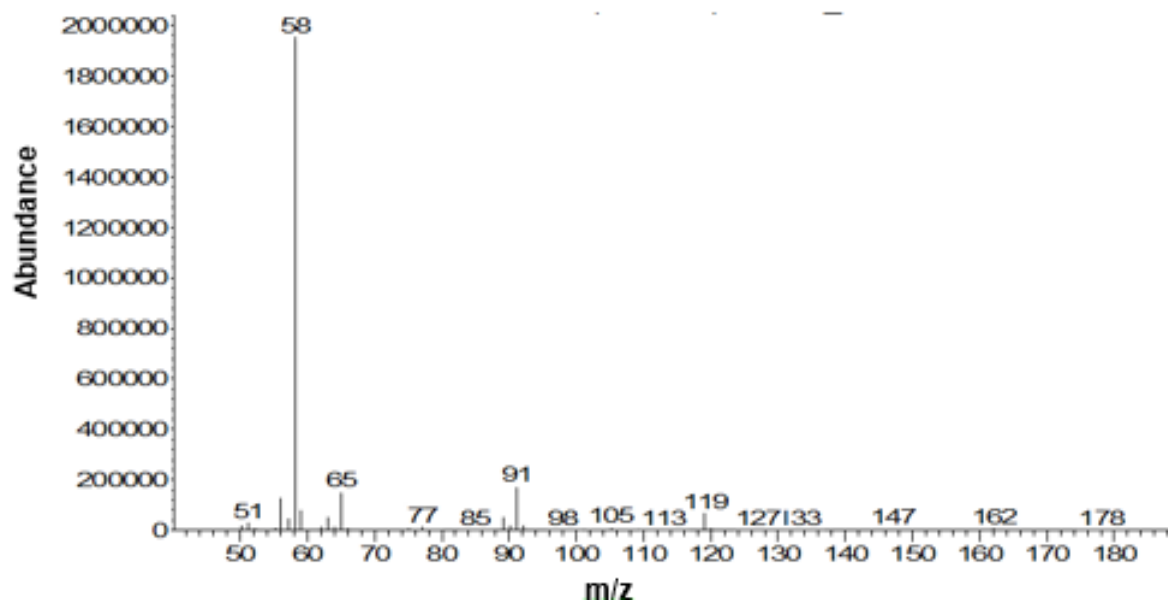


Figure 5.10 Mass spectra of 100 $\mu\text{g mL}^{-1}$ of (±)-mephedrone.

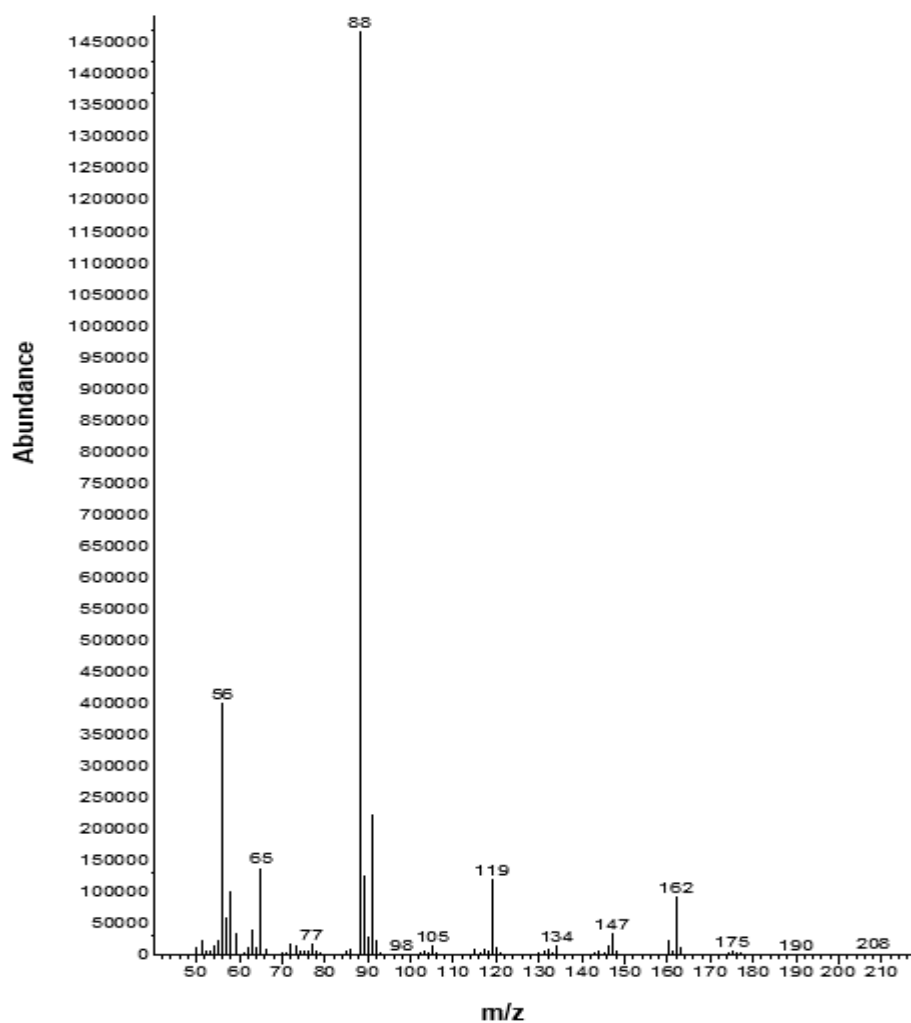


Figure 5.11 Mass spectra of 100 $\mu\text{g mL}^{-1}$ of (±)-mexedrone.

5.5 Ultraviolet-visible spectroscopy (UV-vis) (determination of λ_{\max})

The UV spectrum of (±)-mephedrone in mobile phase 3 shows λ_{\max} at 263 nm ($A = 1.195$, $c = 9.1 \times 10^{-4}$ g 100 mL⁻¹). Likewise, in the ultraviolet spectrum of (±)-mexedrone, λ_{\max} at 263 nm ($A = 0.382$, $c = 9.1 \times 10^{-4}$ g 100 mL⁻¹). This is similar to that reported by Santali et al. for (±)-mephedrone obtained in deionised water ($\lambda_{\max} = 263.5$ nm, $A = 0.651$, $c = 9.1 \times 10^{-4}$ g 100 mL⁻¹) or 0.1 M aqueous hydrochloric acid ($\lambda_{\max} = 263.5$ nm, $A = 0.662$, $c = 9.1 \times 10^{-4}$ g 100 mL⁻¹) (Santali et al., 2011).

5.6 HPLC method development

Mephedrone and mexedrone have been previously characterised using various chromatographic, spectroscopic, and mass-spectrometric methods and X-ray crystal structure analysis (McLaughlin et al., 2017). The previously published data were used to confirm the purity of the reference materials prior to developing a chromatographic method for their separation and detection. As it can be seen from Section 5.4, it is easy to separate and discriminate between these compounds using GC-MS, the most commonly used method for routine screening of unknown bulk forensic samples. However, the interest was in further developing the application of electrochemical detection of new psychoactive substances based on the recent success with mephedrone and its N-ethyl derivative (4-MEC) (Zuway et al., 2015; Khreit et al., 2012).

In this study, for the first time, high performance liquid chromatography combined with an amperometric detection protocol was used for the separation and quantitation of mephedrone and mexedrone. The HPLC-UV chromatographic method was developed by employing change in an isocratic elution to ensure both optimal detection of the analytes and a rapid analysis time. The starting point was to develop an HPLC-UV method that could separate and identify (±)-mephedrone and

(±)-Mexedrone in a mixture with good resolution and shorter relative retention time. The method development was carried out using an adaptation of the HPLC-UV method was reported in chapter 4. The original method in chapter 4 used 30:70 % v/v methanol: 10 mM ammonium acetate buffer containing a suitable electrolyte (100 mM KCl) to analyse the (±)-mephedrone and (±)-4-MEC, but in this study, the organic modifier was increased. To improve the resolution between (±)-mephedrone and (±)-mexedrone, the percentage of organic modifier was changed to 38:62 % v/v methanol: 10 mM ammonium acetate buffer containing a suitable electrolyte (100 mM KCl) and the flow rate decreased to 0.8 mL min⁻¹. The pH of the eluent was adjusted to 3.5 by added as dropwise of acetic acid to ensure (±)-mexedrone and (±)-mephedrone were fully ionised. By the above modification, (±)-mephedrone and (±)-Mexedrone were eluted at 5.75 and 6.55 min respectively using the HPLC-UV (UV detection) with the LC-FC-A system. The resolution between the two peaks was 2.41 which implies “baseline resolution” under the published ICH guidelines (ICH, 1996).

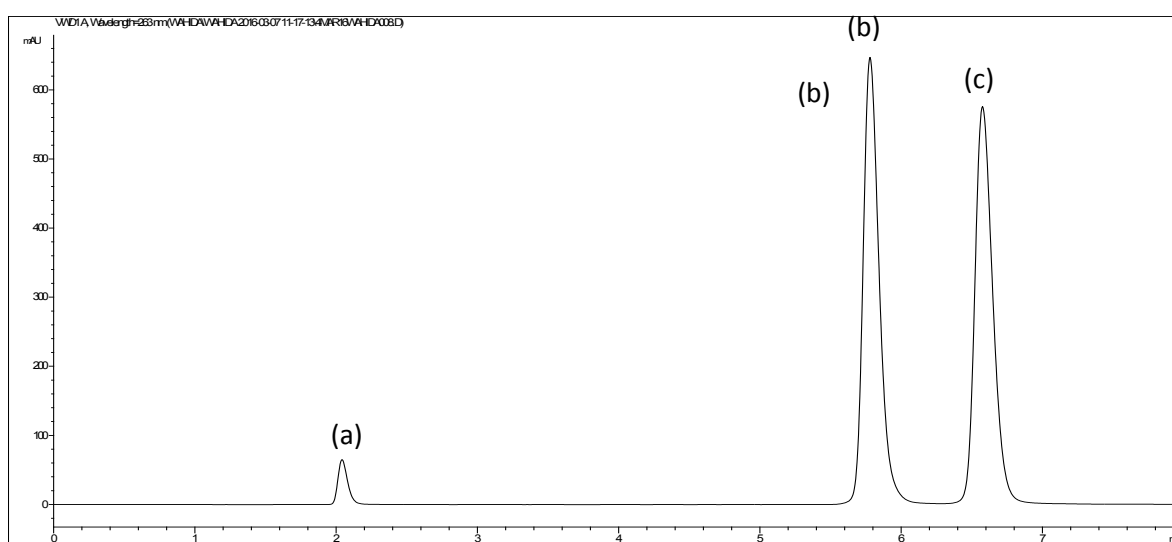


Figure 5.12 The chromatogram of a solution containing uracil (a) 200 µg mL⁻¹, (±)-mephedrone (b), - and (±)-Mexedrone (c) obtained on a HPLC-UV system (UV detection) using an ACE 3 C₁₈ column (150 mm × 4.6 mm i.d., particle size: 3 µm); flow-rate: 0.8 mL min⁻¹; mobile phase 3; detector wavelength (UV): 264 nm.

5.7 Amperometric detection method development

The following optimisation of the anodic potential, linear velocity and pH had to be performed to achieve the optimal detector response and get the optimum conditions of electrochemical response before applying this method to the purchased street samples.

5.7.1 Optimisation of anodic potential by amperometric detection (AD)

By using same HPLC-UV optimal conditions that were obtained in the method development in Section 5.6 (temperature = 22°C, flow rate = 0.8 mL min⁻¹ and pH = 3.5) some changes were made in the potential of amperometric detection (HPLC-AD) to find the best potential to produce a high current response and improve the sensitivity. The (±)-mephedrone (300 µg mL⁻¹) and (±)-Mexedrone (300 µg mL⁻¹) anodic potentials in mobile phase 3 (Table 2.3) were determined by using the peak current (µA) in conjunction with the optimised instrumental configuration. The potential required to achieve the optimal detector response for the mixture was determined, for HPLC-AD in the LC-FC-A system by measuring the amperometric response (peak current, µA) as a function of the anodic potential (E V⁻¹), over the range +0.0 to +1.5 V⁻¹. The maximum high current responses (0.602 and 0.688, n=3) were detected at +1.4 V⁻¹ for (±)-mephedrone and (±)-Mexedrone respectively (Table 5.3).

Table 5.3 The anodic potential of 300 µg mL⁻¹ of (±)-mephedrone and (±)-Mexedrone over the range + 1.1 to + 1.5 V⁻¹ using mobile phase 3, ACE 3 C₁₈ column (150 mm x 4.6 mm i.d., particle size: 3 µm); temperature = 22 °C, flow rate = 0.8 mL min⁻¹ and pH = 3.5 using HPLC-AD in the LC-FC-A system.

Potential (v)	Peak high (µA)	
	(±)-Mephedrone	(±)-Mexedrone
1.1	0.119	0.172
1.2	0.301	0.344
1.3	0.452	0.552
1.4	0.602	0.688
1.5	0.231	0.283

5.7.2 Optimisation of the linear velocity of amperometric detection

The same HPLC-UV optimal conditions obtained from optimisation of the potential in Section 5.7.1 were used (temperature = 22°C, potential 1.4 V and pH = 3.5). These conditions were used in the experiment to optimise the linear velocity of the amperometric detection. The linear velocity required to achieve the optimal detector response for the mixture was determined for LC-FC-A by measuring the amperometric response (peak current, μA) as a function of linear velocity over the range 0.8 to 1.2 mL min^{-1} . The maximum high current responses (0.602 and 0.688, $n=3$) were detected at 0.8 mL min^{-1} for (\pm)-mephedrone and (\pm)-Mexedrone respectively (Table 5.4).

Table 5.4 The linear velocity of 300 $\mu\text{g mL}^{-1}$ (\pm)-mephedrone and (\pm)-Mexedrone over the range 0.8 to + 1.2 mL min^{-1} using mobile phase 3, ACE 3 C_{18} column (150 mm x 4.6 mm i.d., particle size: 3 μm); at temperature = 22 °C and pH = 3.5 using HPLC-AD in the LC-FC-A system.

Flow rate mL min^{-1}	Peak high (μA)	
	(\pm)-Mephedrone	(\pm)-Mexedrone
0.8	0.602	0.688
1	0.456	0.477
1.2	0.328	0.383

5.7.3 Optimisation of pH of HPLC-UV and amperometric detection

One of the important parameters affecting the current response is the pH of the mobile phase. The previously used optimised conditions were used to optimise the response of the detector for 300 $\mu\text{g mL}^{-1}$ of (\pm)-mephedrone and 300 $\mu\text{g mL}^{-1}$ of (\pm)-Mexedrone with a various pH values for mobile phase 3 (Table 2.3). The pH of mobile phase 3 required to achieve the optimal detector response for the mixture was determined by measuring the amperometric response (peak current, μA) as a function of pH over the range 3.5 to 7.5 mL min^{-1} . The maximum detector response was found at pH = 3.5 as 0.602 and 0.688, $n=3$ for (\pm)-mephedrone and (\pm)-

Mexedrone respectively (Table 5.5). At pH less than 3.5, an overlap of the mephedrone and mexedrone peaks was observed in the chromatogram of HPLC-UV and a loss of the analytes' activity. At pH values more than 7.5, turbidity was observed in the solution, because the ionisation of these drugs was changed and in basic solution the drugs will be in their free base form and will be precipitating from the solution. By the optimisation of the amperometric detection of HPLC-AD in the LC-FC-A system (Sections 5.7.1, 5.7.2, and 5.7.3), the analytes were eluted at 5.77 and 6.57 minutes for (±)-mephedrone and (±)-Mexedrone respectively (Figure 5.13).

Table 5.5 The effect of pH of the mobile phase on the analysis of (±)-mephedrone and (±)-Mexedrone over the range 3.5 to 7 using mobile phase 3, ACE 3 C₁₈ column (150 mm x 4.6 mm i.d., particle size: 3 µm); at temperature = 22 °C and flow rate = 0.8 mL min⁻¹ using HPLC-AD in the LC-FC-A system.

pH	Peak high (µA)	
	(±)-Mephedrone	(±)-Mexedrone
3.5	0.602	0.688
5.5	0.435	0.457
7.5	0.378	0.383

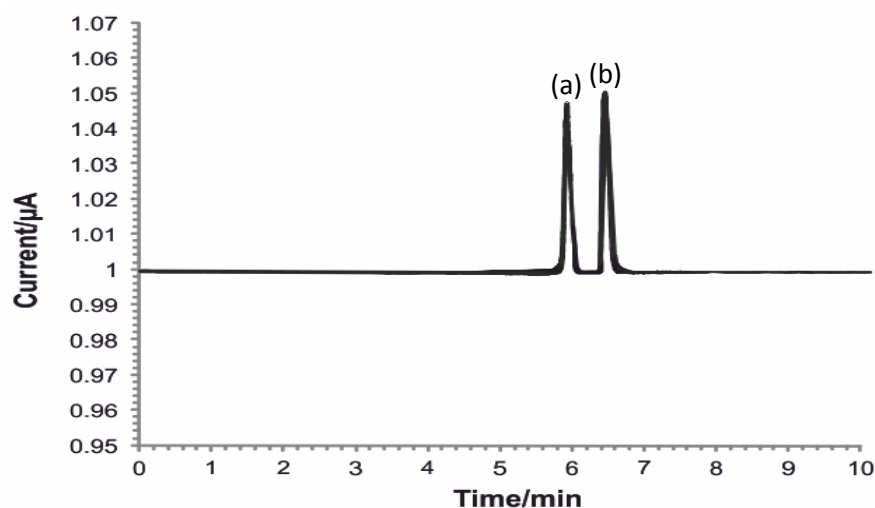


Figure 5.13 Amperogram of a solution containing 200 µg mL (±)-mephedrone (a), and (±)-Mexedrone (b) obtained on the LC-FC-A system (amperometric detection) using an ACE 3 C₁₈ column (150 mm × 4.6 mm i.d., particle size: 3 µm); flow-rate: 0.8 mL min⁻¹; mobile phase 3.

5.8 HPLC-AD method validation

Method validation was used to confirm that the HPLC-AD protocol could rapidly separate and detect (±)-mephedrone and (±)-mexedrone. By the results of

validation it is possible to judge the quality, reliability, and consistency of the HPLC-AD system to use for analysis of MEX-1, MEX-2, MEX-3 (street samples that were obtained from Research Chemicals), and MEX-4 (street sample obtained from Bulkled.eu) Table 2.1. The methods were validated for selectivity, linearity, resolution, detection and quantification limits, robustness, precision, reproducibility, and accuracy in accordance with ICH guidelines (ICH, 1996). Table 5.6 shows the optimal conditions used for method validation.

Table 5.6 Summary of the optimal conditions used for method validation of (±)-mephedrone and (±)-mexedrone using the LC-FC-A system.

Optimised chromatographic conditions	
Column	Column A (Section 2.2.1; ACE 3 C ₁₈ column (150 mm × 4.6 mm i.d., particle size: 3 µm))
Flow rate	0.8 mL min ⁻¹
Solvent	Mobile phase 3 (Table 2.3)
Column temperature (°C)	22
Wavelength (nm)	263
Injection volume (µL)	10
Run-time (mins)	10
pH	3.5
Optimised amperometric detection parameters	
Potential (v)	+1.4
Equilibration time (s)	10
Data interval (s)	0.05
Current range (mA)	1 × 10 ⁻⁶ – 1
Total run time (s)	5000

5.8.1 System suitability test

Retention time, capacity factors, theoretical plates, resolution, and asymmetric factors are presented in Table 5.7. The system suitability test is very important to evaluate the suitability and effectiveness of the entire chromatographic system, not only before use but also during the time of analysis. (±)-Mephedrone was eluted at 5.75 min and (±)-mexedrone eluted at 6.55 min, with high resolution 2.41. Both analytes had theoretical plates within the range >2000, where (±)-mephedrone

theoretical plates were 14000 and (±)-mexedrone were 15000. The asymmetric factor for both analytes was found to be < 2, where (±)-mephedrone was 0.62 and (±)-mexedrone was 0.52.

The summary of the method validation results in Table 5.7 and Table 5.8 were obtained from the standard calibration analyses with their respective correlation coefficients, slopes, and intercepts resulting from the linear regression analysis.

Table 5.7 Summary of HPLC-UV (UV detection) validation data for the quantification of (±)-mephedrone and (±)-Mexedrone using HPLC-UV in the LC-FC-A system, column A (Table 2.3 mobile phase3; wavelength = 263 nm).

System detection	HPLC-UV	
Flow Rate	0.8 mlmin ⁻¹	
Analytes	(±)-Mephedrone	(±)-Mexedrone
t _R (min)(t ₀ = 2.03min) ^a	5.75	6.55
RRT ^b	1	0.9
Capacity factor (k')	1.5	1.83
N (plate)	14000 (68691) ^c	15000 (61904) ^c
H (m)	1.46×10 ⁻⁰⁵	1.62×10 ⁻⁰⁵
Resolution (R _s)	/	2.41
Asymmetry factor (A _s)	0.62	0.52
LOD ^d (µg ml ⁻¹)	6.52	5.15
LOQ ^e (µg ml ⁻¹)	19.75	15.62
Co-efficient of regression(r ²)	0.999 ^f	0.999 ^g
Precision (%RSD) (n=6)		
100 µg mL ⁻¹	0.024	0.019
200 µg mL ⁻¹	0.091	0.004
300 µg mL ⁻¹	0.040	0.013
400 µg mL ⁻¹	0.280	0.012
500 µg mL ⁻¹	0.045	0.009
^a Measured from the retention time of uracil (10 µg mL ⁻¹) eluting from the column. ^b Relative retention time (concerning (±)-mephedrone. ^c N expressed in plates per m. ^d Limit of detection. ^e Limit of quantification. ^f y = 50.834x - 5.4499. ^g y = 33.976x + 1312.		

Table 5.8 Summary of HPLC-AD (amperometric detection) validation data for the quantification of (±)-mephedrone and (±)-mexedrone using HPLC-AD in the LC-FC-A system, column A, (Table 2.2), mobile phase 3; detector wavelength = 263 nm.

System detection	HPLC-AD	
Flow Rate	0.8 ml min ⁻¹	
Analytes	(±)-mephedrone	(±)-mexedrone
t _R (min)(t ₀ = 2.03min) ^a	5.77	6.57
RRT ^b	1	0.9
LOD ^c (µg mL ⁻¹)	13.21	9.95
LOQ ^d (µg mL ⁻¹)	40.03	30.16
Co-efficient of regression(r ²)	0.996 ^e	0.998 ^f
Precision (%RSD) (n=6)		
100 µg mL ⁻¹	0.65	0.81
200 µg mL ⁻¹	0.14	2.56
300 µg mL ⁻¹	1.41	0.31
400 µg mL ⁻¹	0.68	0.61
500 µg mL ⁻¹	0.27	0.63
^a Measured from the retention time of uracil (10 µg mL ⁻¹) eluting from the column. ^b Relative retention time (concerning (±)-mephedrone. ^c Limit of detection. ^d Limit of quantification. ^e y = 0.0012x - 0.0068. ^f y = 0.0013x + 0.0311.		

5.8.2 Resolution (Rs)

Resolution in this study explains the separation between (±)-mephedrone and (±)-mexedrone as shown in Table 5.7. (±)-mephedrone was eluted at 5.77 and (±)-mexedrone was eluted at 6.57 with an excellent resolution of 2.41 that explains this method has a good separation between (±)-mephedrone and (±)-mexedrone because of their resolution was more than two which implies “baseline resolution” under the published ICH guidelines (ICH, 1996).

5.8.3 Linearity

The linearity was evaluated by using a calibration curve to calculate the coefficient of correlation, slope, and intercept values. The linearity was obtained for the HPLC-UV system by a plot constructed from the concentration and peak area (Figure 5.14 a). In this study, the high concentration standards' range used in this study was (100-500 µg mL⁻¹); the 50 µg mL⁻¹ as was that run in the previous chapter

4 could not be used because the amperometric detection in this study needed a high concentration to have a good detection for both the (±)-mephedrone and (±)-mexedrone. , Six replicates were injected under the optimal conditions used in the method development.

The calibration standards all showed excellent linearity responses. That for (±)-mephedrone was $R^2 = 0.999$ with good repeatability and RSD values in the range 0.02-0.28%; $n = 6$ (Appendix: Table 9.22), and for (±)-mexedrone, $R^2 = 0.999$ with RSD values in the range of 0.003–0.02%; $n = 6$ (Appendix: Table 9.23).

The corresponding liquid chromatography-amperometric detection system, the impinging jet, flow cell LC-FC-A was used. The calibration standard (100-500 $\mu\text{g mL}^{-1}$, with six replicated injections) showed good linearity by a plot constructed from the concentration and peak high (Figure 5.14b). The (±)-mephedrone linearity of was $R^2 = 0.996$ with good repeatability with RSD values in the range 0.14-0.722%; $n = 6$ (Appendix: Table 9.24) and for (±)-mexedrone, $R^2 = 0.997$ with RSD values in the range 0.31–0.81%; $n = 6$ (Appendix: Table 9.25). However, both HPLC-UV and HPLC-AD in the LC-FC-A system have a good linearity but the linearity of HPLC-UV was better than the linearity of HPLC-AD in LC-FC-A system due to the HPLC-UV detection having a higher sensitivity to the analytes than HPLC-AD in the LC-FC-A system.

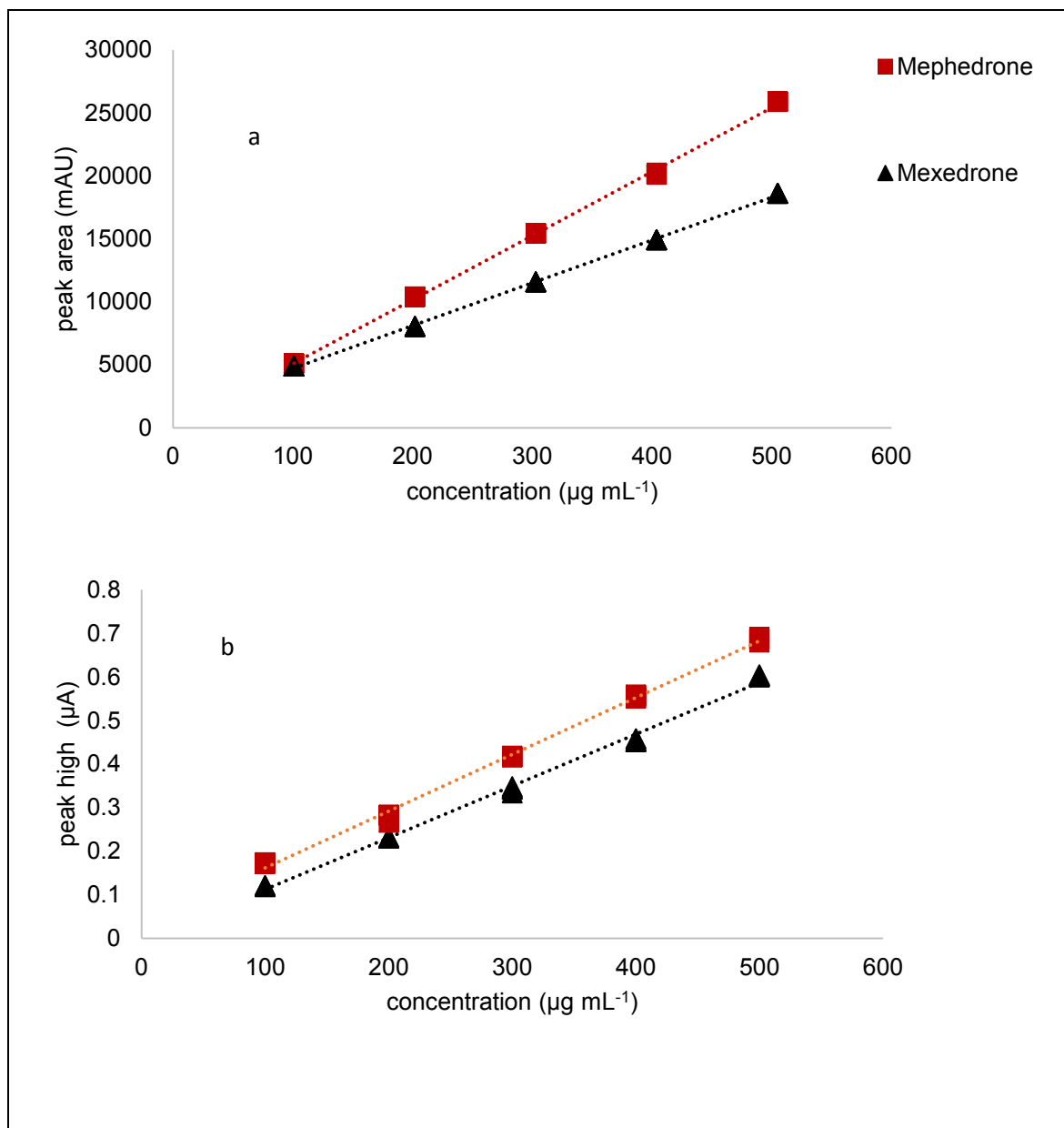


Figure 5.14 The linearity of (±)-mephedrone (squares) and (±)-mexedrone (triangles) by using a) HPLC-UV in the LC-FC-A system b) HPLC-AD in the LC-FC-A system.

5.8.4 Limit of detection (LOD)

LOD was estimated from the calibration standard curve. The standards were used over a concentration range of 100-500 µg mL⁻¹ and injected as six replicates. The LOD of analysis (±)-mephedrone was determined using HPLC-UV in the LC-FC-A system (UV detector) and found to be 6.52 µg mL⁻¹ which was slightly similar to the previous study in chapter 4 where it was 2.5 µg mL⁻¹, and that was due to the change in concentration range of the calibration standard in both studies. The LOD of (±)-mexedrone was 5.15 µg mL⁻¹. Even although the McLaughlin et al.

(McLaughlin et al., 2017) published a liquid chromatographic method for the characterisation of (±)-mexedrone, no LOD and LOQ were reported, therefore, this study is the first to report the LOD for (±)-mexedrone within bulk forensic samples.

The LOD of analysis of (±)-mephedrone was determined using HPLC-AD in the LC-FC-A system (amperometric detector) and was found to be 13.21 $\mu\text{g mL}^{-1}$, similar to the previously reported levels of 14.66 $\mu\text{g mL}^{-1}$ in chapter 4. The LOD of (±)-mexedrone was 9.95 $\mu\text{g mL}^{-1}$. In both detection systems, the LOD of the LC-FC-A system was two times higher than the LOD of HPLC-UV. Which previously observed, HPLC-UV has higher sensitivity than HPLC-AD in this study (Table 5.7 and Table 5.8).

5.8.5 Limit of quantification (LOQ)

LOQ was calculated using a calibration standard curve (standard range 100-500 $\mu\text{g mL}^{-1}$ and injected six replicates). The LOQ for (±)-mephedrone was determined to be 19.75 $\mu\text{g mL}^{-1}$ by using HPLC-UV and 40.03 $\mu\text{g mL}^{-1}$ by using HPLC-AD in the LC-FC-A system. Compared to a previous study (chapter 4), the LOQ was 7.58 $\mu\text{g mL}^{-1}$ using HPLC-UV and 44.42 $\mu\text{g mL}^{-1}$ using HPLC-AD in the LC-FC-A system. In comparing between the previous and this study, there was a clear difference in the LOQ due to a change in the concentrations of the calibration range utilised in this study. In addition, the LOQ for (±)-mexedrone was 15.62 $\mu\text{g mL}^{-1}$ using the HPLC-UV system and 30.16 $\mu\text{g mL}^{-1}$ by using HPLC-AD in the LC-FC-A system (Table 5.7 and Table 5.8).

5.8.6 Robustness

A robustness test was performed in this study to confirm this method can be used for analysis of mixture solutions of 300 $\mu\text{g mL}^{-1}$ of (±)-mephedrone and 300 $\mu\text{g mL}^{-1}$ of (±)-mexedrone which were prepared in Section 2.8.7, although with a minor

change in some parameters such as temperature and organic composition ratio. Table 5.9 shows the effect of a minor change in temperature on the analysis of (±)-mephedrone and (±)-mexedrone using HPLC-UV in the LC-FC-A system. Temperature plays a very important role in confirming the robustness of the analytical method. The temperatures used were 20°C, 22°C and 24°C and the relative standard deviation (RSD %) of relative retention time (RRT) was found to be less than 1% for (±)-mephedrone and (±)-mexedrone using HPLC-UV in the LC-FC-A system, therefore this method is robust.

Table 5.10 shows the effect of a minor change in mobile phase: Mobile phase 3 (Table 2.3), the ratios between methanol: buffer solution A (Section 2.3.1) used were 40:60, 38:62, and 36:64. The relative standard deviation (RSD %) of relative retention time was found to be less than 1% for (±)-mephedrone and (±)-mexedrone respectively, using HPLC-UV in the LC-FC-A system. Due to no significant change in RSD%, this confirmed this method is robust.

Table 5.9 The effect of minor changes of temperature on relative retention time (RRT) of analysis of 300 µg mL⁻¹ of (±)-mephedrone and (±)-mexedrone using HPLC-UV in the LC-FC-A system. (The highlighted area is a standardised condition for this study).

Concentration	RRT					
	(20 °C)		(22 °C)		(24 °C)	
	Mephedrone	Mexedrone	Mephedrone	Mexedrone	Mephedrone	Mexedrone
400	0.876	1.000	0.878	1.000	0.878	1.000
400	0.876	1.000	0.878	1.000	0.878	1.000
400	0.876	1.000	0.878	1.000	0.879	1.000
400	0.874	1.000	0.876	1.000	0.876	1.000
400	0.876	1.000	0.878	1.000	0.878	1.000
400	0.876	1.000	0.879	1.000	0.879	1.000
Average	0.875	1.000	0.878	1.000	0.878	1.000
RSD%	0.110	0.000	0.108	0.000	0.108	0.000

Table 5.10 The effect of a minor change in organic composition of mobile phase 3 on the relative retention time (RRT) of 300 µg mL⁻¹ of (±)-mephedrone and (±)-mexedrone using HPLC-UV in the LC-FC-A system. (The highlighted area is a standardised condition for this study).

Concentration	RRT
---------------	-----

	(40:60% v/v methanol: buffer solution pH = 3.5, Section 2.4		(38:62% v/v methanol: buffer solution pH = 3.5, Section 2.4		(36:64% v/v methanol: buffer solution pH = 3.5, Section 2.4	
	Mephedrone	Mexedrone	Mephedrone	Mexedrone	Mephedrone	Mexedrone
400	0.876	1.000	0.878	1.000	0.878	1.000
400	0.876	1.000	0.878	1.000	0.878	1.000
400	0.876	1.000	0.878	1.000	0.879	1.000
400	0.874	1.000	0.876	1.000	0.876	1.000
400	0.876	1.000	0.878	1.000	0.878	1.000
400	0.876	1.000	0.879	1.000	0.879	1.000
Average	0.875	1.000	0.878	1.000	0.878	1.000
RSD%	0.110	0.000	0.108	0.000	0.108	0.000

5.8.7 Inter- and intra-day precision

12 replicate injections of a mixture solution of 300 µg mL⁻¹ of (±)-mephedrone and 300 µg mL⁻¹ of (±)-mexedrone were prepared as in Section 2.8.7. The intra-day test was performed on the same day (6 in the morning and 6 in the afternoon), and inter-day test was performed by the same procedure with six injections on the following day. However, the results' precision showed little change between HPLC-UV and HPLC-AD in the LC-FC-A system, but HPLC-UV had excellent precision for (±)-mephedrone and (±)-mexedrone, as shown by the RSD % of the peak area being less than 1% (Table 5.11). HPLC-AD achieved good precision for both compounds (±)-mephedrone and (±)-mexedrone as shown by the RSD% values (Table 5.11) of the peak current being less than 1% (Appendix: Table 9.26). The value of RSD% is suggested to be ≤ 1% as an appropriate precision criterion for repetitive injections to assess the precision of an instrument in analytical method validation (Green, 1996). Little drifting of either compound was found, and these results illustrate the ability of this method and the efficiency of these systems to be applied to routine analysis.

Table 5.11 The relative standard deviation (RSD %) of inter- and intra-day precision for (±)-mephedrone and (±)-mexedrone by using HPLC-UV and HPLC-AD in the LC-FC-A system.

System	RSD% of LC-FC-A (n = 12)	
Detection	HPLC-UV	HPLC-AD

		Peak area (mAU)	Peak current (μ A)
Inter-day precision	(\pm)-mephedrone	0.040	0.657
	(\pm)-mexedrone	0.019	0.584
intra-day precision	(\pm)-mephedrone	0.218	0.703
	(\pm)-mexedrone	0.174	0.631

5.8.8 Accuracy

To test the accuracy of the method, two standards, of (\pm)-mephedrone and (\pm)-mexedrone, were prepared as 240, 300 and 360 μ g mL⁻¹. All prepared solutions were injected three times and showed excellent recovery in the range of 99.9-100.9 %, and repeatability with RSD % values 0.01-0.8 % using the HPLC-UV system. The recovery range was 99.9-101.6 % and repeatability RSD % values were in the range 0.3-0.8 % by using HPLC-AD in the LC-FC-A system for (\pm)-mephedrone and (\pm)-mexedrone. In both systems, the recovery range was within the acceptable limits according to ICH (ICH, 1996), therefore this method has a good accuracy.

Table 5.12 Accuracy data expressed as the percentage recovery of a mixture of (\pm)-mephedrone and (\pm)-Mexedrone by using both HPLC-UV and HPLC-AD in the LC-FC-A system.

System			LC-FC-A			
Detection			HPLC-UV		HPLC-AD	
Analyte	Concentration (μ g mL ⁻¹)	Theoretical recovery (μ g mL ⁻¹)	Actual recovery (μ g mL ⁻¹)	%recovery (n=3)	Actual recovery (μ g mL ⁻¹)	%recovery (n=3)
Mephedrone	240 (80%)	242.5	243.09	100.3 (\pm 0.09)	241.35	99.6 (\pm 0.34)
Mexedrone		242.5	242.47	100.1 (\pm 0.04)	242.79	100.1 (\pm 0.6)
Mephedrone	300 (100%)	303.0	303.87	100.3 (\pm 0.04)	303.13	100.4 (\pm 1.0)
Mexedrone		303.0	302.21	99.7 (\pm 0.01)	304.44	100.5 (\pm 0.3)
Mephedrone	360 (120%)	363.6	360.60	99.2 (\pm 0.23)	365.09	100.4 (\pm 0.57)
Mexedrone		363.6	360.62	99.1 (\pm 0.01)	360.09	99.3 (\pm 0.65)

5.9 Application of the methodology to forensic analysis

Street samples containing mexedrone and mephedrone were purchased (Table 2.1) and the purity of the analytes were analysed using HPLC-UV and HPLC-AD in the LC-FC-A system. A new electrode was used for each sample. MEX-1 and MEX-3 contained 95% of mexedrone and no mephedrone was observed. The MEX-

2 contained approximately 80% mexedrone and only 20% mephedrone, in contrast, MEX-4 was shown to contain $99.84 \pm 0.84\%$ mephedrone but mexedrone was not observed in MEX-4 sample. The results of the HPLC-UV analysis are summarised in Table 5.13. In terms of using HPLC-AD in the LC-FC-A system, the results have supported those obtained from the HPLC-UV analysis. Table 5.13 also shows the results of the analysis of street samples using HPLC-AD in the LC-FC-A system. MEX-1 and MEX-3 contained only mexedrone were more than 95% pure in both street samples and were similar to the results obtained by using HPLC-UV in the LC-FC-A system. In addition, MEX-2 contained $80.71 \pm 0.32\%$ of mexedrone and only $18.48 \pm 1.25\%$ of mephedrone. In addition, MEX-4 was shown to contain $99.9 \pm 1.07\%$ of mephedrone.

Table 5.13 Summary of the quantification analysis of street samples by using HPLC-UV and LC-FC-A systems.

System	LC-FC-A			
Detection	HPLC-UV (%w/w) (n =6)		HPLC-AD (%w/w) (n= 6)	
Analyte	mephedrone	mexedrone	mephedrone	mexedrone
tR (min)	5.75	6.55	5.79	6.57
MEX-1	n.d.	99.27 ± 0.39	n.d.	98.35 ± 0.35
MEX-2	18.16 ± 1.09	82.27 ± 0.35	18.48 ± 1.25	80.71 ± 0.32
MEX-3	n.d.	99.26 ± 0.04	n.d.	96.02 ± 1.38
MEX-4	99.84 ± 0.84	n.d.	99.9 ± 1.07	n.d.
n.d. not detected				

5.10 Conclusion

The combination of high performance liquid chromatography with amperometric detection (HPLC-AD) for qualitative and quantitative analysis of (\pm)-mephedrone and the new derivative (\pm)-mephedrone called (\pm)-mexedrone have been reported using an imaging jet flow cell for electrochemical detection (LC-FC-A) incorporating disposable embedded graphite screen-printed electrodes (GSPE). In addition, the validation of the HPLC-AD protocol has been shown by using HPLC-

UV to have a higher limit of detection for (±)-mephedrone ($6.52 \mu\text{g mL}^{-1}$) than that obtained for (±)-mephedrone. In chapter 4 it was $2.5 \mu\text{g mL}^{-1}$ and these differences are due to the change in concentration range utilised in the calibration run. However, in terms of using amperometric detection (HPLC-AD), the limit of detection for (±)-mephedrone was $13.21 \mu\text{g mL}^{-1}$ and similar to the LOD in chapter 4 where it was $14.66 \mu\text{g mL}^{-1}$. Finally, the study in this chapter confirmed the last study in chapter 4 and this new protocol distinguished between mephedrone and its derivatives.

Since this work carried out, the New Psychoactive Substances Act came into force (UK-Government, 2016), and subsequently all psychoactive compounds including (±)-mephedrone have become banned under the new legalisation. Since the ban, it is highly possible that compounds which were previously available in a highly pure form may now have become more adulterated with potential cutting agents such as caffeine and paracetamol. Therefore, this work will in future be extended taking into account possible adulterants.

6 Chapter 6: Detection and quantification of regioisomers of new psychoactive substances (NPS) using high performance liquid chromatography-amperometric detection (HPLC-AD)

6.1 Introduction

Dissociative anaesthetics such as dextromorphan, ketamine and phencyclidine (PCP) affect the central nervous system to produce feelings of detachment and induce a state of anaesthesia due to antagonising ionotropic *N*-methyl-*D*-aspartate receptors (NMDAR) (Morris and Wallach, 2014). The spread of PCP and ketamine derivatives, a new dissociative anaesthetic known as diarylethylamine based on leftamine (Table 6. 1a). Diarylethylamine is not a new compound, and was actually reported in 1924. one of diarylethylamine can be found in the NPS market, as crystals or a powder, is ephenidine and this has mild psychedelic effects (Beharry and Gibbons, 2016). Recently, ephenidine became available and anecdotally appears popular with dissociative users (e.g as an alternative to ketamine). The previous study reported the comparison between ephenidine and ketamine and showed that ephenidine is a relatively selective, voltage-dependent NMDA antagonist, which explains the psychotomimetic effects of ephenidine and predicts the side-effects including memory impairments (Kang et al., 2017). Ephenidine, also known as NEDPA (N-ethyl-1,2-diphenyl ethylamine) and EPE, is a dissociative anaesthetic that exerts its pharmacological action as an N-methyl-*D*-aspartate receptor antagonist (NMDAR) and has been used as a potential general anaesthetic for animals and humans (Kang et al., 2017). Therefore, ephenidine is referred to as a "dissociative anaesthetic" and is used as a recreational drug (Morris and Wallach, 2014). In many countries, ephenidine is

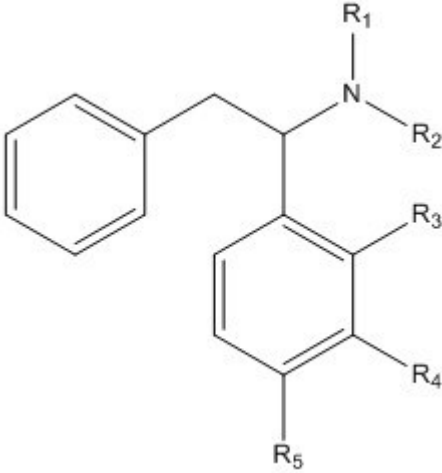
illegal as the structural isomer of the banned opioid drug lefetamine (Wink et al., 2014; Wink et al., 2015).

The variety and evolution of drug types have resulted in a continual analytical challenge for detection, identification, and measurement. This challenge has seen the use of techniques such as HPLC–DAD and LC or GC coupled with accurate mass spectrometry (Favretto et al., 2013). Electrochemistry, as an analytical tool, has the advantages of sensitivity and selectivity toward many target analytes (Smith et al., 2014a; Smith et al., 2015; Metters et al., 2011). An electrochemistry protocol was used in the previous study by Smith et al. for the analysis of the synthetic cathinones, (±)-mephedrone and (±)-4-MEC, either in their pure form by using electroanalytical oxidation (Smith et al., 2014a), or in an impure form (with adulterants) by using direct electrochemical reduction (Smith et al., 2014b). Electrochemical analysis using graphite screen-printed macro electrodes (GSPEs) has the ability to be a rapid, simple and cost-effective analytical screening tool. Moreover, in chapter 4, the HPLC-AD system (high performance liquid chromatography combined with amperometric detection) was used in the separation, detection and quantification of the NPSs (±)-mephedrone and (±)-4-MEC in presence of caffeine as adulterant (Zuway et al., 2015).

In this chapter, the developed HPLC-AD protocol was applied to the qualitative and quantitative analysis of NPSs' regioisomers (regioisomers of methoxyphenidine and fluoroephenidine). Three regioisomer methoxy derivatives of ephenidine, namely (±)-2-methoxyephenidine [(±)-2-MEP; Table 6. 1c], (±)-3-methoxyephenidine [(±)-3-MEP; Table 6. 1d] and (±)-4-methoxyephenidine [(±)-4-MEP; Table 6. 1e] were analysed for the first time in this study. The second study explained the analysis of three regioisomers of fluoroephenidine, namely (±)-2-

fluoroephedrine [(±)-2-FEP; Table 6. 1f], 3-fluoroephedrine [(±)-3-FEP; Table 6. 1g] and (±)-4- fluoroephedrine [(±)-4-FEP; Table 6. 1h]. Methoxyephedrine and fluoroephedrine are derivatives of ephedrine.

Table 6. 1 Chemical structure of ephedrine, lefetamine, and regioisomers of methoxyephedrine, and of fluoroephedrine.

						
Compound		R ₁	R ₂	R ₃	R ₄	R ₅
a	Lefetamine	CH ₃	CH ₃	H	H	H
b	Ephedrine	H	CH ₂ CH ₃	H	H	H
c	2-Methoxyephedrine	H	CH ₂ CH ₃	OCH ₃	H	H
d	3-Methoxyephedrine	H	CH ₂ CH ₃	H	OCH ₃	H
e	4-Methoxyephedrine	H	CH ₂ CH ₃	H	H	OCH ₃
f	2-Fluoroephedrine	H	CH ₂ CH ₃	F	H	H
g	3-Fluoroephedrine	H	CH ₂ CH ₃	H	F	H
h	4-Fluoroephedrine	H	CH ₂ CH ₃	H	H	F

6.2 Detection and quantification of regioisomers of methoxyephedrine using HPLC-AD

This study presents the development and full validation data of the analysis of 2-MEP, 3-MEP, and 4-MEP using high performance liquid chromatography combined with amperometric detection. In terms of the use of amperometric detection, the impinging jet flow cell (LC-FC-A) was used to obtain the peak current (μA) of all the analytes. In addition, it presents the limit of detection and limit of quantification data for all the analytes using UV with amperometric detection for all the analytes.

6.2.1 Ultraviolet-visible spectroscopy (UV) determination of λ_{max}

In this study, the wavelength 279 nm was used to detect and quantify the regioisomers of methoxyephedrine, through their absorbance. The UV maximum (λ_{max}) for (\pm)-2-MEP at 279 nm ($A = 0.793$, 1.0×10^{-2} g 100mL^{-1}), for (\pm)-3-MEP at 279 nm ($A = 0.662$, 1.0×10^{-2} g 100mL^{-1}) and (\pm)-4-MEP (0.761 , 1.0×10^{-2} g 100mL^{-1}) at 279 nm in mobile phase 4 (Table 2.3).

6.2.2 HPLC method development

Due to the new regioisomers of ephedrine having no fully validated methods (or limits of detection and quantification) reported, different parameters were used to develop the HPLC chromatographic method to ensure both optimal detection of the analytes and a rapid analysis time. The starting point was to develop a HPLC-UV method that could separate and identify (\pm)-2-MEP, (\pm)-3-MEP and (\pm)-4-MEP with good resolution and shorter retention time.

By this modification, (\pm)-4-MEP, (\pm)-2-MEP and (\pm)-3-MEP were eluted at 21.61, 23.84 and 25.83 mins respectively using HPLC-UV detection in the LC-FC-A

system. The resolution for all analytes in both systems was in the range > 2 (Figure 6.1).

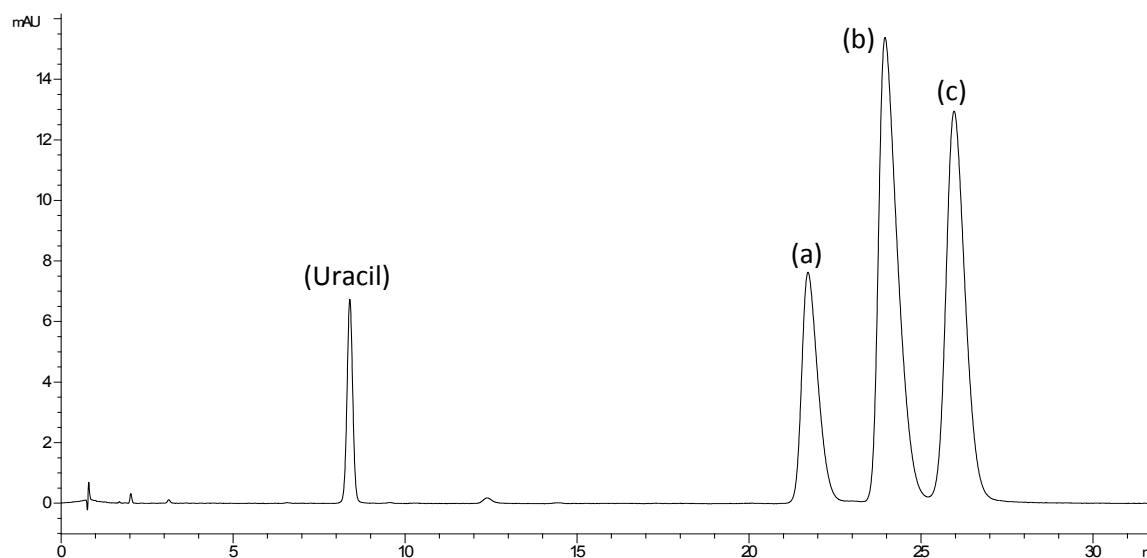


Figure 6.1 The chromatogram of a solution containing $300 \mu\text{g mL}^{-1}$ of (\pm)-4-MEP (a), (\pm)-2-MEP (b) and (\pm)-3-MEP (c) obtained using HPLC-UV in the LC-FC-A system using an ACE 5 C₁₈AR column ($150 \text{ mm} \times 4.6 \text{ mm i.d.}$, particle size: $5 \mu\text{m}$); mobile phase 4 detector wavelength (UV): 279 nm .

6.2.3 Amperometric detection method development

6.2.3.1 Optimisation of potential of amperometric detection

The anodic potentials for (\pm)-2-MEP ($100.0 \mu\text{g mL}^{-1}$), (\pm)-3-MEP ($100.0 \mu\text{g mL}^{-1}$) and (\pm)-4-MEP ($100.0 \mu\text{g mL}^{-1}$) mixture in mobile phase 4 (Table 2.3) were determined using the peak current, in conjunction with the optimised instrumental configuration. The HPLC optimal conditions were used for optimisation of the potential according to the method development in Section 6.4 (temperature = 50°C , flow rate = 2 mL min^{-1} and $\text{pH} = 7$). The potentials required to achieve the optimal detector response for the mixture were determined for LC-FC-A by measuring the amperometric response (peak current, μA) as a function of anodic potential, over the range $+0.0$ to $+1.5 \text{ E V}^{-1}$. The maximum high current responses (0.51 , 0.25 and 0.29 , $n=3$) were detected at $+1.2 \text{ E V}^{-1}$ for (\pm)-2-MEP, (\pm)-3-MEP and (\pm)-4-MEP respectively (Table 6. 1).

Table 6.1 The anodic potentials for 100 $\mu\text{g mL}^{-1}$ of (\pm)-2-MEP, (\pm)-3-MEP and (\pm)-4-MEP over the range 1.0 to + 1.5 V^{-1} using mobile phase 4, column: ACE 5 C_{18}AR column (150 mm \times 4.6 mm i.d., particle size: 5 μm). Temperature = 50 $^{\circ}\text{C}$, flow rate = 2 mL min^{-1} and pH = 7 using HPLC-AD detection in the LC-FC-A system.

Potential(v)	Peak height μA		
	(\pm)-4-MEP	(\pm)-2-MEP	(\pm)-3-MEP
1.0	0.27	0.15	0.16
1.2	0.53	0.28	0.32
1.3	0.44	0.26	0.25
1.4	0.34	0.17	0.19
1.5	0.30	0.15	0.18

6.2.3.2 Optimisation of linear velocity of amperometric detection

The flow rate used in Section 6.1.3.1 was 2 mL min^{-1} because this produced the optimal response. However, in this section, due to the effect of the internal chamber volumes of the flow cells (LC-FC-A = 8 μL) a solution of the mixture (100 $\mu\text{g mL}^{-1}$) was injected ($n = 10$) at range of flow rates 1-2 mL min^{-1} . The amperometric response was measured to determine the optimal linear velocity required for the maximum amperometric response of the LC-FC-A system. Table 6.2 shows the peak current of (\pm)-4-MEP, (\pm)-2-MEP and (\pm)-3-MEP with a good amperometric response [(\pm)-4-MEP = 0.58 μA , (\pm)-2-MEP = 0.28 μA and (\pm)-3-MEP = 0.33] at 1.2 E V^{-1} and (pH = 7) using HPLC-AD in LC-FC-A system. In addition, there was no response observed at flow rates less than 1 mL min^{-1} , and at flow rates more than 2 mL min^{-1} , the peaks on the HPLC-UV (UV detection) system overlapped.

Table 6.2 The linear velocity for 100 $\mu\text{g mL}^{-1}$ of (\pm)-2-MEP, (\pm)-3-MEP and (\pm)-4-MEP over the range 0.9 to 1.2 ml min^{-1} using mobile phase 4, column: ACE 5 C_{18}AR column (150 mm \times 4.6 mm i.d. particle size: 5 μm); at temperature = 50 $^{\circ}\text{C}$, and pH = 7 using HPLC-AD detection in the LC-FC-A system.

Flow rate mL min^{-1}	Peak current		
	(\pm)-4-MEP	(\pm)-2-MEP	(\pm)-3-MEP
1	0.46	0.25	0.29
1.5	0.53	0.28	0.32
2	0.58	0.28	0.33

6.2.3.3 Optimisation of pH of HPLC-UV and amperometric detection

Table 6.3 shows the different pH (3-7) used to find the best pH to obtain the highest response for the analytes. But the best amperometric response for the HPLC-UV and HPLC-AD systems was with a mobile phase of pH = 7, because the pH of the mobile phase cannot be more than 9 or less than 2 to protect the silica from degrading and that affects in the column's performance as explained in Section 3.6. As well as no amperometric response being observed at a mobile phase with pH = 3, the maximum responses using HPLC-AD in the LC-FC-A system were 0.58 μA for (\pm)-4-MEP, 0.28 μA for (\pm)-2-MEP and 0.32 μA for (\pm)-3-MEP, which were observed at a potential = +1.2 E V^{-1} and flow rate 2 mL min^{-1} using a mobile phase with pH = 7. Moreover, the mobile phase pH effect on the response of the HPLC-UV system when using a mobile phase with a pH=5, the peaks in HPLC-UV in the LC-FC-A system overlapped and the resolution of the peaks decreased.

Table 6.3 The effect of the pH of mobile phase on the analysis of 100 $\mu\text{g mL}^{-1}$ of (\pm)-2-MEP, (\pm)-3-MEP and (\pm)-4-MEP over the range 3 to 7 mL min^{-1} using mobile phase 4, column: ACE 5 C_{18}AR column (150 mm \times 4.6 mm i.d. particle size: 5 μm); temperature = 50 $^{\circ}\text{C}$, potential = 1.2 E V^{-1} and flow rate 2 mL min^{-1} using HPLC-AD detection in the LC-FC-A system.

pH	Peak current		
	(\pm)-4-MEP	(\pm)-2-MEP	(\pm)-3-MEP
3	n.d.	n.d.	n.d.
5	0.34	0.16	0.197
7	0.58	0.28	0.32
n.d.=not detected			

By the optimisation of amperometric detection (Section 6.3.1, 6.3.2, and 6.3.3) in the LC-FC-A systems, the analytes were eluted at 21.63, 23.86 and 25.85 minutes for (\pm)-4-MEP, (\pm)-2-MEP and (\pm)-3-MEP respectively in the LC-FC-A (amperometric detection) system (Figure 6.2).

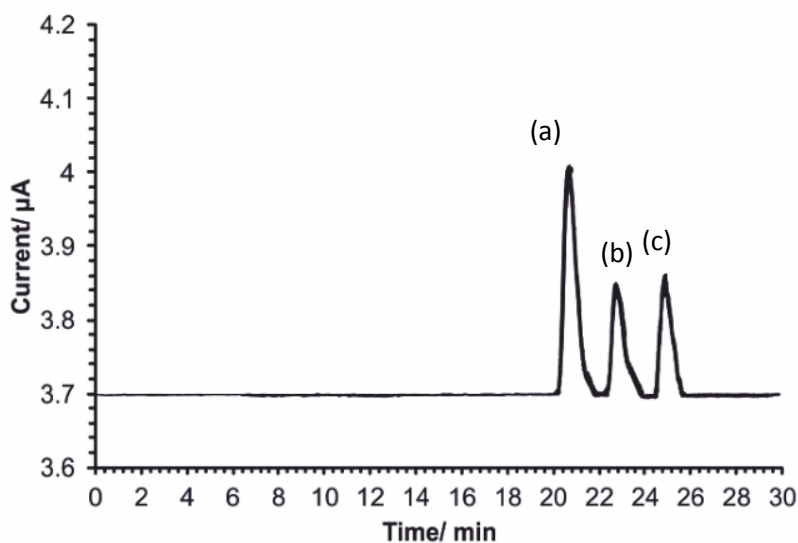


Figure 6.2 Amperogram of a solution containing $300 \mu\text{g mL}^{-1}$ of (\pm)-4-MEP (a), (\pm)-2-MEP (b) and (\pm)-3-MEP (c) obtained on the LC-FC-A system (amperometric detection) using an ACE 5 C₁₈AR column (150 mm \times 4.6 mm i.d., particle size: 5 μm); flow-rate: 2 mL min⁻¹; mobile phase 4.

6.2.4 HPLC-AD method validation

The validation of the LC-FC-A system technique was a procedure aimed at obtaining experimentally justified evidence of the ability of this technique to give results characterised by the required accuracy and precision (ICH, 1996). The LC-FC-A analytical techniques used for analysis the methoxyphenidine hydrochloride regioisomers required validation prior to deploying them in the analysis of the purchased street samples. The LC-FC-A system employing the commercial impinging jet flow cell and was validated (in terms of UV- detection) using a standard mixture of regioisomers of methoxyphenidine hydrochloride with strong UV absorption: (\pm)-4-MEP, (\pm)-2-MEP and (\pm)-3-MEP over the 100-500 $\mu\text{g mL}^{-1}$ range. The optimal conditions used in this study are shown in Table 6.4.

Table 6.4 Summary of the optimal conditions utilised in the analysis of (±)-4-FEP, (±)-2-FEP and (±)-3-FEP.

Optimised chromatography conditions	
Column	Column B (Section 2.2.1) ACE 5 C ₁₈ AR column (150 mm × 4.6 mm i.d., particle size: 5 µm);
Flow rate (mL min ⁻¹)	2
Solvent	Mobile phase 4 (Table 2.3)
Column temperature (°C)	50
Wavelength (nm)	279
Injection volume (µL)	10
Run time (mins)	30
pH	7.0
Optimised amperometric detection parameters	
Potential (V)	+1.2
Equilibrium time (s)	10
Data interval (s)	0.05
Current range (mA)	1×10 ⁻⁶ -1
Total run time (s)	5000

Table 6.5 shows the summary of the validation parameters used for analysis the methoxyphenidine hydrochloride regioisomers [(±)-4-MEP, (±)-2-MEP and 3-MEP] using HPLC-UV in the LC-FC-A system, and

Table 6.6 shows the summary of validation parameters of the analysis methoxyphenidine hydrochloride regioisomers using HPLC-AD in the LC-FC-A (amperometric detection) system.

Table 6.5 Summary of HPLC-UV (UV detection) validation data for the quantification of (±)-4-MEP, (±)-2-MEP and (±)-3-MEP obtained in the LC-FC-A systems using column B, (Table 2.2); mobile phase: 4C (Section 2.4); UV wavelength: 279 nm.

System detection	LC-FC-A (HPLC-UV detection)		
Flow Rate	2 ml min ⁻¹		
Analytes	4-MEP	2-MEP	3-MEP
t _R (min)(t ₀ = 0.854min) ^a	21.61	23.84	25.83
RRT ^b	0.91	1	1.08
Capacity factor (k')	20.61	22.84	24.83
N (plates)	10304 (68691) ^c	9286 (61904) ^c	10395 (69300) ^c
H (m)	1.46×10 ⁻⁰⁵	1.62×10 ⁻⁰⁵	1.44×10 ⁻⁰⁵
Resolution (R _s)	/	2.41	2.05
Asymmetry factor (A _s)	0.62	0.52	0.71
LOD ^d (µg ml ⁻¹)	3.26	6.25	6.78
LOQ ^d (µg ml ⁻¹)	9.89	18.95	20.54
Co-efficient of regression(r ²)	1 ^f	0.999 ^g	0.999 ^h
Precision (%RSD) (n=6)			
100 µg mL ⁻¹	0.17	0.09	0.10
200 µg mL ⁻¹	0.25	0.07	0.08
300 µg mL ⁻¹	0.16	0.03	0.08
400 µg mL ⁻¹	0.16	0.02	0.07
500 µg mL ⁻¹	0.08	0.01	0.01
^a Measured from the retention time of uracil (10 µg mL ⁻¹) eluting from the column. ^b Relative retention time (with respect to 2-MEP). ^c N expressed in plates per m. ^d Limit of detection. ^e Limit of quantification. ^f y = 0.8194x - 0.168. ^g y = 1.873x + 10.301. ^h y = 1.587x + 6.9073.			

Table 6.6 Summary of HPLC-AD (amperometric detection) validation data for the quantification of (±)-4-MEP, (±)-2-MEP and (±)-3-MEP obtained in the LC-FC-A (impinging jet flow cell) system using column B, (Table 2.2. Mobile phase: 4C (Section 2.4); UV wavelength: 279 nm.

System detection	LC-FC-A (AD)		
Flow Rate	2 ml min ⁻¹		
Analytes	4-MEP	2-MEP	3-MEP
t _R (min)(t ₀ = 0.854min) ^a	21.63	23.86	25.85
RRT ^b	0.91	1	1.08
LOD ^c (µg ml ⁻¹)	15.93	24.54	23.62
LOQ ^d (µg ml ⁻¹)	48.28	74.37	71.57
Co-efficient of regression(r ²)	0.994 ^e	0.986 ^f	0.987 ^g
Precision (%RSD) (n=6)			
100 µg mL ⁻¹	0.52	2.97	3.03
200 µg mL ⁻¹	2.8	3.43	4.17
300 µg mL ⁻¹	3.35	3.38	3.10
400 µg mL ⁻¹	1.49	1.95	1.31
500 µg mL ⁻¹	1.37	1.33	1.27
^a Measured from the retention time of uracil (10 µg mL ⁻¹) eluting from the column. ^b Relative retention time (with respect to 2-MEP). ^c Limit of detection. ^d Limit of quantification. ^e y = 0.0013x + 0.0145. ^f y = 0.0008x + 0.0424. ^g y = 0.0008x + 0.0488.			

6.2.4.1 System suitability test

The system suitability principle was explained in Section 3.5.1. In the LC-FC-A system, the resolution, effectiveness and reproducibility of the chromatograph system were confirmed by the system suitability test. This was established using HPLC-UV detection data (resolution, number of plates, capacity factors and asymmetric in Table 6.5). Figure 6.2 shows the elution time of (±)-4-MEP at 21.61, (±)-2-MEP at 23.84 with a good resolution of 2.41 and (±)-3-MEP at 25.83 mins respectively, with a resolution of 2.05. The theoretical plates numbers (N) were 10604 for (±)-4-MEP, 9286 for (±)-2-MEP and 10395 for (±)-3-MEP, that explained the excellent effectiveness of the sharpness of the peak and good efficiency of the column. In addition, the capacity factors that showed the effect of the stationary phase on compound retention were calculated from HPLC-UV data and found to be 20.61, 22.84 and 24.83 for (±)-4-MEP, (±)-2-MEP and (±)-3-MEP respectively. Moreover, the asymmetric factor was calculated from the HPLC-UV data to be found more than 1 meaning there was no peak tailing.

6.2.4.2 Resolution (Rs)

The resolution of separation of the three compounds is shown in Table 5.6 where (±)-4-MEP was eluted at 21.61 mins, (±)-2-MEP was eluted at 23.84 mins, with an excellent resolution of 2.41, and (±)-3-MEP was eluted at 25.83 mins with a good resolution of 2.05. Therefore, from the resolutions mentioned above, this method has a good separation for the three compounds because their resolution was more than 1.5 which is accepted according ICH validation (ICH, 1996).

6.2.4.3 Selectivity factor (α)

The selectivity principle was explained in Section 3.5.3. In this study, the results of the HPLC-UV system were that (±)-2-MEP was eluted at 21.61 mins and

(±)-3-MEP was eluted at 23.84 mins, with a high resolution of 2.41, and (±)-4-MEP was eluted at 25.83 mins with a resolution of 2.05. That means this method has a good selectivity to separate the regioisomers of methoxyphenidine from each other in the mixture (Figure 6.2). In addition, the specificity of this method was expressed using the solutions of the UV-inactive analytes sucrose, mannitol, and lactose (which are commonly used as diluents, prepared in Section 2.9.7). These were not observed to interfere with the analytes, thereby confirming the specificity of the proposed method.

6.2.4.4 Linearity

The linearity principle was explained in Section 3.5.4. In this study the linearity of (±)-2-MEP, (±)-3-MEP and (±)-4-MEP using the LC-FC-A (HPLC-UV) system was obtained from the calibration standards. The standards were used between 100-500 $\mu\text{g mL}^{-1}$ and injected as six replicates using the optimised chromatographic condition at 279 nm, temperature 50°C and flow rate 2 mL min^{-1} using an ACE 5 C₁₈AR column (150 mm × 4.6 mm i.d., particle size: 5 μm). The linearity plot was constructed from the concentration and peak area obtained (Figure 6.3a). The good linear response of the HPLC-UV system for (±)-4-MEP was $R^2 = 1$ with %RSD = 0.08-0.25%; n = 6, Appendix: Table 9.27, for (±)-2-MEP was $R^2 = 0.999$, with %RSD = 0.01–0.9%; n = 6, Appendix: Table 9.28) and for (±)-3-MEP was $R^2 = 0.999$ with %RSD = 0.01–0.10%; n = 6, Appendix: Table 9.29). That explains the excellent linearity for the HPLC-UV system.

The corresponding liquid chromatography-amperometric detection system, (LC-FC-A), employing the commercially available, impinging jet, flow cell, was validated using the same standard mixtures as were used in HPLC-UV detection containing 100-500 $\mu\text{g mL}^{-1}$ of (±)-2-MEP, (±)-3-MEP and (±)-4-MEP. The good

linear response of the HPLC-AD system (Figure 6.3b) for (\pm)-4-MEP was $R^2 = 0.994$ with %RSD = 0.52–1.89%; $n = 6$, Appendix: Table 9.30, for (\pm)-2-MEP was $R^2 = 0.9863$ with %RSD = 0.67–1.05%; $n = 6$, Appendix: Table 9.31 and for (\pm)-3-MEP was $R^2 = 0.9874$ with %RSD = 0.64–1.76%; $n = 6$, Appendix: Table 9.32. That explained the linearity for the LC-FC-A system. In comparing the linearity of HPLC-UV and HPLC-AD systems, the linearity of HPLC-AD was less than the linearity of HPLC-UV because HPLC-UV has a higher sensitivity to the analytes than HPLC-AD.

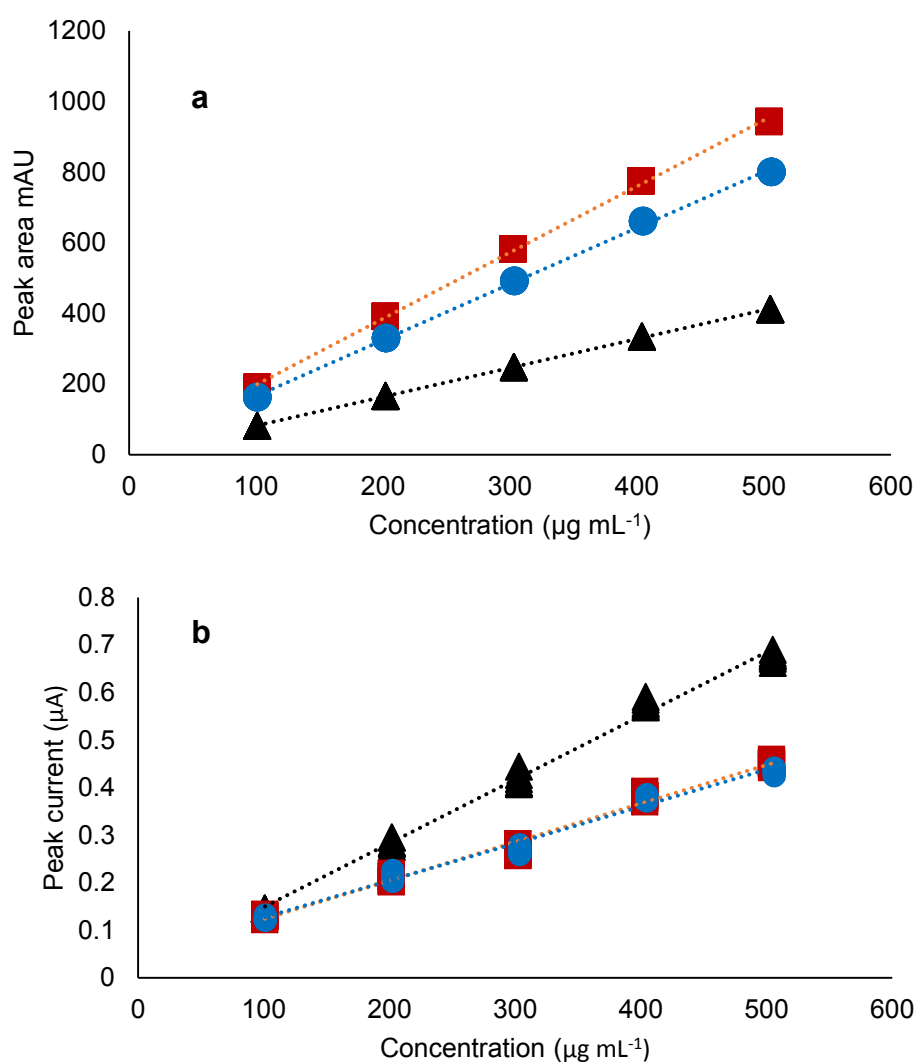


Figure 6.3 The linearity of (\pm)-4-MEP (triangles), (\pm)-2-MEP (squares) and (\pm)-3-MEP (circles) using the LC-FC-A system a) HPLC-UV (UV detection), b) HPLC-AD (amperometric detection).

6.2.4.5 Limit of detection (LOD)

The LOD principle was explained in Section 3.5.5. In this study, the LOD was estimated from calibration standard curves by six injections performed over a concentration range 100-500 $\mu\text{g mL}^{-1}$. The LODs for analysis of the methoxyphenidine hydrochloride regioisomers were determined using the LC-FC-A (HPLC-UV detection) system and were found to be 3.26 $\mu\text{g mL}^{-1}$ for (\pm)-4-MEP, 6.25 $\mu\text{g mL}^{-1}$ for (\pm)-2-MEP and 6.78 $\mu\text{g mL}^{-1}$ (\pm)-3-MEP. The LODs of analysis of methoxyphenidine hydrochloride regioisomers were determined by using the LC-FC-A (amperometric detection) system and found to be 15.93 $\mu\text{g mL}^{-1}$ for (\pm)-4-MEP, 24.54 $\mu\text{g mL}^{-1}$ for (\pm)-2-MEP and 23.62 $\mu\text{g mL}^{-1}$ for (\pm)-3-MEP.

To compare the reliability of the presented results of LODs for the two approaches, these values are undoubtedly different because the LODs of HPLC-UV are less than the LODs of HPLC-AD due to HPLC-UV having a higher sensitivity than HPLC-AD. In addition, in amperometric detection, a high concentrations of the analytes need to be used. However, in the literature there is no fully validated method for detecting regioisomers of methoxyphenidine to compare the LODs, but for the first time this method explains a fully validated method using the HPLC-AD protocol for analysis of these regioisomers.

6.2.4.6 Limit of quantification

The LOQ principle was explained in Section 3.5.6. In this study, the LOQ was estimated from calibration standard curves by six injections performed over a concentration range 100-500 $\mu\text{g mL}^{-1}$. The LOQs of analysing the methoxyphenidine hydrochloride regioisomers were determined using the LC-FC-A system (HPLC-UV detection) and found to be 9.89 $\mu\text{g mL}^{-1}$ for (\pm)-4-MEP, 18.95 $\mu\text{g mL}^{-1}$ for (\pm)-2-MEP and 20.54 $\mu\text{g mL}^{-1}$ (\pm)-3-MEP. The LOQs of analysis for

methoxyphenidine hydrochloride regioisomers were determined by using the LC-FC-A (amperometric detection) system and found to be 48.28 $\mu\text{g mL}^{-1}$ for (\pm)-4-MEP, 74.37 $\mu\text{g mL}^{-1}$ for (\pm)-2-MEP and 71.57 $\mu\text{g mL}^{-1}$ for (\pm)-3-MEP. On comparing the reliability of the results of LOQs for the two approaches, these values are different for the same reason that LODs differ (Section 6.1.7). In addition, as explained in Section 6.2.4.4, due to no fully validated method being in the literature, comparison of the LOQs in this method cannot be compared with the literature.

6.2.4.7 Robustness

The robustness test principle was explained in chapter 3 section 3.7.7. In this study, the effect of temperature variation and change of composition ratio of the mobile phase were analysed to ensure if this method was unaffected by these changes.

The first parameter of the robustness test was the minor change in temperature using different temperatures of 48°C, 50°C and 52°C, as shown in Table 6.7. The method was carried out using column ACE 5 C₁₈-AR (150 x 4.6 mm, 5 μm particle size) and a solution containing the three components at a concentration of 300 $\mu\text{g mL}^{-1}$. The relative retention times of the three analytes were measured and the %RSD calculated to determine the precision. Table 6.7 shows the analysis of (\pm)-4-MEP, (\pm)-2-MEP and (\pm)-3-MEP using the optimum conditions obtained from the method development with minor changes in temperature. In comparing the relative retention time (RRt), all the results were similar and gave %RSDs which were <1% and within the guidelines stipulated by the ICH. These data indicate that this method is robust and should be suitable for use in the routine analysis of seized samples. Highlighted data in Table 6.7 represent the optimal conditions used in this validation study.

Table 6.7 The effect of minor changes of temperature on relative retention time (RRT) of the analysis of 300 $\mu\text{g mL}^{-1}$ of (\pm)-4-MEP, (\pm)-2-MEP and (\pm)-3-MEP using HPLC-UV in the LC-FC-A system, (the highlighted area is a standardised condition for this study).

Concentration $\mu\text{g mL}^{-1}$	RRT								
	(48°C)			(50°C)			(52°C)		
	4-MEP	2-MEP	3-MEP	4-MEP	2-MEP	3-MEP	4-MEP	2-MEP	3-MEP
300	0.903	1.000	1.074	0.905	1.000	1.081	0.906	1.000	1.083
300	0.902	1.000	1.074	0.905	1.000	1.081	0.906	1.000	1.084
300	0.902	1.000	1.073	0.905	1.000	1.081	0.906	1.000	1.083
300	0.903	1.000	1.074	0.905	1.000	1.081	0.906	1.000	1.083
300	0.902	1.000	1.074	0.905	1.000	1.080	0.907	1.000	1.086
300	0.902	1.000	1.073	0.906	1.000	1.083	0.907	1.000	1.086
Average	0.902	1.000	1.074	0.905	1.000	1.081	0.906	1.000	1.084
RSD%	0.024	0.000	0.019	0.047	0.000	0.105	0.047	0.000	0.139

The second parameter of the robustness test was minor changes in the ratio of the mobile phase to determine whether this method is robust or not. In addition, the method was performed by injecting 300 $\mu\text{g mL}^{-1}$ of (\pm)-4-MEP, (\pm)-2-MEP and (\pm)-3-MEP and Table 6.8 shows the similarity in results of relative retention time by using minor changes of mobile phase 4 ratios, section 2.4, to analysis methoxyphenidine hydrochloride regioisomers and from the results, this method is robust. Highlighted data in Table 6.8 presents the optimal conditions used in validation of this study.

Table 6.8 The effect of a minor change inorganic composition of the mobile phase 4 on the relative retention time (RRT) of 300 $\mu\text{g mL}^{-1}$ of (\pm)-4-MEP, (\pm)-2-MEP and (\pm)-3-MEP using HPLC-UV in the LC-FC-A system. The highlighted area is a standardised condition for this study.

Concentration $\mu\text{g mL}^{-1}$	RRT								
	(20:80 v/v)			(18:82 v/v)			(16:84 v/v)		
	4-MEP	2-MEP	3-MEP	4-MEP	2-MEP	3-MEP	4-MEP	2-MEP	3-MEP
300	0.907	1.000	1.086	0.907	1.000	1.088	0.903	1.000	1.074
300	0.907	1.000	1.086	0.907	1.000	1.088	0.902	1.000	1.074
300	0.907	1.000	1.086	0.907	1.000	1.088	0.905	1.000	1.081
300	0.907	1.000	1.087	0.907	1.000	1.089	0.905	1.000	1.081
300	0.915	1.000	1.096	0.907	1.000	1.088	0.907	1.000	1.086
300	0.907	1.000	1.086	0.917	1.000	1.097	0.907	1.000	1.086
Average	0.908	1.000	1.088	0.909	1.000	1.090	0.905	1.000	1.080
RSD%	0.364	0.000	0.381	0.420	0.000	0.342	0.213	0.000	0.517

6.2.4.8 Inter-and intra-day precision

One of the most important tests has been expressed as the precision of the analytical procedure used in this study to analyse the methoxyphenidine hydrochloride regioisomers and this was the inter- and intra-day test. This test has been done under the same conditions over a short interval of time (repeatability). 12 replicate injections of a mixture solution of 300 $\mu\text{g mL}^{-1}$ of (\pm)-4-MEP, 300 $\mu\text{g mL}^{-1}$ of (\pm)-2-MEP and 300 $\mu\text{g mL}^{-1}$ of (\pm)-3-MEP were prepared as in Section 2.9.6. This test was performed on the same day (6 in the morning and 6 in the afternoon), and the same procedure with six injections repeated the following day to obtained the relative standard deviation for all analytes in both detection systems (HPLC-UV and HPLC-AD). However, the precision results showed little change in both systems (HPLC-UV, HPLC-AD), but both systems have good precision for the three compounds ((\pm)-4-MEP, (\pm)-2-MEP and (\pm)-3-MEP) as shown by RSD% of less than 1% (Table 6.9). The value of RSD% was calculated from the supplementary data in Appendix: Table 9.39 found to be < 1% for all analytes. This is an appropriate precision criterion for repetitive injections to assess the precision of the instrument in analytical method validation (Green, 1996). In addition, these results illustrate the ability of this method and the efficiency of these systems to be applied to routine analysis.

Table 6.9 The relative standard deviation (RSD %) of inter- and intra-day measurements for (300 $\mu\text{g mL}^{-1}$) (\pm)-4-MEP, (\pm)-2-MEP and (\pm)-3-MEP using HPLC-UV detection and amperometric detection in the LC-FC-A system.

n=12	analytes	RSD % of LC-FC-A	
		HPLC-UV (peak area)	Amperometric detection (peak current)
Inter-day precision	4-MEP	0.15	0.98
	2-MEP	0.03	0.81
	3-MEP	0.08	0.72
intra-day precision	4-MEP	0.83	0.7
	2-MEP	0.16	0.76
	3-MEP	0.17	0.83

6.2.4.9 Accuracy test

Accuracy test principle was explained in Section 3.5.8. The test performed at the 80, 100 and 120% level of target concentration. Recovery data were in triplicate at each level of label claim. Percentage recovery for (±)-4-MEP, (±)-2-MEP and (±)-3-MEP were calculated for each sample and demonstrated excellent accuracy range 98±0.09% to 102±0.53% for HPLC-UV in LC-FC-A system (Table 6.10). In addition, the recovery percentages for amperometric detection of LC-FC-A system were 99.7±0.51 % to 101.8±0.94 % by using HPLC-AD in LC-FC-A system (Table 6.10).

Table 6.10 Percentage recovery of (±)-4-MEP, (±)-2-MEP and (±)-3-MEP using both system HPLC-UV and LC-FC-A

System			LC-FC-A			
Detection			HPLC-UV		HPLC-AD	
Compound	Concentration µg mL ⁻¹	Theoretical recovery µg mL ⁻¹	Actual recovery µg mL ⁻¹	%recovery (n=3)	Actual recovery µg mL ⁻¹	%recovery (n=3)
4-MEP	240 (80%)	241	241	100±0.05	237	101.8±0.94
2-MEP		240	236	102±0.53	241	99.7±0.51
3-MEP		242	242	100±0.22	239	101.4±0.56
4-MEP	300 (100%)	304	305	99±0.05	302	100.7±0.44
2-MEP		303	297	102±0.12	300	100.7±0.77
3-MEP		303	302	100±0.42	303	99.9±0.54
4-MEP	360 (120%)	363	366	99±0.18	360	100.9±0.32
2-MEP		362	365	98±0.09	362	99.9±0.55
3-MEP		362	364	99±0.21	360	100.5±0.35

6.2.5 Forensic Application

The two street samples were obtained from Great Manchester Police (GMP). These samples were homogenised and labelled as MEP-1 and MEP-2. Both street samples were analysed with duplicated weight (in triplicate) by using the validated LC-FC-A system, and using the commercial impinging flow cell for amperometric detection, at concentration 300 µg ml⁻¹. The HPLC-UV results (Table 6.11) confirmed that the first street sample (MEP-1) contained 101±0.6 %w/w of pure 3-

MEP but another sample contained 11.8 ± 0.86 %w/w of 2-MEP and 90.3 ± 0.2 of 3-MEP. In term of amperometric detection by using HPLC-AD in LC-FC-A system were 101.6 ± 1.4 of 3-MEP (pure form) in the first street sample (MEP-1) and 10.1 ± 1.7 and 91.9 ± 1.8 of 2-MEP and 3-MEP in second street sample (MEP-2) with the ratio (10:90) respectively.

Table 6.11 Direct comparison between quantitative data obtained by HPLC-UV and HPLC-AD (impinging jet flow cell) system, for the analysis $300 \mu\text{g mL}^{-1}$ of the regioisomer of methoxyphenidine in a selection of purchased street samples

System	LC-FC-A					
Detection	HPLC-UV (%w/w) (n= 6)			HPLC-AD (%w/w) (n =6)		
Analyte	4-MEP	2-MEP	3-MEP	4-MEP	2-MEP	3-MEP
MEP-1	n.d.	n.d.	101 ± 0.6	n.d.	n.d.	101.6 ± 1.4
MEP-2	n.d.	11.8 ± 0.86	90.3 ± 0.2	n.d.	10.1 ± 1.7	91.9 ± 1.8
n.d. = not detected.						

6.3 Detection and quantification of regioisomer of fluoroephenidine by using HPLC-AD protocol:

The previous Section represents the analysis of regioisomers of methoxyephenidine as new psychoactive substances by using high performance liquid chromatography in combined with amperometric detection protocol. This protocol was succeeded for detection, separation, and quantification the regioisomers of methoxyephenidine. Therefore, the HPLC-AD protocol will used in this Section to detect, separate and quantify the regioisomers of fluoroephenidine as new psychoactive substances with the same analogue manner of regioisomers of methoxyephenidine.

6.3.1 Ultraviolet-Visible Spectroscopy (UV) (Determination of λ_{\max})

The fluoroephenidine regioisomers can be detected at 270 nm and the UV max (nm) measurement of regioisomers of fluoroephenidine were (±)-2-FEP at 270 nm ($A = 0.89, 4.0 \times 10^{-2} \text{g } 100\text{mL}^{-1}$), (±)-3-FEP at 270 nm ($A = 1.3, 4.0 \times 10^{-2} \text{g } 100\text{mL}^{-1}$), and (±)-4-FEP at 270 nm ($A = 0.98, 4.0 \times 10^{-2} \text{g } 100\text{mL}^{-1}$) in mobile phase 5 (Table 2.3).

6.3.2 HPLC Method Development:

The started point was to developed HPLC-UV method that could separate and identify (±)-2-FEP, (±)-3-FEP and (±)-4-FEP with good resolution and shorter retention time Figure 6.4. The method development was carried out by using an adaptation of HPLC-UV method was used for analysis regioisomers of methoxyephenidine in the first Section of this chapter with the following modification: change the ration of mobile phase by using (25: 75) Acetonitrile: 20mM ammonium acetate and 100mM KCl at pH=7.

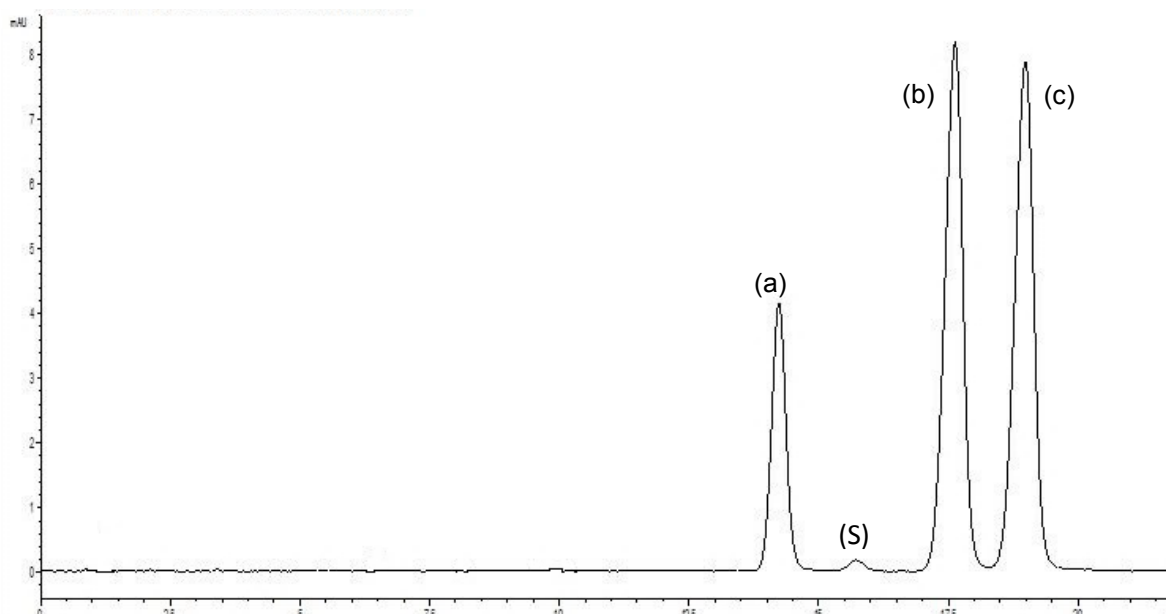


Figure 6.4 The chromatogram for $200 \mu\text{g mL}^{-1}$ of (\pm)-4-FEP (a), (\pm)-2-FEP (b) and (\pm)-3-FEP (c) obtained by using HPLC-UV detection in LC-FC-A system using an ACE 5 C18AR column (150 mm \times 4.6 mm i.d., particle size: 5 μm); Mobile phase: mobile phase 4; UV wavelengths 279 nm, the peak (S) is a system peaks associated with the sample.

6.3.3 Amperometric detection method development:

6.3.3.1 Optimization of potential of Amperometric detection:

The anodic potential for (\pm)-2-FEP ($300.0 \mu\text{g mL}^{-1}$), (\pm)-3-FEP ($300.0 \mu\text{g mL}^{-1}$) and (\pm)-4-FEP ($300.0 \mu\text{g mL}^{-1}$) mixture in the Mobile Phase 5 (Table 2.3) were determined by using the peak current, in conjunction with the optimised instrumental configuration. The optimal conditions were used for optimization of potential according to the best condition were obtained in method development in Section 6.3.2 (temperature = 50°C , flow rate = 1.5 mL min^{-1} at pH = 7). The potential required to achieve the optimal detector response for the mixture were determined, for LC-FC-A system by measuring the amperometric response (peak current, μA) as a function of anodic potential (E V^{-1}), over the range +0.0 to +1.5 E V^{-1} . The maximum high current responses (1.26, 0.93 and 1.06, $n=3$) were detected at +1.2 E V^{-1} for (\pm)-4-FEP, (\pm)-2-FEP and (\pm)-3-FEP respectively (Table 6.12).

Table 6.12 The anodic potential of 300 $\mu\text{g mL}^{-1}$ (\pm)-4-FEP, (\pm)-2-FEP and (\pm)-3-FEP over the range + 0.0 to + 1.5 V at temperature = 50 $^{\circ}\text{C}$, flow rate = 1.5 mL min^{-1} and pH = 7 by using LC-FC-A

potential (v)	Peak current(μA)		
	(\pm)-4-MEP	(\pm)-2-MEP	(\pm)-3-MEP
0	n.d.	n.d.	n.d.
0.8	0.15	0.09	0.12
1	0.79	0.54	0.65
1.2	1.26	0.93	1.06
1.5	0.32	0.29	0.30
Key: n.d. not detected			

6.3.3.2 Optimization of linear velocity of Amperometric Detection:

The linear velocity of fluoroephenidine regioisomers was measured as methoxyephenidine regioisomers. The mixture of (\pm)-4-FEP, (\pm)-2-FEP and (\pm)-3-FEP (300 $\mu\text{g mL}^{-1}$) was injected ($n = 10$) at range of flow rates 0.5-1.5 mL min^{-1} . Table 6.12 shown the peak current of (\pm)-4-FEP, (\pm)-2-FEP and (\pm)-3-FEP with a good amperometric response [(\pm)-4-FEP = 1.26 μA , (\pm)-2-FEP = 0.93 μA and (\pm)-3-FEP = 1.06 μA] at 1.2 E V^{-1} and (pH = 7) by using LC-FC-A system. In addition, there is not any response observed at flow rate less than 0.5 mL min^{-1} and if the flow rate more than 1.5 mL min^{-1} the peaks on the HPLC-UV system will overlap.

Table 6.13 the linear velocity of 300 $\mu\text{g mL}^{-1}$ of (\pm)-4-FEP, (\pm)-2-FEP and (\pm)-3-FEP over the range 0.5 to 1.5 mL min^{-1} at temperature = 50 $^{\circ}\text{C}$, potential = 1.2 E V^{-1} and pH = 7) by using LC-FC-A system.

Flow rate mL min^{-1}	Peak current(μA)		
	(\pm)-4-FEP	(\pm)-2-FEP	(\pm)-3-FEP
1	0.77	0.52	0.62
1.5	1.26	0.93	1.06
2	1.06	0.74	0.82

6.3.3.3 Optimization of pH of HPLC-UV and Amperometric detection:

Table 6.14 shown the different pH (3-7) of mobile phase 5 was used to find the best pH could use to obtain the highest response for the analytes. This method carried out by injected 100 $\mu\text{g mL}^{-1}$ of regioisomer of fluoroephenidine in LC-FC-AD system. The best response for HPLC-UV and HPLC-AD in LC-FC-A system was pH

= 7, because cannot increase the pH of the mobile phase more than 9 or less than 2 to protect the column from degradation as explained in chapter 3 Section 3.6. As well as low amperometric response was observed at mobile phase 5C with pH = 3 which is 0.043 μA for (\pm)-4-FEP, 0.045 μA for (\pm)-2-FEP and 0.415 μA for (\pm)-3-FEP. The maximum responses by using LC-FC-A system were 1.24 μA for (\pm)-4-FEP, 0.919 μA for (\pm)-2-FEP and 1.055 μA for (\pm)-3-FEP which observed at potential = +1.2 E V^{-1} and flow rate 1.5 mL min^{-1} mobile phase with pH = 7.

Table 6.14 The effect of pH of mobile phase on analysis 100 $\mu\text{g mL}^{-1}$ of (\pm)-4-FEP, (\pm)-2-FEP and (\pm)-3-FEP over the range 3 to 7 at temperature = 50 $^{\circ}\text{C}$, potential = 1.2 E V^{-1} by using LC-FC-A system.

pH	Peak current (μA)		
	(\pm)-4-FEP	(\pm)-2-FEP	(\pm)-3-FEP
3	0.043	0.045	0.0415
5	0.039	0.046	0.0336
7	1.24	0.919	1.055

By optimization of amperometric detection (Section 6.3.3) in LC-FC-A system, the fluoroephenidine regioisomer were eluted at 14.37 of (\pm)-4-MEP, 17.78 of (\pm)-2-FEP and 19.15 of (\pm)-3-FEP in HPLC-AD of LC-FC-A system (Figure 6.5).

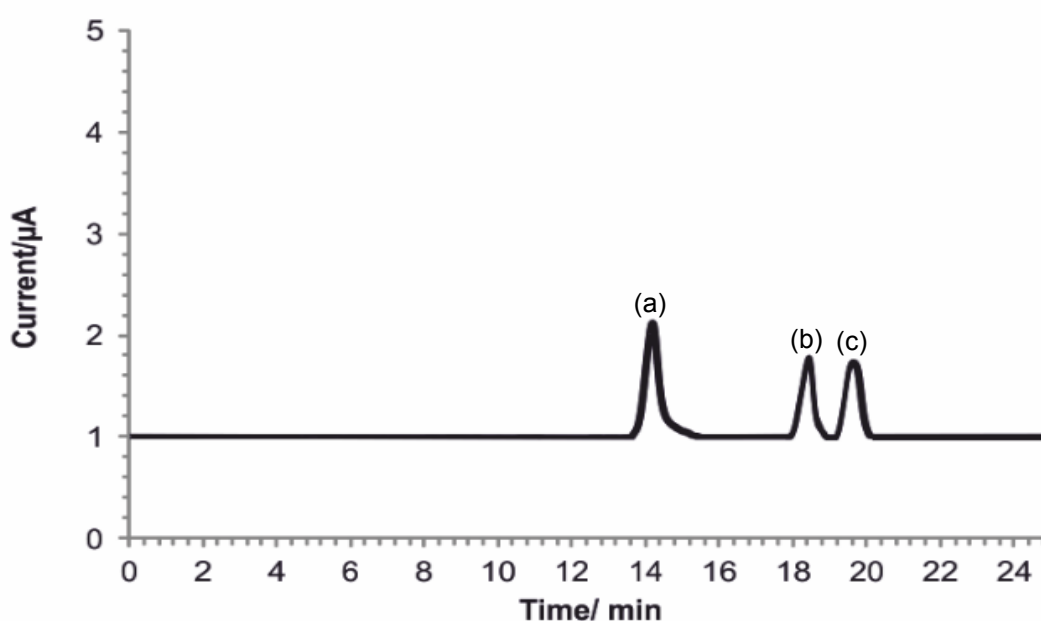


Figure 6.5 Amperogram of 200 $\mu\text{g mL}^{-1}$ (\pm)-4-FEP (a), (\pm)-2-FEP (b) and (\pm)-3-FEP (c) obtained on the HPLC-AD system using an ACE 5 C_{18}AR column (150 mm \times 4.6 mm i.d., particle size: 5 μm); mobile phase 5; detector wavelengths (UV): 279 nm.

6.3.4 Method Validation

HPLC-AD analytical techniques used for analysis the regioisomers of fluoroephedrine hydrochloride required validation prior to deploying them in the analysis of the purchased street samples. The LC-FC-A system was validated (in term of UV- detection) using a standard mixture of regioisomer of fluoroephedrine hydrochloride with strongly UV- absorbing: (±)-4-FEP, (±)-2-FEP and (±)-3-FEP over 50-300 µg mL⁻¹ range. Table 6.15 shows the optimal condition was used for validation the standard mixture of fluoroephedrine regioisomer in both HPLC-UV and HPLC-AD.

Table 6.16 shows the summary of the validation parameters that were used for analysis the fluoroephedrine hydrochloride regioisomers [(±)-4-FEP, (±)-2-FEP and (±)-3-FEP] using the HPLC-UV system, and Table 6.17 shows the summary of validation parameters of the analysis of fluoroephedrine hydrochloride regioisomers using HPLC-AD in the LC-FC-A system.

Table 6.15 Summary of the optimal conditions utilised in the analysis (±)-4-FEP, (±)-2-FEP and (±)-3-FEP

Optimised chromatographic conditions	
Column	ACE 5 C ₁₈ AR (150 mm × 4.6 mm i.d., particle size: 5 µm)
Flow rate	2 mL min ⁻¹
Solvent	Mobile phase 5 (Table 2.3)
Column temperature (°C)	50
Wavelength (nm)	270
Injection volume (µL)	10
Run time (mins)	30
Optimised amperometric detection parameters	
Potential (V)	+1.2
Equilibration time (s)	10
Data interval (s)	0.05
Current range (mA)	1×10 ⁻⁶
Total run time (s)	5000

Table 6.16 Summary of HPLC-UV validation data for the quantification of regioisomers of fluoroephenedine obtained on the LC-FC-A (impinging jet flow cell) system, using column B, (Table 2.2) mobile phase 5; detector wavelength (UV): 270 nm.

System detection	LC-FC-A (HPLC-UV)		
Flow Rate	1.5ml/min		
Analytes	4-FEP	2-FEP	3-FEP
tR(min) (t0= 1.078 min) ^a	14.35	17.76	19.13
RRT ^b	0.81	1.00	1.08
Capacity factor (k')	13.35	16.76	18.13
N (plate) ^c	12267(80032)	11327(73660)	12077(79318)
H (m)	1.25×10 ⁻⁰⁵	1.36×10 ⁻⁰⁵	1.26×10 ⁻⁰⁵
Resolution (Rs)	/	5.68	2.03
Asymmetry factor (As)	1.14	1.54	1.46
LOD ^d (µg ml ⁻¹)	3.58	3.74	3.52
LOQ ^e (µg ml ⁻¹)	10.86	11.34	10.70
Coefficient of regression (R ²)	0.999 ^f	0.999 ^g	0.999 ^h
Precision (%RSD) (n=6)			
50 µg ml ⁻¹	0.62	0.29	0.23
100 µg ml ⁻¹	0.32	0.28	0.33
150 µg ml ⁻¹	0.22	0.15	0.18
200 µg ml ⁻¹	0.31	0.04	0.17
250 µg ml ⁻¹	0.22	0.11	0.16
300 µg ml ⁻¹	0.20	0.12	0.09
^a Measured from the retention time of uracil (10 µg mL ⁻¹) eluting from the column. ^b Relative retention time (with respect to 2-MEP). ^c N expressed in plates per m. ^d Limit of detection. ^e Limit of quantification. ^f y = 0.3912x + 0.7088. ^g y = 0.957x + 1.3817. ^h y = 0.9731x + 0.4059.			

Table 6.17 Summary of validation data for regioisomers of fluoroephedrine obtained on the LC-FC-A (impinging jet flow cell) system using column B, (Table 2.2 mobile phase 5, detector wavelength (UV): 270 nm.

System detection	LC-FC-A (HPLC-AD)		
Flow Rate	1.5ml/min		
Analytes	4-FEP	2-FEP	3-FEP
tR(min) (t0= 1.078min) ^a	14.37	17.78	19.15
RRT ^b	0.81	1.00	1.08
Capacity factor (k')	13.37	16.78	18.15
LOD ^c (µg ml ⁻¹)	4.69	6.38	4.62
LOQ ^d (µg ml ⁻¹)	15.11	19.34	13.99
Co-efficient of regression(R ²)	0.999 ^e	0.997 ^f	0.998 ^g
Precision (%RSD) (n=6)			
50 µg ml ⁻¹	0.24	1.88	1.1384
100 µg ml ⁻¹	0.25	1.70	1.26
150 µg ml ⁻¹	0.64	1.19	1.44
200 µg ml ⁻¹	0.36	0.27	0.23
250 µg ml ⁻¹	0.16	0.21	0.44
300 µg ml ⁻¹	0.56	0.88	0.62
^a Measured from the retention time of uracil (10 µg mL ⁻¹) eluting from the column. ^b Relative retention time (with respect to 2-FEP). ^c limit of detection. ^d Limit of quantification. ^e y = 0.0028x + 0.0002. ^f y = 0.0024x + 0.0066. ^g y = 0.0024x - 0.0016.			

6.3.4.1 System suitability test

This test was performed to confirm this method is stable and the effectiveness of the chromatographic system before use for analysis of street samples. Figure 6.4 shows excellent separation between the analytes and the resolution was more than 2. The numbers of theoretical plates in this study for all analytes were > 2000, confirming that the column has great efficiency in separating the analytes in a mixture. In addition, the capacity factors were calculated and found to be 13.35, 16.76 and 18.13 minutes for (±)-4-FEP, (±)-2-FEP and (±)-3-FEP respectively and that represents the retention of the analyte in the stationary phase. The asymmetric factor in this study was less than 1 that confirms no peak tailing in this system (Table 6.16).

6.3.4.2 Resolution (Rs)

In this study the resolution of separation of the three regioisomers of fluoroephedrine hydrochloride shown in Table 6.16 were that (±)-4-FEP was eluted at 14.35 min, (±)-2-FEP was eluted at 17.76 min with excellent resolution 5.68 and (±)-3-FEP was eluted at 19.13 min with good resolution 2.03. Therefore, from the resolution mentioned above, this method has a good separation for regioisomers of fluoroephedrine hydrochloride because their resolution was more than 2 which is acceptable according to ICH validation (ICH, 1996; ICH, 2017).

6.3.4.3 Selectivity factor (α)

The selectivity principle was explained in Section 3.5.3. In this study the results of the HPLC-UV system were that (±)-4-FEP was eluted at 14.35 mins and (±)-2-FEP was eluted at 17.76 mins with high resolution 5.68 and (±)-3-FEP was eluted at 19.13 mins with resolution 2.03. These results of this method have a good separation for the regioisomers of fluoroephedrine from each other in a mixture (Figure 6.4 and Figure 6.5). In addition, the specificity of this method was expressed using solutions of the UV-inactive analytes sucrose, mannitol, and lactose (which are commonly used as diluents, prepared in Section 2.10.7). These were not observed to interfere with the analytes, thereby confirming the specificity of the proposed method.

6.3.4.4 Linearity

In this study the linearity of (±)-4-FEP, (±)-2-FEP and (±)-3-FEP using the HPLC-UV system was obtained from the calibration standards. The calibration standards were used (50-300 $\mu\text{g mL}^{-1}$) and injected (six replicates) using the optimised chromatographic conditions at 270 nm, temperature 50°C and flow rate 1.5 mL min^{-1} using ACE 5 C₁₈AR column (150 mm × 4.6 mm i.d., particle size: 5

μm). The linearity plot was constructed from the concentration and peak area obtained (Figure 6.6a). The good linear response of the HPLC-UV system for (\pm)-4-FEP $R^2 = 0.999$ with precision $\%RSD = 0.19\text{--}0.62\%$; $n = 6$ (Appendix: Table 9.33), for (\pm)-2-FEP $R^2 = 0.999$ with precision ($\%RSD = 0.04\text{--}0.29\%$; $n = 6$) (Appendix: Table 9.34) and for (\pm)-3-FEP $R^2 = 0.999$ with precision ($\%RSD = 0.09\text{--}0.33\%$; $n = 6$) (Appendix: Table 9.35). That explained the excellent linearity for HPLC-UV in LC-FC-A system.

The corresponding liquid chromatography-amperometric detection system, [LC-FC-A], employing the commercially available, impinging jet, flow cell (LC-FC-A), was validated using the same standard mixtures as were used for HPLC-UV containing $50\text{--}300\ \mu\text{g mL}^{-1}$ of (\pm)-4-FEP, (\pm)-2-FEP and (\pm)-3-FEP. The good linear response of LC-FC-A system (Figure 6.6b) for (\pm)-4-FEP $R^2 = 0.999$ with precision ($\%RSD = 0.15\text{--}0.64\%$; $n = 6$) (Appendix: Table 9.36), (\pm)-2-FEP $R^2 = 0.997$ with precision ($\%RSD = 0.20\text{--}1.23\%$; $n = 6$) (Appendix: Table 9.37) and for (\pm)-3-FEP $R^2 = 0.999$ with precision ($\%RSD = 0.23\text{--}1.43\%$; $n = 6$) (Appendix: Table 9.38). That explained the linearity for HPLC-AD in LC-FC-A system. In comparing the linearity of HPLC-UV and HPLC-AD in LC-FC-A systems, the linearity of HPLC-AD (amperometric detection) was less than the linearity of HPLC-UV, the same as the linearity results obtained in analysis of regioisomers of methoxyphenidine, because the HPLC-UV is more highly sensitive to the analytes more HPLC-AD in the LC-FC-A system.

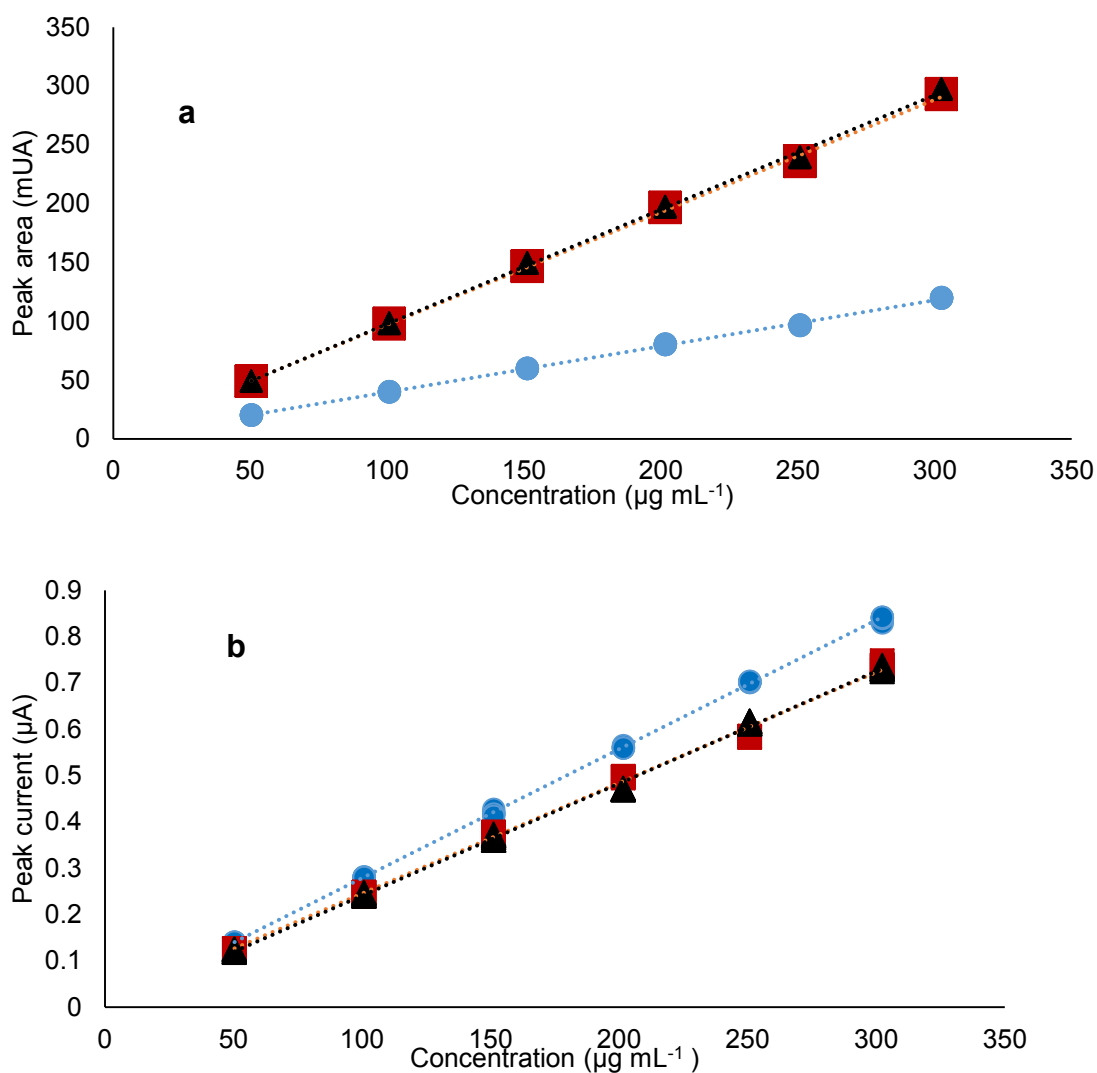


Figure 6.6 The linearity of (±)-4-FEP (circles), (±)-2-FEP (squares) and (±)-3-FEP (triangles) by using a) HPLC-UV and b) HPLC-AD in LC-FC-A system.

6.3.4.5 Limit of detection (LOD):

The LOD was estimated from calibration standard curve by six injections performed over concentration range 50-300 $\mu\text{g mL}^{-1}$. The LOD of analysis the fluoroephedrine hydrochloride regioisomers were determined using HPLC-UV (UV detector) in the LC-FC-A system and found to be 3.58 $\mu\text{g mL}^{-1}$ for (±)-4-FEP, 3.74 $\mu\text{g mL}^{-1}$ for (±)-2-FEP and 3.52 $\mu\text{g mL}^{-1}$ (±)-3-FEP (Table 6.16). The LOD of analysis of fluoroephedrine hydrochloride regioisomers were determined by using the HPLC-AD (amperometric detector) in the LC-FC-A system and found to be 4.69 $\mu\text{g mL}^{-1}$ for (±)-4-FEP, 6.38 $\mu\text{g mL}^{-1}$ for (±)-2-FEP and 4.62 $\mu\text{g mL}^{-1}$ for (±)-2-FEP (Table 6.17).

As in previous chapters, the LOD of HPLC-UV (UV detection) always lower than the LOD of HPLC-AD because the LOD for HPLC-UV is less than LOD of HPLC-AD in this study.

6.3.4.6 Limit of quantification

The LOQ of regioisomers of fluoroephenidine were estimated from the calibration standard curve by six injections performed over the concentration range 50-300 $\mu\text{g mL}^{-1}$. The LOQ of the analysis of the fluoroephenidine hydrochloride regioisomers were determined by using HPLC-UV system (UV detector) and found to be 10.86 $\mu\text{g mL}^{-1}$ for (\pm)-4-FEP, 11.34 $\mu\text{g mL}^{-1}$ for (\pm)-2-FEP and 10.70 $\mu\text{g mL}^{-1}$ (\pm)-3-FEP (Table 6.16). The LOQ of analysis of fluoroephenidine hydrochloride regioisomers were determined by using the HPLC-AD in the LC-FC-A system (amperometric detector) and found to be 15.11 $\mu\text{g mL}^{-1}$ for (\pm)-4-FEP, 19.34 $\mu\text{g mL}^{-1}$ for (\pm)-2-FEP and 13.99 $\mu\text{g mL}^{-1}$ for (\pm)-3-FEP (Table 6.17). To compare results of LOQ for the two approaches (HPLC-UV and HPLC-AD), LOQ were different due to the high concentration range of calibration standard concentrations that were used in this study, which is for the same reason as for the LOD.

6.3.4.7 Robustness

In this study the effect of temperature variation and change of composition ratio of the mobile phase were analysed to ensure that the LC-FC-A method was unaffected by these changes.

The first parameter of the robustness test was a minor change in temperature (by using 48°C, 50°C and 52°C, as show in Table 6.18) to ensure whether this method is robust or not. Table 6.18 shows the analysis of (\pm)-4-FEP, (\pm)-2-FEP and (\pm)-3-FEP using the optimum conditions (highlighted) that were obtained from method development with minor changes in temperature to ensure this method is

robust. In comparing the relative retention time (RRT) in Table 6.18, all results had similar relative retention times, therefore the minor change in temperature did not affect the analysis and this method is robust.

Table 6.18 The effect of minor changes of temperature on relative retention time (RRT) of analysis of 300 $\mu\text{g mL}^{-1}$ of (\pm)-4-FEP, (\pm)-2-FEP and (\pm)-3-FEP using HPLC-UV in the LC-FC-A system, (the highlighted area is a standardised condition for this study).

Concentration ($\mu\text{g mL}^{-1}$)	RRT								
	(48°C)			(50°C)			(52°C)		
	4-FEP	2-FEP	3-FEP	4-FEP	2-FEP	3-FEP	4-FEP	2-FEP	3-FEP
300	0.807	1.000	1.077	0.809	1.000	1.077	0.807	1.000	1.077
300	0.806	1.000	1.077	0.808	1.000	1.077	0.807	1.000	1.078
300	0.807	1.000	1.076	0.808	1.000	1.077	0.807	1.000	1.078
300	0.807	1.000	1.076	0.808	1.000	1.077	0.807	1.000	1.077
300	0.807	1.000	1.076	0.808	1.000	1.077	0.808	1.000	1.077
300	0.807	1.000	1.076	0.807	1.000	1.077	0.808	1.000	1.077
Average	0.807	1.000	1.076	0.808	1.000	1.077	0.808	1.000	1.077
RSD%	0.037	0.000	0.006	0.054	0.000	0.012	0.033	0.000	0.006

The second parameter of the robustness test used in this study was a minor change in ratio of mobile phase 5 (section 2.4) to ensure this method is robust. Table 6.19 shows the similarity of results of relative retention time using minor changes of mobile phase ratio to analyse fluoroephendine regioisomers. These results explain this method is robust. The highlighted data in Table 6.19 represents the optimal conditions used in this study for analysis of the regioisomers of fluoroephendine.

Table 6.19 The effect of a minor changes in organic composition of mobile phase 4 on the relative retention time (RRT) of 300 $\mu\text{g mL}^{-1}$ of (\pm)-4-FEP, (\pm)-2-FEP and (\pm)-3-FEP using HPLC-UV in the LC-FC-A system, (the highlighted area is a standardised condition for this study).

Concentration ($\mu\text{g mL}^{-1}$)	RRT								
	(23:77 v/v)			(25:75 v/v)			(27:73 v/v)		
	4-FEP	2-FEP	3-FEP	4-FEP	2-FEP	3-FEP	4-FEP	2-FEP	3-FEP
300	0.810	1.000	1.077	0.808	1.000	1.076	0.808	1.000	1.076
300	0.810	1.000	1.076	0.808	1.000	1.076	0.807	1.000	1.076
300	0.810	1.000	1.077	0.809	1.000	1.077	0.808	1.000	1.077
300	0.810	1.000	1.077	0.808	1.000	1.076	0.808	1.000	1.077
300	0.810	1.000	1.077	0.808	1.000	1.076	0.807	1.000	1.076
300	0.809	1.000	1.077	0.808	1.000	1.076	0.808	1.000	1.077
Average	0.810	1.000	1.077	0.808	1.000	1.076	0.808	1.000	1.076
RSD%	0.0003	0.000	0.0002	0.0002	0.000	0.0001	0.0002	0.000	0.0001

6.3.4.8 Inter-and intra-day precision

This test has been done under the optimum conditions obtained in development method Section 6.3.2 over a short interval of time (repeatability). The 12 replicate injections of mixture solution of 300 $\mu\text{g mL}^{-1}$ of (\pm)-4-FEP, 300 $\mu\text{g mL}^{-1}$ of (\pm)-2-FEP and 300 $\mu\text{g mL}^{-1}$ of (\pm)-3-FEP were prepared as in Section 2.10.6. The intra- and inter-day test was performed on the same day (6 in the morning and 6 in the afternoon), and the same procedure repeated with six injections on the following day to obtained the relative standard deviation for all analytes in both detection systems (HPLC-UV and HPLC-AD). However, the results' precision showed little change in the two detection systems (HPLC-UV, HPLC-AD), but HPLC-UV has excellent precision for the three compounds ((\pm)-4-FEP, (\pm)-2-FEP and (\pm)-3-FEP) as shown in Table 6.20 with the RSD% of the peak area being less than 1%.

The HPLC-AD system achieved good precision for all compounds ((\pm)-4-FEP, (\pm)-2-FEP and (\pm)-3-FEP) as shown in Table 6.20. The RSD% values of the peak current were less than 1%. The value of RSD% is suggested to be <1% as an appropriate precision criterion for repetitive injections to assess the precision of the instrument in analytical method validation (Green, 1996). In addition, these results

illustrate the ability of this method and the efficiency of these systems to be applied to the routine analysis. The value of RSD% was calculated by the supplementary data in Appendix: Table 9.39 and found to be < 1% for all analytes. This is an appropriate precision criterion for repetitive injections to assess the precision of the instrument in analytical method validation (Green, 1996).

Table 6.20 Relative standard deviation (RSD %) of inter- and intra-day peak values for (±)-4-FEP, (±)-2-FEP and (±)-3-FEP.

System		LC-FC-A	
Detection		HPLC-UV (Peak area)	Amperometric detection (Peak current)
Inter-day precision (n=12)	4-FEP	0.18	0.66
	2-FEP	0.10	0.68
	3-FEP	0.09	0.56
Intra-day precision (n=12)	4-FEP	0.23	0.23
	2-FEP	0.07	0.99
	3-FEP	0.09	0.69

6.3.4.9 Accuracy test

The principle of accuracy test was explained in Section 3.7.9. The test performed at the 80, 100 and 120% level of target concentration. Recovery data were in triplicate at each level of label claim. Percentage recovery for (±)-4-FEP , (±)-2-FEP and (±)-3-FEP were calculated for each sample and demonstrated excellent accuracy range 100±0.11% to 102±0.14% for the HPLC-UV system (Table 6.21), and 100±0.19% to 102±0.56% using the HPLC-AD system (Table 6.21).

Table 6.21 Percentage recovery of (±)-4-FEP, (±)-2-FEP and (±)-3-FEP using both HPLC-UV and HPLC-AD in the LC-FC-A system.

System			LC-FC-A			
Detection			HPLC-UV		HPLC-AD	
Compound	Concentration (µg mL ⁻¹)	Theoretical recovery (µg mL ⁻¹)	Actual recovery (µg mL ⁻¹)	% Recovery (n=3)	Actual recovery (µg mL ⁻¹)	% Recovery (n=3)
4-FEP	240 (80%)	243	240	101±0.4	242	100±0.19
2-FEP		242	240	101±0.11	241	100±0.61
3-FEP		244	243	100±0.23	242	100±0.77
4-FEP	300 (100%)	305	304	100±0.47	299	102±0.56
2-FEP		301	297	101±0.12	300	100±0.89
3-FEP		303	302	100±0.18	301	100±0.62
4-FEP	360 (120%)	364	363	100±0.37	361	100±0.77
2-FEP		371	369	101±0.15	368	100±0.93
3-FEP		370	364	102±0.14	369	100±0.98

6.3.5 Forensic Application

The three street samples were obtained from Great Manchester Police (GMP). These samples were homogenised and labelled as FEP-1, FEP-2, and FEP-3. All samples were analysed with duplicated weight (in triplicate) with the validated LC-FC-A system, using UV detection and the commercial impinging flow cell for amperometric detection, at concentration 300 µg ml⁻¹. The HPLC-UV results in LC-FC-A system (Table 6.22) confirmed that the first sample (FEP-1) contained about 48.2±0.5 % of 2-FEP and 51.8±0.5 % of 3-FEP but the second sample (FEP-2) contained 100.2±0.3 % of 2-FEP. Last sample (FEP-3) contained about 80:20 % of 2-FEP and 3-FEP respectively. By using amperometric detection (HPLC-AD) for analysis of the three street samples (Table 6.22) that confirmed the results were obtained by using UV detection (HPLC-UV) in LC-FC-A system. The FEP-1, contain 2-FEP and 3-FEP nearly about 50:50 and FEP-2 contain pure 2-FEP with 100.3±0.4%. The third street sample FEP-3 contain 79.6±0.6% of 2-FEP and 20.4±2.1% 3-FEP.

Table 6.22 Direct comparison between quantitative data obtained by HPLC-UV and HPLC-AD (impinging jet flow cell) in LC-FC-A system, for the analysis of the regioisomers of fluoroephedrine in a selection of purchased street samples

System	LC-FC-A					
Detection	HPLC-UV (%w/w) (n= 6)			HPLC-AD (%w/w) (n =6)		
Analytes	4-FEP	2-FEP	3-FEP	4-FEP	2-FEP	3-FEP
FEP-1	n.d.	48.2±0.5	51.8±0.5	n.d.	48.5±0.4	51.5±0.4
FEP-2	n.d.	100.2±0.3	n.d.	n.d.	100.3±0.4	n.d.
FEP-3	n.d.	78.5±0.7	21.5±2.7	n.d.	79.6±0.6	20.4±2.1
n.d. = not detected.						

6.4 Conclusions

Overall, this chapter has been shown for the first time that high performance liquid chromatography in combination with amperometric detection can be used for analysis of the regioisomers of new psychoactive substances (ephedrine derivatives). This chapter presented two studies for the detection and quantification of the regioisomers of methoxyephedrine and of fluoroephedrine. This work improves previous work in chapters 3, 4 and 5. However, the HPLC-UV system has a higher sensitivity than HPLC-AD in the LC-FC-A system, but this study obtained new separation and electrochemical detection method. The limits of detection of regioisomers of methoxyephedrine (±)-4-MEP, (±)-2-MEP and (±)-3-MEP were 3.26, 6.25 and 6.78 $\mu\text{g mL}^{-1}$ respectively using UV detection (HPLC-UV), and by using amperometric detection (HPLC-AD) the LODs were 15.93 $\mu\text{g mL}^{-1}$ for (±)-4-MEP, 24.54 $\mu\text{g mL}^{-1}$ and 23.62 for (±)-2-MEP and (±)-3-MEP respectively. In the same way the limit of detection for regioisomer of fluoroephedrine using HPLC-UV were 3.58, 3.74 and 3.52 $\mu\text{g mL}^{-1}$ for (±)-4-FEP, (±)-2-FEP and (±)-3-FEP respectively. In terms of the amperometric detection (HPLC-AD), the limits of detection were 4.69, 6.38 and 4.62 for (±)-4-FEP, (±)-2-FEP and (±)-3-FEP respectively.

Separation of the analytes by chromatography demonstrated a rapid separation and discrimination between the regioisomers of methoxyephedrine and

between the regioisomers of fluoroephedrine within the purchased street samples. This indicates this protocol for HPLC-AD can be considered suitable for the routine quantification and detection of regioisomers of new psychoactive substances. In addition, in these studies, the same limitations were reported in the conclusion of chapter 3 Section 3.7. Additionally, in this study there were two λ_{max} (220 nm and 279 nm) that can be used for detecting the regioisomers of methoxyephedrine. However, the peak absorbance was obtained when $\lambda_{\text{max}} = 220$ nm was used, but at the same time, there were some small peaks observed in the chromatogram because an ingredient in the mobile phase or analytical sample could be detected at this wavelength and produced noise. In addition, further work to this study will use $\lambda_{\text{max}} 220$ nm, to detect and quantifying the regioisomers of methoxyephedrine and to improve the absorbance of UV detection.

7 Chapter 7: Conclusions & Future Perspectives

This thesis demonstrates the application of fully validated methods combining high performance liquid chromatography with amperometric detection (HPLC-AD) for the analysis of three different classes of the new psychoactive substances (NPS) (namely: amphetamines [Chapter 3], cathinones [Chapters 4 and 5] and dissociative anaesthetics [Chapter 6]), within purchased or seized samples. Method development and optimisation of the key experimental parameters has facilitated a rapid and sensitive method of separation and detection of the illicit drugs in both their pure form and in the presence of common adulterants – these methods are comparable to standard detection by HPLC-UV.

The methods have demonstrated an ability to separate chemical entities which are different in structure (e.g. PMA vs. MDMA), derivatives of each other (e.g. methcathinone vs. *N*-ethylcathinones) and/or regioisomers of the same NPS (e.g. methoxy-ephedrine derivatives). The last example is of significance as regioisomeric discrimination is normally difficult to achieve in some classes of NPS and requires complex and expensive approaches (e.g. high-field NMR).

Amperometric detection incorporating disposable embedded graphite screen-printed macroelectrodes (GSPE) has been developed/optimised in each study using both a commercially available impinging jet flow cell (LC-FC-A system), or a custom-made iCell channel flow cell (LC-FC-B system).

This work also demonstrates that the design of the flow-cell affects the overall sensitivity of the measurement system, with the flow-cell (having the smaller fluid volume), giving a greater response. However, the two designs are significantly

different in terms of the flow delivery to the electrode, yet the iCell (having a volume 15 times that of the impinging jet flow cell) gives detection results of a similar order. This suggests that further optimisation of the shape may yield greater sensitivity; such work is underway with NPSs and the HPLC-AD protocol.

The simultaneous HPLC-UV and amperometric detection protocol detailed herein shows a marked improvement and advantage over previously reported electroanalytical methods, which were either unable to selectively discriminate between structurally related synthetic cathinones or utilised harmful and restrictive materials in their design. In addition, the cost effectiveness of the approach of using amperometric detection, rather than a more expensive secondary technique (for example: mass spectrometry), is clearly apparent as the cost of a disposable GSPE is approximately a few pence compared to a mass spectrometer (circa. £50K) and is significantly less complicated/expensive in terms of technological complexity, running/repair costs and specialised technical training. It is envisaged that the proof-of-concept study will be invaluable to analytical scientists and law enforcement officials, for the development of miniaturised and robust, electroanalytical detection systems for new psychoactive substances and related compounds as they emerge on the recreational drugs market.

Clearly, the global battle against drug (mis)use is showing no signs of relenting and the potential application of HPLC-AD to the general/wider detection and quantification of controlled/NPSs is clearly apparent. Nevertheless, our application of this technique has been applied only to bulk forensic samples, the wide range of potential stationary and mobile phase combinations (for example hydrophilic interaction liquid chromatography, HILIC) opens up the possibility of expanding this method to metabolites and/or biomarkers associated with clinical detection and/or

post-mortem toxicology in drug users. At present, the technology is limited to a laboratory environment, however, with the advent of customised microfluidic cells (for example: labs-on-a-chip incorporating a stationary phase material), the potential for reducing the system is possible and therefore opens up the potential for field-deployable separation/detection for use by law enforcement, first-responders and other relevant agencies.

8 References

Aboul-Enein, H. Y. (2000) 'Selectivity versus specificity in chromatographic analytical methods.' *Accreditation and Quality Assurance*, 5(5) pp. 180-181.

ACMD, A. C. o. t. M. o. D. (2011) *Consideration of the Novel Psychoactive Substances ('Legal Highs')*. London: Home office.

Adamowicz, P., Tokarczyk, B., Stanaszek, R. and Slopianka, M. (2013) 'Fatal mephedrone intoxication--a case report.' *J Anal Toxicol*, 37(1), Jan-Feb, pp. 37-42.

Addiction, E. E. M. C. f. D. a. D. (2012) *Annual report on the state of the drugs problem in Europe*.

Adenier, A., Chehimi, M. M., Gallardo, I., Pinson, J. and Vila, N. (2004) 'Electrochemical oxidation of aliphatic amines and their attachment to carbon and metal surfaces.' *Langmuir*, 20(19), Sep 14, pp. 8243-8253.

Al-Motarreb, A., Baker, K. and Broadley, K. J. (2002) 'Khat: pharmacological and medical aspects and its social use in Yemen.' *Phytother Res*, 16(5), Aug, pp. 403-413.

Alvarez, J. C., Etting, I., Abe, E., Villa, A. and Fabresse, N. (2017) 'Identification and quantification of 4-methylethcathinone (4-MEC) and 3,4-methylenedioxypyrovalerone (MDPV) in hair by LC-MS/MS after chronic administration.' *Forensic Sci Int*, 270, Jan, pp. 39-45.

Arora, B., Velpandian, T., Saxena, R., Lalwani, S., Dogra, T. D. and Ghose, S. (2016) 'Development and validation of an ESI-LC-MS/MS method for simultaneous identification and quantification of 24 analytes of forensic relevance in vitreous humour, whole blood and plasma.' *Drug Test Anal*, 8(1), Jan, pp. 86-97.

Arunotayanun, W. and Gibbons, S. (2012) 'Natural product 'legal highs'.' *Natural Product Reports*, 29(11), Nov, pp. 1304-1316.

Ayres, T. C. and Bond, J. W. (2012) 'A chemical analysis examining the pharmacology of novel psychoactive substances freely available over the internet and their impact on public (ill)health. Legal highs or illegal highs?' *BMJ Open*, 2(4)

Balbino, M. A., Eleoterio, I. C., de Oliveira, M. F. and McCord, B. R. (2016) 'Electrochemical Study of Delta-9-Tetrahydrocannabinol by Cyclic Voltammetry Using Screen Printed Electrode, Improvements in Forensic Analysis.' *Sensors & Transducers*, 207(12) p. 73.

- Baldania, S. L., Bhatt, K. K., Mehta, R. S., Shah, D. A. and Gandhi, T. R. (2008) 'RP-HPLC Estimation of Venlafaxine Hydrochloride in Tablet Dosage Forms.' *Indian J Pharm Sci*, 70(1), Jan, pp. 124-128.
- Beharry, S. and Gibbons, S. (2016) 'An overview of emerging and new psychoactive substances in the United Kingdom.' *Forensic Science International*, 267, 10//, pp. 25-34.
- Bhoomaiah, B. (2012) 'RP-HPLC Method for the Quantification of Cladribine in Pharmaceutical formulation.' *International Journal of Science and Technology*, 2(2) pp. 93-101.
- Blanco, E., Banks, C. E., Foster, C. W., Cumba, L. R. and do Carmo, D. R. (2016) 'Can solvent induced surface modifications applied to screen- printed platforms enhance their electroanalytical performance?' *Analyst*, 141(9) pp. 2783-2790.
- Bogusz, M. J. (2000) 'Liquid chromatography–mass spectrometry as a routine method in forensic sciences: a proof of maturity.' *Journal of Chromatography B: Biomedical Sciences and Applications*, 748(1) pp. 3-19.
- Borges, K. B., Freire, E. F., Martins, I. and de Siqueira, M. E. P. B. (2009) 'Simultaneous determination of multibenzodiazepines by HPLC/UV: Investigation of liquid–liquid and solid-phase extractions in human plasma.' *Talanta*, 78(1) pp. 233-241.
- Bourquin, D. and Brenneisen, R. (1987) 'Confirmation of cannabis abuse by the determination of 11-nor- Δ^9 -tetrahydrocannabinol-9-carboxylic acid in urine with high-performance liquid chromatography and electrochemical detection.' *Journal of Chromatography B: Biomedical Sciences and Applications*, 414 pp. 187-191.
- Brandt, S. D., Sumnall, H. R., Measham, F. and Cole, J. (2010) 'Analyses of second-generation 'legal highs' in the UK: Initial findings.' *Drug Testing and Analysis*, 2(8) pp. 377-382.
- Brunt, T. M., Poortman, A., Niesink, R. J. M. and van den Brink, W. (2011) 'Instability of the ecstasy market and a new kid on the block: mephedrone.' *Journal of Psychopharmacology*, 25(11), Nov, pp. 1543-1547.
- Butler, D. and Guilbault, G. G. (2004) 'Analytical Techniques for Ecstasy.' *Analytical Letters*, 37(10), 2004/12/27, pp. 2003-2030.
- Caldicott, D. G., Edwards, N. A., Kruys, A., Kirkbride, K. P., Sims, D. N., Byard, R. W., Prior, M. and Irvine, R. J. (2003) 'Dancing with "death": p-methoxyamphetamine overdose and its acute management.' *J Toxicol Clin Toxicol*, 41(2) pp. 143-154.

- Carhart-Harris, R. L., King, L. A. and Nutt, D. J. (2011) 'A web-based survey on mephedrone.' *Drug Alcohol Depend*, 118(1), Oct 1, pp. 19-22.
- Carmo, H., Remião, F., Carvalho, F., Fernandes, E., de Boer, D., dos Reis, L. A. and de Lourdes Bastos, M. (2003) '4-Methylthioamphetamine-induced hyperthermia in mice: influence of serotonergic and catecholaminergic pathways.' *Toxicology and applied pharmacology*, 190(3) pp. 262-271.
- Carvalho, M., Carmo, H., Costa, V. M., Capela, J. P., Pontes, H., Remiao, F., Carvalho, F. and Bastos, M. D. (2012) 'Toxicity of amphetamines: an update.' *Archives of Toxicology*, 86(8), Aug, pp. 1167-1231.
- Castaneto, M. S., Barnes, A. J., Concheiro, M., Klette, K. L., Martin, T. A. and Huestis, M. A. (2015) 'Biochip array technology immunoassay performance and quantitative confirmation of designer piperazines for urine workplace drug testing.' *Analytical and Bioanalytical Chemistry*, 407(16) pp. 4639-4648.
- Chèze, M., Deveaux, M., Martin, C., Lhermitte, M. and Pépin, G. 'Simultaneous analysis of six amphetamines and analogues in hair, blood and urine by LC-ESI-MS/MS.' *Forensic Science International*, 170(2) pp. 100-104.
- Clemens, K. J., McGregor, I. S., Hunt, G. E. and Cornish, J. L. (2007) 'MDMA, methamphetamine and their combination: possible lessons for party drug users from recent preclinical research.' *Drug Alcohol Rev*, 26(1), Jan, pp. 9-15.
- Cole, J. C., Bailey, M., Sumnall, H. R., Wagstaff, G. F. and King, L. A. (2002) 'The content of ecstasy tablets: implications for the study of their long-term effects.' *Addiction*, 97(12), Dec, pp. 1531-1536.
- Cosbey, S. H., Peters, K. L., Quinn, A. and Bentley, A. (2013) 'Mephedrone (methylethcathinone) in toxicology casework: a Northern Ireland perspective.' *J Anal Toxicol*, 37(2), Mar, pp. 74-82.
- Council Decision, E. (2010) *Submitting 4-methylmethcathinone (mephedrone) to control measures*.
- Council Decision, J. (2005) *The information exchange, risk-assessment and control of new psychoactive substances*.
- Cumba, L. R., Smith, J. P., Zuway, K. Y., Sutcliffe, O. B., do Carmo, D. R. and Banks, C. E. (2016) 'Forensic electrochemistry: simultaneous voltammetric detection of MDMA and its fatal counterpart "Dr Death" (PMA).' *Analytical Methods*, 8(1) pp. 142-152.

Cumba, L. R., Smith, J. P., Brownson, D. A. C., Iniesta, J., Metters, J. P., do Carmo, D. R. and Banks, C. E. (2015) 'Electroanalytical detection of pindolol: comparison of unmodified and reduced graphene oxide modified screen-printed graphite electrodes.' *Analyst*, 140(5) pp. 1543-1550.

D. J. Pike, N. K., P. A. Milner and D. I. Stewart, *Sensors*, 2013, 13, 58–70.

da Costa, J. L. and Chasin, A. A. d. M. (2004) 'Determination of MDMA, MDEA and MDA in urine by high performance liquid chromatography with fluorescence detection.' *Journal of Chromatography B*, 811(1), 2004/11/05/, pp. 41-45.

Dams, R., De Letter, E. A., Mortier, K. A., Cordonnier, J. A., Lambert, W. E., Piette, M. H. A., Van Calenbergh, S. and De Leenheer, A. P. (2003) 'Fatality Due To Combined Use of the Designer Drugs MDMA and PMA: A Distribution Study.' *Journal of Analytical Toxicology*, 27(5) pp. 318-323.

Dargan, P. I. and Wood, D. M. (2013) *Novel Psychoactive Substances: Classification, Pharmacology and Toxicology*. (9780124159112)

Dargan, P. I., Albert, S. and Wood, D. M. (2010) 'Mephedrone use and associated adverse effects in school and college/university students before the UK legislation change.' *QJM*, 103(11), Nov, pp. 875-879.

Daws, L. C., Irvine, R. J., Callaghan, P. D., Toop, N. P., White, J. M. and Bochner, F. (2000) 'Differential behavioural and neurochemical effects of para-methoxyamphetamine and 3, 4-methylenedioxymethamphetamine in the rat.' *Progress in Neuro-Psychopharmacology and Biological Psychiatry*, 24(6) pp. 955-977.

de Figueiredo, N., Oiye, E., de Menezes, M., de Andrade, J., Silva, M. and de Oliveira, M. (2010) 'Determination of 3, 4-methylenedioxymethamphetamine (MDMA) in confiscated tablets by High-Performance Liquid Chromatography (HPLC) with Diode Array Detector.' *J Forensic Res*, 1(2) pp. 1-4.

de MenezesA, M. M. T., de AndradeA, J. F., de Oliveira, M. F., TristãoB, H. M., Aparecida, A. and SaczkC, L. L. O. (2012) 'Analysis of Δ9-THC in cosmetics by high performance liquid chromatography with UV-Vis detection.' *Br J Anal Chem*, 8 pp. 341-344.

de Oliveira, L. S., Balbino, M. A., de Menezes, M. M. T., Dockal, E. R. and de Oliveira, M. F. (2013) 'Voltammetric analysis of cocaine using platinum and glassy carbon electrodes chemically modified with Uranyl Schiff base films.' *Microchemical Journal*, 110 pp. 374-378.

Dhakane, V. D. and Ubale, M. B. (2012) 'A Validated Stability-Indicating HPLC Related substances method for Carmustine in bulk drug.' *Elixir Int. J*, 50 pp. 10383-10386.

Dragan, R. (2003) 'Definition and classification of drug addiction and drug misuse issues.' *Sociologija*, 45(1) pp. 1-14.

Dunne, F. J., Jaffar, K. and Hashmi, S. (2015) 'Legal Highs-Not so new and still growing in popularity.' *British Journal of Medical Practitioners*, 8(1)

ElSohly, M. A., ElSohly, H. N., Jones, A. B., Dimson, P. A. and Wells, K. E. (1983) 'Analysis of the major metabolite of delta 9-tetrahydrocannabinol in urine II. A HPLC procedure.' *J Anal Toxicol*, 7(6), Nov-Dec, pp. 262-264.

EMCDDA, E. M. C. f. D. a. D. A. (2007) *Early-warning system on new psychoactive substances — operating guidelines*.

EMCDDA, E. M. C. f. D. a. D. A. (2010) *Europol–EMCDDA Joint Report on a new psychoactive substance: 4-methylmethcathinone (mephedrone)*.

EMCDDA, E. M. C. f. D. a. D. A. (2011) *New drugs and emerging trends*.

EMCDDA, E. M. C. f. D. a. D. A. (2013) *EU drug markets report: a strategic analysis*.

EMCDDA, E. M. C. f. D. a. D. A. (2015) *New psychoactive substances in Europe. An update from the EU Early Warning System (March 2015)*.

EMCDDA, E. M. C. f. D. a. D. A. (2016) *EMCDDA–Europol 2016 Annual Report on the implementation of Council Decision 2005/387/JHA*.

Farghaly, O., Hameed, R. A. and Abu-Nawwas, A.-A. H. (2014) 'Analytical application using modern electrochemical techniques.' *Int. J. Electrochem. Sci*, 9(1)

Fass, J. A., Fass, A. D. and Garcia, A. S. (2012) 'Synthetic cathinones (bath salts): legal status and patterns of abuse.' *Annals of Pharmacotherapy*, 46(3) pp. 436-441.

Favretto, D., Pascali, J. P. and Tagliaro, F. (2013) 'New challenges and innovation in forensic toxicology: focus on the "New Psychoactive Substances".' *J Chromatogr A*, 1287, Apr 26, pp. 84-95.

Freeman, S. and Alder, J. F. (2002) 'Arylethylamine psychotropic recreational drugs: a chemical perspective.' *European Journal of Medicinal Chemistry*, 37(7), 2002/07/01/, pp. 527-539.

Garrido, E. M., Garrido, J. M., Milhazes, N., Borges, F. and Oliveira-Brett, A. M. (2010) 'Electrochemical oxidation of amphetamine-like drugs and application to electroanalysis of ecstasy in human serum.' *Bioelectrochemistry*, 79(1), Aug, pp. 77-83.

Gibbons, S. and Zloh, M. (2010) 'An analysis of the 'legal high' mephedrone.' *Bioorg Med Chem Lett*, 20(14), Jul 15, pp. 4135-4139.

Gil, D., Adamowicz, P., Skulska, A., Tokarczyk, B. and Stanaszek, R. (2013) 'Analysis of 4-MEC in biological and non-biological material—Three case reports.' *Forensic Science International*, 228(1), 2013/05/10/, pp. 11-15.

Gillman, P. K. (2005) 'Monoamine oxidase inhibitors, opioid analgesics and serotonin toxicity.' *BJA: British Journal of Anaesthesia*, 95(4) pp. 434-441.

Glover, S. J. and Allen, K. R. (2010) 'Measurement of benzodiazepines in urine by liquid chromatography-tandem mass spectrometry: confirmation of samples screened by immunoassay.' *Ann Clin Biochem*, 47(Pt 2), Mar, pp. 111-117.

Green, J. M. (1996) 'Peer Reviewed: A Practical Guide to Analytical Method Validation.' *Analytical Chemistry*, 68(9), 1996/05/01, pp. 305A-309A.

Greifenstein, F. E., Devault, M., Yoshitake, J. and Gajewski, J. E. (1958) 'A study of a 1-aryl cyclo hexyl amine for anesthesia.' *Anesth Analg*, 37(5), Sep-Oct, pp. 283-294.

Guidelli, R. (1971a) 'Diffusion toward planar, spherical, and dropping electrodes at constant potential: II. Examples.' *Journal of Electroanalytical Chemistry and Interfacial Electrochemistry*, 33(2), 1971/12/01/, pp. 303-317.

Guidelli, R. (1971b) 'Diffusion toward planar, spherical, and dropping electrodes at constant potential: I. Theory.' *Journal of Electroanalytical Chemistry and Interfacial Electrochemistry*, 33(2), 1971/12/01/, pp. 291-302.

Gulaboski, R., Cordeiro, M. N., Milhazes, N., Garrido, J., Borges, F., Jorge, M., Pereira, C. M., Bogeski, I., Morales, A. H., Naumoski, B. and Silva, A. F. (2007) 'Evaluation of the lipophilic properties of opioids, amphetamine-like drugs, and metabolites through electrochemical studies at the interface between two immiscible solutions.' *Anal Biochem*, 361(2), Feb 15, pp. 236-243.

Gunasingham, H. (1984) 'Large-volume wall-jet cells as electrochemical detectors for high-performance liquid chromatography.' *Analytica Chimica Acta*, 159, 1984/01/01, pp. 139-147.

Gunasingham, H., Tay, B. T., Ang, K. P. and Koh, L. L. (1984) 'Electrochemical detection of polynuclear aromatic hydrocarbons following reversed-phase gradient

high-performance liquid chromatography using a large-volume wall-jet detector.' *Journal of Chromatography A*, 285, 1984/01/01/, pp. 103-114.

Gura, S., Guerra-Diaz, P., Lai, H. and Almirall, J. R. (2009) 'Enhancement in sample collection for the detection of MDMA using a novel planar SPME (PSPME) device coupled to ion mobility spectrometry (IMS).' *Drug Test Anal*, 1(7), Jul, pp. 355-362.

Hadlock, G. C., Webb, K. M., McFadden, L. M., Chu, P. W., Ellis, J. D., Allen, S. C., Andrenyak, D. M., Vieira-Brock, P. L., German, C. L., Conrad, K. M., Hoonakker, A. J., Gibb, J. W., Wilkins, D. G., Hanson, G. R. and Fleckenstein, A. E. (2011) '4-Methylmethcathinone (mephedrone): neuropharmacological effects of a designer stimulant of abuse.' *J Pharmacol Exp Ther*, 339(2), Nov, pp. 530-536.

Hanson, G., Venturelli, P. J. and Fleckenstein, A. E. (2015) *Drugs and society*. Vol. Twelfth. Burlington, MA: Jones & Bartlett Learning.

He, H., Shay, S. D., Caraco, Y., Wood, M. and Wood, A. J. (1998) 'Simultaneous determination of codeine and its seven metabolites in plasma and urine by high-performance liquid chromatography with ultraviolet and electrochemical detection.' *Journal of Chromatography B: Biomedical Sciences and Applications*, 708(1) pp. 185-193.

Helmlin, H.-J., Bracher, K., Bourquin, D., Vonlanthen, D., Brenneisen, R. and Styk, J. (1996) 'Analysis of 3,4-Methylenedioxymethamphetamine (MDMA) and its Metabolites in Plasma and Urine by HPLC-DAD and GC-MS.' *Journal of Analytical Toxicology*, 20(6) pp. 432-440.

Hill, S. L. and Thomas, S. H. L. (2011) 'Clinical toxicology of newer recreational drugs.' *Clinical Toxicology*, 49(8), 2011/10/01, pp. 705-719.

HomeOffice. (2009) *Drug Misuse Declared: Findings from the 2008/09 British Crime Survey*

Honeychurch, K. (2016) 'Review: The Application of Liquid Chromatography Electrochemical Detection for the Determination of Drugs of Abuse.' *Separations*, 3(4) p. 28.

Honeychurch, K. C. and Hart, J. P. (2008) 'Determination of flunitrazepam and nitrazepam in beverage samples by liquid chromatography with dual electrode detection using a carbon fibre veil electrode.' *Journal of Solid State Electrochemistry*, 12(10) pp. 1317-1324.

Honeychurch, K. C., Smith, G. C. and Hart, J. P. (2006) 'Voltammetric behavior of nitrazepam and its determination in serum using liquid chromatography with redox mode dual-electrode detection.' *Analytical chemistry*, 78(2) pp. 416-423.

Hudson, J. H., J.; Wagner, R., Harper, C. and Friel, P. (2013) *Validation of a Cannabinoid Quantitation Method Using an Agilent 6430 LC/MS/MS*.

Huettl, P., Koester, S., Hoffer, L. and Gerhardt, G. A. (1999) 'Separation and identification of drugs of abuse in drug cottons by high performance liquid chromatography coupled with electrochemical array detectors.' *Electroanalysis*, 11(5) pp. 313-319.

Hysek, C. M., Domes, G. and Liechti, M. E. (2012) 'MDMA enhances "mind reading" of positive emotions and impairs "mind reading" of negative emotions.' *Psychopharmacology (Berl)*, 222(2), Jul, pp. 293-302.

Hysek, C. M., Schmid, Y., Simmler, L. D., Domes, G., Heinrichs, M., Eisenegger, C., Preller, K. H., Quednow, B. B. and Liechti, M. E. (2014) 'MDMA enhances emotional empathy and prosocial behavior.' *Soc Cogn Affect Neurosci*, 9(11), Nov, pp. 1645-1652.

ICH, I. C. f. H. (1996) *Validation of analytical procedure: Text and Methodology*.

ICH, I. C. f. H. (2017) *The International Council for Harmonisation of Technical Requirements for Pharmaceuticals for Human Use*.

Isabel Colado, M., O'Shea, E. and Richard Green, A. (2007) 'MDMA and Other "Club Drugs".' *In Handbook of Contemporary Neuropharmacology*. John Wiley & Sons, Inc.,

Iversen, L. (2008) *Speed, ecstasy, ritalin: the science of amphetamines*. Oxford University Press.

Iversen, L., White, M. and Treble, R. (2014) 'Designer psychostimulants: pharmacology and differences.' *Neuropharmacology*, 87 pp. 59-65.

Jankovics, P., Varadi, A., Tolgyesi, L., Lohner, S., Nemeth-Palotas, J. and Koszegi-Szalai, H. (2011) 'Identification and characterization of the new designer drug 4'-methylethcathinone (4-MEC) and elaboration of a novel liquid chromatography-tandem mass spectrometry (LC-MS/MS) screening method for seven different methcathinone analogs.' *Forensic Sci Int*, 210(1-3), Jul 15, pp. 213-220.

Johnson, L. A., Johnson, R. L. and Portier, R. B. (2013) 'Current "legal highs".' *J Emerg Med*, 44(6), Jun, pp. 1108-1115.

Jordan, P. H. and Hart, J. P. (1991) 'Voltammetric behaviour of morphine at a glassy carbon electrode and its determination in human serum by liquid

chromatography with electrochemical detection under basic conditions.' *Analyst*, 116(10), Oct, pp. 991-996.

Kalix, P. (1981) 'Cathinone, an alkaloid from khat leaves with an amphetamine-like releasing effect.' *Psychopharmacology (Berl)*, 74(3) pp. 269-270.

Kalix, P. (1983) 'A Comparison of the Catecholamine Releasing Effect of the Khat Alkaloids (-)-Cathinone and (+)-Norpseudoephedrine.' *Drug and Alcohol Dependence*, 11(3-4) pp. 395-401.

Kalix, P. (1991) 'The Pharmacology of Psychoactive Alkaloids from Ephedra and Catha.' *Journal of Ethnopharmacology*, 32(1-3), Apr, pp. 201-208.

Kalix, P. (1992) 'Cathinone, a Natural Amphetamine.' *Pharmacology & Toxicology*, 70(2), Feb, pp. 77-86.

Kalix, P. (1996) 'Catha edulis, a plant that has amphetamine effects.' *Pharmacy World & Science: PWS*, 18(2) pp. 69-73.

Kalix, P. and Braenden, O. (1985) 'Pharmacological aspects of the chewing of khat leaves.' *Pharmacological Reviews*, 37(2), Jun, pp. 149-164.

Kang, H., Park, P., Bortolotto, Z. A., Brandt, S. D., Colestock, T., Wallach, J., Collingridge, G. L. and Lodge, D. (2017) 'Ephenidine: A new psychoactive agent with ketamine-like NMDA receptor antagonist properties.' *Neuropharmacology*, 112(Part A), 2017/01/01/, pp. 144-149.

Kato, N., Fujita, S., Ohta, H., Fukuba, M., Toriba, A. and Hayakawa, K. (2008) 'Thin layer chromatography/fluorescence detection of 3,4-methylenedioxy-methamphetamine and related compounds.' *J Forensic Sci*, 53(6), Nov, pp. 1367-1371.

Kaur, J., Srinivasan, K. K., Joseph, A., Gupta, A., Singh, Y., Srinivas, K. S. and Jain, G. (2010) 'Development and validation of stability indicating method for the quantitative determination of venlafaxine hydrochloride in extended release formulation using high performance liquid chromatography.' *J Pharm Bioallied Sci*, 2(1), Jan, pp. 22-26.

Kazakevich, Y. and Lobrutto, R. (2007) *HPLC for pharmaceutical scientists*. John Wiley & Sons.

Kelly, J. P. (2011) 'Cathinone derivatives: a review of their chemistry, pharmacology and toxicology.' *Drug Test Anal*, 3(7-8), Jul-Aug, pp. 439-453.

Khreit, O. I. G., Irving, C., Schmidt, E., Parkinson, J. A., Nic Daeid, N. and Sutcliffe, O. B. (2012) 'Synthesis, full chemical characterisation and development of validated methods for the quantification of the components found in the evolved "legal high" NRG-2.' *Journal of Pharmaceutical and Biomedical Analysis*, 61(Supplement C), 2012/03/05/, pp. 122-135.

King, L. and Kicman, A. (2011) 'A brief history of 'new psychoactive substances'.' *Drug testing and analysis*, 3(7-8) pp. 401-403.

Kokubun, H., Uezono, Y. and Matoba, M. (2014) 'Novel method of determination of D9-tetrahydrocannabinol (THC) in human serum by high-performance liquid chromatography with electrochemical detection.' *Gan to kagaku ryoho. Cancer & chemotherapy*, 41(4) pp. 471-473.

Kumar, K. K., Nagoji, K. E. and Nadh, R. V. (2012) 'A Validated RP-HPLC Method for the Estimation of Lapatinib in Tablet Dosage form using Gemcitabine Hydrochloride as an Internal Standard.' *Indian J Pharm Sci*, 74(6), Nov, pp. 580-583.

Kumar, K. R., Rao, C. M. P., Rao, C. B. and Chandra, K. (2010) 'RP-HPLC method development and validation for estimation of capecitabine in capsules.' *International Journal of ChemTech Research*, 2(1) pp. 307-311.

Kumihashi, M., Ameno, K., Shibayama, T., Suga, K., Miyauchi, H., Jamal, M., Wang, W., Uekita, I. and Ijiri, I. (2007) 'Simultaneous determination of methamphetamine and its metabolite, amphetamine, in urine using a high performance liquid chromatography column-switching method.' *Journal of chromatography. B, Analytical technologies in the biomedical and life sciences*, 845(1), 2007/01//, pp. 180-183.

Kusu, F. (2015) 'Development and Application of Electroanalytical Methods in Biomedical Fields.' *Yakugaku Zasshi-Journal of the Pharmaceutical Society of Japan*, 135(3), Mar, pp. 415-430.

Le Gall, E., Haurena, C., Sengmany, S., Martens, T. and Troupel, M. (2009) 'Three-component synthesis of alpha-branched amines under Barbier-like conditions.' *J Org Chem*, 74(20), Oct 16, pp. 7970-7973.

Lee, Y. W. (2013) 'Simultaneous Screening of 177 Drugs of Abuse in Urine Using Ultra-performance Liquid Chromatography with Tandem Mass Spectrometry in Drug-intoxicated Patients.' *Clin Psychopharmacol Neurosci*, 11(3), Dec, pp. 158-164.

Liechti, M. (2015) 'Novel psychoactive substances (designer drugs): overview and pharmacology of modulators of monoamine signaling.' *Swiss Med Wkly*, 145 p. w14043.

Liechti, M. E. and Vollenweider, F. X. (2001) 'Which neuroreceptors mediate the subjective effects of MDMA in humans? A summary of mechanistic studies.' *Hum Psychopharmacol*, 16(8), Dec, pp. 589-598.

Liechti, M. E., Kunz, I. and Kupferschmidt, H. (2005) 'Acute medical problems due to Ecstasy use. Case-series of emergency department visits.' *Swiss Med Wkly*, 135(43-44), Oct 29, pp. 652-657.

Litman, A., Levav, I., Saltz-Rennert, H. and Maoz, B. (1986) 'The use of khat. An epidemiological study in two Yemenite villages in Israel.' *Cult Med Psychiatry*, 10(4), Dec, pp. 389-396.

Liu, H. C., Lee, H. T., Hsu, Y. C., Huang, M. H., Liu, R. H., Chen, T. J. and Lin, D. L. (2015) 'Direct Injection LC-MS-MS Analysis of Opiates, Methamphetamine, Buprenorphine, Methadone and Their Metabolites in Oral Fluid from Substitution Therapy Patients.' *J Anal Toxicol*, 39(6), Jul-Aug, pp. 472-480.

Logan, B. K. (2002) 'Methamphetamine - Effects on Human Performance and Behavior.' *Forensic Sci Rev*, 14(1-2), Feb, pp. 133-151.

Lurie, Y., Gopher, A., Lavon, O., Almog, S., Sulimani, L. and Bentur, Y. (2012) 'Severe paramethoxymethamphetamine (PMMA) and paramethoxyamphetamine (PMA) outbreak in Israel.' *Clin Toxicol (Phila)*, 50(1), Jan, pp. 39-43.

Maldener, G. (1989) 'Requirements and tests for HPLC apparatus and methods in pharmaceutical quality control.' *Chromatographia*, 28(1) pp. 85-88.

Marchand, D. H., Croes, K., Dolan, J. W. and Snyder, L. R. (2005) 'Column selectivity in reversed-phase liquid chromatography. VII. Cyanopropyl columns.' *J Chromatogr A*, 1062(1), Jan 7, pp. 57-64.

Martin, T. L. (2001) 'Three cases of fatal paramethoxyamphetamine overdose.' *J Anal Toxicol*, 25(7), Oct, pp. 649-651.

Maskell, P. D., De Paoli, G., Seneviratne, C. and Pounder, D. J. (2011) 'Mephedrone (4-methylmethcathinone)-related deaths.' *J Anal Toxicol*, 35(3), Apr, pp. 188-191.

Masui, M., Sayo, H. and Tsuda, Y. (1968) 'Anodic oxidation of amines. Part I. Cyclic voltammetry of aliphatic amines at a stationary glassy-carbon electrode.' *Journal of the Chemical Society B: Physical Organic*, pp. 973-976.

McElrath, K. and O'Neill, C. (2011) 'Experiences with mephedrone pre- and post-legislative controls: Perceptions of safety and sources of supply.' *International Journal of Drug Policy*, 22(2), Mar, pp. 120-127.

- McLaughlin, G., Morris, N., Kavanagh, P. V., Power, J. D., O'Brien, J., Talbot, B., Elliott, S. P., Wallach, J., Hoang, K., Morris, H. and Brandt, S. D. (2016) 'Test purchase, synthesis, and characterization of 2-methoxydiphenidine (MXP) and differentiation from its meta- and para-substituted isomers.' *Drug Test Anal*, 8(1), Jan, pp. 98-109.
- McLaughlin, G., Morris, N., Kavanagh, P. V., Power, J. D., Dowling, G., Twamley, B., O'Brien, J., Talbot, B., Walther, D., Partilla, J. S., Baumann, M. H. and Brandt, S. D. (2017) 'Synthesis, characterization and monoamine transporter activity of the new psychoactive substance mexedrone and its N-methoxy positional isomer, N-methoxymephedrone.' *Drug testing and analysis*, 9(3), 09/21, pp. 358-368.
- Metters, J. P., Kadara, R. O. and Banks, C. E. (2011) 'New directions in screen printed electroanalytical sensors: an overview of recent developments.' *Analyst*, 136(6), Mar 21, pp. 1067-1076.
- Michel, R. E., Rege, A. B. and George, W. J. (1993) 'High-pressure liquid chromatography/electrochemical detection method for monitoring MDA and MDMA in whole blood and other biological tissues.' *Journal of Neuroscience Methods*, 50(1), 1993/10/01/, pp. 61-66.
- Milhazes, N., Martins, P., Uriarte, E., Garrido, J., Calheiros, R., Marques, M. P. M. and Borges, F. (2007) 'Electrochemical and spectroscopic characterisation of amphetamine-like drugs: Application to the screening of 3,4-methylenedioxymethamphetamine (MDMA) and its synthetic precursors.' *Analytica Chimica Acta*, 596(2), 2007/07/23/, pp. 231-241.
- Min, J. Z., Yamashita, K., Toyo'oka, T., Inagaki, S., Higashi, T., Kikura-Hanajiri, R. and Goda, Y. (2010) 'Simultaneous and group determination methods for designated substances by HPLC with multi-channel electrochemical detection and their application to real samples.' *Biomedical Chromatography*, 24(12) pp. 1287-1299.
- Moeller, K. E., Lee, K. C. and Kissack, J. C. (2008) 'Urine drug screening: practical guide for clinicians.' *Mayo Clin Proc*, 83(1), Jan, pp. 66-76.
- Moeller, M. R., Steinmeyer, S. and Kraemer, T. (1998) 'Determination of drugs of abuse in blood.' *Journal of Chromatography B: Biomedical Sciences and Applications*, 713(1) pp. 91-109.
- Moreno, D., Diaz de Grenu, B., Garcia, B., Ibeas, S. and Torroba, T. (2012) 'A turn-on fluorogenic probe for detection of MDMA from ecstasy tablets.' *Chem Commun (Camb)*, 48(24), Mar 21, pp. 2994-2996.
- Morgan, C. J., Noronha, L. A., Muetzfeldt, M., Feilding, A. and Curran, H. V. (2013) 'Harms and benefits associated with psychoactive drugs: findings of an

international survey of active drug users.' *Journal of Psychopharmacology*, 27(6) pp. 497-506.

Morris, H. and Wallach, J. (2014) 'From PCP to MXE: a comprehensive review of the non-medical use of dissociative drugs.' *Drug Test Anal*, 6(7-8), Jul-Aug, pp. 614-632.

Morris, K. (2010) UK places generic ban on mephedrone drug family. Elsevier.

Muller, I. B. and Windberg, C. N. (2005) 'Validation of an HPLC method for quantitation of MDMA in tablets.' *J Chromatogr Sci*, 43(8), Sep, pp. 434-437.

Nakahara, Y. and Sekine, H. (1985) 'Studies on confirmation of cannabis use. I. Determination of the cannabinoid contents in marijuana cigarette, tar, and ash using high performance liquid chromatography with electrochemical detection.' *J Anal Toxicol*, 9(3), May-Jun, pp. 121-124.

Nakahara, Y., Sekine, H. and Cook, C. E. (1989) 'Confirmation of cannabis use. II. Determination of tetrahydrocannabinol metabolites in urine and plasma by HPLC with ECD.' *J Anal Toxicol*, 13(1), Jan-Feb, pp. 22-24.

Nakashima, K., Kaddoumi, A., Ishida, Y., Itoh, T. and Taki, K. (2003) 'Determination of methamphetamine and amphetamine in abusers' plasma and hair samples with HPLC-FL.' *Biomedical Chromatography*, 17(7) pp. 471-476.

Natalia Biziak de Figueiredo¹, É. N. O., Matheus Manoel Teles de Menezes¹, José Fernando de Andrade¹, Maria Cristina Brunini and Oliveira^{1*}, S. a. M. F. d. (2010) 'Determination of 3,4-methylenedioxymethamphetamine (MDMA) in Confiscated Tablets by High-Performance Liquid Chromatography (HPLC) with Diode Array Detector.' *Journal of Forensic Research*, 1(2)

Nencini, P., Amiconi, G., Befani, O., Abdullahi, M. A. and Anania, M. C. (1984) 'Possible Involvement of Amine Oxidase Inhibition in the Sympathetic Activation Induced by Khat (Catha-Edulis) Chewing in Humans.' *Journal of Ethnopharmacology*, 11(1) pp. 79-86.

Neue, U. D. (1997) 'HPLC troubleshooting: Complex sample matrices.' *American Laboratory*, 29(14), Jul, pp. 48-49.

Neue, U. D. (2010) 'Geometrically deformed tubes as efficient vessels for post-column derivatization in high-performance liquid chromatography.' *Chemical Engineering and Processing*, 49(7), Jul, pp. 662-671.

Neville, T. (1995) 'The Case of the Frozen Addicts - Langston,Jw, Palfreman,J.' *Library Journal*, 120(7), Apr 15, pp. 105-105.

- Nieddu, M., Boatto, G., Sini, L. and Dessì, G. (2007) 'Determination of p-Methoxyamphetamine by Capillary Electrophoresis with Diode Array Detection from Urine and Plasma Samples.' *Journal of Liquid Chromatography & Related Technologies*, 30(3), 2007/02/01, pp. 431-438.
- Nyoni, E. C., Sitaram, B. R. and Taylor, D. A. (1996) 'Determination of Δ^9 -tetrahydrocannabinol levels in brain tissue using high-performance liquid chromatography with electrochemical detection.' *Journal of Chromatography B: Biomedical Sciences and Applications*, 679(1), 1996/04/26/, pp. 79-84.
- Ochiai, L. M., Agustini, D., Figueiredo-Filho, L. C. S., Banks, C. E., Marcolino-Junior, L. H. and Bergamini, M. F. (2017) 'Electroanalytical thread-device for estriol determination using screen-printed carbon electrodes modified with carbon nanotubes.' *Sensors and Actuators B: Chemical*, 241(Supplement C), 2017/03/31/, pp. 978-984.
- Oldham, K. B. (1973) 'Diffusive transport to planar, cylindrical and spherical electrodes.' *Journal of Electroanalytical Chemistry and Interfacial Electrochemistry*, 41(3), 1973/02/09/, pp. 351-358.
- Osorio-Olivares, M., Rezende, M. C., Sepulveda-Boza, S., Cassels, B. K. and Fierro, A. (2004) 'MAO inhibition by arylisopropylamines: the effect of oxygen substituents at the beta-position.' *Bioorganic & Medicinal Chemistry*, 12(15), Aug 1, pp. 4055-4066.
- Pápai, Z. and Pap, T. L. (2002) 'Analysis of peak asymmetry in chromatography.' *Journal of Chromatography A*, 953(1), 2002/04/12/, pp. 31-38.
- Paton, D. M., Bell, J. I., Yee, R. and Cook, D. A. (1975) 'Pharmacology and toxicity of 3,4-methylenedioxyamphetamine, para-methoxyamphetamine and related dimethoxyamphetamines.' *Proc West Pharmacol Soc*, 18 pp. 229-231.
- Pecková, K. (2011) 'Utilization of Unmodified Screen-Printed Carbon Electrodes in Electroanalysis of Organic Compounds (An Overview).'
- Phillips, D. J., Capparella, M., Neue, U. D. and ElFallah, Z. (1997) 'A new small particle packing for faster analysis with high resolution.' *Journal of Pharmaceutical and Biomedical Analysis*, 15(9-10), Jun, pp. 1389-1395.
- Pichini, S., Navarro, M., Pacifici, R., Zuccaro, P., Ortuno, J., Farre, M., Roset, P. N., Segura, J. and de la Torre, R. (2003) 'Usefulness of sweat testing for the detection of MDMA after a single-dose administration.' *J Anal Toxicol*, 27(5), Jul-Aug, pp. 294-303.
- Pike, D. J., Kapur, N., Millner, P. A. and Stewart, D. I. (2012) 'Flow cell design for effective biosensing.' *Sensors (Basel)*, 13(1), Dec 20, pp. 58-70.

Prosser, J. M. and Nelson, L. S. (2012) 'The toxicology of bath salts: a review of synthetic cathinones.' *J Med Toxicol*, 8(1), Mar, pp. 33-42.

PYLA, S., SRINIVAS, K., YVV, J. and PANDA, J. 'DEVELOPMENT AND VALIDATION OF NEW ANALYTICAL METHOD FOR PACLITAXEL IN BULK AND PHARMACEUTICAL DOSAGE FORM BY REVERSE PHASE HPLC (RP-HPLC).'

R. J. Flanagan, D. P. a. R. W., *Electrochemical Detection in HPLC: Analysis of Drugs and Poisons*, RSC Chromatography Monographs, 2005, vol. 10, pp. 1–244.

Ren, D.-B., Yang, Z.-H., Liang, Y.-Z., Fan, W. and Ding, Q. (2013) 'Effects of injection volume on chromatographic features and resolution in the process of counter-current chromatography.' *Journal of Chromatography A*, 1277, 2013/02/15/, pp. 7-14.

Reuter, P. and Pardo, B. (2017) 'Can new psychoactive substances be regulated effectively? An assessment of the British Psychoactive Substances Bill.' *Addiction*, 112(1), Jan, pp. 25-31.

Ribeiro, M., Fernanda, M., da Cruz Júnior, J. W., Dockal, E. R., McCord, B. R. and de Oliveira, M. F. (2016) 'Voltammetric Determination of Cocaine Using Carbon Screen Printed Electrodes Chemically Modified with Uranyl Schiff Base Films.' *Electroanalysis*, 28(2) pp. 320-326.

Riezzo, I., Cerretani, D., Fiore, C., Bello, S., Centini, F., D'Errico, S., Fiaschi, A. I., Giorgi, G., Neri, M., Pomara, C., Turillazzi, E. and Fineschi, V. (2010) 'Enzymatic-nonenzymatic cellular antioxidant defense systems response and immunohistochemical detection of MDMA, VMAT2, HSP70, and apoptosis as biomarkers for MDMA (Ecstasy) neurotoxicity.' *J Neurosci Res*, 88(4), Mar, pp. 905-916.

Roberts, L., Ford, L., Patel, N., Vale, J. A. and Bradberry, S. M. (2017) '11 analytically confirmed cases of mephedrone use among polydrug users.' *Clinical Toxicology*, 55(3), 2017/03/16, pp. 181-186.

Saito, K., Saito, R., Kikuchi, Y., Iwasaki, Y., Ito, R. and Nakazawa, H. (2011) 'Analysis of Drugs of Abuse in Biological Specimens.' *Journal of Health Science*, 57(6) pp. 472-487.

Sandhya, P., Vishnu, P. and Anjali, N. (2013) 'Method development and validation of Imatinib Mesylate in Pharmaceutical dosage form by RP-HPLC.' *World Journal of Pharmacy and Pharmaceutical Sciences*, 3(1) pp. 682-688.

Santagati, N. A., Ferrara, G., Marrazzo, A. and Ronsisvalle, G. (2002) 'Simultaneous determination of amphetamine and one of its metabolites by HPLC

with electrochemical detection.' *Journal of pharmaceutical and biomedical analysis*, 30(2) pp. 247-255.

Santali, E. Y., Cadogan, A.-K., Daeid, N. N., Savage, K. A. and Sutcliffe, O. B. (2011) 'Synthesis, full chemical characterisation and development of validated methods for the quantification of (\pm)-4'-methylmethcathinone (mephedrone): A new "legal high".' *Journal of Pharmaceutical and Biomedical Analysis*, 56(2), 2011/09/10/, pp. 246-255.

Sawyer, W. R., Waterhouse, G. A., Doedens, D. J. and Forney, R. B. (1988) 'Heroin, morphine, and hydromorphone determination in postmortem material by high performance liquid chromatography.' *J Forensic Sci*, 33(5), Sep, pp. 1146-1155.

Schifano, F., Albanese, A., Fergus, S., Stair, J. L., Deluca, P., Corazza, O., Davey, Z., Corkery, J., Siemann, H., Scherbaum, N., Farre, M., Torrens, M., Demetrovics, Z., Ghodse, A. H., Psychonaut Web, M. and Re, D. R. G. (2011) 'Mephedrone (4-methylmethcathinone; 'meow meow'): chemical, pharmacological and clinical issues.' *Psychopharmacology (Berl)*, 214(3), Apr, pp. 593-602.

Seger, C. (2012) 'Usage and limitations of liquid chromatography-tandem mass spectrometry (LC-MS/MS) in clinical routine laboratories.' *Wien Med Wochenschr*, 162(21-22), Nov, pp. 499-504.

Shabir, G. A. (2003) 'Validation of high-performance liquid chromatography methods for pharmaceutical analysis.' *Journal of Chromatography A*, 987(1), 2003/02/14/, pp. 57-66.

Shevyrin, V., Melkozerov, V., Eltsov, O., Shafran, Y. and Morzherin, Y. (2016) 'Synthetic cannabinoid 3-benzyl-5-[1-(2-pyrrolidin-1-ylethyl)-1H-indol-3-yl]-1,2,4-oxadiazole. The first detection in illicit market of new psychoactive substances.' *Forensic Science International*, 259, 2//, pp. 95-100.

Shulgin, A. T. (1978) 'Psychotomimetic drugs: Structure-activity relationships.' *In Stimulants*. Springer, pp. 243-333.

Siegel, G. J. and Agranoff, B. W. (1999) *Basic neurochemistry : molecular, cellular, and medical aspects*. 6th ed. / editors Bernard W. Agranoff ... [et al.], illustrations by Lorie M. Gavulic. ed., Philadelphia: Lippincott-Raven Publishers.

Simmler, L. D. (2018) 'Monoamine Transporter and Receptor Interaction Profiles of Synthetic Cathinones.' *In* Zawilska, J. B. (ed.) *Synthetic Cathinones: Novel Addictive and Stimulatory Psychoactive Substances*. Cham: Springer International Publishing, pp. 97-115.

- Simmler, L. D., Hysek, C. M. and Liechti, M. E. (2011) 'Sex differences in the effects of MDMA (ecstasy) on plasma copeptin in healthy subjects.' *J Clin Endocrinol Metab*, 96(9), Sep, pp. 2844-2850.
- Simmler, L. D., Wandeler, R. and Liechti, M. E. (2013b) 'Bupropion, methylphenidate, and 3,4-methylenedioxypyrovalerone antagonize methamphetamine-induced efflux of dopamine according to their potencies as dopamine uptake inhibitors: implications for the treatment of methamphetamine dependence.' *BMC Res Notes*, 6, Jun 05, p. 220.
- Simmler, L. D., Rickli, A., Hoener, M. C. and Liechti, M. E. (2014) 'Monoamine transporter and receptor interaction profiles of a new series of designer cathinones.' *Neuropharmacology*, 79(Supplement C), 2014/04/01/, pp. 152-160.
- Simmler, L. D., Buser, T. A., Donzelli, M., Schramm, Y., Dieu, L. H., Huwyler, J., Chaboz, S., Hoener, M. C. and Liechti, M. E. (2013a) 'Pharmacological characterization of designer cathinones in vitro.' *Br J Pharmacol*, 168(2), Jan, pp. 458-470.
- Smith, J. P., Sutcliffe, O. B. and Banks, C. E. (2015) 'An overview of recent developments in the analytical detection of new psychoactive substances (NPSs).' *Analyst*, Jun 2,
- Smith, J. P., Metters, J. P., Irving, C., Sutcliffe, O. B. and Banks, C. E. (2014a) 'Forensic electrochemistry: the electroanalytical sensing of synthetic cathinone-derivatives and their accompanying adulterants in "legal high" products.' *Analyst*, 139(2) pp. 389-400.
- Smith, J. P., Metters, J. P., Khreit, O. I. G., Sutcliffe, O. B. and Banks, C. E. (2014b) 'Forensic Electrochemistry Applied to the Sensing of New Psychoactive Substances: Electroanalytical Sensing of Synthetic Cathinones and Analytical Validation in the Quantification of Seized Street Samples.' *Analytical Chemistry*, 86(19), 2014/10/07, pp. 9985-9992.
- Smith, J. P., Metters, J. P., Kampouris, D. K., Lledo-Fernandez, C., Sutcliffe, O. B. and Banks, C. E. (2013) 'Forensic electrochemistry: the electroanalytical sensing of Rohypnol (R) (flunitrazepam) using screen-printed graphite electrodes without recourse for electrode or sample pre-treatment.' *Analyst*, 138(20) pp. 6185-6191.
- Soar, K., Turner, J. J. and Parrott, A. C. (2001) 'Psychiatric disorders in Ecstasy (MDMA) users: a literature review focusing on personal predisposition and drug history.' *Hum Psychopharmacol*, 16(8), Dec, pp. 641-645.
- Soares, M., Carvalho, M., Carmo, H., Remiao, F., Carvalho, F. and Bastos, M. (2004) 'Simultaneous determination of amphetamine derivatives in human urine after SPE extraction and HPLC-UV analysis.' *Biomedical Chromatography*, 18(2) pp. 125-131.

Somaini, L., Saracino, M. A., Marcheselli, C., Zanchini, S., Gerra, G. and Raggi, M. A. (2011) 'Combined liquid chromatography-coulometric detection and microextraction by packed sorbent for the plasma analysis of long acting opioids in heroin addicted patients.' *Anal Chim Acta*, 702(2), Sep 30, pp. 280-287.

Sreedevi, A., Rao, L. and Kalyani, L. (2013) 'Stability-indicating HPLC Method for analysis of Epirubicin in Pharmaceutical dosage form.' *Indo American Journal of Pharmaceutical Research*, 3(10) pp. 8249-8259.

Stoll, D. R., Paek, C. and Carr, P. W. (2006) 'Fast gradient elution reversed-phase high-performance liquid chromatography with diode-array detection as a high-throughput screening method for drugs of abuse. I. Chromatographic conditions.' *J Chromatogr A*, 1137(2), Dec 29, pp. 153-162.

Stradiotto, N. R., Yamanaka, H. and Zanoni, M. V. B. (2003) 'Electrochemical sensors: a powerful tool in analytical chemistry.' *Journal of the Brazilian Chemical Society*, 14(2) pp. 159-173.

Švorc, L., Vojs, M., Michniak, P., Marton, M., Rievaj, M. and Bustin, D. (2014) 'Electrochemical behavior of methamphetamine and its voltammetric determination in biological samples using self-assembled boron-doped diamond electrode.' *Journal of Electroanalytical Chemistry*, 717, 2014/03/15/, pp. 34-40.

Tadini, M. C., Balbino, M. A., Eleoterio, I. C., de Oliveira, L. S., Dias, L. G., Jean-François Demets, G. and de Oliveira, M. F. (2014) 'Developing electrodes chemically modified with cucurbit[6]uril to detect 3,4-methylenedioxymethamphetamine (MDMA) by voltammetry.' *Electrochimica Acta*, 121, 2014/03/01/, pp. 188-193.

Tagliaro, F., Franchi, D., Dorizzi, R. and Marigo, M. (1989) 'High-performance liquid chromatographic determination of morphine in biological samples: An overview of separation methods and detection techniques.' *Journal of Chromatography B: Biomedical Sciences and Applications*, 488(1), 1989/03/17/, pp. 215-228.

UK-Government. (1971) *Misuse of Drugs Act 1971(c.38)*. London.

UK-Government (1973) 'The Misuse of Drugs (Safe Custody) Regulations 1973.'

UK-Government. (2001) *The Misuse of Drugs Regulations 2001*.

UK-Government (2012) 'The Human Medicines Regulations.'

UK-Government. (2016) *Psychoactive Substances Act 2016*.

UNODC (1961) 'United Nations Single Convention on Narcotic Drugs.'

UNODC, U. N. O. o. D. a. C. (2013) *The International Drug Control Conventions*.

USE, I. C. O. H. O. T. R. F. R. O. P. F. H. (2005) 'VALIDATION OF ANALYTICAL PROCEDURES: TEXT AND METHODOLOGY Q2(R1) '

Uslu, B. and Ozkan, S. A. (2011) 'Electroanalytical Methods for the Determination of Pharmaceuticals: A Review of Recent Trends and Developments.' *Analytical Letters*, 44(16), 2011/11/01, pp. 2644-2702.

V. Krishnaiah, Y. V. R. R., V. Hanuman Reddy, M. Thirupalu Reddy, G. M. Rao, *Int. J. Sci Res.*, 2012, 1, 14 – 17.

Valente, M. J., Guedes de Pinho, P., de Lourdes Bastos, M., Carvalho, F. and Carvalho, M. (2014) 'Khat and synthetic cathinones: a review.' *Arch Toxicol*, 88(1), Jan, pp. 15-45.

Verschraagen, M., Maes, A., Ruiter, B., Bosman, I. J., Smink, B. E. and Lusthof, K. J. (2007) 'Post-mortem cases involving amphetamine-based drugs in The Netherlands. Comparison with driving under the influence cases.' *Forensic Sci Int*, 170(2-3), Aug 06, pp. 163-170.

Vessman, J. (1996) 'Selectivity or specificity? Validation of analytical methods from the perspective of an analytical chemist in the pharmaceutical industry.' *J Pharm Biomed Anal*, 14(8-10), Jun, pp. 867-869.

Wada, M., Ochi, Y., Nogami, K., Ikeda, R., Kuroda, N. and Nakashima, K. (2012) 'Evaluation of hair roots for detection of methamphetamine and 3,4-methylenedioxymethamphetamine abuse by use of an HPLC-chemiluminescence method.' *Anal Bioanal Chem*, 403(9), Jul, pp. 2569-2576.

Waddell, S. A., Fernandez, C., Inverarity, C. C. and Prabhu, R. (2017) 'Extending the capability of forensic electrochemistry to the novel psychoactive substance benzylpiperazine.' *Sensing and Bio-Sensing Research*, 13, 2017/04/01/, pp. 28-39.

Wallach, J., Kavanagh, P. V., McLaughlin, G., Morris, N., Power, J. D., Elliott, S. P., Mercier, M. S., Lodge, D., Morris, H., Dempster, N. M. and Brandt, S. D. (2015) 'Preparation and characterization of the 'research chemical' diphenidine, its pyrrolidine analogue, and their 2,2-diphenylethyl isomers.' *Drug Test Anal*, 7(5), May, pp. 358-367.

Whelpton, R. (2007) 'Speed, Ecstasy, Ritalin: The Science of Amphetamines.' *British Journal of Clinical Pharmacology*, 63(6) pp. 763-763.

White, C., Edwards, M., Brown, J. and Bell, J. (2014) 'The impact of recreational MDMA 'ecstasy' use on global form processing.' *J Psychopharmacol*, 28(11), Nov, pp. 1018-1029.

Wilkins, C. (2014) 'A critical first assessment of the new pre-market approval regime for new psychoactive substances (NPS) in New Zealand.' *Addiction*, 109(10) pp. 1580-1586.

Wink, C. S., Meyer, G. M., Wissenbach, D. K., Jacobsen-Bauer, A., Meyer, M. R. and Maurer, H. H. (2014) 'Lefetamine-derived designer drugs N-ethyl-1,2-diphenylethylamine (NEDPA) and N-iso-propyl-1,2-diphenylethylamine (NPDPA): metabolism and detectability in rat urine using GC-MS, LC-MSn and LC-HR-MS/MS.' *Drug Test Anal*, 6(10), Oct, pp. 1038-1048.

Wink, C. S. D., Meyer, G. M. J., Meyer, M. R. and Maurer, H. H. (2015) 'Toxicokinetics of lefetamine and derived diphenylethylamine designer drugs- Contribution of human cytochrome P450 isozymes to their main phase I metabolic steps.' *Toxicology Letters*, 238(3), Nov 4, pp. 39-44.

Winstock, A. R., Marsden, J. and Mitcheson, L. (2010) 'What should be done about mephedrone?' *BMJ*, 340 p. c1605.

Winstock, A. R., Mitcheson, L. R., Deluca, P., Davey, Z., Corazza, O. and Schifano, F. (2011) 'Mephedrone, new kid for the chop?' *Addiction*, 106(1), Jan, pp. 154-161.

Wolff, K. and Winstock, A. R. (2006) 'Ketamine: from medicine to misuse.' *CNS Drugs*, 20, 2006/03//

//, p. 199+.

Xiang, P., Shen, M. and Drummer, O. H. (2015) 'Review: Drug concentrations in hair and their relevance in drug facilitated crimes.' *J Forensic Leg Med*, 36, Nov, pp. 126-135.

Xu, F., Gao, M., Wang, L., Zhou, T., Jin, L. and Jin, J. (2002) 'Amperometric determination of morphine on cobalt hexacyanoferrate modified electrode in rat brain microdialysates.' *Talanta*, 58(3), 2002/09/12/, pp. 427-432.

Zanda, M. T. and Fattore, L. (2017) 'Chapter 29 - Novel Psychoactive Substances: A New Behavioral and Mental Health Threat A2 - Watson, Ronald Ross.' In Zibadi, S. (ed.) *Addictive Substances and Neurological Disease*. Academic Press, pp. 341-353.

Zhao, H., Brenneisen, R., Scholer, A., McNally, A. J., ElSohly, M. A., Murphy, T. P. and Salamone, S. J. (2001) 'Profiles of urine samples taken from Ecstasy users at

Rave parties: analysis by immunoassays, HPLC, and GC-MS.' *J Anal Toxicol*, 25(4), May-Jun, pp. 258-269.

Zuba, D. (2012) 'Identification of cathinones and other active components of 'legal highs' by mass spectrometric methods.' *Trac-Trends in Analytical Chemistry*, 32, Feb, pp. 15-30.

Zuway, K. Y., Smith, J. P., Foster, C. W., Kapur, N., Banks, C. E. and Sutcliffe, O. B. (2015) 'Detection and quantification of new psychoactive substances (NPSs) within the evolved "legal high" product, NRG-2, using high performance liquid chromatography-amperometric detection (HPLC-AD).' *Analyst*, 140(18), Sep 21, pp. 6283-6294.

9 Appendix

Table 9.1 Results of linearity measurements for (±)-MA using HPLC-UV detection in the LC-FC-A system, column A (Table 2.2), Mobile phase 1, detector wavelength (UV): 210 nm.

(±)-MA						
Concentration (µg mL ⁻¹)	10	20	40	60	80	100
Peak area 1	180.46	371.38	736.63	1123.78	1493.72	1852.48
Peak area 2	182.01	371.66	735.68	1124.83	1494.54	1852.47
Peak area 3	183.24	370.15	740.69	1124.99	1493.97	1853.36
Peak area 4	182.92	371.31	738.51	1125.37	1492.49	1856.64
Peak area 5	180.04	372.04	739.72	1124.00	1494.07	1851.54
Peak area 6	181.33	371.49	739.43	1122.15	1492.50	1847.63
Average	181.67	371.34	738.44	1124.19	1493.55	1852.35
RSD%	0.71	0.17	0.26	0.10	0.06	0.16

Table 9.2 Results of linearity measurements for (±)-PMA using HPLC-UV detection in the LC-FC-A system, column A (Table 2.2), Mobile phase 1, detector wavelength (UV): 210 nm.

(±)-PMA						
Concentration (µg mL ⁻¹)	10	20	40	60	80	100
Peak area 1	140.83	283.62	562.49	859.49	1146.62	1421.60
Peak area 2	140.81	284.72	560.55	859.57	1144.25	1425.26
Peak area 3	143.00	283.84	565.50	861.99	1143.09	1424.07
Peak area 4	140.81	283.05	563.86	860.75	1142.99	1424.11
Peak area 5	143.74	283.67	560.07	860.25	1143.91	1420.69
Peak area 6	142.97	286.05	565.36	855.30	1142.58	1417.41
Average	142.03	284.16	562.97	859.56	1143.91	1422.19
RSD%	0.95	0.38	0.42	0.27	0.13	0.20

Table 9.3 Results of linearity measurements for (±)-MDMA using HPLC-UV detection in the LC-FC-A system, column A (Table 2.2), mobile phase 1, detector wavelength (UV): 210 nm.

(±)-MDMA						
Concentration (µg mL ⁻¹)	10	20	40	60	80	100
Peak area 1	134.54	289.03	571.74	870.28	1157.05	1425.17
Peak area 2	135.35	290.59	570.04	868.03	1156.29	1427.81
Peak area 3	134.58	290.54	570.67	868.87	1156.28	1424.35
Peak area 4	135.97	288.47	572.12	869.47	1155.60	1426.27
Peak area 5	135.21	289.04	570.14	868.48	1155.37	1425.50
Peak area 6	134.51	290.10	571.66	867.96	1156.49	1425.29
Average	135.03	289.63	571.06	868.85	1156.18	1425.73
RSD%	0.44	0.31	0.16	0.10	0.05	0.08

Table 9.4 Results of linearity measurements for (±)-PMA by using HPLC-AD detection in the LC-FC-A system, column A (Table 2.2), mobile phase 1.

(±)-PMA						
Concentration ($\mu\text{g mL}^{-1}$)	10	20	40	60	80	100
Peak current 1	0.079	0.154	0.246	0.565	0.840	0.962
Peak current 2	0.079	0.152	0.241	0.561	0.826	0.958
Peak current 3	0.078	0.154	0.241	0.560	0.833	0.965
Peak current 4	0.077	0.154	0.243	0.557	0.828	0.965
Peak current 5	0.079	0.154	0.244	0.556	0.828	0.958
Peak current 6	0.077	0.155	0.244	0.558	0.830	0.956
Average	0.07	0.154	0.243	0.559	0.831	0.961
RSD%	0.99	0.62	0.71	0.58	0.60	0.39

Table 9.5 Results of linearity measurements for (±)-MDMA using HPLC-AD detection in the LC-FC-A system, column A (Table 2.2), mobile phase 1.

(±)-MDMA						
Concentration ($\mu\text{g mL}^{-1}$)	10	20	40	60	80	100
Peak current 1	0.123	0.206	0.393	0.884	1.163	1.457
Peak current 2	0.122	0.206	0.392	0.883	1.160	1.460
Peak current 3	0.122	0.206	0.392	0.882	1.160	1.457
Peak current 4	0.124	0.206	0.392	0.883	1.162	1.458
Peak current 5	0.123	0.205	0.392	0.884	1.163	1.458
Peak current 6	0.122	0.207	0.392	0.881	1.162	1.457
Average	0.120	0.210	0.390	0.880	1.160	1.460
RSD%	0.52	0.25	0.11	0.13	0.12	0.08

Table 9.6 Results of linearity measurements for (±)-PMA using HPLC-AD detection in the LC-FC-B system, column (A) Table 2.2, mobile phase 1.

(±)-PMA						
Concentration ($\mu\text{g mL}^{-1}$)	10	20	40	60	80	100
Peak current 1	0.0871	0.144	0.164	0.223	0.274	0.297
Peak current 2	0.089	0.142	0.162	0.227	0.269	0.298
Peak current 3	0.088	0.143	0.164	0.223	0.269	0.295
Peak current 4	0.087	0.143	0.162	0.224	0.273	0.297
Peak current 5	0.088	0.143	0.163	0.224	0.274	0.295
Peak current 6	0.087	0.143	0.164	0.223	0.274	0.295
Average	0.087	0.140	0.160	0.224	0.272	0.296
RSD%	0.88	0.50	0.65	0.74	0.94	0.45

Table 9.7 Raw data of the inter- and intra-day peak values and relative standard deviations (RSD %) for (±)-MA, (±)-PMA and (±)-MDMA using HPLC-UV detection and amperometric detection in the LC-FC-A and LC-FC-B systems.

LC-FC-A												
Concentration ($\mu\text{g mL}^{-1}$)	Intra-day values of HPLC-UV peak area (mA)			Intra-day values of HPLC-AD peak current (μA)			Inter-day values of HPLC-UV peak area (mA)			Inter-day values of HPLC-AD peak current (μA)		
	MA	PMA	MDMA	MA	PMA	MDMA	MA	PMA	MDMA	MA	PMA	MDMA
60	1123.78	859.48	870.27	n.d.	0.550	0.830	1123.78	859.48	868.27	n.d.	0.550	0.830
60	1124.83	859.57	868.03	n.d.	0.560	0.826	1124.83	859.574	866.03	n.d.	0.560	0.820
60	1124.98	861.99	868.86	n.d.	0.580	0.820	1124.98	861.99	868.86	n.d.	0.580	0.820
60	1125.36	860.74	869.47	n.d.	0.560	0.830	1125.36	860.74	869.47	n.d.	0.560	0.830
60	1125.99	860.25	868.48	n.d.	0.540	0.840	1125.99	860.25	868.48	n.d.	0.540	0.840
60	1124.15	855.30	867.95	n.d.	0.560	0.810	1124.15	855.30	867.95	n.d.	0.560	0.820
60	1123.78	860.48	870.27	n.d.	0.560	0.884	1123.78	860.48	870.27	n.d.	0.550	0.830
60	1123.83	859.57	870.03	n.d.	0.560	0.883	1125.83	859.57	870.03	n.d.	0.550	0.820
60	1123.98	861.99	870.86	n.d.	0.550	0.882	1124.98	861.99	870.86	n.d.	0.560	0.820
60	1122.36	860.74	869.47	n.d.	0.550	0.883	1125.36	862.74	870.47	n.d.	0.550	0.830
60	1123.99	860.25	869.48	n.d.	0.550	0.884	1125.99	861.25	870.48	n.d.	0.550	0.820
60	1122.15	860.30	867.95	n.d.	0.550	0.881	1125.15	859.30	869.95	n.d.	0.550	0.830
Average	1124.10	860.05	869.26	n.d.	0.553	0.883	1125.02	860.22	869.26	n.d.	0.552	0.825
RSD%	0.09	0.19	0.11	n.d.	0.933	0.128	0.06	0.22	0.16	n.d.	0.740	0.664
n.d. = not detected												

Table 9.8 Results of linearity measurements for (±)-caffeine using HPLC-UV in the LC-FC-A system, column A (Table 2.2), mobile phase 2, detector wavelength (UV): 264 nm.

Concentration ($\mu\text{g mL}^{-1}$)	50	100	200	300	400	500
Peak area(μA) 1	1454.60	2824.40	5635.50	8224.10	11214.80	13923.30
Peak area(μA) 2	1454.90	2824.20	5635.80	8223.30	11213.00	13923.40
Peak area(μA) 3	1454.60	2823.80	5635.70	8223.10	11213.80	13925.50
Peak area(μA) 4	1453.50	2823.90	5636.80	8224.90	11212.30	13925.40
Peak area(μA) 5	1453.40	2824.20	5636.60	8223.90	11213.00	13923.30
Peak area(μA) 6	1453.50	2823.80	5635.90	8224.40	11212.00	13924.30
Average	1454.08	2824.05	5636.05	8223.95	11213.15	13924.20
RSD%	0.05	0.01	0.01	0.01	0.01	0.01

Table 9.9 Results of linearity measurements for (±)-mephedrone using HPLC-UV in the LC-FC-A system, column A (Table 2.2), mobile phase 2, detector wavelength (UV): 264 nm.

Concentration ($\mu\text{g mL}^{-1}$)	50	100	200	300	400	500
Peak area(μA) 1	2166.70	4211.40	8464.80	12386.30	16984.30	21224.20
Peak area(μA) 2	2166.30	4211.30	8467.40	12383.00	16983.10	21224.00
Peak area(μA) 3	2166.50	4211.80	8463.80	12385.80	16983.80	21223.50
Peak area(μA) 4	2165.80	4212.10	8465.00	12386.50	16982.50	21224.10
Peak area(μA) 5	2166.10	4211.70	8460.60	12386.60	16983.00	21223.60
Peak area(μA) 6	2166.90	4211.90	8462.30	12385.10	16982.50	21222.80
Average	2166.383	4211.700	8463.983	12385.550	16983.200	21223.700
RSD%	0.40	0.30	2.35	1.37	0.72	0.52

Table 9.10 Results of linearity measurements for (±)-4-MEC using HPLC-UV in the LC-FC-A system, column A (Table 2.2), mobile phase 2 C, detector wavelengths (UV): 264 nm.

Concentration ($\mu\text{g mL}^{-1}$)	50	100	200	300	400	500
Peak area(μA) 1	2051.90	3991.20	8022.80	11763.00	16133.10	20177.00
Peak area(μA) 2	2050.90	3991.10	8025.70	11763.00	16135.20	20172.00
Peak area(μA) 3	2051.4	3990.10	8025.00	11767.60	16133.33	20170.00
Peak area(μA) 4	2051.60	3990.80	8025.90	11766.80	16133.90	20177.40
Peak area(μA) 5	2050.70	3991.60	8024.10	11764.10	16134.70	20174.70
Peak area(μA) 6	2051.90	3991.40	8024.40	11766.40	16135.50	20273.20
Average	2051.400	3991.033	8024.65	11765.15	16134.28	20190.71
RSD%	0.028	0.013	0.014	0.017	0.006	0.20

Table 9.11 Results of linearity measurements for (±)-caffeine using HPLC-AD in the LC-FC-A system, column A (Table 2.2), mobile phase 2, detector wavelength (UV): 264 nm.

Linearity of caffeine						
Concentration ($\mu\text{g mL}^{-1}$)	50	100	200	300	400	500
Peak current(μA) 1	0.650	1.228	2.514	3.219	4.427	5.370
Peak current(μA) 2	0.641	1.232	2.522	3.245	4.467	5.375
Peak current(μA) 3	0.647	1.234	2.528	3.231	4.432	5.431
Peak current(μA) 4	0.641	1.236	2.542	3.203	4.411	5.437
Peak current(μA) 5	0.649	1.231	2.548	3.247	4.431	5.437
Peak current(μA) 6	0.643	1.225	2.543	3.217	4.496	5.397
Average	0.645	1.231	2.533	3.227	4.444	5.408
RSD%	0.004	0.004	0.014	0.017	0.031	0.031

Table 9.12 Results of linearity measurements for (±)-mephedrone using HPLC-AD in the LC-FC-A system, column A (Table 2.2), mobile phase 2, detector wavelength (UV): 264 nm.

Linearity of (±)-4-MMC						
Concentration ($\mu\text{g mL}^{-1}$)	50	100	200	300	400	500
Peak current(μA) 1	0.129	0.214	0.498	0.670	0.926	1.252
Peak current(μA) 2	0.127	0.217	0.487	0.677	0.930	1.265
Peak current(μA) 3	0.128	0.212	0.497	0.680	0.930	1.262
Peak current(μA) 4	0.129	0.213	0.488	0.687	0.942	1.254
Peak current(μA) 5	0.128	0.213	0.496	0.678	0.928	1.263
Peak current(μA) 6	0.129	0.216	0.49	0.679	0.946	1.283
Average	0.128	0.214	0.493	0.678	0.934	1.263
RSD%	0.550	0.870	0.005	0.808	0.913	0.872

Table 9.13 Results of linearity measurements for (±)-4-MEC using HPLC-AD in the LC-FC-A system, column A (Table 2.2), mobile phase 2, detector wavelength (UV): 264 nm.

Linearity of (±)-4-MEC						
Concentration ($\mu\text{g mL}^{-1}$)	50	100	200	300	400	500
Peak current(μA) 1	4393.81	6458.28	8642.43	10909.90	4393.81	6458.28
Peak current(μA) 2	4392.52	6453.37	8655.18	10934.80	4392.52	6453.37
Peak current(μA) 3	4393.04	6457.33	8556.70	10944.00	4393.04	6457.33
Peak current(μA) 4	4393.91	6454.09	8555.94	10948.00	4393.91	6454.09
Peak current(μA) 5	4394.15	6457.41	8554.57	10912.90	4394.15	6457.41
Peak current(μA) 6	4392.98	6452.50	8551.02	10911.10	4392.98	6452.50
Average	4393.40	6455.50	8585.97	10926.78	4393.40	6455.50
RSD%	0.02	0.04	0.57	0.16	0.02	0.04

Table 9.14 Results of linearity measurements for (±)-caffeine using HPLC-UV in the LC-FC-B system, column A (Table 2.2), mobile phase 2, detector wavelength (UV): 264 nm.

Concentration ($\mu\text{g mL}^{-1}$)	200	300	400	500
Peak current(μA) 1	4393.81	6458.28	8642.43	10909.90
Peak current(μA) 2	4392.52	6453.37	8655.18	10934.80
Peak current(μA) 3	4393.04	6457.33	8556.70	10944.00
Peak current(μA) 4	4393.91	6454.09	8555.94	10948.00
Peak current(μA) 5	4394.15	6457.41	8554.57	10912.90
Peak current(μA) 6	4392.98	6452.50	8551.02	10911.10
Average	4393.40	6455.50	8585.97	10926.78
RSD%	0.02	0.04	0.57	0.16

Table 9.15 Results of linearity measurements for (±)-mephedrone using HPLC-UV in the LC-FC-B system, column A (Table 2.2), mobile phase 2, detector wavelength (UV): 264 nm.

Concentration ($\mu\text{g mL}^{-1}$)	200	300	400	500
Peak current(μA) 1	6682.87	9866.16	13216.60	17087.90
Peak current(μA) 2	6688.88	9869.84	13203.30	17017.90
Peak current(μA) 3	6685.21	9867.37	13164.00	16953.30
Peak current(μA) 4	6689.61	9864.71	13123.40	16899.00
Peak current(μA) 5	6684.94	9865.10	13131.50	16858.40
Peak current(μA) 6	6688.56	9865.36	13102.10	16861.00
Average	6686.68	9866.42	13156.82	16946.25
RSD%	0.04	0.02	0.35	0.54

Table 9.16 Results of linearity measurements for (±)-4-MEC by using HPLC-UV in the LC-FC-B system, column A (Table 2.2), mobile phase 2, detector wavelength (UV): 264 nm.

Concentration ($\mu\text{g mL}^{-1}$)	200	300	400	500
Peak current(μA) 1	6583.34	9761.26	13031.30	16867.00
Peak current(μA) 2	6585.96	9724.31	13035.10	16809.10
Peak current(μA) 3	6587.77	9723.58	12985.80	16746.00
Peak current(μA) 4	6587.31	9720.96	12947.60	16687.70
Peak current(μA) 5	6586.41	9720.03	12952.80	16749.00
Peak current(μA) 6	6585.35	9723.60	12924.40	16746.20
Average	6586.02	9728.96	12979.50	16767.50
RSD%	0.02	0.16	0.35	0.37

Table 9.17 Results of linearity measurements for (±)-mephedrone using HPLC-AD in the LC-FC-B system, column A (Table 2.2), mobile phase 2, detector wavelength (UV): 264 nm.

Concentration ($\mu\text{g mL}^{-1}$)	200	300	400	500
Peak current(μA) 1	0.307	0.468	0.597	0.704
Peak current(μA) 2	0.307	0.469	0.596	0.703
Peak current(μA) 3	0.307	0.467	0.594	0.704
Peak current(μA) 4	0.306	0.465	0.596	0.703
Peak current(μA) 5	0.306	0.468	0.595	0.704
Peak current(μA) 6	0.306	0.468	0.596	0.705
Average	0.307	0.468	0.596	0.704
RSD%	0.179	0.295	0.173	0.107

Table 9.18 Results of linearity measurements for caffeine using HPLC-AD in the LC-FC-B system, column A (Table 2.2), mobile phase 2, detector wavelength (UV): 264 nm.

Linearity of (±)-mephedrone				
Concentration ($\mu\text{g mL}^{-1}$)	200	300	400	500
Peak current(μA) 1	0.055	0.103	0.123	0.147
Peak current(μA) 2	0.056	0.103	0.124	0.144
Peak current(μA) 3	0.055	0.104	0.124	0.147
Peak current(μA) 4	0.055	0.102	0.125	0.145
Peak current(μA) 5	0.055	0.103	0.124	0.144
Peak current(μA) 6	0.055	0.102	0.124	0.145
Average	0.055	0.103	0.124	0.145
RSD%	0.740	0.732	0.510	0.940

Table 9.19 Results of linearity measurements for (±)-4-MEC using HPLC-AD in the LC-FC-B system, column A (Table 2.2), mobile phase 2, detector wavelength (UV): 264 nm.

Concentration ($\mu\text{g mL}^{-1}$)	200	300	400	500
Peak current(μA) 1	0.045	0.053	0.066	0.073
Peak current(μA) 2	0.045	0.054	0.065	0.073
Peak current(μA) 3	0.044	0.054	0.066	0.072
Peak current(μA) 4	0.045	0.053	0.066	0.073
Peak current(μA) 5	0.044	0.054	0.066	0.073
Peak current(μA) 6	0.045	0.054	0.065	0.072
Average	0.045	0.054	0.066	0.073
RSD%	0.74	0.68	0.44	0.37

Table 9.20 Raw data of inter- and intra-day peak area values and relative standard deviations (RSD %) for (±)-caffeine, (±)-mephedrone and (±)-4-MEC using HPLC-UV detection and amperometric detection in the LC-FC-A system.

Concentration ($\mu\text{g mL}^{-1}$)	Intra-day values of HPLC-UV peak area (mA)			Intra-day values of HPLC-AD peak current (μA)			Intra-day values of HPLC-UV peak area (mA)			Intra-day values of HPLC-AD peak current (μA)		
	Caffeine	4-MMC	4-MEC	Caffeine	4-MMC	4-MEC	Caffeine	4-MMC	4-MEC	Caffeine	4-MMC	4-MEC
400	11214.8	16984.3	16133.1	4.427	0.926	0.458	11214.8	16984.3	16133.1	4.427	0.926	0.458
400	11213.0	16983.1	16135.2	4.467	0.930	0.452	11213.0	16983.1	16135.2	4.467	0.930	0.452
400	11213.8	16983.8	16133.3	4.432	0.930	0.460	11213.8	16983.8	16133.3	4.432	0.930	0.460
400	11212.3	16982.5	16133.9	4.411	0.942	0.455	11212.3	16982.5	16133.9	4.411	0.942	0.455
400	11213.0	16983.0	16134.7	4.431	0.928	0.460	11213.0	16983.0	16134.7	4.431	0.928	0.460
400	11212.0	16982.5	16135.5	4.496	0.946	0.460	11212.0	16982.5	16135.5	4.496	0.946	0.460
400	11267.0	16969.2	16115.3	4.410	0.917	0.463	11212.8	16719.2	15845.0	4.421	0.922	0.455
400	11265.9	16964.7	16115.3	4.446	0.927	0.463	11212.1	16718.8	15844.8	4.435	0.924	0.456
400	11265.6	16968.5	16121.6	4.426	0.931	0.464	11210.3	16720.8	15840.8	4.442	0.920	0.450
400	11268.0	16969.5	16120.5	4.388	0.941	0.463	11210.9	16721.9	15843.4	4.450	0.927	0.456
400	11266.7	16969.6	16116.8	4.448	0.929	0.458	11211.8	16720.6	15846.7	4.432	0.927	0.449
400	11267.3	16967.5	16119.9	4.407	0.930	0.464	11210.4	16721.3	15845.7	4.410	0.927	0.447
Average	11239.9	16975.7	16126.2	4.43	0.93	0.46	11212.3	16851.8	15989.3	4.44	0.93	0.45
RSD%	0.249	0.047	0.053	0.656	0.860	0.829	0.012	0.814	0.947	0.544	0.830	0.967

Table 9.21 Raw data of the inter- and intra-day peak area values and relative standard deviations (RSD %) of for (±)-caffeine, (±)-mephedrone and (±)-4-MEC using HPLC-UV detection and amperometric detection in the LC-FC-B system.

Concentration ($\mu\text{g mL}^{-1}$)	Intra-day values of HPLC-UV peak area (mA)			Intra-day values of HPLC-AD peak current (μA)			Intra-day values of HPLC-UV peak area (mA)			Intra-day values of HPLC-AD peak current (μA)		
	Caffeine	4-MMC	4-MEC	Caffeine	4-MMC	4-MEC	Caffeine	4-MMC	4-MEC	Caffeine	4-MMC	4-MEC
400	11214.8	16984.3	16133.1	4.427	0.926	0.458	11214.8	16984.3	16133.1	4.427	0.926	0.458
400	11213.0	16983.1	16135.2	4.467	0.930	0.452	11213.0	16983.1	16135.2	4.467	0.930	0.452
400	11213.8	16983.8	16133.3	4.432	0.930	0.460	11213.8	16983.2	16133.3	4.432	0.930	0.460
400	11212.3	16982.5	16133.9	4.411	0.942	0.455	11212.3	16982.5	16133.9	4.411	0.942	0.455
400	11213.0	16983.0	16134.7	4.431	0.928	0.460	11213.0	16983.	16134.7	4.431	0.928	0.460
400	11212.0	16982.5	16135.5	4.496	0.946	0.460	11212.0	16982.5	16135.5	4.496	0.946	0.460
400	11267.0	16969.2	16115.3	4.410	0.917	0.463	11212.8	16719.2	15845.0	4.421	0.922	0.455
400	11265.9	16964.7	16115.3	4.446	0.927	0.463	11212.1	16718.8	15844.8	4.435	0.924	0.456
400	11265.6	16968.5	16121.6	4.426	0.931	0.464	11210.3	16720.8	15840.8	4.442	0.920	0.450
400	11268.0	16969.5	16120.5	4.388	0.941	0.463	11210.9	16721.9	15843.4	4.450	0.927	0.456
400	11266.7	16969.6	16116.8	4.448	0.929	0.458	11211.8	16720.6	15846.7	4.432	0.927	0.449
400	11267.3	16967.5	16119.9	4.407	0.930	0.464	11210.4	16721.3	15845.7	4.410	0.927	0.447
Average	11239.9	16975.7	16126.2	4.43	0.93	0.46	11212.3	16851.8	15989.3	4.44	0.93	0.45
RSD%	0.249	0.047	0.053	0.656	0.860	0.829	0.012	0.814	0.947	0.544	0.830	0.967

Table 9.22 Results of linearity measurements for (±)-mephedrone using HPLC-UV in the LC-FC-A system, column A (Table 2.2), mobile phase 3, detector wavelength (UV): 263 nm.

Concentration ($\mu\text{g mL}^{-1}$)	100	200	300	400	500
Peak high (μA)-1	5101.70	10414.80	15431.60	20107.70	25880.30
Peak high (μA)-2	5101.00	10389.90	15444.80	20087.90	25902.40
Peak high (μA)-3	5102.30	10395.70	15445.30	20141.20	25912.00
Peak high (μA)-4	5100.70	10392.30	15437.01	20139.80	25904.30
Peak high (μA)-5	5103.30	10396.20	15443.60	20249.30	25887.10
Peak high (μA)-6	5103.80	10389.70	15447.80	20166.30	25896.60
Average	5102.10	10396.40	15441.70	20148.70	25897.10
RSD%	0.02	0.09	0.03	0.28	0.04

Table 9.23 Results of linearity measurements for (±)-mexedrone using HPLC-UV in the LC-FC-A system, column A (Table 2.2), mobile phase 3, detector wavelength (UV): 263 nm.

Concentration ($\mu\text{g mL}^{-1}$)	100	200	300	400	500
Peak high (μA)-1	4888.2	8037.7	11578.4	14923.3	18604.2
Peak high (μA)-2	4888.41	8038.45	11579.3	14920.5	18606.7
Peak high (μA)-3	4889.82	8038.12	11582	14922.6	18602.6
Peak high (μA)-4	4886.96	8038.57	11579.1	14923.6	18603.0
Peak high (μA)-5	4887.69	8038.3	11581.7	14920.5	18603.6
Peak high (μA)-6	4888.2	8038.3	11581.3	14924.8	18602.2
Average	4888.21	8038.2	11580.30	14922.5	18603.7
RSD%	0.02	0.003	0.01	0.01	0.01

Table 9.24 Results of linearity measurements for (±)-mephedrone using HPLC-AD in the LC-FC-A system, column A (Table 2.2), mobile phase 3, detector wavelength (UV): 263 nm.

Concentration ($\mu\text{g mL}^{-1}$)	100	200	300	400	500
Peak high (μA)-1	0.1200	0.2309	0.3436	0.4509	0.6047
Peak high (μA)-2	0.1194	0.2303	0.3430	0.4523	0.6030
Peak high (μA)-3	0.1206	0.2300	0.3380	0.4515	0.6021
Peak high (μA)-4	0.1185	0.2305	0.3412	0.4525	0.6020
Peak high (μA)-5	0.1200	0.2307	0.3428	0.4577	0.6000
Peak high (μA)-6	0.1190	0.2305	0.3452	0.4576	0.6010
Average	0.1196	0.2305	0.3425	0.4538	0.6021
RSD%	0.65	0.14	0.722	0.67	0.27

Table 9.25 Results of linearity measurements for (±)-mexedrone using HPLC-AD in the LC-FC-A system, column A (Table 2.2), mobile phase 3, detector wavelength (UV): 263 nm.

Concentration ($\mu\text{g mL}^{-1}$)	100	200	300	400	500
Peak high (μA)-1	0.1741	0.2826	0.4166	0.5567	0.6922
Peak high (μA)-2	0.1730	0.2834	0.4160	0.5584	0.6865
Peak high (μA)-3	0.1730	0.2830	0.4174	0.5524	0.6864
Peak high (μA)-4	0.1720	0.2820	0.4193	0.5554	0.6884
Peak high (μA)-5	0.1700	0.2810	0.4160	0.5598	0.6844
Peak high (μA)-6	0.1730	0.2790	0.4160	0.5510	0.6791
Average	0.1725	0.2818	0.4169	0.5556	0.6862
RSD%	0.81	0.58	0.31	0.61	0.63

Table 9.26 Raw data of the inter- and intra-day peak values and relative standard deviations (RSD %) of for (±)-mephedrone, and (±)-mexedrone using HPLC-UV detection and amperometric detection in the LC-FC-A system.

Concentration ($\mu\text{g mL}^{-1}$)	Intra-day HPLC-UV peak area (mAU)		Intra-day HPLC-AD peak current (μA)		Inter-day HPLC-UV peak area (mAU)		Inter-day HPLC-AD peak area (μA)	
	4-MMC	Mexedrone	4-MMC	Mexedrone	4-MMC	Mexedrone	4-MMC	Mexedrone
300	15431.6	11578.4	0.344	0.417	15431.6	11578.4	0.344	0.417
300	15444.8	11579.3	0.343	0.416	15444.8	11579.3	0.343	0.416
300	15445.3	11582.0	0.344	0.417	15445.3	11582.0	0.344	0.417
300	15437.1	11579.1	0.341	0.419	15437.1	11579.1	0.341	0.419
300	15443.6	11581.7	0.348	0.416	15443.6	11581.7	0.348	0.416
300	15447.8	11581.3	0.345	0.416	15447.8	11581.3	0.345	0.416
300	15392.9	11557.5	0.343	0.420	15432.9	11577.5	0.348	0.414
300	15382.9	11535.2	0.344	0.424	15432.9	11585.2	0.345	0.417
300	15391.8	11552.1	0.344	0.421	15431.8	11582.1	0.348	0.410
300	15490.0	11548.3	0.345	0.421	15440.0	11578.3	0.345	0.412
300	15394.8	11539.3	0.342	0.422	15444.8	11579.3	0.345	0.416
300	15385.3	11532.0	0.338	0.420	15445.3	11582.0	0.348	0.414
Average	15424.0	11562.2	0.343	0.419	15439.8	11580.5	0.345	0.415
STD	33.661	20.137	0.002	0.003	6.211	2.222	0.002	0.002
RSD%	0.218	0.174	0.703	0.631	0.040	0.019	0.657	0.584

Table 9.27 Results of linearity measurements for (±)-4-MEP using HPLC-UV in the LC-FC-A system, column B (Table 2.2), mobile phase 4, detector wavelength (UV): 279 nm.

Concentration ($\mu\text{g mL}^{-1}$)	100	200	300	400	500
Peak area 1	81.47	166.01	248.23	334.67	411.02
Peak area 2	81.21	166.79	247.57	333.52	411.74
Peak area 3	81.15	166.56	248.15	333.63	411.48
Peak area 4	81.28	165.91	247.22	333.99	411.36
Peak area 5	81.29	165.97	247.57	333.69	411.02
Peak area 6	81.48	166.79	247.65	333.08	411.75
Average	81.31	166.34	247.73	333.76	411.40
RSD%	0.17	0.25	0.16	0.16	0.08

Table 9.28 Results of linearity measurements for (±)-2-MEP using HPLC-UV in the LC-FC-A system, column B (Table 2.2), mobile phase 4, detector wavelength (UV): 279 nm.

Concentration ($\mu\text{g mL}^{-1}$)	100	200	300	400	500
Peak area 1	191.22	391.28	582.20	775.08	943.50
Peak area 2	191.48	391.24	582.38	775.49	943.36
Peak area 3	191.04	391.15	582.29	775.02	943.20
Peak area 4	191.25	391.60	581.92	775.09	943.36
Peak area 5	191.19	391.76	582.38	775.37	943.13
Peak area 6	191.05	391.82	582.29	775.17	943.35
Average	191.20	391.47	582.24	775.20	943.32
RSD%	0.09	0.07	0.03	0.02	0.01

Table 9.29 Results of linearity measurements for (±)-3-MEP using HPLC-UV in the LC-FC-A system, column B (Table 2.2), mobile phase 4, detector wavelength (UV): 279 nm.

Concentration ($\mu\text{g mL}^{-1}$)	100	200	300	400	500
Peak area 1	162.07	329.85	491.08	661.18	799.86
Peak area 2	162.17	329.23	491.32	660.31	799.64
Peak area 3	162.43	329.48	491.74	661.28	799.72
Peak area 4	162.49	329.40	491.68	660.37	799.68
Peak area 5	162.20	329.68	491.32	660.44	799.67
Peak area 6	162.14	329.23	492.23	660.22	799.65
Average	162.25	329.48	491.56	660.63	799.71
RSD%	0.10	0.08	0.08	0.07	0.01

Table 9.30 Results of linearity measurements for (±)-4-MEP using HPLC-UV in the LC-FC-A system, column B (Table 2.2), mobile phase 4, detector wavelength (UV): 279 nm.

Concentration ($\mu\text{g mL}^{-1}$)	100	200	300	400	500
Peak current(μA)-1	0.15	0.29	0.41	0.58	0.69
Peak current(μA)-2	0.15	0.29	0.41	0.57	0.68
Peak current(μA)-3	0.14	0.29	0.41	0.57	0.68
Peak current(μA)-4	0.15	0.29	0.42	0.57	0.68
Peak current(μA)-5	0.15	0.28	0.42	0.58	0.67
Peak current(μA)-6	0.15	0.29	0.41	0.59	0.66
Average	0.15	0.29	0.41	0.58	0.68
RSD%	0.52	1.89	1.25	1.40	1.35

Table 9.31 Results of linearity measurements for (±)-2-MEP using HPLC-AD in the LC-FC-A system, column B (Table 2.2), mobile phase 4, amperometric detector

Concentration ($\mu\text{g mL}^{-1}$)	100	200	300	400	500
Peak current(μA)-1	0.13	0.20	0.26	0.38	0.44
Peak current(μA)-2	0.13	0.20	0.26	0.38	0.45
Peak current(μA)-3	0.13	0.21	0.26	0.38	0.46
Peak current(μA)-4	0.13	0.20	0.26	0.38	0.45
Peak current(μA)-5	0.13	0.20	0.26	0.38	0.45
Peak current(μA)-6	0.13	0.2	0.26	0.37	0.4
Average	0.130	0.20	0.26	0.38	0.45
RSD%	1.05	0.67	0.95	0.71	1.02

Table 9.32 Results of linearity measurements for (±)-3-MEP using HPLC-AD in the LC-FC-A system, column B (Table 2.2), mobile phase 4, amperometric detector

Concentration ($\mu\text{g mL}^{-1}$)	100	200	300	400	500
Peak current(μA)-1	0.13	0.22	0.27	0.39	0.43
Peak current(μA)-2	0.13	0.22	0.27	0.38	0.43
Peak current(μA)-3	0.12	0.22	0.27	0.38	0.44
Peak current(μA)-4	0.13	0.22	0.27	0.37	0.44
Peak current(μA)-5	0.13	0.22	0.27	0.38	0.44
Peak current(μA)-6	0.13	0.22	0.28	0.38	0.43
Average	0.13	0.22	0.27	0.38	0.43
RSD%	1.57	0.64	1.17	1.30	1.24

Table 9.33 Results of linearity measurements for (±)-4-FEP using HPLC-UV in the LC-FC-A system, column B (Table 2.2), mobile phase 5; detector wavelength (UV): 270 nm.

Concentration ($\mu\text{g mL}^{-1}$)	50	100	150	200	250	300
Peak area 1	20.41	40.27	59.83	80.76	96.90	119.92
Peak area 2	20.37	40.14	59.93	80.32	96.77	119.73
Peak area 3	20.44	40.00	60.14	80.33	96.77	119.91
Peak area 4	20.46	40.26	60.18	80.90	96.71	120.32
Peak area 5	20.44	40.00	60.03	80.46	96.41	119.86
Peak area 6	20.13	40.01	60.06	80.34	97.06	120.28
Average	20.37	40.12	60.03	80.52	96.78	120.00
RSD%	0.62	0.32	0.218	0.31	0.22	0.19

Table 9.34 Results of linearity measurements for (±)-2-FEP using HPLC-UV in the LC-FC-A system, column B (Table 2.2), mobile phase 5, detector wavelength (UV): 270 nm.

Concentration ($\mu\text{g mL}^{-1}$)	50	100	150	200	250	300
Peak area 1	49.19	97.67	146.82	196.86	235.84	292.74
Peak area 2	48.93	98.01	146.63	196.82	236.21	293.05
Peak area 3	49.25	98.29	147.19	196.77	235.74	292.84
Peak area 4	49.16	97.91	146.96	196.81	236.12	293.38
Peak area 5	48.94	98.27	146.82	196.71	236.39	293.40
Peak area 6	48.95	98.39	146.60	196.63	236.37	293.65
Average	49.07	98.09	146.83	196.77	236.11	293.18
RSD%	0.29	0.28	0.15	0.04	0.11	0.12

Table 9.35 Results of linearity measurements for (±)-3-FEP using HPLC-UV in the LC-FC-A system, column B, (Table 2.2), mobile phase 5, detector wavelength (UV): 270 nm.

Concentration ($\mu\text{g mL}^{-1}$)	50	100	150	200	250	300
Peak area 1	49.22	97.81	149.69	197.41	239.05	297.32
Peak area 2	49.01	98.27	149.29	197.65	239.85	297.29
Peak area 3	48.99	98.56	149.70	197.23	239.21	297.76
Peak area 4	49.04	98.37	149.77	197.95	239.69	297.47
Peak area 5	49.25	98.36	149.41	197.16	239.07	297.66
Peak area 6	49.06	98.76	149.08	197.08	239.87	297.04
Average	49.09	98.36	149.49	197.41	239.46	297.42
RSD%	0.23	0.33	0.18	0.17	0.16	0.09

Table 9.36 Results of linearity measurements for (±)-4-FEP using HPLC-AD in LC-FC-A system, column B (Table 2.2), mobile phase 5, amperometric detector

Concentration ($\mu\text{g mL}^{-1}$)	50	100	150	200	250	300
Peak current(μA) 1	0.140	0.281	0.421	0.563	0.704	0.830
Peak current(μA) 2	0.141	0.282	0.419	0.561	0.703	0.842
Peak current(μA) 3	0.141	0.281	0.418	0.560	0.703	0.841
Peak current(μA) 4	0.140	0.280	0.417	0.565	0.702	0.842
Peak current(μA) 5	0.140	0.282	0.418	0.561	0.702	0.840
Peak current(μA) 6	0.141	0.281	0.413	0.560	0.704	0.843
Average	0.141	0.281	0.418	0.562	0.71	0.839
RSD%	0.24	0.25	0.64	0.36	0.15	0.56

Table 9.37 Results of linearity measurements for (±)-2-FEP using HPLC-AD in the LC-FC-A system, column B (Table 2.2), mobile phase 5, amperometric detector

Concentration ($\mu\text{g mL}^{-1}$)	50	100	150	200	250	300
Peak current(μA) 1	0.125	0.248	0.248	0.379	0.583	0.739
Peak current(μA) 2	0.127	0.249	0.249	0.375	0.586	0.737
Peak current(μA) 3	0.126	0.247	0.247	0.369	0.585	0.728
Peak current(μA) 4	0.128	0.249	0.249	0.369	0.584	0.739
Peak current(μA) 5	0.127	0.249	0.249	0.369	0.583	0.734
Peak current(μA) 6	0.127	0.248	0.241	0.378	0.583	0.748
Average	0.127	0.248	0.247	0.373	0.584	0.738
RSD%	0.76	0.39	1.23	1.19	0.20	0.87

Table 9.38 Results of linearity measurements for (±)-3-FEP using HPLC-AD in the LC-FC-A system, column B (Table 2.2), mobile phase 5, amperometric detector

Concentration ($\mu\text{g mL}^{-1}$)	50	100	150	200	250	300
Peak current(μA)-1	0.124	0.246	0.365	0.471	0.612	0.731
Peak current(μA)-2	0.125	0.245	0.366	0.473	0.618	0.738
Peak current(μA)-3	0.124	0.245	0.364	0.470	0.617	0.735
Peak current(μA)-4	0.123	0.246	0.361	0.471	0.617	0.725
Peak current(μA)-5	0.123	0.247	0.365	0.469	0.613	0.732
Peak current(μA)-6	0.124	0.248	0.361	0.471	0.613	0.729
Average	0.124	0.246	0.364	0.471	0.615	0.732
RSD%	0.608	0.475	0.594	0.230	0.440	0.610

Table 9.39 Raw data of inter- and intra-day peak area values and relative standard deviations (RSD %) for (±)-4-MEP, (±)-2-MEP and (±)-3-MEP by using HPLC-UV detection and amperometric detection in the LC-FC-A system.

Concentration ($\mu\text{g mL}^{-1}$)	Intra-day of HPLC-UV peak area (mA)			Intra-day of HPLC-AD peak current (μA)			Inter-day of HPLC-AD peak area (mA)			Inter-day of HPLC-AD peak current (μA)		
	4-MEP	2-MEP	3-MEP	4-MEP	2-MEP	3-MEP	4-MEP	2-MEP	3-MEP	4-MEP	2-MEP	3-MEP
300	248.23	582.2	491.08	0.417	0.262	0.268	244.23	580.2	493.08	0.417	0.262	0.268
300	247.57	582.38	491.32	0.419	0.259	0.273	243.57	580.38	493.32	0.419	0.259	0.273
300	248.15	582.29	491.74	0.424	0.262	0.269	243.15	580.29	492.74	0.424	0.262	0.269
300	247.22	581.92	491.68	0.417	0.261	0.270	244.22	581.92	492.68	0.41	0.261	0.270
300	247.57	582.38	491.32	0.426	0.262	0.270	244.57	580.38	493.32	0.426	0.262	0.270
300	247.65	582.29	492.23	0.419	0.262	0.273	243.65	581.29	493.23	0.419	0.262	0.273
300	248.23	582.2	491.08	0.417	0.261	0.268	248.23	582.2	491.08	0.418	0.257	0.273
300	247.57	582.38	491.32	0.418	0.257	0.273	247.57	582.38	491.32	0.419	0.262	0.273
300	248.15	582.29	491.74	0.424	0.263	0.268	248.15	582.29	491.74	0.417	0.261	0.268
300	247.22	581.92	491.68	0.417	0.261	0.271	247.22	581.92	491.68	0.418	0.257	0.273
300	247.57	582.38	491.32	0.426	0.259	0.270	247.57	582.38	491.32	0.417	0.262	0.268
300	247.65	582.29	492.23	0.417	0.261	0.270	247.65	582.29	492.23	0.419	0.259	0.273
Average	247.73	582.24	491.56	0.42	0.26	0.27	245.82	581.49	492.31	0.42	0.26	0.27
RSD%	0.15	0.03	0.08	0.90	0.66	0.71	0.83	0.16	0.17	0.70	0.76	0.83

Table 9.40 Raw data of the inter and intra-day peak values and relative standard deviations (RSD %) for (±)-4-FEP, (±)-2-FEP and (±)-3-FEP using HPLC-UV detection and amperometric detection in the LC-FC-A system.

Concentration ($\mu\text{g mL}^{-1}$)	Intra-day of HPLC-UV peak area (mA)			Intra-day of HPLC-AD peak current (μA)			Inter-day of HPLC-AD peak area (mA)			Inter-day of HPLC-AD peak current (μA)		
	4-FEP	2-FEP	3-FEP	4-FEP	2-FEP	3-FEP	4-FEP	2-FEP	3-FEP	4-FEP	2-FEP	3-FEP
300	119.92	292.74	297.32	0.838	0.740	0.731	119.92	292.74	297.32	0.838	0.740	0.731
300	119.73	293.05	297.30	0.842	0.738	0.738	119.73	293.05	297.30	0.842	0.738	0.738
300	119.91	292.84	297.76	0.841	0.729	0.736	119.91	292.84	297.76	0.841	0.729	0.736
300	120.32	293.38	297.47	0.842	0.740	0.725	120.32	293.38	297.47	0.842	0.740	0.725
300	119.86	293.40	297.66	0.840	0.735	0.732	119.86	293.40	297.66	0.840	0.735	0.732
300	120.28	293.20	297.04	0.843	0.749	0.730	120.28	293.20	297.04	0.843	0.749	0.730
300	119.78	293.04	297.29	0.829	0.730	0.724	120.14	293.39	297.77	0.841	0.729	0.738
300	119.93	292.87	297.72	0.849	0.734	0.734	119.25	293.28	297.09	0.838	0.729	0.736
300	120.31	293.38	297.43	0.829	0.740	0.726	120.01	293.20	297.03	0.840	0.726	0.725
300	119.87	293.40	297.09	0.844	0.736	0.728	119.88	293.21	297.32	0.840	0.734	0.730
300	119.72	293.07	297.74	0.839	0.736	0.731	119.73	292.98	297.23	0.836	0.721	0.723
300	119.82	292.49	297.08	0.842	0.741	0.728	120.21	293.34	297.54	0.840	0.740	0.726
Average	119.95	293.07	297.41	0.840	0.737	0.730	119.94	293.17	297.38	0.840	0.734	0.731
RSD%	0.18	0.10	0.09	0.659	0.678	0.558	0.23	0.07	0.09	0.227	0.991	0.688